

PROBING PHYSICS BEYOND THE STANDARD MODEL THROUGH  
NEUTRINO-ELECTRON SCATTERINGS

A THESIS SUBMITTED TO  
THE GRADUATE SCHOOL OF NATURAL AND APPLIED SCIENCES  
OF  
MIDDLE EAST TECHNICAL UNIVERSITY

SELÇUK BİLMİŞ

IN PARTIAL FULFILLMENT OF THE REQUIREMENTS  
FOR  
THE DEGREE OF DOCTOR OF PHILOSOPHY  
IN  
PHYSICS

AUGUST 2016



Approval of the thesis:

**PROBING PHYSICS BEYOND THE STANDARD MODEL THROUGH  
NEUTRINO-ELECTRON SCATTERINGS**

submitted by **SELÇUK BİLMİŞ** in partial fulfillment of the requirements for the degree of **Doctor of Philosophy in Physics Department, Middle East Technical University** by,

Prof. Dr. Gülbin Dural Ünver  
Dean, Graduate School of **Natural and Applied Sciences**

\_\_\_\_\_

Prof. Dr. Sadi Turgut  
Head of Department, **Physics**

\_\_\_\_\_

Assoc. Prof. Dr. İsmail Turan  
Supervisor, **Physics Department, METU**

\_\_\_\_\_

**Examining Committee Members:**

Prof. Dr. Ali Ulvi Yilmazer  
Physics Engineering Department, Ankara University

\_\_\_\_\_

Assoc. Prof. Dr. İsmail Turan  
Physics Department, METU

\_\_\_\_\_

Prof. Dr. Tahmasib Aliev  
Physics Department, METU

\_\_\_\_\_

Prof. Dr. İnanç Şahin  
Physics Department, Ankara University

\_\_\_\_\_

Prof. Dr. Mehmet Zeyrek  
Physics Department, METU

\_\_\_\_\_

**Date:**

\_\_\_\_\_

**I hereby declare that all information in this document has been obtained and presented in accordance with academic rules and ethical conduct. I also declare that, as required by these rules and conduct, I have fully cited and referenced all material and results that are not original to this work.**

Name, Last Name: SELÇUK BILMIŞ

Signature :



## ABSTRACT

### PROBING PHYSICS BEYOND THE STANDARD MODEL THROUGH NEUTRINO-ELECTRON SCATTERINGS

Bilmiş, Selçuk

Ph.D., Department of Physics

Supervisor : Assoc. Prof. Dr. İsmail Turan

August 2016, 270 pages

Neutrino interactions are well explained with the electroweak theory. Hence, as an alternative to collider experiments, new physics can be searched in neutrino experiments as well. Using the neutrino-electron scattering data taken by several experiments (TEXONO, GEMMA, LSND, CHARM II, BOREXINO), which were chosen according to their incoming neutrino energy as well as recoil energy of the electron, possible effects on the neutrino scattering data originating from the presence of non-commutativity in space as well as the existence of a hidden sector in the form of dark photon have been studied.

Once QED is extended into non-commutative space, coupling of neutral particles to photons becomes possible at tree level. Using this new vertex, contribution to the cross section is calculated and bounds for the non-commutative energy scale  $\Lambda_{NC}$  are set. We find that the results from CHARM II experiments give the stringent bounds as  $\Lambda_{NC} > 3.3$  TeV at 95% confidence level and improve the bounds over the collider

experiments.

In the second part of the thesis, as an alternative scenario, the effects of the hidden sector through a light gauge boson  $A'$ , associated with a group  $U(1)_{B-L}$  is searched in the neutrino electron scattering experiments. This new gauge boson can interact with neutrinos at tree level even though it has no charge, hence named as dark photon. The bounds are set for the mass of the dark photon  $m_{A'}$  and the coupling constant  $g_{B-L}$ . The exclusion plot at the 90% C.L. for the  $m_{A'}-g_{B-L}$  plane is plotted. It is shown that the interference term can not be neglected and improves the bounds. Our results provide more stringent bounds to some regions of the parameter space.

Keywords: Neutrino Scattering, Texono, Non-commutative Space, Dark Photon

# ÖZ

## NÖTRİNO-ELEKTRON SAÇILIMLARINDA YENİ FİZİK ARAŞTIRILMASI

Bilmiş, Selçuk

Doktora, Fizik Bölümü

Tez Yöneticisi : Doç. Dr. İsmail Turan

Ağustos 2016 , 270 sayfa

Nötrino etkileşimleri elektrozayıf teori ile çok iyi şekilde açıklanabilmektedir. Bu sayede, çarpıştırıcı deneylerine alternatif olarak nötrino deneylerinde de yeni fizik araştırması yapılabilir. Nötrinoların enerjileri ve elektronun geri tepme enerjileri göz önüne alınarak seçilen nötrino deneylerinin (TEXONO, GEMMA, LSND, CHARM II, BOREXINO) saçılım verileri kullanılarak “saklı sektörün” karanlık foton formunda etkilerinin yanında komütatif olmayan uzayın varlığının nötrino saçılım dasetindeki etkileri çalışılmıştır.

Kuantum elektrodinamiği komütatif olmayan uzay-zamanda incelendiğinde yüksüz parçacıkların ağaç mertebesinde fotonlar ile etkileşebildiği anlaşılır. Bu yeni etkileşmenin tesir kesitine yaptığı katkılar hesaplanarak komütatif olmayan enerji skalasına,  $\Lambda_{NC}$ , sınırlar konuldu. CHARM II deneyinin, %95 güvenilirlik düzeyinde en yüksek sınır değerini,  $\Lambda_{NC} > 3.3$  TeV olarak verdiğini bulduk ki, bu sınır değeri çarpıştırıcı deneyinde elde edilen sınır değerlerini daha yukarı çekmiştir.

Tezin ikinci kısmında, alternatif senaryo olarak, “saklı sektörün” etkileri  $U(1)_{B-L}$  grubu ile ilişkili hafif ayar bozonu olan  $A'$  aracılığıyla nötrino elektron saçılım deneylerinde araştırıldı. Bu yeni ayar bozonu yüksüz olmasına rağmen nötrinolar ile ağaç mertebesinde etkileşebilmektedir ki bu yüzden karanlık foton olarak adlandırılır. Karanlık fotonun kütlesi ( $m_{A'}$ ) ve bağdaşım sabiti ( $g_{B-L}$ ) için sınır değerler bulundu. %90 güvenilirlik ölçeğinde  $m_{A'}-g_{B-L}$  düzleminde dışlama diyagramı çizildi. Girişim teriminin ihmal edilemeyeceği hatta sınır değerlerini daha da iyilestireceği gösterildi. Elde ettiğimiz sonuçlar parametre uzayının bazı bölgeleri için var olan sınır değerlerini daha da yukarı çeker.

Anahtar Kelimeler: Nötrino Saçılımı, Texono, Komütatif Olmayan Uzay, Karanlık Foton

*To my cat psinoza (aka pisu)*

## ACKNOWLEDGMENTS

First and foremost I want to thank my advisor Assoc. Prof. Dr. İsmail Turan for the continuous support of my Ph.D. study and related research. It has been an honor to be his first Ph.D. student.

I am very grateful to Prof. Dr. T. M. Aliev for his patience, insightful discussions, scientific advice and knowledge.

I also thank to Prof. Dr. Mehmet Zeyrek and Assoc. Prof. Dr. Muhammed Deniz for paving the way for being a member of TEXONO collaboration.

Besides, I would like to thank to Prof. Dr. Ali Ulvi Yılmaz and Prof. Dr. İnanç Şahin who were in my thesis committee, for their time, interest, insightful comments and encouragement.

My sincere thanks also goes to Prof. Dr. Henry Wong, who provided me an opportunity to join TEXONO collaboration and who gave access to the research facilities and several data. Moreover, I would like to thank him for his useful comments and guidance throughout this research.

I am grateful for the support by the TUBITAK-2211 program.

I would like to thank to Doğan, Ender and Ozan for their friendships. I am also thankful to Hülya for her friendship especially for the times we were in Japan. Thanks to Sinan for his support on skype even though he was far away.

I would like to thank to Makbule for her love and great support. Without the “baklavas” she bought from “Mado”, this thesis would not have been completed.

Last but not the least, I would like to thank to my family for supporting me spiritually throughout writing this thesis and my life in general.

# TABLE OF CONTENTS

ABSTRACT . . . . .	v
ÖZ . . . . .	vii
ACKNOWLEDGMENTS . . . . .	x
TABLE OF CONTENTS . . . . .	xi
LIST OF TABLES . . . . .	xv
LIST OF FIGURES . . . . .	xvii
LIST OF ABBREVIATIONS . . . . .	xxvi
CHAPTERS	
1 INTRODUCTION . . . . .	1
1.1 Outline of the Thesis . . . . .	5
2 NEUTRINOS IN THE STANDARD MODEL . . . . .	7
2.1 A Brief History of Neutrinos . . . . .	7
2.2 Neutrino Sources . . . . .	16
2.3 The Standard Model . . . . .	21
2.3.1 The Electromagnetic Force . . . . .	22
2.3.2 The Weak Force . . . . .	22

2.3.3	The Strong Force . . . . .	23
2.3.4	The Electroweak Theory . . . . .	24
2.4	Helicity and Chirality of Neutrinos . . . . .	29
3	NEUTRINO ELECTRON SCATTERING IN THE STANDARD MODEL	35
3.1	The Golden Rule for Scattering . . . . .	35
3.2	$ \mathcal{M} ^2$ for the Neutrino-Electron Scattering . . . . .	42
3.2.1	The $\nu_\mu - e^-$ Scattering . . . . .	43
3.2.2	The $\bar{\nu}_\mu - e^-$ Scattering . . . . .	52
3.2.3	The $\nu_e - e^-$ Scattering . . . . .	54
3.2.4	The $\bar{\nu}_e - e^-$ Scattering . . . . .	57
3.3	The Differential Cross Section for the $\nu - e$ Scatterings . . . . .	60
3.4	Neutrino Electron Scattering for High Energy Neutrinos . . . . .	66
3.5	The Neutrino Electron Scattering With Respect to the Scat- tering Angle of Electron . . . . .	68
4	$\nu - e$ SCATTERING EXPERIMENTS . . . . .	73
4.1	TEXONO . . . . .	73
4.2	GEMMA . . . . .	81
4.3	LSND . . . . .	82
4.4	CHARM II . . . . .	86
4.5	BOREXINO . . . . .	89
5	NONCOMMUTATIVE SPACE . . . . .	93
5.1	The Landau Problem . . . . .	95



5.2	A Brief History of the Non-commutative Space . . . . .	101
5.3	Weyl-Moyal Product . . . . .	102
5.4	Non-commutative QED . . . . .	103
5.4.1	Neutrino-electron Scattering in Non-Commutative Space . . . . .	110
5.4.2	Anti-neutrino Electron Scattering In Non-commutative Space . . . . .	133
5.5	Analysis & Results . . . . .	135
5.5.1	TEXONO . . . . .	136
5.5.2	LSND . . . . .	139
5.5.3	CHARM II . . . . .	140
5.5.4	Bounds from Other Channels . . . . .	140
6	DARK PHOTON . . . . .	145
6.1	Hidden Sector . . . . .	147
6.2	The $\nu - e$ Scattering Under the $U(1)_{B-L}$ Symmetry . . . . .	153
6.3	The $\bar{\nu} - e$ Scattering Under the $U(1)_{B-L}$ Symmetry . . . . .	158
6.4	Interference of Dark Photon and Standard Model Diagrams . . . . .	159
6.5	Analysis & Results . . . . .	161
6.5.1	Roles of Interference Terms . . . . .	166
6.5.2	Dark Photon Bounds in the Literature . . . . .	169
6.5.3	Dark Photon Production Mechanisms . . . . .	170
6.5.4	Beam Dump Experiments . . . . .	174

6.5.4.1	Electron Beam Dump Experiments . . .	175
6.5.4.2	Proton Beam Dump Experiments . . .	176
6.5.5	Fixed Target Experiments . . . . .	178
6.5.6	Flavor Factories & Colliders . . . . .	180
6.5.7	Light Shining through Walls (LSW) . . . . .	183
6.5.8	Anomalous Magnetic Moment of the Electron and Muon (g-2) . . . . .	183
6.5.9	Helioscopes . . . . .	184
6.5.10	CMB . . . . .	184
7	CONCLUSIONS . . . . .	189
APPENDICES		
A	FIERZ IDENTITIES . . . . .	225
B	SCALAR PRODUCTS IN THE REST FRAME OF THE ELECTRON	235
C	MAXIMUM RECOIL ENERGY OF THE ELECTRON . . . . .	239
D	INTERFERENCE TERM FOR $\nu_\mu - e^-$ SCATTERING IN THE NON- COMMUTATIVE SPACE . . . . .	243
E	COMPUTATIONAL FILES . . . . .	257
E.1	CalcHEP Model Files . . . . .	257
E.2	Contents of the “sum_22_low_weak.m” . . . . .	260
E.3	Mathematica Notebook File to Calculate the Cross-section for $\bar{\nu}_e - e^-$ Scattering . . . . .	261
	CURRICULUM VITAE . . . . .	267

## LIST OF TABLES

### TABLES

Table 2.1 Quantum numbers of the leptons and quarks are shown. $I$ and $I_3$ are the total and third component of the weak isospin, respectively. $Q$ is the electromagnetic charge of the fermions and $Y$ corresponds to the hypercharge. . . . .	25
Table 3.1 The values of vector and axial couplings of fermions in the SM is shown. . . . .	52
Table 3.2 The parameters $a$ and $b$ in the SM cross section expression in Equation (3.116). $\alpha$ corresponds to $\mu$ or $\tau$ . . . . .	63
Table 4.1 Key parameters of the TEXONO experiments are summarized. . . .	80
Table 5.1 The key parameters of the TEXONO, LSND and CHARM-II measurements on the $\nu - e$ scattering, and the derived bounds on NC physics. The best-fit values in $\Theta^2$ and the 95% CL lower limits on $\Lambda_{NC}$ are shown.	140
Table 5.2 Summary of experimental constraints on the NC energy scale $\Lambda_{NC}$ . The quoted bounds for the direct experiments on scattering processes at colliders are at 95% C.L. These are complemented by order-of-magnitude estimates for the model-dependent bounds with the atomic, hadronic and astrophysical systems. The projected sensitivities from current and future collider experiments are also listed. (Table is adapted from [115].) . . . .	143
Table 6.1 Various hidden sector models are summarized. . . . .	148

Table 6.2 The key parameters of the TEXONO, LSND, CHARM II, BOREX-INO and GEMMA experiments on the  $\nu - e$  scattering is shown. (Table is adapted from [170].) . . . . . 162

Table 6.3 The key parameters of the electron-beam dump experiments used to constrain the dark photon parameters is shown. For more details see [182] where the table is adapted from. . . . . 176

Table 6.4 The relevant parameters of the most common experiments are shown. (Table is adapted from [155].) . . . . . 179

Table 6.5 The bounds on the gauge coupling constant of the dark photon from different sources are listed with a brief summary about the experiments as well as the relevant references. . . . . 185

## LIST OF FIGURES

### FIGURES

- Figure 2.1 Expected energy distribution of the emitted electron for the two body decay is a sharp peak (red curve). However, the observed spectrum was continuous for the  $\beta$  decay (black curve) (Figure is adapted from [1]). . . . . 8
- Figure 2.2 Four-point interaction model of Enrico Fermi to describe  $\beta$  decay. . . . . 9
- Figure 2.3 The schematic view of the idea of Wu experiment. Number of electrons emitted by  $\alpha$  and  $\pi - \alpha$  degrees expected to be equal if the parity is conserved (Figure is adapted from [5]). . . . . 11
- Figure 2.4 Schematic view of the detection process for the Reines-Cowan experiment (Figure is adapted from [15]). . . . . 14
- Figure 2.5 Decay rate of  $Z$  boson implies the existence of three neutrino flavors (Figure is adapted from [18]). . . . . 15
- Figure 2.6 The chain reactions in the fusion process for the pp cycle is shown according to the SSM. Neutrinos produced in the pp, pep,  ${}^7\text{Be}$ , hep and  ${}^8\text{B}$  cycles are electron neutrinos ( $\nu_e$ ). 1.5% of the fusion process occurs via CNO cycle which is not depicted here (Figure is adapted from [26]). . . . . 17
- Figure 2.7 The measured and predicted solar neutrino rates are compared. Figure is adapted from [32]. . . . . 18
- Figure 2.8 The SSM prediction of the energy vs flux of the neutrinos are depicted for each cycle of the fusion mechanism in the sun (Figure is adapted from [32]). . . . . 19

Figure 2.9 The measured and calculated fluxes of all neutrino sources are depicted with respect to the energy of the neutrinos (Figure is adapted from [41]). . . . .	20
Figure 2.10 The particle content of the Standard Model is shown with their characteristic properties such as spin, charge and mass (Figure is adapted from [53]). . . . .	21
Figure 2.11 The helicity for neutrinos and antineutrinos are shown. If $m_\nu = 0$ then the helicity and chirality corresponds to same meaning. . . . .	31
Figure 3.1 Symbolic illustration of two body scattering is shown in the rest frame of the target material. . . . .	36
Figure 3.2 The electroweak vertex factors are shown for the neutral and charged currents. Here $f$ corresponds to any lepton or quark and the values of $c_V$ and $c_A$ are shown in Table (3.1). . . . .	43
Figure 3.3 Feynman Diagram of $\nu_\mu - e^-$ scattering is depicted. Interaction takes place via neutral current exchange only. . . . .	43
Figure 3.4 The Feynman diagram of the $\bar{\nu}_\mu - e^-$ scattering. The interaction takes place via the exchange of $Z$ boson. . . . .	52
Figure 3.5 The $\nu_e - e^-$ scattering takes place via the charged current ( $W$ boson) as well as the neutral current ( $Z$ boson) exchange. . . . .	54
Figure 3.6 The $\bar{\nu}_e - e^-$ scattering takes place via the charged current as well as the neutral current. However, the interaction with $W$ boson takes place in the s-channel unlike the $\nu_e - e^-$ scattering. . . . .	57
Figure 3.7 Dependence of the maximum recoil energy of the electron with respect to the incoming neutrino energy is demonstrated. . . . .	64
Figure 3.8 The recoil energy spectra of the $\nu - e$ scattering for the incident neutrino energy $E_\nu = 10$ MeV is shown. . . . .	65

Figure 3.9	The neutrino electron scattering with respect to the incoming neutrino energy, $E_\nu$ is shown for two cases. In the first case, we neglected the threshold value, i.e. $T_{th} = 0$ , which is practically impossible (left side of the Figure). In the second case 3 MeV threshold value is used, which is generally the range for the reactor neutrino experiments (right side of the Figure).	66
Figure 3.10	The differential cross section for the neutrino electron scattering with respect to the scattering angle of the electron is shown for all neutrino flavors as well as anti-neutrinos.	70
Figure 4.1	The schematic view of the KSNPS is shown (Figure is adapted from [62]).	74
Figure 4.2	Two different detectors are placed in the shielded space (Figure is adapted from [62]).	75
Figure 4.3	The schematic view of the shielding design of the TEXONO collaboration (Figure is adapted from [62]).	75
Figure 4.4	Typical $\bar{\nu}_e$ spectrum for reactor neutrinos is shown (Figure is adapted from [62]).	76
Figure 4.5	The schematic view for the scintillating crystals are shown. The signals are recorded with PMTs at both ends (Figure is adapted from [62]).	77
Figure 4.6	Measured event rate with respect to the recoil energy is shown with the SM prediction is fitted (Figure is adapted from [62]).	78
Figure 4.7	The spectrum for a $\bar{\nu}_e = 10^{13} \text{ cm}^{-2} \text{ s}^{-1}$ is shown with SM and magnetic moments at $\mu_\nu = 10^{-10} \mu_B$ (Figure is adapted from [69]).	79
Figure 4.8	The schematic view of the experiment with its inner shieldings is shown for HPGe detector (Figure is adapted from [69]).	79
Figure 4.9	The residual spectrum is depicted with respect to recoil energy (Figure is adapted from [69]).	80

Figure 4.10 The schematic view of the experimental set-up for the NPCGe is shown with its shielding structure (Figure is adapted from [72]). . . . .	81
Figure 4.11 The Reactor ON-OFF data taken by NPCGe detector is shown with respect to recoil energy. The fitted region is for the analysis of $\bar{\nu}_e$ milicharge (Figure is adapted from [73]). . . . .	82
Figure 4.12 The schematic view of the GEMMA Experiment with its shielding structure is shown (Figure is adapted from [74]). . . . .	83
Figure 4.13 The spectra of Reactor ON and OFF as well as ON-OFF is shown with respect to the recoil energy of electron. The analysis threshold achieved is 2.8 keV (Figure is adapted from [74]). . . . .	84
Figure 4.14 The schematic view of the LSND detector is depicted (Figure is adapted from [80]). . . . .	84
Figure 4.15 The schematic view of the target area and detector enclosure (top) as well as the experimental area is shown (bottom) (Figure is adapted from [78]). . . . .	85
Figure 4.16 The shape of the flux for neutrinos in LSND experiment is shown. The flux values are normalized (Figure is adapted from [81]). . . . .	86
Figure 4.17 Schematic view of the neutrino beam of CHARM II experiment is shown. While in (a), general view is shown, in (b) neutrino cave area is shown schematically (Figure is adapted from [84]). . . . .	87
Figure 4.18 The schematic view of the CHARM II detector is depicted (Figure is adapted from [82]). . . . .	88
Figure 4.19 The schematic view of the Borexino detector is shown (Figure is adapted from [87]). . . . .	89
Figure 4.20 The schematic drawing of the Borexino detector is shown (Figure is adapted from [92]). . . . .	90



Figure 4.21 Observed neutrino spectrum with an analytic fit over the 290 – 1270 keV range is shown (Figure is adapted from [93]). . . . .	91
Figure 5.1 An example of noncommutativity of finite rotations is shown. . . . .	94
Figure 5.2 Coupling of neutral particles to photons is allowed in NCQED. . . . .	110
Figure 5.3 Feynman Diagram of $\nu - e^-$ scattering in non-commutative space is displayed. Even though neutrinos are neutral they can still interact with photons. . . . .	111
Figure 5.4 Feynman Diagram of $\bar{\nu} - e^-$ scattering in non-commutative space is displayed. Even though neutrinos are chargeless they can still interact with photons. . . . .	133
Figure 5.5 The differential cross-sections as a function of the recoil energy is depicted for (a) Top: TEXONO experiment with reactor $\bar{\nu}_e$ [62, 69, 68], (b) Middle: LSND experiment with $\nu_\mu$ from stopped-pion [81], and (c) Bottom: CHARM-II experiment with accelerator $\nu_\mu(\bar{\nu}_\mu)$ [114, 85]. Both SM and NC contributions are displayed. (Figure is adapted from [115].) . . . . .	137
Figure 5.6 Data sets of TEXONO adapted for the noncommutative analysis. SM+NC effects are fitted to data. . . . .	138
Figure 5.7 Weinberg angle measurements are shown with respect to energy. For more details See [13]. . . . .	141
Figure 6.1 Interactions of neutrinos with electron via $t$ channel dark photon ( $A'$ ) exchange in panel (a). The panels (b) and (c) are for the kinetic mixing between photon-dark photon and Z boson-dark photon, respectively. (Figure is adapted from [170].) . . . . .	152
Figure 6.2 The dark photon couples to charged leptons and neutrinos in a different way. The relevant vertex factors are depicted. . . . .	153

Figure 6.3	The Neutrino electron scattering can also take place via the dark photon exchange in the $U(1)_{B-L}$ model as well as $W$ and $Z$ boson exchanges. The interaction is independent of the neutrino flavors. . . . .	153
Figure 6.4	The anti-neutrino electron scattering diagram via dark photon exchange. . . . .	158
Figure 6.5	The $\nu-e^-$ scattering takes place via the exchange of $W$ and $Z$ boson as well as the dark photon contribution. To calculate the interference term, all these diagrams must be considered. On the other hand for the $\nu_\mu - e^-$ scattering one just needs to consider the diagram shown in panel (a) and (b) since $W$ exchange is not allowed. . . . .	160
Figure 6.6	The differential cross-section spectrum is shown for various $M_{A'}$ at a fixed arbitrarily chosen $g_{B-L}$ over the recoil energy for the TEXONO experiment. For this plot, the neutrino flux is normalized to 1. (Figure is adapted from [170].) . . . . .	163
Figure 6.7	TEXONO-CsI and TEXONO-HPGe data is fitted for a fixed value of $m_{A'} = 1$ keV and bounds are set for $g_{B-L}$ . This procedure is conducted over the $A'$ mass-range, keV to 10 GeV, so that the bounds are obtained in $m_{A'} - g_{B-L}$ plane. . . . .	164
Figure 6.8	Bounds acquired from Borexino data for the DP parameters are shown in the $m_{A'} - g_{B-L}$ plane by taking into account and neglecting the interference terms. The bounds from [173] is also shown for comparison. . . . .	165
Figure 6.9	The 90% CL exclusion limits in the $g_{B-L} - M_{A'}$ plane for various TEXONO experiments (left) and for the LSND and CHARM II experiments (right) are depicted. The results with and without the interference contributions are shown for highlighting its significance. (Figure is adapted from [170].) . . . . .	166

Figure 6.10 The 90% C.L. exclusion limits of the gauge coupling constant $g_{B-L}$ of the $U(1)_{B-L}$ group as a function of the dark photon mass $M_{A'}$ by including the interference effects. The regions above the curves are excluded. (Figure is adapted from [170].)	168
Figure 6.11 Direct dark photon production mechanism via the electron-positron annihilation channel is shown.	170
Figure 6.12 Feynman diagram of the dark photon production from $\pi^0$ decay is shown.	171
Figure 6.13 Dark photons can be produced similar to the Bremsstrahlung process called as $A'$ -strahlung.	171
Figure 6.14 The partial width for the dark photons decaying into the SM particles in the kinetic mixing model by considering the Equations (6.58) and (6.59) are shown. (Figure is adapted from [155].)	174
Figure 6.15 A schematic view of the electron beam-dump experiment is shown. $L_{sh}$ and $L_{dec}$ show the length of the shielding material and the length of the decay tube respectively. When the electron with energy $E_0$ hits on the target, the dark photon with energy $E_{\gamma'}$ is expected to be produced via the bremsstrahlung like process. The produced dark photons pass through the shielding without interacting and decay into the lepton pairs via mixing with the photon. (Figure is adapted from [182].)	175
Figure 6.16 The bounds acquired from the electron beam dump experiments is shown in $m_{\gamma'} (m_{A'})$ (mass of the dark photon) and $\chi (\epsilon)$ (kinetic mixing parameter) plane. The depicted regions are excluded. (Figure is adapted from [182]).	177
Figure 6.17 The bounds obtained from different proton beam dump experiments are shown for the kinetic-mixing model. (Figure is adapted from [181].)	178

Figure 6.18 The schematic view of the APEX experiment. Electrons are im-  
pinged on a Tungsten target. Two septum magnets with opposite polar-  
ity are used to deflect the charged particles to large angles through the  
high resolution (HPS) spectrometers where the energy and momentum of  
the particles are accurately measured. Invariant mass distribution of the  
electron-positron pair is measured via this mechanism. (Figure is adapted  
from [195].) . . . . . 179

Figure 6.19 The bounds for the dark photon parameters are shown for the fixed  
target experiments as well as the flavor factories and colliders. (The figure  
is adapted from [200].) . . . . . 180

Figure 6.20 Exclusion limits obtained for the DP parameters from flavor facto-  
ries are shown. (Figure is adapted from [208]. . . . . 182

Figure 6.21 The schematic view of the detection mechanism of the dark photons  
via the LSW experiment is shown. If the incoming photon oscillates into  
the dark photon, then due to feebly interaction of dark photons they are  
expected to pass through the wall and oscillate back to photons which are  
tried to be detected. . . . . 183

Figure 6.22 The bounds acquired from the LSW experiments are shown with a  
comparison from the bounds solar, cast and atomic force experiments. For  
more information see [212] where the figure is adapted from. . . . . 184

Figure 6.23 The combined limits obtained from the neutrino-electron scattering  
(this work) is overlaid on the bounds from different laboratory experiments  
as well as cosmological and astrophysical sources at 90% C.L. (Figure is  
adapted from [170].) . . . . . 186

Figure B.1 The neutrino electron scattering is illustrated schematically in the  
rest frame of the initial electron. . . . . 236

Figure D.1 Feynman Diagram of $\nu_\mu - e^-$ scattering takes place with $Z$ boson exchange as well as the photon exchange which takes place only in non-commutative space. Interference term between two diagrams must be calculated. . . . .	244
Figure E.1 Contents of the func.mdl file is presented for the DP model. . . . .	257
Figure E.2 Contents of the prtcls.mdl file is shown for the DP model. . . . .	258
Figure E.3 Contents of the vars.mdl file is shown for the DP model. . . . .	258
Figure E.4 Contents of the lgrng.mdl file is shown for the DP model. . . . .	259
Figure E.5 Contents of the “sum_22_low_weak.m” file is shown. . . . .	260

## LIST OF ABBREVIATIONS

AGN	Active Galactic Nuclei
ALPs	Axion Like Particles
AS	Anti-symmetric
BOREXINO	Boron Experiment
BSM	Beyond the Standard Model
CC	Charged Current
CHARM	Cern-Hamburg-Rome-Moscow Collaboration
C.L.	Confidence Level
CMB	Cosmic Microwave Background
CNB	Cosmic Neutrino Background
CNO	Carbon-Nitrogen-Oxygen
DONUT	Direct Observation of NU Tau
DP	Dark Photon
GEMMA	Germanium Experiment for measurement of Magnetic Moment Antineutrino
hep	$^3\text{He} + \text{p}$ fusion reaction in the sun
HPGe	High Purity Germanium
IMB	Irvine-Michigan-Brookhaven (Detector)
IR	Infrared
Kamiokande	Kamioka Neutrino Detection Experiment
KNPP	Kalinin Nuclear Power Plant
KSNPS	Kuo-Sheng Nuclear Power Station
LAMPF	Los Alamos Physics Facility
LMA	Large Mixing Angle
LSND	Liquid Scintillator Neutrino Detector
MSW	Mikheyev-Smirnov-Wolfenstein
m.w.e	meter water equivalent
NC	Neutral Current
NCQED	Non-commutative QED

NPCGe	n-type Point Contact Germanium
QCD	Quantum Chromodynamics
QED	Quantum Electrodynamics
pep	Proton-Electron-Proton
PMT	Photo Multiplier Tube
pp	Proton-Proton
S	Symmetric
SM	Standard Model
SPS	Super Proton Synchotron
SSM	Standard Solar Model
TEXONO	Taiwan Experiment On Neutrino
UV	Ultraviolet
V-A	Vector minus Axial Vector
WISPs	Weakly Interacting sub-eV Particles





# CHAPTER 1

## INTRODUCTION

Classical physics which is a concentration of Newtonian mechanics and electromagnetism had been considered as an ultimate theory in a century ago. From the orbits of the planets to the interaction of charged particles were successfully explained by the model and the measurements at that time were in total agreement with the predictions. The inadequacy of classical physics was understood when the experiments in atomic scale achieved to be conducted in addition to strange properties of light being discovered. Spectrum of black-body radiation, photoelectric effect as well as hydrogen energy levels were some of the unexplained phenomena by classical physics. With the foundation of quantum mechanics, anomalies that classical physics could not resolve had been explained clearly and it is understood that classical physics can be considered as an effective theory which functions best for long distances and low velocity regions and a more fundamental theory as quantum mechanics exists.

In the classical physics era the only known forces were the electromagnetism and gravity. On the other hand, with the discovery of nucleus and its constituents nucleons (protons and neutrons) the atomic model had been started to be formulated. Moreover, with the enhancements in technology, experiments achieved to find more elementary particles like quarks which constitute the nucleon as well as some new *electron like* elementary particles. The interactions of newly discovered particles are explained with the introduction of new forces as the strong and the weak forces. Yukawa and Fermi's models to explain the strong and weak interactions in 1935 can be considered as the beginning of the modern particle physics era.

With the developments in the accelerator technology, from 1937 (discovery of the

muon) to 2000 (discovery of the tau neutrino) elementary particles that form the matter and comprises the particle content of the Standard Model (SM) had been discovered. The interactions of these elementary particles among each other are well explained by the electromagnetic, weak and strong interactions which are unified under the standard model.

SM predictions have been tested in the collider experiments as well as the data collected from cosmology and astrophysical experiments which can also be considered as “natural” accelerator and is found extremely successful. Moreover, when we contemplate the developments in the history of the SM, we find out that, SM had predicted the existence of new particles such as  $Z$ -boson and  $\tau$  lepton before their discoveries for the model to be consistent. The discovery of these particles is also a big success story of the model. Furthermore, the missing piece of the model, the Higgs boson, which is responsible for the fermions and gauge particles being massive through the spontaneous symmetry breaking, has been discovered in 2012 by the CMS and ATLAS collaborations at LHC. With this latest discovery as well as the compatibility with the experimental results conducted so far, the standard model can be considered as an ultimate theory at least at a scale of  $1/1000th$  of a nucleus which is the current experimental reach by the experiments.

Even though the SM is very successful in explaining the experiments conducting at a TeV scale, it is nevertheless still reasonable to consider SM as an effective theory of some other new physics theory as an analogy with classical physics being an effective theory of quantum physics.

Moreover, SM is not considered as an ultimate theory since the model contains so many arbitrary parameters and needs fine tuning. Hence, the naturalness and hierarchy issues remain unsolved in the SM even it has a high success rate in the predictions of the experimental results up to high accuracy. On the other hand, it is also thought among some scientists that the issues like naturalness and hierarchy are not real physics problems but instead problems due to aesthetic criterion. Even this belief empowers the SM, on the questions of the description of dark matter, dark energy as well as the neutrino mass mechanism, the model can not give clear predictions and this comprises the most weak points of the model. Furthermore, the neutrino oscillation

mechanism does not fit into the SM, however, the phenomenon still can be integrated to the theory with a small modifications.

The standard model has been under threat by the advanced developments in the detector technologies due to the huge increment in the collision energies as well as the sensitivity measurements. With the data acquired by telescope experiments like Fermi, Atic, AMS as well as cold dark matter search experiments COGENT, DAMA it was announced that they observed more events (excess events) than the SM predictions. In addition to this discrepancy, on the other hand, with the enhancements in the detection sensitivities, muon magnetic moment anomaly became apparent. There is a  $3.6\sigma$  discrepancy between the SM prediction and the measured value. These kinds of anomalies that the SM lacks to explain are the main motivations for the new physics searches.

The general expectation of finding beyond the standard model (BSM) signals is towards to discovering a new massive particle at collider experiments. The reason behind this lies in the history due to the discovery of massive particles chronologically with the increasing energy of colliders. On the other hand, LHC which is having collisions at 13 TeV in the center-of-mass frame in 2016 has not discovered a “new particle” yet. This gives a new direction to the research program towards the so-called “hidden valley” in which it is considered that, new particles that feebly interacts with SM sector exist. If such a sector existed, those new particles and interactions would give a description where the SM fails to illustrate. However, it is better to search these new particles at low energy and high precision experiments especially if the mass of these particles are smaller than 10 GeV. At this energy scale, however, the background is very large for the detection of these weakly interacting particles at LHC.

In addition to the motivations mentioned for beyond the standard model searches, since any new physics models are also compatible with the SM predictions, there is no reason to ignore them and as a quest for the underlying rules that govern the nature, new physics searches must be contemplated carefully and should be searched in various channels to test the new theory. However, this kind of search strategy requires somewhat advanced detector technology, since the new signals are generally expected to be very small.

One of the common problems in new physics scenarios is that they contain many free parameters. Hence, it becomes almost impossible to claim that these new theories verified to be inconsistent. Instead, what can be done is to exclude the parameter region by comparing the data with the BSM prediction. In this sense, new physics scenarios may seem as never ending stories. However, every new physics models are proposed at least to explain an anomaly and this is generally satisfied only for the specific regions of the free parameters of the model. Hence, ruling out the favored region is crucial for the BSM phenomenology. For this reason the studies should be investigated in a wide range of areas in addition to testing the new physics in various channels. Even if it is not possible to claim that proposed new physics model is wrong due to number of free parameters that model contains, once the favored parameter region is excluded then the motivation is lost. On the other hand, if the new theory does not point any signal that can be searched but claims that it explains every anomaly, in that case one just needs to obey without questioning.

Searching for the Non-commutative space effects comprises one of the example of BSM studies. The ideas that the spacetime may not be commutative at very small scales has been around as a possibility, providing a remedy to infinities popping up in field theory calculations and it has other motivations from string theory as well. Indeed, once the Quantum Electrodynamics (QED) is extended in non-commutative spacetime, the coupling of neutral particles to photons is allowed at tree level. This new vertex contributes to the cross section through which new bounds for the non-commutative energy scale  $\Lambda_{NC}$  are set.

Nowadays most of the effort has gone to search physics beyond the Standard Model in the so-called energy frontiers while there are some smoking guns that *new physics* might lie way below the electroweak scale to which the energy frontiers are insensitive, motivating searches alternatively in the intensity frontiers. If new particles interacted very weakly with the SM sector, then we would not have discovered such particles at high energy colliders. Existence of such “hidden sector” particles can propose solutions to problems that SM lacks to answer like dark matter and anomalous magnetic moment of muon. If the hidden sector is gauged under a group  $U(1)_{B-L}$ , the gauge field  $A'$ , named dark photon, will couple any standard model particle with a nonzero  $B - L$  number. This opens up a direct tree level neutrino interaction vertex

with  $A'$ . Hence, these new interactions apart from the SM predictions can be searched for the sake of BSM studies.

Neutrino interactions taking place rather at low energies are well understood within the electroweak theory. Hence, as an alternative to high-energy collider experiments, neutrino experiments could be used as a probe to test the Standard Model as well as to look for any mimics from low lying *new physics*. Moreover, neutrino interactions are purely leptonic processes with robust standard model predictions, creating ideal testing ground for *new physics*.

In this thesis, neutrino electron scattering experiments are used to constrain new physics models; dark photons and non-commutative (NC) space and bounds are acquired for the free parameters of the model.

## 1.1 Outline of the Thesis

This thesis is organized as follow;

- **CHAPTER 2:** In this chapter, the neutrino properties in the Standard Model with a brief history are explained. Along with them, a brief information about the SM is given as well as the electroweak interaction of neutrinos explained.
- **CHAPTER 3:** Differential cross-section of all type of neutrinos and anti-neutrinos are calculated in the electroweak theory in this chapter. The cross-section is also expressed with respect to the recoil energy of the electron so that the SM prediction is tested via neutrino experiments. Moreover, the case for high energetic neutrinos as well as the relation between the incoming energy of the neutrino and the recoil energy is analyzed in detail.
- **CHAPTER 4:** The main goal of this chapter is to give a brief summary for the neutrino experiments whose data were used to constrain the new physics scenarios. The set-up configurations of the experiments and the data published are summarized along with the key parameters of the experiments.
- **CHAPTER 5:** In this part of the thesis, the effects of neutrino-electron scattering in the noncommutative-space are searched. After explaining the motivations

for the NC-space, QED is constructed in the NC-space using the Weyl-Moyal product as well as the Seiberg-Witten Map. Then, the cross-section is calculated for the  $\nu - e^-$  scattering in the NC-space and by analyzing the data of TEXONO, LSND and CHARM II, the chapter is ended with the bounds acquired for the NC scale  $\Lambda_{NC}$  at 95% C.L.

- **CHAPTER 6:** Motivations for the Hidden sector are explained by mentioning the anomalies that the SM lacks of addressing. Focusing on the so-called vector portal, the consequences of the additional  $U(1)_{B-L}$  symmetry are discussed. Having showed that the  $\nu - e^-$  scattering is possible via the dark photon exchange, the differential cross-section with the interference term between the SM diagrams is calculated. The data sets from TEXONO, LSND, CHARM II, GEMMA and BOREXINO data is analyzed and the bounds are obtained in the  $g_{B-L}$  and  $m_{A'}$  plane. And this chapter is finalized wby comparing our bounds with the ones in the literature.
- **CHAPTER 7:** The conclusions that we derived from this thesis study and future prospects are presented in this chapter.

## CHAPTER 2

### NEUTRINOS IN THE STANDARD MODEL

#### 2.1 A Brief History of Neutrinos

In 1920s, one of the unexplained phenomena was the continuous energy spectrum of electrons emitted by a radioactive nuclei. In a two body decay, (assuming a mother nucleus decaying into a daughter one and an electron), once we calculate the energy of the emitted electrons using conservation of energy and momentum, we find the energy of the emitted electron in the lab frame as;

$$\begin{aligned}p_A &= p_B + p_C \\p_B &= p_A - p_C \\p_B^2 &= p_A^2 + p_C^2 - 2p_A \cdot p_C \\m_B^2 &= m_A^2 + m_C^2 - 2(E_A E_C - \vec{p}_A \cdot \vec{p}_C) \\m_B^2 &= m_A^2 + m_C^2 - 2m_A E_C\end{aligned}\tag{2.1}$$

in which particles  $A$  &  $B$  represent mother and daughter nuclei, respectively, and particle  $C$  corresponds to the emitted electron.<sup>1</sup> Hence, we can write for the electron energy;

$$E_C = \frac{m_A^2 + m_C^2 - m_B^2}{2m_A}\tag{2.2}$$

Since the mass of the particles are constant, it is expected that emitted electrons have fixed energy, however, observed spectrum was continuous (see Figure (2.1)). This was one of the unexplained phenomena at those times. To explain this mystery at that time, Bohr was even ready to abandon the idea of conservation of energy. As a desperate

---

<sup>1</sup> Throughout this thesis, natural units are used;  $\hbar = 1$ ,  $c = 1$ . If there is not a vector sign on top of the momentum symbols, then it represents 4-vectors, 3 vectors are denoted with a vector sign on top of the symbols.

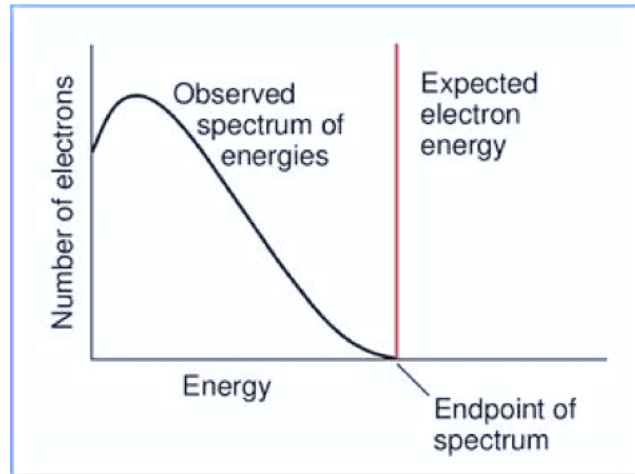


Figure 2.1: Expected energy distribution of the emitted electron for the two body decay is a sharp peak (red curve). However, the observed spectrum was continuous for the  $\beta$  decay (black curve) (Figure is adapted from [1]).

remedy, he proposed that, bound electrons may have interacted different than the free ones, in a way that conservation of energy and momentum are violated. This idea had appeared even in the textbooks in 1930s as; “This would mean that that the idea of energy and its conservation fails in dealing with processes involving the emission or capture of nuclear electrons. This does not sound improbable if we remember all that has been said about peculiar properties of electrons inside the nucleus” [2]. It is important to note that, in 1920s nuclear physics, the common belief was the nuclei being composed of electrons and protons and neutron had not been discovered yet. A nuclei ( ${}^AZ$ ) believed to contain  $A$  protons and  $A - Z$  electrons such that the charge of the nuclei is  $Z$ . For instance  ${}^4He$  was believed to contain 4 protons and 2 electrons leading to the charge of the nucleus  $+2$ .

Another remedy to explain the continuous energy spectrum of electrons was suggested by Pauli in 1930, with a letter to a workshop in Tübingen, Germany, where the radioactivity was discussed by the leading scientists of the era [3]. He proposed a new particle emitted in the  $\beta$  decay. This particle should have been neutral, spin  $1/2$ , massive at the order of electron’s mass at most and very weakly interacted with matter. He called the particle as “neutron”. Thus, if this new particle was also emitted with the electron, then sum of the energies of the “neutron” and electron would be constant and this would explain the continuous spectrum of the electron.



In 1932, Chadwick, while studying the neutral radiation of the decay in the process,  ${}^9\text{Be} + \alpha \rightarrow {}^{12}\text{C} + n$ , discovered a neutral particle which is slightly heavier than the proton. This particle was highly penetrating but different from the  $\gamma$  rays and named as “neutron” although it was not the particle that Pauli proposed.

In 1934, Fermi renamed the Pauli’s particle as “neutrino” which is expected to be much more lighter than the neutron. Moreover, he formulated four-fermion interaction for the decay process  $n \rightarrow p + e^- + \bar{\nu}_e$  in 1934 (see Figure (2.2)). He wrote the amplitude for the interaction as;

$$\mathcal{M} = \frac{G_F}{\sqrt{2}}(\bar{p}\Gamma n)(\bar{e}\Gamma'\nu) + H.c. \quad (2.3)$$

where  $G_F$  is the dimensionful Fermi coupling constant that gives information about the strength of the interaction and  $\Gamma$  ( $\Gamma'$ ) are the linear combinations of bilinear co-variants,  $\{\mathbb{1}, \gamma^5, \gamma^\mu, \gamma^\mu\gamma^5, \sigma^{\mu\nu}\}$ . To know the exact form of the interaction, precise measurements were needed for the  $\beta$  decay. This formulation also enabled to calculate cross-sections of other processes such as  $\bar{\nu}_e + p \rightarrow e^+ + n$ , which is the neutrino detection process that I am going to mention.

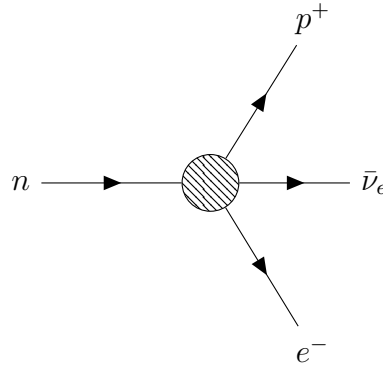


Figure 2.2: Four-point interaction model of Enrico Fermi to describe  $\beta$  decay.

New particles had continued to be discovered in cosmic-ray experiments in 1930s. A new particle that we know now is the muon was discovered in 1936 even though it was believed at first that it was the particle that Yukawa predicted. On the other hand,  $\pi$  mesons, which are the predicted particles of Yukawa, were discovered in 1947.

With the discovery of new particles, new puzzles arose. In 1924, Laporte had showed that parity is conserved in electromagnetic interactions [4] and in 1927, Wigner identified that this conservation rule is a consequence of the reflection symmetry of the

electromagnetic force. Moreover, there was not any reason to think that laws of nature are not parity invariant, at least until 1950s, the so-called  $\theta - \tau$  puzzle.

The idea of parity conservation seemed so natural that this rule is even used for the derivation of particle quantum numbers. In 1954, two particles, named as  $\theta$  and  $\tau$  had been identified with the same mass, charge, spin and lifetime but with different decay modes as following;

$$\begin{aligned}\tau^+ &\rightarrow \pi^+\pi^+\pi^- \\ \theta^+ &\rightarrow \pi^+\pi^0.\end{aligned}\tag{2.4}$$

Depending on how particles behave under mirror reflection, intrinsic parities are assigned to particles as 1 and  $-1$ . The intrinsic parity of the  $\pi$  mesons are determined experimentally as  $P(\pi) = -1$ . Hence the parity of the  $\theta^+$  can be determined as;

$$\begin{aligned}P(\theta^+) &= \underbrace{P(\pi^+)}_{-1} \underbrace{P(\pi^+)}_{-1} \underbrace{P(\pi^0)}_{-1} (-1)^l \\ &= +1\end{aligned}\tag{2.5}$$

where the orbital angular momentum,  $l$ , of two pions is zero due to the conservation of total angular momentum. Also note that, the spins of all the particles above are zero. On the other hand for the  $\tau^+$  we have;

$$\begin{aligned}P(\tau^+) &= \underbrace{P(\pi^+)}_{-1} \underbrace{P(\pi^+)}_{-1} \underbrace{P(\pi^-)}_{-1} P_{spatial} \\ &= -P_{spatial}.\end{aligned}\tag{2.6}$$

In order to decide the orbital angular momentum, let us divide the situation into two parts. First let us think about the angular momentum between two  $\pi^+$  mesons and then consider the angular momentum between the center of mass of these particles and the remaining particle  $\pi^-$ . To conserve angular momentum, we find that this sum of the angular momentum must be 0, thus the angular momentum must be same in magnitude. Hence, we deduce that;

$$P_{spatial} = (-1)^l (-1)^l = 1.\tag{2.7}$$

From this result we find that parity of the  $\tau^+$  is equal to  $-1$ . The puzzling situation is that, the two particles ( $\theta$  and  $\tau$ ) with the same properties (mass, spin, decay time etc.), decay in different channels. The only difference is the parity of those particles and this was a mystery.

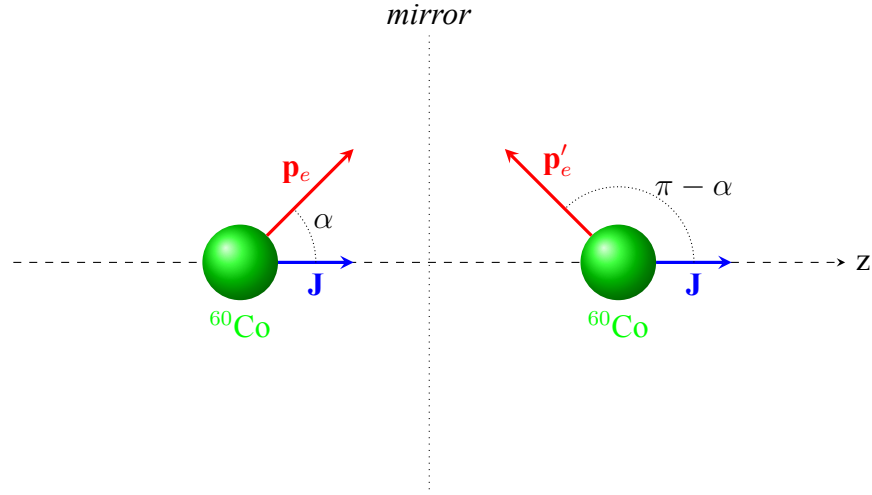
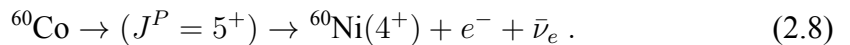


Figure 2.3: The schematic view of the idea of Wu experiment. Number of electrons emitted by  $\alpha$  and  $\pi - \alpha$  degrees expected to be equal if the parity is conserved (Figure is adapted from [5]).

In 1956, Lee and Yang questioned the idea that what if parity is violated in weak interaction and  $\theta$  and  $\tau$  are the actually the same particle. To test the idea, first, they reanalyzed experimental data to see the effect of parity violation. In strong interaction, there was solid evidence that parity is conserved, however there was no evidence of parity conservation in  $\beta$  decay startlingly [6]. The idea that nature should not behave in a different way for left and right was so strong that parity conservation was believed without experimental evidence. Lee and Yang proposed experiments to test the parity violation in weak interactions.

The proposed interaction was the beta decay of the cobalt;



The quantity expected to be measured is the momentum of the electron projection on to total spin  $J$  of the cobalt. Note that, momentum changes sign under parity but total angular momentum does not. If the parity is conserved, then the number of electrons emitted by any angle  $\alpha$  and  $\pi - \alpha$  degrees should be same, otherwise parity is violated in  $\beta$  decay (see Figure (2.3)).

The experiment was so difficult to conduct with the technology in those years. One of the challenges was the necessity of setting the temperature around  $10^{-3}K$  in order to align the spin of cobalt. Chien-Shiung Wu and her colleagues achieved to conduct

the experiment and found out startling result that number of electrons emitted at an angle  $\alpha = \pi$  was much more than the ones emitted at an angle  $\alpha = 0$  [7]. With this experiment, it was verified that parity is violated in  $\beta$  decay which also meant that reflection symmetry does not hold in nature.

In addition to Wu's experiment, Lederman and his collaborators also set-up an experiment to check parity violation in weak decays to test the Lee and Yang's proposal. They analyzed the decay chain of the pion,



and looked for the asymmetry in the polarization of the muon along the direction of motion. By observing the angular distribution of electrons from the muon decay, it would be possible to determine the muon polarization [8]. The results also verified that parity is violated in weak interactions. Observation of parity violation enlightens the  $\theta - \tau$  puzzle and it is realized that those particles are actually same particle that we denote as  $K$  meson today.

After it was understood that experimental results were satisfactory enough, theory of the weak interactions that leads to parity violation was settled with the developments by Feynman, Gellmann, Marshak and Sudarshan. They found out that the weak interaction is in the form of  $V - A$  (vector - axial vector) so that purely left handed states are favored and parity is violated in weak interactions.

While forming the weak interaction theory was in progress, there were still doubts about the existence of neutrinos. Pauli even said after proposing the existence of neutrino that; "I have done a terrible thing, I have postulated a particle that cannot be detected" [9]. Existence of a particle with the properties of interacting very weakly with matter, being very light and neutral made the neutrinos to be considered very hard to be detected.

Using the Fermi theory for the weak interaction, it was possible to estimate the interaction rate of the neutrino with the nucleus and feasibility study for the detector size could be performed, however it seemed improbable. In the early 1950s, Reines and Cowan started the "Project Poltergeist", to make the dream real [10].

To be able to benefit from nuclear reactors being intense source for  $\beta$  decays (with luminosity  $\sim 10^{13} \text{ s}^{-1} \text{ cm}^{-2}$ ), an experiment was set-up near the Savannah-River reactor site with a target of 200 liters of water in which 40 kg  $\text{CdCl}_2$  was solved in it. The hypothesis was to observe the inverse beta decay,

$$\nu + p \rightarrow n + e^+ .$$

The outgoing positron is expected to interact in a short time with the electrons in the material and due to pair production, two photon with 0.5 MeV energy is expected to be emitted back to back ( $e^- + e^+ \rightarrow \gamma\gamma$ ). In addition to this, emitted neutron is interacted with the cadmium, which is a good neutron absorber. When neutron was absorbed by cadmium, following reaction would take place,



When cadmium absorbs a neutron it becomes excited and turns to its original state by emitting a photon after  $5 \mu\text{s}$  (see Figure (2.4)). Hence, two photon signals from the pair production following with a single photon signal from the excited cadmium after  $5 \mu\text{s}$  would mean that neutrinos exist. In 1956, Reines and Cowan declared that they observed neutrino [11, 12].

Another project to detect the neutrinos in the same years was led by Ray Davis, who tried to observe neutrino in the inverse chlorine decay,



However, this interaction could not be observed, which is inferred as neutrinos and anti-neutrinos are different particles. Once we assign lepton numbers for leptons as  $L = 1$  and for anti-leptons  $L = -1$ , and dictate that lepton number must be conserved in the interactions, then it becomes obvious why neutrino could not be detected in the inverse chlorine decay, since  $\Delta L = 2$ .

This lepton number conservation also explains why two neutrinos should be emitted in  $\mu$  decay ( $\mu^- \rightarrow e^- + 2\nu$ ). The puzzling situation was that although muons were expected to decay into electrons, no interactions like  $\mu^- \rightarrow e^- + \gamma$  had been observed [13]. This brings the question whether types of neutrinos emitted in the  $\mu$  decay

are same or not? A new conservation law (muon lepton number and electron lepton number conservation separately) would ban the decay of muon to electron. Discovery of muon neutrino in 1962 by Lederman-Schwartz-Steinberger also showed that this additional conservation law actually holds [14] and it is understood that the decaying of the muon into electron actually takes place as  $\mu^- \rightarrow e^- + \bar{\nu}_e + \nu_\mu$ .

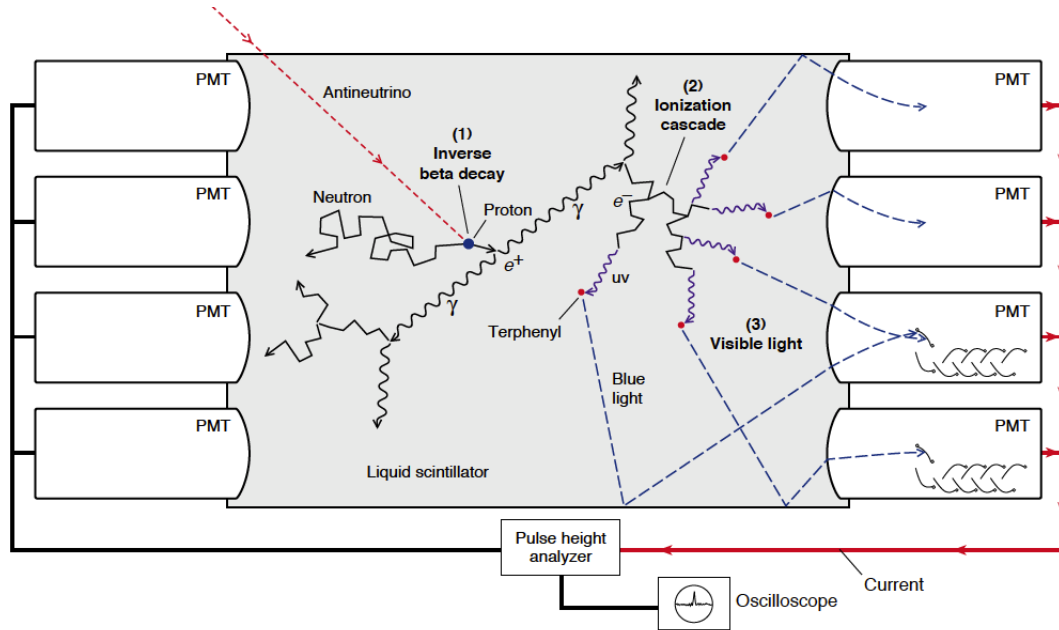


Figure 2.4: Schematic view of the detection process for the Reines-Cowan experiment (Figure is adapted from [15]).

To test the idea, Lederman and his colleagues set up a beam-dump experiment so that neutrinos were produced from the pion decay, hence muon neutrinos ( $\nu_\mu$ ) were emitted and the following interactions were aimed to be observed:

$$\begin{aligned} \nu_\mu + X &\rightarrow \mu + Y \\ \nu_\mu + X &\rightarrow e + Y \end{aligned} \quad (2.12)$$

where  $X$  and  $Y$  were the initial and final states. The first interaction was observed but not the second one and this verified the conservation of lepton flavor.

During the years 1974–1977, the group led by Martin Lewis Perl discovered a lepton called tau-lepton ( $\tau$ ) whose mass is 1.78 GeV [16]. After the discovery of  $\tau$ , the search for its neutrino partner had also started. There were indirect signals of the existence of this new type of neutrino from the decay width of the  $Z$  boson.  $Z$  boson can decay into lepton pairs ( $Z \rightarrow l^+l^-$ ), quark pairs ( $Z \rightarrow q\bar{q}$ ) and neutrino pairs ( $Z \rightarrow \nu_\alpha + \bar{\nu}_\alpha$ )

where  $\alpha$  corresponds to the type of neutrino, which was two since  $\nu_e$  and  $\nu_\mu$  neutrinos had been the only discovered ones yet. The measurement of full decay rate of the  $Z$  boson at CERN [17] implied that there were three flavors of neutrinos as shown in Figure (2.5).

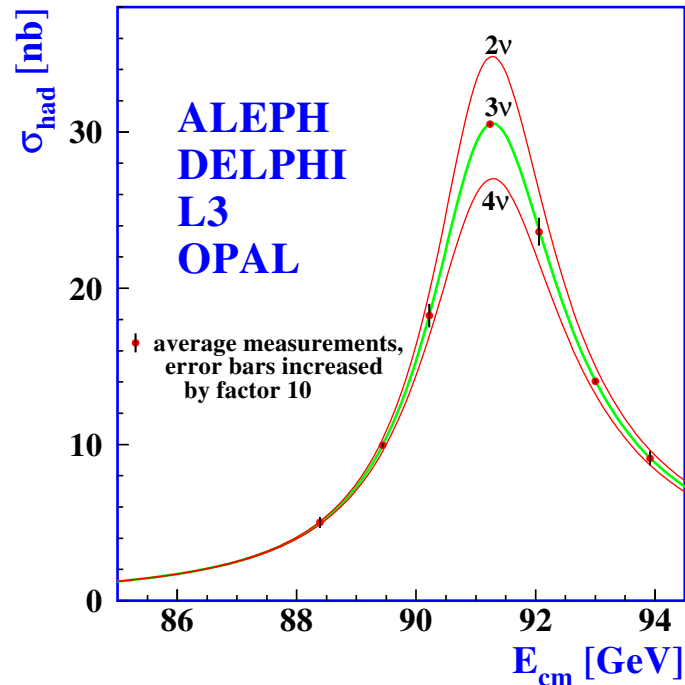


Figure 2.5: Decay rate of  $Z$  boson implies the existence of three neutrino flavors (Figure is adapted from [18]).

The expected  $\tau$  neutrino was discovered by DONUT (“Direct Observation of NU Tau”) experiment in 2000 [19].

The idea of neutrino emerged as a desperate remedy to save the law of conservation of energy and momentum and there were already three flavors of neutrinos as the Standard Model predicted.

After giving a brief history <sup>2</sup> about such an elusive particle, in the next section, we will give information about the sources of neutrinos.

---

<sup>2</sup> For good reviews about history of neutrinos, see [1, 20, 21, 22, 23].

## 2.2 Neutrino Sources

In general, sources of neutrinos can be classified as natural and artificial ones. Moreover, natural and artificial sources can also be divided into more sub-groups with respect to their origin as;

### **Class I: The Natural Sources:**

- **Solar Neutrinos:** Every star, hence the sun, is a very powerful source of neutrinos due to thermonuclear reactions occurring in the core. Since neutrinos interact very weakly with matter, almost all the neutrinos produced in the core of the sun reach the Earth with a large flux (about  $\sim 6 \times 10^{10} \text{ cm}^{-2} \text{ s}^{-1}$ ) according to the Standard Solar Model (SSM) prediction. Since the mean free path of photons in the sun is  $\sim 10^{-12}$  of the radius of the sun [24], it takes around  $10^{13}$  seconds for photons to reach the surface of the sun. On the other hand, since neutrinos interact very weakly, it takes only  $\sim 2.3$  s for neutrinos to reach the surface of the sun. Hence, this peculiar property of the neutrinos make them as best candidate to test the solar model hypothesis. In this sense, apart from particle physics, neutrinos play crucial role in astrophysics also.

According to the SSM, the sun produces its energy via pp (proton-proton) and CNO (Carbon-Nitrogen-Oxygen) cycles. The decay probabilities of pp and CNO cycles are 98.5% and 1.5%, respectively, hence, pp dominates over CNO cycle. Neutrinos produced in these fusion reactions are electron-type neutrinos (see Figure (2.6)).

Detecting neutrinos such an elusive particles is so difficult. Detectors must be built in underground (in general abandoned mines are used for this purpose) to be shielded by rock from cosmic rays. Solar neutrinos were first detected in 1968 by R. Davis in the Homestake experiment [25] which operated till 1994. After that, several experiments with different detection techniques measured the solar neutrino flux. However, the measured  $\nu_e$  flux was not compatible with the SSM prediction as shown in Figure (2.7). On the other hand, the measured total neutrino flux ( $\nu_e + \nu_\mu + \nu_\tau$ ) fit into the SSM prediction. The anomaly of the deficit of the  $\nu_e$  neutrinos was explained by the oscillation of neutrinos



$(\nu_e \rightarrow \nu_\mu)$  (for more information see [26, 27, 28]).

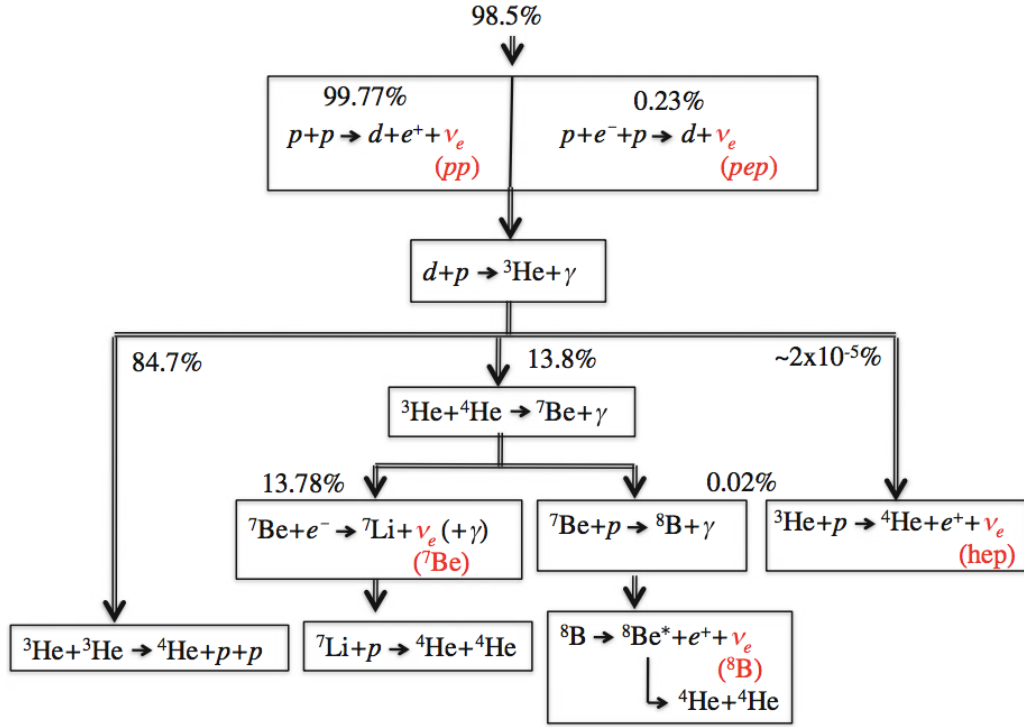


Figure 2.6: The chain reactions in the fusion process for the pp cycle is shown according to the SSM. Neutrinos produced in the pp, pep,  ${}^7\text{Be}$ , hep and  ${}^8\text{B}$  cycles are electron neutrinos ( $\nu_e$ ). 1.5% of the fusion process occurs via CNO cycle which is not depicted here (Figure is adapted from [26]).

The energy range of the solar neutrinos is in between keV and MeV depending on the channels that neutrinos are produced as shown in Figure (2.8).

- **Atmospheric Neutrinos:** The energy range of the atmospheric neutrinos is very broad from MeV to TeV scale. However, as the energy of the atmospheric neutrinos increase then the flux decreases as shown in Figure (2.9). When the cosmic rays interact with the nuclei in the atmosphere, hadrons mostly pions are produced. From the decay of the mesons, neutrinos are emitted and these neutrinos are named as atmospheric neutrinos which have been first detected in 1965 [29, 30]. The expected neutrino emission channels were due to the decay of pions and muons as;

$$\begin{aligned} \pi^- &\rightarrow \mu^- + \bar{\nu}_\mu, \\ \mu^- &\rightarrow e^- + \bar{\nu}_e + \nu_\mu. \end{aligned} \tag{2.13}$$

Hence, the expected ratio of the muon neutrinos to electron neutrinos was  $\frac{N_{\nu_\mu}}{N_{\nu_e}} = 2$ , however, the data did not agree with this estimation. This discrepancy is explained by the oscillation of  $\nu_\mu \rightarrow \nu_\tau$ . For a review about atmospheric neutrinos see [31].

- **Relic or Cosmological Neutrinos:** As cosmic microwave background radiation (CMB) corresponds to the radiation left over from the big bang (2.7 K), cosmic neutrino background (CNB or  $C\nu$ B) is the radiation of the neutrinos from the big bang (1.9 K). These neutrinos are named as “relic neutrinos”. Since the relevant energy is very low, they are not expected to be detected in the near future.

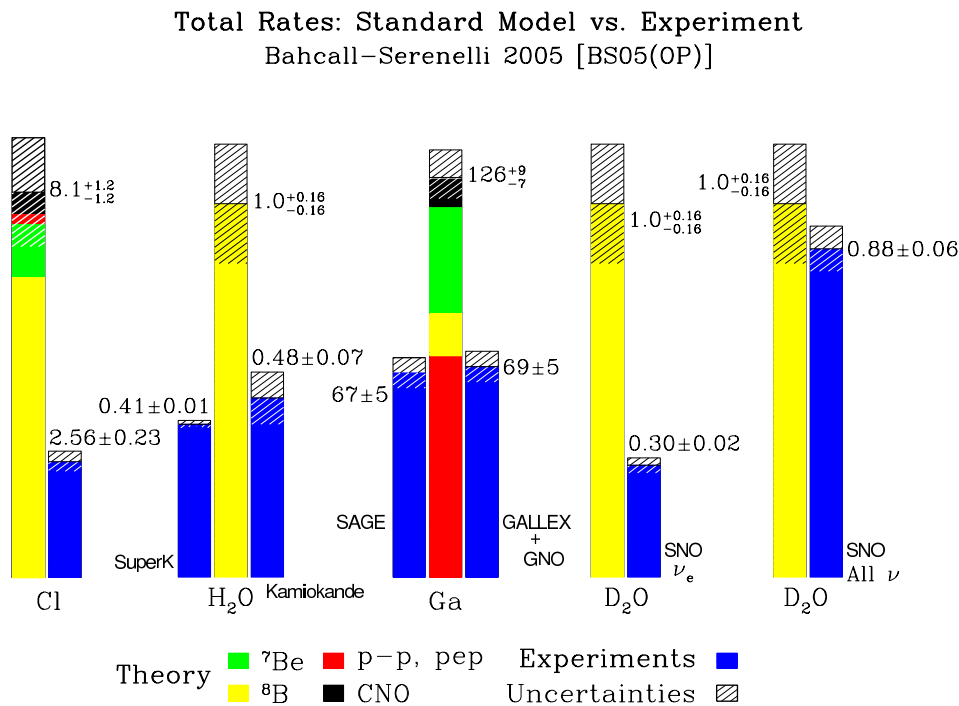


Figure 2.7: The measured and predicted solar neutrino rates are compared. Figure is adapted from [32].

- **Supernova Neutrinos:** When a massive star completes its lifecycle, it explodes and this process is named as supernova. Neutrinos with energy range 10 – 30 MeV are emitted in a very small time scale during this explosion.

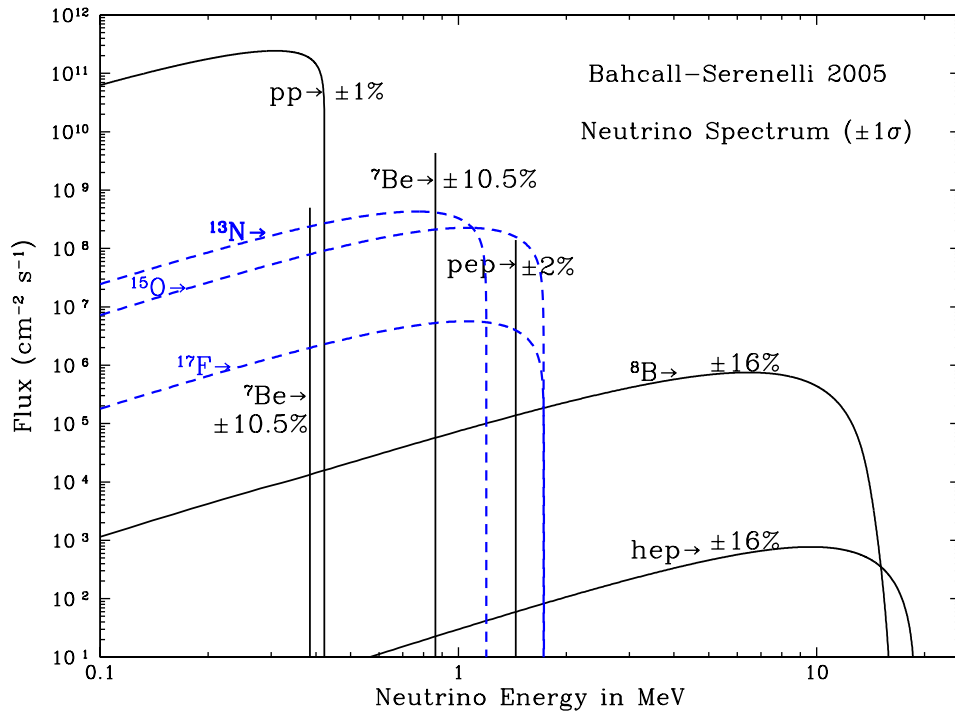


Figure 2.8: The SSM prediction of the energy vs flux of the neutrinos are depicted for each cycle of the fusion mechanism in the sun (Figure is adapted from [32]).

Neutrinos from supernova, as called 1987A in the Large Magellanic Cloud were observed by Kamiokande [33] (in Japan), IMB [34] (in USA) and BAKSAN [35] (in Russia) detectors.

- **Geophysical Neutrinos:** Due to the beta decay of the naturally occurring elements in the interior of the Earth, neutrinos are emitted. These neutrinos are called as “geo-neutrinos” or “terrestrial-neutrinos”. The keV-MeV range geoneutrinos are detected by KAMLAND [36] and BOREXINO [37] collaborations.
- **Cosmogenic Neutrinos:** Cosmogenic neutrinos are the most energetic ones with the lowest flux. It is believed that when the ultrahigh energetic cosmic rays interacted with the 2.7 K cosmic microwave background, the so called “cosmogenic neutrinos” are emitted with energy at the order of  $10^{15}$  PeV –  $10^{18}$  EeV [38]. The flux of the cosmogenic neutrinos depends on the model. They have not been observed yet, however, with the neutrino telescopes being built in this era like Askaryan Radio Array [39] and ARIANNA [40], the hopes

for their detection is high.

## Class II: Artificial Sources

- Reactor Neutrinos:** Nuclear reactors produce energy using the fission of the radioactive elements. The radioactive elements used like  $^{235}\text{U}$ ,  $^{238}\text{U}$ ,  $^{239}\text{Pu}$  and  $^{241}\text{Pu}$  are intense source of electron-type anti neutrinos. Depending on the fuel used in the reactor the energy of the anti-neutrinos varies between 1 – 10 MeV.
- Accelerator Neutrinos:** It is possible to produce neutrino beams using accelerators. When electron or proton beams are impinged on a fixed target, then hadrons, mostly pions and kaons, are produced. With the applied magnetic field, the charged mesons are directed into a long tunnel in which they decay into neutrinos. The energy of the neutrinos depend on the electron-or proton beam and varies between MeV to TeV.

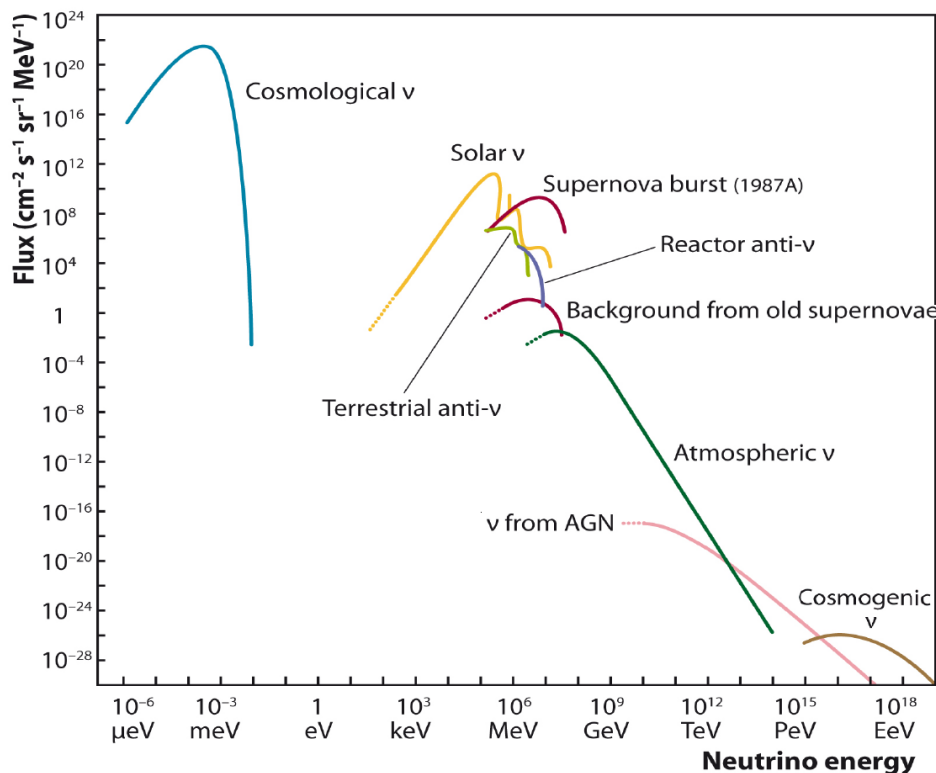


Figure 2.9: The measured and calculated fluxes of all neutrino sources are depicted with respect to the energy of the neutrinos (Figure is adapted from [41]).

### 2.3 The Standard Model

The Standard Model is the most successful quantum field theory that unified the electromagnetic, strong and weak interaction of elementary particles [42, 43, 44]. One of the recent success story of the model has been the discovery of the long time missing particle, Higgs boson [45, 46], predicted by SM [47, 48, 49, 50, 51, 52]. Even though there are still unexplained phenomena like existence of dark matter, neutrinos being massive etc., Standard Model achieves explaining vast experimental results [13].

Elementary particles are classified in the model according to their spins as fermions (spin-half particles) and bosons (spin-integer particles). While leptons and quarks being spin half particles constitute the fermions, bosons, which are the mediator of the interactions, include the  $W^\pm$ ,  $Z$  bosons, photons, gluons and Higgs boson. While the spin of the Higgs boson is zero, the other bosons are spin 1 particles. The particle content of the model is summarized in Figure (2.10).

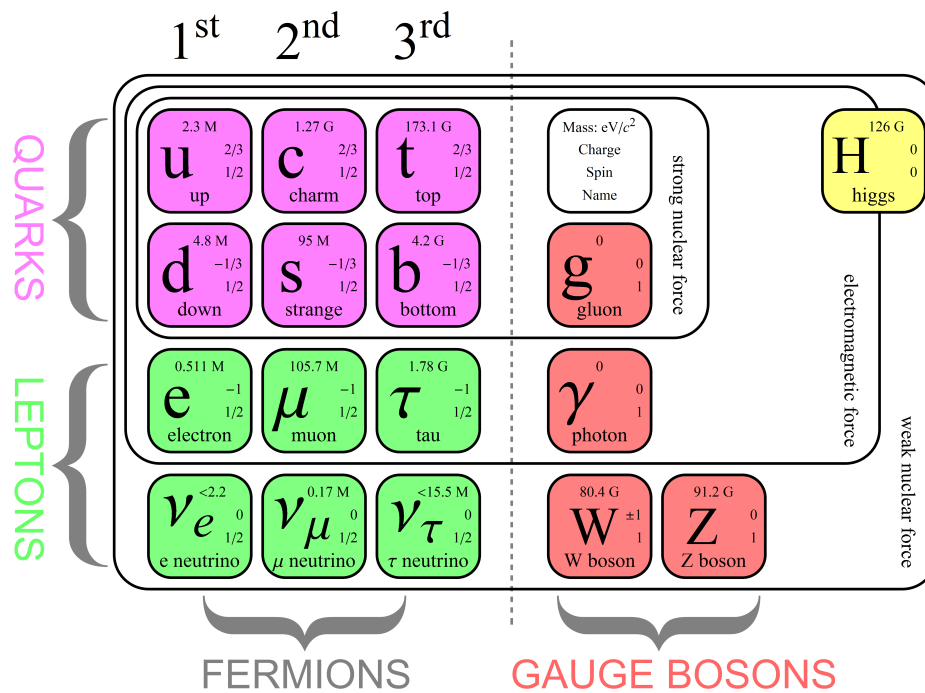


Figure 2.10: The particle content of the Standard Model is shown with their characteristic properties such as spin, charge and mass (Figure is adapted from [53]).

Leptons can be classified as charged leptons (electron, muon and tau) and their neutral counterparts, neutrinos ( $\nu_e$ ,  $\nu_\mu$  and  $\nu_\tau$ ). Now, experimentally it is established that

there are three generations of leptons as shown in Figure (2.10). Each generation is composed of left handed doublets with non-zero weak isospin and right-handed states with zero weak isospin which we will discuss. On the other hand, each generation of quarks comprise left handed doublets with non-zero weak isospin and two right handed singlets with zero weak isospin. Different from the leptons, quarks can also interact with gluons since they carry additional quantum numbers named as “color”.

Bosons are responsible for the carriers of the forces described by the Standard Model. Photons,  $W^\pm$ ,  $Z$  bosons and gluons are the mediator of the electromagnetic, weak and strong forces respectively. Besides, recently discovered Higgs boson is responsible for the particles being massive via Higgs mechanism.

Let us briefly mention about the properties of the fundamental forces.

### 2.3.1 The Electromagnetic Force

The electromagnetic interaction takes place between the charged particles by the exchange of photons. Since the photon is massless, the interaction range is infinity and the interaction mechanism is described by Quantum Electrodynamics (QED). Electromagnetic force is the first known interaction among the others. Thus, the weak and strong force are named by comparing the strength of these forces with respect to the electromagnetic force.

### 2.3.2 The Weak Force

Both leptons and quarks interact weakly via the exchange of massive  $W^\pm$  and  $Z$  bosons. The mass of the  $W$  boson is  $m_W = 80.4$  GeV and  $m_Z = 91.2$  GeV. Since these bosons have large mass, the interaction range is very short  $R \sim 10^{-18}$  m. When compared with the electromagnetic force, the strength is approximately  $10^{-5}$  times weaker. It should be noted that, while the  $Z$  boson interacts with both left and right handed fermions (anti-fermions),  $W^\pm$ -boson interacts only with the left-handed fermions and their right handed anti-particles. Note also that, the quarks flavors can only be changed via the interaction with  $W^\pm$  bosons.

### 2.3.3 The Strong Force

Only quarks have strong interaction since they carry color. The interaction is mediated via the exchange of 8 gluons, which are massless, spin 1 and electrically neutral particles. Since gluons also carry colors, they can have self-interactions as well. Strong force is around 100 times stronger than the electromagnetic force and is explained well with Quantum Chromodynamics (QCD). As opposed to the other forces, the strength of the strong force does not decrease as the distance between interacting particles increase. Hence, isolated quarks have not been observed but instead hadrons which are color-neutral particles are observed and this phenomena is named as confinement. The interaction range of the force is  $10^{-15}$  m.

In the Standard Model, which have local gauge invariance, it is possible to explain the dynamics of the elementary particles. This means that the forces are related with the associated gauge groups. For instance the Standard Model is a gauge theory which is described by  $SU(3)_C \times SU(2)_L \times U(1)_Y$  symmetry group.

$SU(3)_C$  is the symmetry group responsible for strong interaction through the color quantum number, in which the subscript "C" corresponds to. There are 8 generators of this group that correspond to the 8 gluons involved in QCD.

Subscript "L" in  $SU(2)_L$  corresponds to left-handed chirality and this symmetry group represents the weak interaction with the associated weak isospin as the local symmetry. The only particles interact with the weak bosons are the left-handed particles with weak isospin,  $I = \frac{1}{2}$ . There are 3 generators in this group hence, 3 gauge bosons,  $W^\pm$  and  $Z^0$ . It is important to note that,  $W$  and  $Z$  bosons had not been discovered when the theory was proposed. Hence, discovery of these gauge bosons can also be considered as the milestone of the Standard Model.

$U_1(Y)$  represents the symmetry group for the electromagnetic interaction where "Y" corresponds to the weak hypercharge. This symmetry group contains one generator which corresponds to photon.

Electromagnetic and weak interactions are unified based on the concept of local gauge invariance by Sheldon Glashow, Steven Weinberg and Abdus Salam [43, 44, 54] and

named as electroweak interaction. The corresponding symmetry group for this unification is the  $SU(2)_L \times U(1)_Y$ . There exist three generators of  $SU(2)_L$ , denoted as  $W^i$  and one boson corresponding to  $U(1)_Y$  group, denoted as  $B$ . With spontaneous symmetry breaking mechanism, the gauge bosons  $W^\pm$ ,  $Z^0$  and  $\gamma$  appear as a combination of  $W^i$  and  $B$ .

Even though with the concept of local gauge invariance unification of electromagnetic and weak force is achieved, since this idea requires all fermions and gauge bosons being massless the model had a shortcoming. With the idea of Higgs mechanism, which proposes self-interacting spin-0 field around all over the space, the problem of massless fermions and gauge bosons have been overcome. The particle of this field is named as ‘‘Higgs’’ boson and discovered in 2012 [45, 46]. The Higgs field interacts with all fermions and the vacuum expectation value is different from zero and needs to be determined by experiments. With the spontaneous symmetry breaking of  $SU(2)_L \times U(1)_Y$  symmetry,  $W$  and  $Z$  bosons as well as charged fermions gain mass and photons, gluons and neutrinos remain massless.

The addition of the strong force gauge group,  $SU(3)_C$ , to that of the electroweak part is rather trivial with no mixing and since we will deal with neutrinos, it is important to give brief information about the electroweak theory in the next section.

### 2.3.4 The Electroweak Theory

For obtaining part of the Lagrangian responsible for neutrino interactions, as mentioned, it is enough to consider only  $SU(2)_L \times U(1)_Y$  part of the symmetry group of SM.  $SU(2)_L$  symmetry group can be described by the weak isospin ( $I$ ), which is assigned non-zero values only to left handed leptons and quarks as shown in Table 2.1, so that parity symmetry is broken and  $V - A$  theory could be set. In general,  $SU(N)$  group has  $N^2 - 1$  generators, hence,  $SU(2)_L$  group has three generators and can be described by  $I_i$  ( $i = 1, 2, 3$ ). These generators satisfy the following commutation relations which have non-abelian character,

$$[I_i, I_j] = i\epsilon_{ijk}I_k . \quad (2.14)$$



Thus, the weak isospin can be described in terms of Pauli matrices as;

$$I_i = \frac{1}{2}\sigma_i. \quad (2.15)$$

Moreover, hypercharge is related to the third component of the weak isospin,  $I_3$  and the charge operator,  $Q$ , by Gell-Mann-Nishijima relation as (See Table 2.1 for the related quantum numbers);

$$Q = I_3 + \frac{Y}{2}. \quad (2.16)$$

This relation mimics the unification of electromagnetic and weak interaction. To have the local gauge invariance, three vector gauge boson fields,  $W_i^\mu$  ( $i = 1, 2, 3$ ) associated with 3 generators  $I_i$  and one vector gauge boson field  $B^\mu$  associated with the generator  $Y$  are required.

Table2.1: Quantum numbers of the leptons and quarks are shown.  $I$  and  $I_3$  are the total and third component of the weak isospin, respectively.  $Q$  is the electromagnetic charge of the fermions and  $Y$  corresponds to the hypercharge.

Fermions	Generation			$I$	$I_3$	$Q$	$Y$
	1 <sup>st</sup>	2 <sup>nd</sup>	3 <sup>rd</sup>				
Leptons	$\begin{pmatrix} \nu_e \\ e \end{pmatrix}_L$	$\begin{pmatrix} \nu_\mu \\ \mu \end{pmatrix}_L$	$\begin{pmatrix} \nu_\tau \\ \tau \end{pmatrix}_L$	1/2	$\begin{pmatrix} 1/2 \\ -1/2 \end{pmatrix}$	$\begin{pmatrix} 0 \\ -1 \end{pmatrix}$	-1
	$e_R$	$\mu_R$	$\tau_R$	0	0	-1	-2
Quarks	$\begin{pmatrix} u \\ d \end{pmatrix}_L$	$\begin{pmatrix} c \\ s \end{pmatrix}_L$	$\begin{pmatrix} t \\ b \end{pmatrix}_L$	1/2	$\begin{pmatrix} 1/2 \\ -1/2 \end{pmatrix}$	$\begin{pmatrix} 2/3 \\ -1/3 \end{pmatrix}$	1/3
	$u_R$	$c_R$	$t_R$	0	0	2/3	4/3
	$d_R$	$s_R$	$b_R$	0	0	-1/3	-2/3

With the above mentioned basics of the electroweak theory let us try to construct the Lagrangian of the theory and for the sake of simplicity we will neglect the mass of the fermions and deal only with the first generation of the leptons. Extension to the other generations and quarks is straightforward (see [27, 28, 55] for detailed information).

To start with, once we assume there is no weak and electromagnetic interaction, the

Lagrangian for the free Dirac fields can be written as

$$\mathcal{L} = (\bar{\nu}_{eL} \bar{e}_L)(i\gamma^\mu \partial_\mu) \begin{pmatrix} \nu_{eL} \\ e_L \end{pmatrix} + \bar{e}_R i\gamma^\mu \partial_\mu e_R. \quad (2.17)$$

Although this Lagrangian is invariant under global SU(2) transformations on the fields  $\nu_{eL}$  and  $e_L$ , it is not invariant under the local weak isospin transformations. However, it is possible to solve this problem by introducing corresponding gauge vector fields.

With the addition of these fields, Lagrangian turns out to be

$$\mathcal{L} = -\frac{1}{2}Tr(W_{\mu\rho}W^{\mu\rho}) + (\bar{\nu}_{eL} \bar{e}_L)i\gamma^\mu(\partial_\mu + igW_\mu) \begin{pmatrix} \nu_{eL} \\ e_L \end{pmatrix} + \bar{e}_R i\gamma^\mu \partial_\mu e_R. \quad (2.18)$$

Some of the gauge bosons are electrically charged and defined in terms of these three vector fields as;

$$\begin{aligned} W_\mu^0 &= W_\mu^3 \\ W_\mu^+ &= \frac{1}{\sqrt{2}}(W_\mu^1 - iW_\mu^2) \\ W_\mu^- &= \frac{1}{\sqrt{2}}(W_\mu^1 + iW_\mu^2). \end{aligned} \quad (2.19)$$

Hence with these definitions, from Equation (2.18), the coupling term for  $\nu - e - W$  can be found as

$$\begin{aligned} \mathcal{L} &= -g(\bar{\nu}_{eL} \bar{e}_L)\gamma^\mu W_\mu^i \frac{\sigma_i}{2} \begin{pmatrix} \nu_{eL} \\ e_L \end{pmatrix} \\ &= -g(\bar{\nu}_{eL} \bar{e}_L)\gamma^\mu \frac{1}{2} \begin{pmatrix} W_\mu^0 & \sqrt{2}W_\mu^+ \\ \sqrt{2}W_\mu^- & -W_\mu^0 \end{pmatrix} \begin{pmatrix} \nu_{eL} \\ e_L \end{pmatrix} \\ &= -\frac{g}{2}\{W_\mu^0(\bar{\nu}_{eL}\gamma^\mu\nu_{eL} - \bar{e}_L\gamma^\mu e_L) + \sqrt{2}W_\mu^+\bar{\nu}_{eL}\gamma^\mu e_L + \sqrt{2}W_\mu^-\bar{e}_L\gamma^\mu\nu_{eL}\} \end{aligned} \quad (2.20)$$

where  $\sigma_i$  is the Pauli matrices.

Since

$$\bar{\psi}_L\gamma^\mu\psi_L = \frac{1}{2}\bar{\psi}\gamma^\mu(1 - \gamma^5)\psi \quad (2.21)$$

the above Lagrangian can be written in terms of chirality operator,  $\gamma^5$

$$\begin{aligned} \mathcal{L} &= -\frac{g}{4}\{W_\mu^0(\bar{\nu}_e\gamma^\mu(1 - \gamma^5)\nu_e - \bar{e}\gamma^\mu(1 - \gamma^5)e) + \sqrt{2}W_\mu^+\bar{\nu}_e\gamma^\mu(1 - \gamma^5)e \\ &\quad + \sqrt{2}W_\mu^-\bar{e}\gamma^\mu(1 - \gamma^5)\nu_e\}. \end{aligned} \quad (2.22)$$

It is clearly seen that only the left-handed leptons interact with the charged weak gauge bosons, hence parity is violated maximally.

Electroweak interaction is the unification of electromagnetic and weak force. However, the Lagrangian in Equation (2.22) describes only the weak interaction. The  $W_\mu^0$  field could be thought as the photon field at first, however, the coupling of this gauge boson is different than the photon. For instance,  $W_\mu^0$  couples to neutrinos but not to  $e_R$  unlike the photon.

With the help of additional invariance under  $U(1)$  transformations with quantum numbers  $y_L, y_R$ ;

$$\begin{aligned} \begin{pmatrix} \nu_{eL} \\ e_L \end{pmatrix} &\rightarrow e^{iy_L X} \begin{pmatrix} \nu_{eL} \\ e_L \end{pmatrix} \\ e_R &\rightarrow e^{iy_R X} e_R \end{aligned} \quad (2.23)$$

electromagnetic interaction can also be described. However, this description would mean the existence of two photon like gauge bosons which we know is not correct. To overcome this problem, it is possible to choose one special combinations of these quantum numbers as;

$$\begin{aligned} y_L &= -\frac{1}{2} \\ y_R &= -1. \end{aligned} \quad (2.24)$$

This  $U(1)$  group is named as the weak hypercharge  $Y$  and Gell-Mann-Nishijima relation,  $Q = I_3 + \frac{Y}{2}$  holds as mentioned before. For this group, the vector field is  $B_\mu$  and corresponding coupling constant is  $g'$ . Hence, with the addition of  $U(1)$  group, there are two neutral, massless vector fields;  $W_\mu^3$  and  $B_\mu$ . It is possible to combine them to describe weak neutral currents by defining two orthogonal linear combination of normalized fields  $Z_\mu$  and  $A_\mu$ ;

$$\begin{aligned} Z_\mu &= \frac{1}{\sqrt{g^2 + g'^2}} (gW_\mu^3 - g'B_\mu) \\ A_\mu &= \frac{1}{\sqrt{g^2 + g'^2}} (g'W_\mu^3 + gB_\mu) \end{aligned} \quad (2.25)$$

With a redefinition of coupling constants as;

$$\begin{aligned}\sin \theta_W &= \frac{g'}{\sqrt{g^2 + g'^2}} \\ \cos \theta_W &= \frac{g}{\sqrt{g^2 + g'^2}}\end{aligned}\quad (2.26)$$

the fields can be rewritten as;

$$\begin{aligned}Z_\mu &= \cos \theta_W W_\mu^0 - \sin \theta_W B_\mu \\ A_\mu &= \sin \theta_W W_\mu^0 + \cos \theta_W B_\mu\end{aligned}\quad (2.27)$$

where  $\sin \theta_W$  is the fundamental constant parameter of the Standard Model and named as the Weinberg angle. With these definitions, the Lagrangian in Equation (2.22) can be written as;

$$\begin{aligned}\mathcal{L} = & -\frac{g}{\sqrt{2}} [W_\mu^+ \bar{\nu}_{eL} \gamma^\mu e_L + W_\mu^- \bar{e}_L \gamma^\mu \nu_{eL} \\ & - \sqrt{g^2 + g'^2} Z_\mu (\frac{1}{2} \bar{\nu}_{eL} \gamma^\mu \nu_{eL} - \frac{1}{2} \bar{e}_L \gamma^\mu e_L \\ & - \sin^2 \theta_W (-\bar{e}_L \gamma^\mu e_L + y_R \bar{e}_R \gamma^\mu e_R)] \\ & - \frac{gg'}{\sqrt{g^2 + g'^2}} A_\mu (-\bar{e}_L \gamma^\mu e_L + y_R \bar{e}_R \gamma^\mu e_R).\end{aligned}\quad (2.28)$$

As seen from the above Lagrangian, while  $Z_\mu$  couples to neutral fermions,  $A_\mu$  couples to charged leptons but not to neutrinos. Thus,  $A_\mu$  is the candidate for the desired photon field. To get the electromagnetic interaction, the coupling constants need to be chosen as;

$$\begin{aligned}y_R &= -1 \\ \frac{gg'}{\sqrt{g^2 + g'^2}} &= e\end{aligned}\quad (2.29)$$

When comparing this equation with Equation (2.26) we deduce that

$$\sin \theta_W = \frac{e}{g}.\quad (2.30)$$

Consequently, the Lagrangian describing the weak and electromagnetic interaction can be written in terms of the corresponding currents

$$\begin{aligned}\mathcal{L} = & -e [A_\mu J_{em} + \frac{1}{\sqrt{2} \sin \theta_W} (W_\mu^+ \bar{\nu}_{eL} \gamma^\mu e_L + W_\mu^- \bar{e}_L \gamma^\mu \nu_{eL}) \\ & + \frac{1}{\sin \theta_W \cos \theta_W} Z_\mu J_{NC}^\mu]\end{aligned}\quad (2.31)$$

where the currents are

$$\begin{aligned} J_{em}^\mu &= -\bar{e}_L \gamma^\mu e_L - \bar{e}_R \gamma^\mu e_R = -\bar{e} \gamma^\mu e \\ J_{NC}^\mu &= \frac{1}{2} \bar{\nu}_{eL} \gamma^\mu \nu_{eL} - \frac{1}{2} \bar{e}_L \gamma^\mu e_L - \sin^2 \theta_W J_{em}^\mu . \end{aligned} \quad (2.32)$$

## 2.4 Helicity and Chirality of Neutrinos

Fermions are described by 4-component wave function  $\psi(x)$  (spinors) and these spinors are the solutions of the Dirac equation

$$(i\gamma^\mu \frac{\partial}{\partial x^\mu} - m)\psi = 0 \quad (2.33)$$

where  $\gamma$  matrices are denoted in Dirac representation as

$$\gamma^0 = \begin{pmatrix} 0 & 1 \\ 1 & 0 \end{pmatrix}, \quad \gamma^i = \begin{pmatrix} 0 & \sigma^i \\ -\sigma^i & 0 \end{pmatrix} \quad (2.34)$$

in which  $\sigma^i$  are the Pauli matrices and  $i = 1, 2, 3$ . (For more detailed information see [56]). In addition  $\gamma^5$  is defined as

$$\gamma^5 = i\gamma^0\gamma^1\gamma^2\gamma^3 = \begin{pmatrix} 0 & 1 \\ 1 & 0 \end{pmatrix}. \quad (2.35)$$

Once we multiply the Dirac equation with  $\gamma^0$  from left, we get

$$\begin{aligned} (i\gamma^0\gamma^\mu \frac{\partial}{\partial x^\mu} - m\gamma^0)\psi &= 0 \\ (i\underbrace{\gamma^0\gamma^0}_1 \frac{\partial}{\partial x^0} - i\gamma^0\gamma^i \frac{\partial}{\partial x^i} - m\gamma^0)\psi &= 0 \end{aligned} \quad (2.36)$$

$$\boxed{(i\frac{\partial}{\partial x^0} - i\gamma^0\gamma^i \frac{\partial}{\partial x^i} - m\gamma^0)\psi = 0}$$

Furthermore, since  $\gamma^0\gamma^5\Sigma^i = \gamma^i$  we can write the above equation as

$$\begin{aligned} (i\frac{\partial}{\partial x^0} - i\underbrace{\gamma^0\gamma^0\gamma^5\Sigma^i}_1 \frac{\partial}{\partial x^i} - m\gamma^0)\psi &= 0 \\ (i\frac{\partial}{\partial x^0} - i\gamma^5\Sigma^i \frac{\partial}{\partial x^i} - m\gamma^0)\psi &= 0 \end{aligned} \quad (2.37)$$

$$\boxed{(i\frac{\partial}{\partial x^0} - i\Sigma^i\gamma^5 \frac{\partial}{\partial x^i} - m\gamma^0)\psi = 0}$$

where  $\Sigma^i$  corresponds to

$$\Sigma^i = \begin{pmatrix} \sigma^i & 0 \\ 0 & \sigma^i \end{pmatrix}. \quad (2.38)$$

Once we multiply Equation (2.37) from left with  $\gamma^5$  we get

$$(i\gamma^5 \frac{\partial}{\partial x^0} - i \underbrace{\gamma^5 \gamma^5}_{\mathbb{1}} \Sigma^i \frac{\partial}{\partial x^i} - m \underbrace{\gamma^5 \gamma^0}_{-\gamma^0 \gamma^5}) \psi = 0 \quad (2.39)$$

$$\boxed{(i\gamma^5 \frac{\partial}{\partial x^0} - i\Sigma^i \frac{\partial}{\partial x^i} + m\gamma^0 \gamma^5) \psi = 0}$$

When we add Equation (2.39) and 2.37 we get;

$$(i(1 + \gamma^5) \frac{\partial}{\partial x^0} - i(\Sigma^i + \underbrace{\gamma^5 \Sigma^i}_{\Sigma^i \gamma^5}) \frac{\partial}{\partial x^i} - m\gamma^0(1 - \gamma^5)) \psi = 0 \quad (2.40)$$

$$\boxed{(i(1 + \gamma^5) \frac{\partial}{\partial x^0} - i\Sigma^i(1 + \gamma^5) \frac{\partial}{\partial x^i} - m\gamma^0(1 - \gamma^5)) \psi = 0}$$

Moreover, once we subtract Equation (2.39) and 2.37 we get;

$$(i(1 - \gamma^5) \frac{\partial}{\partial x^0} - i\Sigma^i(\gamma^5 - 1) \frac{\partial}{\partial x^i} - m\gamma^0(1 + \gamma^5)) \psi = 0 \quad (2.41)$$

$$\boxed{(i(1 - \gamma^5) \frac{\partial}{\partial x^0} + i\Sigma^i(1 - \gamma^5) \frac{\partial}{\partial x^i} - m\gamma^0(1 + \gamma^5)) \psi = 0}$$

Now let us define the projection operators as follows.  $P_L = \frac{1}{2}(1 - \gamma^5)$  and  $P_R = \frac{1}{2}(1 + \gamma^5)$ . Note that, the following identities hold for the projection operators.

$$P_L + P_R = 1 ,$$

$$P_L P_R = P_R P_L = 0 ,$$

$$P_R^2 = P_R ,$$

$$P_L^2 = P_L .$$
(2.42)

In addition we can define the left-handed and right-handed components of fermion function as;

$$\psi_L = P_L \psi$$

$$\psi_R = P_R \psi$$
(2.43)

and it is easy to see  $P_L \psi_R = P_R \psi_L = 0$  as expected.

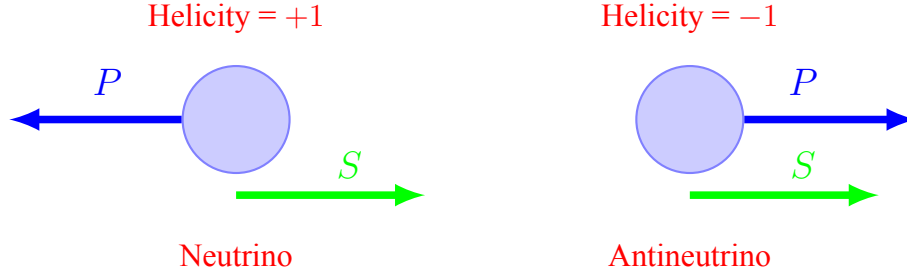


Figure 2.11: The helicity for neutrinos and antineutrinos are shown. If  $m_\nu = 0$  then the helicity and chirality corresponds to same meaning.

Once we solve the eigenequation for  $\gamma^5\psi_{L,R} = \lambda\psi_{L,R}$ , we find

$$\begin{aligned}
 \gamma^5\psi_L &= \lambda\psi_L \\
 \gamma^5\frac{1}{2}(1 - \gamma^5)\psi &= \lambda\frac{1}{2}(1 - \gamma^5)\psi \\
 (\gamma^5 - \underbrace{\gamma^5\gamma^5}_1)\psi &= \lambda(1 - \gamma^5)\psi \\
 (\gamma^5 - 1)\psi &= \lambda(1 - \gamma^5)\psi \\
 \Rightarrow \lambda &= -1
 \end{aligned} \tag{2.44}$$

Similarly eigenequation for  $\psi_R$ ;

$$\begin{aligned}
 \gamma^5\psi_R &= \lambda\psi_R \\
 \gamma^5\frac{1}{2}(1 + \gamma^5)\psi &= \lambda\frac{1}{2}(1 + \gamma^5)\psi \\
 (\gamma^5 + \underbrace{\gamma^5\gamma^5}_1)\psi &= \lambda(1 + \gamma^5)\psi \\
 (\gamma^5 + 1)\psi &= \lambda(1 + \gamma^5)\psi \\
 \Rightarrow \lambda &= 1
 \end{aligned} \tag{2.45}$$

Hence we deduce that;

$$\gamma^5\psi_{L,R} = \mp\psi_{L,R} \tag{2.46}$$

The eigenvalues  $\mp 1$  of  $\gamma^5$  operator are called as ‘‘chirality’’ and  $\psi_{L,R}$  are called as the chiral projections.

It is possible to define any of the spinors in terms of chiral projections (also named as the ‘‘Weyl’’ spinors) as;

$$\psi = (P_L + P_R)\psi = P_L\psi + P_R\psi = \psi_L + \psi_R \tag{2.47}$$

Using the above notation we can write Equations 2.40 and 2.41 in terms of the chiral projections as;

$$\begin{aligned} \left(i\frac{\partial}{\partial x^0} - i\Sigma^i\frac{\partial}{\partial x^i}\right)\psi_R &= m\gamma^0\psi_L \\ \left(i\frac{\partial}{\partial x^0} + i\Sigma^i\frac{\partial}{\partial x^i}\right)\psi_L &= m\gamma^0\psi_R. \end{aligned} \quad (2.48)$$

If the fermion is massless then we can decouple the above equation as

$$\begin{aligned} i\frac{\partial}{\partial x^0}\psi_R &= i\Sigma^i\frac{\partial}{\partial x^i}\psi_R \\ i\frac{\partial}{\partial x^0}\psi_L &= -i\Sigma^i\frac{\partial}{\partial x^i}\psi_L. \end{aligned} \quad (2.49)$$

Notice that, these decoupled equations resemble to the Schrodinger equation,

$$i\frac{\partial}{\partial t}\psi_{L,R} = \mp i\Sigma^i\frac{\partial}{\partial x^i}\psi_{L,R}. \quad (2.50)$$

Indeed, if  $E \rightarrow i\frac{\partial}{\partial t}$  and  $p^i \rightarrow -i\frac{\partial}{\partial x^i}$ , these equations can be written as

$$E\psi_{L,R} = \pm\Sigma^i p^i\psi_{L,R}. \quad (2.51)$$

Note that, the helicity operator is defined as;

$$\mathcal{H} = \frac{\vec{\Sigma} \cdot \vec{p}}{|\vec{p}|} \quad (2.52)$$

Since for a massless particle  $E = |\vec{p}|$ , we can write Equation (2.51) as;

$$\mathcal{H}\psi_{L,R} = \pm\psi_{L,R} \quad (2.53)$$

Hence we see that for eigenspinor  $\psi_L$ ;

$$\begin{pmatrix} h = 1; & \text{for particles} \\ h = -1; & \text{for anti-particles} \end{pmatrix} \quad (2.54)$$

and for eigenspinor  $\psi_R$ ;

$$\begin{pmatrix} h = -1; & \text{for particles} \\ h = +1; & \text{for anti-particles} \end{pmatrix} \quad (2.55)$$

where  $h$  is eigenvalue of the helicity operator,  $\mathcal{H}$ .

Thus, we deduce that if the fermion is massless, then the helicity and chirality can be considered as same. However, if the fermion has mass then decoupling of equations



is not possible, hence chirality eigenspinors  $\psi_L$  and  $\psi_R$  do not describe particles with fixed helicity anymore.

In the Standard Model, the interacting neutrinos (anti-neutrinos) are always left (right) handed according to the two-component theory. Hence, the spinor in weak interaction is described as;

$$\psi_\nu = \frac{1}{2}(1 - \gamma^5)\psi = \psi_L \quad (2.56)$$

In addition, if the mass is equal to zero, then we infer that the neutrinos are particles with helicity  $h = +1$  whereas the anti-neutrinos with helicity  $h = -1$  (see Figure (2.11)).



## CHAPTER 3

### NEUTRINO ELECTRON SCATTERING IN THE STANDARD MODEL

Neutrino-electron scattering process represents a promising and clean way of the testing ground of the Standard Model and precise determination of the Weinberg angle ( $\sin^2\theta_W$ ). In order to test the SM predictions and measure the free parameters of the model, one needs to calculate the cross section of neutrino scattering which enables to predict how many interactions would take place in the experiment. Especially in low energy neutrino experiments, number of events are obtained with respect to recoil energy ( $T$ ) of the target material (electron), hence, one needs to calculate the cross section with respect to recoil energy, i.e.  $\frac{d\sigma}{dT}$  for extracting the parameters of the SM. For this purpose we start with the Fermi's golden rule to construct and then calculate  $\frac{d\sigma}{dT}$ .

#### 3.1 The Golden Rule for Scattering

From quantum field theory it is well known that the differential cross section of the  $1 + 2 \rightarrow 3 + 4$  process is determined as;

$$d\sigma = |\mathcal{M}|^2 \frac{S}{4\sqrt{(p_1 \cdot p_2)^2 - (m_1 m_2)^2}} \left[ \left( \frac{d^3\vec{p}_3}{(2\pi)^3 2E_3} \right) \left( \frac{d^3\vec{p}_4}{(2\pi)^3 2E_4} \right) \right] \times (2\pi)^4 \delta^4(p_1 + p_2 - p_3 - p_4). \quad (3.1)$$

In this expression,  $p_1$ ,  $p_2$ ,  $p_3$  and  $p_4$  are four-momentum of corresponding particles,

while, 3-vectors are denoted with vector sign as  $\vec{p}_i$ . Moreover,  $E_3$  and  $E_4$  are the energy of the outgoing particles after the interaction and  $S$  is the statistical factor as  $\frac{1}{n!}$  for  $n$  identical particles in the final state. The  $\delta$  function in Equation (3.1) describes the conservation of energy and momentum.

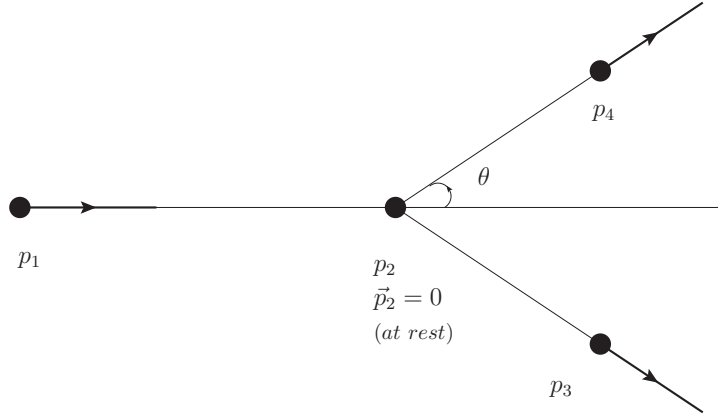


Figure 3.1: Symbolic illustration of two body scattering is shown in the rest frame of the target material.

In the rest frame of particle 2 (target particle) (generally called as the lab frame), obviously  $E_2 = m_2$  and  $\vec{p}_2 = 0$ . Moreover using the relativistic relation between energy and momentum  $E^2 - |p|^2 = m^2$ , we find

$$\begin{aligned}
 (p_1 \cdot p_2)^2 - (m_1 m_2)^2 &= ((E_1 E_2 - \vec{p}_1 \cdot \vec{p}_2)^2 - (m_1 m_2)^2) \\
 &= ((E_1 m_2 - 0)^2 - (m_1 m_2)^2) \\
 &= (E_1^2 m_2^2 - m_1^2 m_2^2) = m_2^2 \underbrace{(E_1^2 - m_1^2)}_{|\vec{p}_1|^2} \\
 &= m_2^2 |\vec{p}_1|^2.
 \end{aligned} \tag{3.2}$$

If we put this equation into Equation (3.1), we get

$$\begin{aligned}
 d\sigma &= |\mathcal{M}|^2 \frac{S}{4m_2 |\vec{p}_1|} \frac{1}{16\pi^2} \frac{1}{E_3 E_4} d^3 \vec{p}_3 d^3 \vec{p}_4 \delta^4(p_1 + p_2 - p_3 - p_4) \\
 &= \frac{|\mathcal{M}|^2}{64\pi^2} \frac{S}{m_2 |\vec{p}_1|} \frac{1}{E_3 E_4} \delta(E_1 + m_2 - E_3 - E_4) \delta^3(\vec{p}_1 - \vec{p}_3 - \vec{p}_4) d^3 \vec{p}_3 d^3 \vec{p}_4
 \end{aligned} \tag{3.3}$$

where  $E_2 = m_2$  &  $\vec{p}_2 = 0$  are implemented.

Using the energy-momentum relation to eliminate  $E_i$ 's, we can write this equation in

terms of momenta

$$\begin{aligned}
d\sigma &= \frac{|\mathcal{M}|^2}{64\pi^2} \frac{S}{m_2|\vec{p}_1|} \frac{1}{\sqrt{|\vec{p}_3|^2 + m_3^2} \sqrt{|\vec{p}_4|^2 + m_4^2}} \\
&\times \delta(\sqrt{|\vec{p}_1|^2 + m_1^2} + m_2 - \sqrt{|\vec{p}_3|^2 + m_3^2} - \sqrt{|\vec{p}_4|^2 + m_4^2}) \\
&\times \delta^3(\vec{p}_1 - \vec{p}_3 - \vec{p}_4) d^3\vec{p}_3 d^3\vec{p}_4 .
\end{aligned} \tag{3.4}$$

In order to obtain  $d\sigma/dT$ , first we perform integration over  $d^3\vec{p}_3$ . From the conservation law of momentum, we can solve for  $\vec{p}_3$  in the rest frame of the second particle as;

$$\begin{aligned}
\vec{p}_1 + \cancel{\vec{p}_2} &= \vec{p}_3 + \vec{p}_4 \\
\Rightarrow \vec{p}_3 &= \vec{p}_1 - \vec{p}_4
\end{aligned} \tag{3.5}$$

and therefore for energy  $E_3$  we have;

$$\begin{aligned}
E_3^2 &= |\vec{p}_3|^2 + m_3^2 \\
E_3 &= \sqrt{|\vec{p}_1 - \vec{p}_4|^2 + m_3^2}
\end{aligned} \tag{3.6}$$

We can perform integration over  $d^3\vec{p}_3$  using the  $\delta$  function. In result, we obtain

$$\begin{aligned}
d\sigma &= \frac{|\mathcal{M}|^2}{64\pi^2} \frac{S}{m_2|\vec{p}_1|} \frac{1}{\sqrt{|\vec{p}_1 - \vec{p}_4|^2 + m_3^2}} \frac{1}{\sqrt{|\vec{p}_4|^2 + m_4^2}} \\
&\times \delta(\sqrt{|\vec{p}_1|^2 + m_1^2} + m_2 - \sqrt{|\vec{p}_1 - \vec{p}_4|^2 + m_3^2} - \sqrt{|\vec{p}_4|^2 + m_4^2}) d^3\vec{p}_4
\end{aligned} \tag{3.7}$$

For performing integration over  $d^3\vec{p}_4$  we use the spherical coordinates. The dimensional volume in spherical coordinates can be written as;

$$d^3\vec{p}_4 = |\vec{p}_4|^2 \sin\theta d\theta d\phi |d\vec{p}_4| \tag{3.8}$$

and

$$(\vec{p}_1 - \vec{p}_4)^2 = |\vec{p}_1|^2 + |\vec{p}_4|^2 - 2|\vec{p}_1||\vec{p}_4| \cos\theta . \tag{3.9}$$

Since we need to find the cross-section in terms of the recoil energy we write the Equation (3.7) as;

$$\begin{aligned}
\frac{d\sigma}{d|\vec{p}_4|} &= \int_0^{2\pi} d\phi \int_0^\pi d\theta \left( \frac{|\mathcal{M}|^2}{64\pi^2} \frac{S}{m_2|\vec{p}_1|} \frac{|\vec{p}_4|^2 \sin \theta}{\sqrt{|\vec{p}_4|^2 + m_4^2}} \right. \\
&\quad \times \frac{1}{\sqrt{|\vec{p}_1|^2 + |\vec{p}_4|^2 - 2|\vec{p}_1||\vec{p}_4| \cos \theta + m_3^2}} \\
&\quad \times \delta(\sqrt{|\vec{p}_1|^2 + m_1^2} + m_2 - \sqrt{|\vec{p}_1|^2 + |\vec{p}_4|^2 - 2|\vec{p}_1||\vec{p}_4| \cos \theta + m_3^2} \\
&\quad \left. - \sqrt{|\vec{p}_4|^2 + m_4^2}) \right), \tag{3.10}
\end{aligned}$$

carrying out  $\phi$  integration and applying the following change of variables

$$\begin{aligned}
\cos \theta &= u, \\
-\sin \theta d\theta &= du, \tag{3.11}
\end{aligned}$$

we can write Equation (3.10) as;

$$\begin{aligned}
\frac{d\sigma}{d|\vec{p}_4|} &= \frac{|\mathcal{M}|^2}{32\pi} \frac{S}{m_2|\vec{p}_1|} \frac{|\vec{p}_4|^2}{\sqrt{|\vec{p}_4|^2 + m_4^2}} \int_{-1}^1 \frac{du}{\sqrt{|\vec{p}_1|^2 + |\vec{p}_4|^2 - 2|\vec{p}_1||\vec{p}_4|u + m_3^2}} \\
&\quad \times \delta(\sqrt{|\vec{p}_1|^2 + m_1^2} + m_2 - \sqrt{|\vec{p}_1|^2 + |\vec{p}_4|^2 - 2|\vec{p}_1||\vec{p}_4|u + m_3^2} - \sqrt{|\vec{p}_4|^2 + m_4^2}). \tag{3.12}
\end{aligned}$$

The integral in Equation (3.12) becomes

$$\begin{aligned}
I &= \int_{-1}^1 \frac{1}{\sqrt{|\vec{p}_1|^2 + |\vec{p}_4|^2 - 2|\vec{p}_1||\vec{p}_4|u + m_3^2}} \\
&\quad \times \delta(\sqrt{|\vec{p}_1|^2 + m_1^2} + m_2 - \sqrt{|\vec{p}_1|^2 + |\vec{p}_4|^2 - 2|\vec{p}_1||\vec{p}_4|u + m_3^2} - \sqrt{|\vec{p}_4|^2 + m_4^2}) \\
&= \frac{1}{|\vec{p}_1||\vec{p}_4|}. \tag{3.13}
\end{aligned}$$

Thus, after performing integration over the polar and azimuthal angles for the differential cross section, Equation (3.12) turns out to be equal to

$$\begin{aligned}
\frac{d\sigma}{d|\vec{p}_4|} &= \frac{|\mathcal{M}|^2}{32\pi} \frac{S}{m_2|\vec{p}_1|} \frac{|\vec{p}_4|^2}{\sqrt{|\vec{p}_4|^2 + m_4^2}} \frac{1}{|\vec{p}_1||\vec{p}_4|} \\
&= \frac{|\mathcal{M}|^2}{32\pi} \frac{S}{m_2|\vec{p}_1|^2} \frac{|\vec{p}_4|}{\sqrt{|\vec{p}_4|^2 + m_4^2}}. \tag{3.14}
\end{aligned}$$

Our purpose is to find the differential cross section in terms of the recoil energy of an electron. Therefore, we first performed the  $d^3\vec{p}_3$  integral. Note that for the elastic collision we denoted  $p_4$  as the four vector of the recoil energy of the target.

If we denote the recoil energy of the electron as  $T$ , it is equal to

$$T = (E_4 - m_4) \quad (3.15)$$

and using the relativistic energy-momentum relation we have;

$$\begin{aligned} E_4^2 - m_4^2 &= |\vec{p}_4|^2 \\ \Rightarrow \underbrace{(E_4 - m_4)}_T \underbrace{(E_4 + m_4)}_{T+2m_4} &= |\vec{p}_4|^2 \\ \Rightarrow T(T + 2m_4) &= |\vec{p}_4|^2 \end{aligned} \quad (3.16)$$

Once we differentiate both sides of Equation (3.16) we get;

$$\begin{aligned} 2|\vec{p}_4|d|\vec{p}_4| &= (2T + 2m_4)dT \\ \Rightarrow |\vec{p}_4|d|\vec{p}_4| &= (T + m_4)dT \end{aligned} \quad (3.17)$$

Putting Equation (3.17) into Equation (3.14), we finally get  $d\sigma/dT$  in the rest frame of the second particle as,

$$\begin{aligned} \frac{d\sigma}{|\vec{p}_4|d|\vec{p}_4|} &= \frac{|\mathcal{M}|^2}{32\pi} \frac{S}{m_2|\vec{p}_1|^2} \frac{1}{\sqrt{|\vec{p}_4|^2 + m_4^2}} = \frac{|\mathcal{M}|^2}{32\pi} \frac{S}{m_2|\vec{p}_1|^2} \frac{1}{E_4} \\ \frac{d\sigma}{(T + m_4)dT} &= \frac{|\mathcal{M}|^2}{32\pi} \frac{S}{m_2|\vec{p}_1|^2} \frac{1}{E_4} \\ \frac{d\sigma}{dT} &= \underbrace{(T + m_4)}_{E_4} \frac{|\mathcal{M}|^2}{32\pi} \frac{S}{m_2|\vec{p}_1|^2} \frac{1}{E_4} \\ \frac{d\sigma}{dT} &= \cancel{E_4} \frac{|\mathcal{M}|^2}{32\pi} \frac{S}{m_2|\vec{p}_1|^2} \cancel{E_4} \\ \boxed{\frac{d\sigma}{dT} = \frac{|\mathcal{M}|^2}{32\pi} \frac{S}{m_2|\vec{p}_1|^2}} \end{aligned} \quad (3.18)$$

For practical purposes, it is also useful to present a relation between  $\frac{d\sigma}{dT}$  and  $\frac{d\sigma}{d\Omega}$ , where  $d\Omega = \sin\theta d\theta d\phi$  (solid angle), since in the literature  $\frac{d\sigma}{d\Omega}$  results are given so often. For this purpose we can write,

$$\begin{aligned} \frac{d\sigma}{dT} &= 2\pi \sin\theta \frac{\partial\theta}{\partial T} \frac{d\sigma}{d\Omega} \\ &= 2\pi \frac{\partial\cos\theta}{dT} \frac{d\sigma}{d\Omega} \end{aligned} \quad (3.19)$$

However note that  $\theta$  is the scattering angle between incoming and outgoing neutrino ( $\vec{p}_1$  and  $\vec{p}_3$ ) different from the angle shown in Figure (3.1). In order to calculate  $\frac{\partial \cos \theta}{\partial T}$ , we need to describe the recoil energy of the electron in terms of the scattering angle  $\theta$ .

Using the energy and momentum conservation we can write;

$$\begin{aligned} p_1 + p_2 &= p_3 + p_4 \\ p_1 - p_3 &= p_2 - p_4 \end{aligned} \quad (3.20)$$

once we square both sides to acquire the scattering angle between  $\vec{p}_1$  and  $\vec{p}_3$ , we get;

$$\begin{aligned} p_1^2 + p_3^2 - 2p_1 \cdot p_3 &= p_2^2 + p_4^2 - 2p_2 \cdot p_4 \\ m_1^2 + m_3^2 - 2(E_1 E_3 - \vec{p}_1 \cdot \vec{p}_3) &= m_2^2 + m_4^2 - 2(E_2 E_4 - \vec{p}_2 \cdot \vec{p}_4) \\ m_1^2 + m_3^2 - 2E_1 E_3 + 2|\vec{p}_1||\vec{p}_3| \cos \theta &= m_2^2 + m_4^2 - 2m_2 E_4, \end{aligned} \quad (3.21)$$

where;  $\vec{p}_2 = 0$  and  $E_2 = m_2$ , are set in the last step.

For the elastic scattering  $m_1 = m_3$  and  $m_2 = m_4$ , hence Equation (3.21) can be written as;

$$\begin{aligned} 2m_1^2 - 2E_1 E_3 + 2|\vec{p}_1||\vec{p}_3| \cos \theta &= 2m_2^2 - 2m_2 E_4 \\ m_1^2 - E_1 E_3 + |\vec{p}_1||\vec{p}_3| \cos \theta &= m_2^2 - m_2 E_4 \\ \cos \theta &= \frac{m_2^2 - m_2 E_4 - m_1^2 + E_1 E_3}{|\vec{p}_1||\vec{p}_3|} \end{aligned} \quad (3.22)$$

In order to find  $\frac{\partial \cos \theta}{\partial T}$  we need to relate  $E_3$  and  $E_4$  with the recoil energy  $T$ .

$E_3$  can be written in terms of electron recoil energy as;

$$\begin{aligned} E_3 &= E_1 + E_2 - E_4 \\ E_3 &= E_1 + m_2 - (T + m_4) \\ E_3 &= E_1 + m_2 - (T + m_2) \\ E_3 &= E_1 - T \end{aligned} \quad (3.23)$$

If we put Equation (3.23) into Equation (3.22) we get;



$$\begin{aligned}
\cos \theta &= \frac{m_2 \overbrace{(m_2 - E_4)}^{-T} - m_1^2 + E_1 \overbrace{(E_1 - T)}^{E_3}}{|\vec{p}_1| |\vec{p}_3|} \\
&= \frac{-m_2 T - m_1^2 + E_1 (E_1 - T)}{\sqrt{E_1^2 + m_1^2} \sqrt{E_3^2 + m_3^2}} \\
&= \frac{-m_2 T - m_1^2 + E_1 (E_1 - T)}{\sqrt{E_1^2 + m_1^2} \sqrt{(E_1 - T)^2 + m_3^2}} \\
\boxed{\cos \theta} &= \frac{-m_2 T - m_1^2 + E_1 (E_1 - T)}{\sqrt{E_1^2 + m_1^2} \sqrt{(E_1 - T)^2 + m_1^2}}.
\end{aligned} \tag{3.24}$$

For our specific case (neutrino-electron elastic scattering) if we neglect neutrino mass  $m_1 = m_3 = m_\nu \simeq 0$ , we can write  $|\vec{p}_1| = E_1$ . And since  $m_2 = m_4 = m_e$ , Equation (3.24) reduces to;

$$\begin{aligned}
\cos \theta &= \frac{-m_e T + E_1 (E_1 - T)}{\sqrt{E_1^2} \sqrt{(E_1 - T)^2}} \\
&= \frac{-m_e T + E_1 (E_1 - T)}{E_1 (E_1 - T)} \\
\boxed{\cos \theta} &= 1 - \frac{m_e T}{E_1 (E_1 - T)}.
\end{aligned} \tag{3.25}$$

When we differentiate with respect to  $T$ , we get;

$$\frac{\partial \cos \theta}{\partial T} = \frac{m_e}{(E_1 - T)^2} \tag{3.26}$$

Using this result in Equation (3.19) we find;

$$\begin{aligned}
\frac{d\sigma}{dT} &= 2\pi \frac{\partial \cos \theta}{dT} \frac{d\sigma}{d\Omega} \\
&= 2\pi \frac{m_e}{(E_1 - T)^2} \frac{d\sigma}{d\Omega}.
\end{aligned} \tag{3.27}$$

Differential elastic-scattering cross section with respect to solid angle when the incoming particle is massless in the lab frame is given in many books [57, 55, 58, 59, 60] as;

$$\frac{d\sigma}{d\Omega} = S |\mathcal{M}|^2 \left( \frac{E_3}{8\pi m_2 E_1} \right)^2. \tag{3.28}$$

When we plug Equations (3.23), (3.26) and (3.28) into Equation (3.27), we get;

$$\begin{aligned}
\frac{d\sigma}{dT} &= S|\mathcal{M}|^2 2\pi \frac{m_e}{(E_1 - T)^2} \left( \frac{\overbrace{E_3}^{E_1 - T}}{8\pi m_e E_1} \right)^2 \\
\frac{d\sigma}{dT} &= S|\mathcal{M}|^2 2\pi \frac{m_e}{(E_1 - T)^2} \frac{(E_1 - T)^2}{(8\pi m_e E_1)^2} \\
\frac{d\sigma}{dT} &= S|\mathcal{M}|^2 \frac{1}{32\pi m_e E_1^2} \\
\boxed{\frac{d\sigma}{dT} &= S|\mathcal{M}|^2 \frac{1}{32\pi m_e |\vec{p}_1|^2}},
\end{aligned} \tag{3.29}$$

which is what we already obtained in Equation (3.18) as expected.

### 3.2 $|\mathcal{M}|^2$ for the Neutrino-Electron Scattering

Neutrinos can only have weak interactions in the SM. The weak interactions are mediated via  $W^\pm$  and  $Z$  bosons and the vertex factors are depicted in Figure (3.2). The constants  $g_z$  and  $g_w$  can be expressed in terms of the Weinberg angle,  $\theta_W$ , and the fine structure constant,  $\alpha$ , as;

$$\begin{aligned}
g_z &= \frac{\sqrt{\alpha}}{\sin \theta_W \cos \theta_W}, \\
g_w &= \frac{\sqrt{\alpha}}{\sin \theta_W},
\end{aligned} \tag{3.30}$$

where  $\alpha = \frac{e^2}{4\pi}$ . Moreover the mass of the electroweak gauge bosons are related as;

$$\frac{m_W}{m_Z} = \cos \theta_W \tag{3.31}$$

and the Fermi coupling constant is defined as;

$$G_F \equiv \frac{\sqrt{2}}{8} \frac{g_z^2}{m_Z^2} \equiv \frac{\sqrt{2}}{8} \frac{g_w^2}{m_W^2}. \tag{3.32}$$

The propagator for  $W$  and  $Z$  bosons in unitary gauge are,

$$D_{\mu\nu} = \frac{-i(g_{\mu\nu} - q_\mu q_\nu / M^2)}{q^2 - M^2}, \tag{3.33}$$

where  $q$  is the four-momentum transfer and  $M$  is  $m_Z$  or  $m_W$ . At low energy limit ( $q^2 \ll M^2$ ), the propagator of the massive vector boson reduces to

$$D_{\mu\nu} = \frac{i g_{\mu\nu}}{M^2}. \tag{3.34}$$

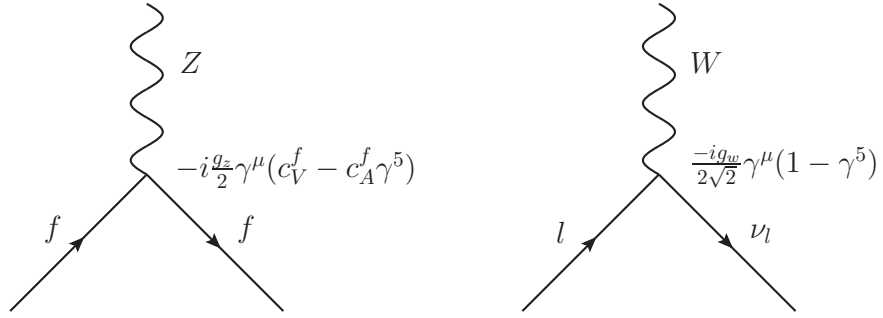


Figure 3.2: The electroweak vertex factors are shown for the neutral and charged currents. Here  $f$  corresponds to any lepton or quark and the values of  $c_V$  and  $c_A$  are shown in Table (3.1).

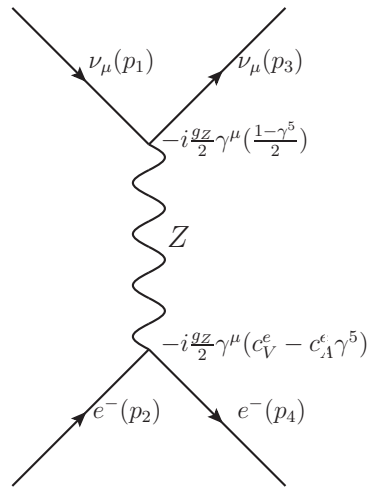


Figure 3.3: Feynman Diagram of  $\nu_\mu - e^-$  scattering is depicted. Interaction takes place via neutral current exchange only.

Now we are in a position to calculate the amplitude for neutrino-electron scattering. Let us first start our calculations with  $\nu_\mu - e^-$  scattering.

### 3.2.1 The $\nu_\mu - e^-$ Scattering

$\nu_\mu - e^-$  scattering in the Standard Model takes place via  $Z$  boson exchange only. The Feynman diagram of the interaction with the related vertex factors are shown in Figure (3.3).

By following the Feynman rules one can write the amplitude of the interaction for low

energies as follows.

$$-i\mathcal{M}_{\nu\mu-e^-} = \left[ \bar{u}(p_3) \frac{-ig_z}{2} \gamma^\mu (c_V^\nu - c_A^\nu \gamma^5) u(p_1) \right] \frac{ig_{\mu\nu}}{m_Z^2} \left[ \bar{u}(p_4) \frac{-ig_z}{2} \gamma^\nu (c_V^e - c_A^e \gamma^5) u(p_2) \right], \quad (3.35)$$

where  $c_V^e$ ,  $c_A^e$ ,  $c_V^\nu$ ,  $c_A^\nu$  are the coupling constants. Once we simplify we can write the amplitude as,

$$\mathcal{M}_{\nu\mu-e^-} = \frac{g_z^2}{4m_Z^2} \left[ \bar{u}(p_3) \gamma^\mu (c_V^\nu - c_A^\nu \gamma^5) u(p_1) \right] \left[ \bar{u}(p_4) \gamma_\mu (c_V^e - c_A^e \gamma^5) u(p_2) \right]. \quad (3.36)$$

To calculate the cross section, we need  $|\mathcal{M}|^2$ . Performing summation over spins of final particles we get,

$$\begin{aligned} \sum_{spins} |\mathcal{M}|_{\nu\mu-e^-}^2 &= \sum_{spins} \frac{g_z^4}{16m_Z^4} \left[ \bar{u}(p_3) \gamma^\mu (c_V^\nu - c_A^\nu \gamma^5) u(p_1) \right] \left[ \bar{u}(p_3) \gamma^\mu (c_V^\nu - c_A^\nu \gamma^5) u(p_1) \right]^* \\ &\quad \left[ \bar{u}(p_4) \gamma_\mu (c_V^e - c_A^e \gamma^5) u(p_2) \right] \left[ \bar{u}(p_4) \frac{-ig_z}{2} \gamma_\mu (c_V^e - c_A^e \gamma^5) u(p_2) \right]^* \end{aligned} \quad (3.37)$$

Using the Casimir's identities, we can write the above equation in terms of traces as,

$$\sum_{spins} |\mathcal{M}|_{\nu\mu-e^-}^2 = \frac{g_z^4}{16m_Z^4} Tr[\Gamma_1(p_1 + m_1) \bar{\Gamma}_2(p_3 + m_3)] Tr[\Gamma_3(p_2 + m_2) \bar{\Gamma}_4(p_4 + m_4)], \quad (3.38)$$

where,

$$\begin{aligned} \Gamma_1 &= \gamma^\mu (c_V^\nu - c_A^\nu \gamma^5), \\ \Gamma_2 &= \gamma^\nu (c_V^\nu - c_A^\nu \gamma^5), \\ \Gamma_3 &= \gamma_\mu (c_V^e - c_A^e \gamma^5), \\ \Gamma_4 &= \gamma_\nu (c_V^e - c_A^e \gamma^5), \end{aligned} \quad (3.39)$$

and  $\bar{\Gamma}$  is defined as,

$$\bar{\Gamma} \equiv \gamma^0 \Gamma^\dagger \gamma^0. \quad (3.40)$$

Hence,  $\bar{\Gamma}_2$  and  $\bar{\Gamma}_4$  can be performed as;

$$\begin{aligned} \bar{\Gamma}_2 &= \gamma^0 (\Gamma_2)^\dagger \gamma^0 \\ &= \gamma^0 [\gamma^\nu (c_V^\nu - c_A^\nu \gamma^5)]^\dagger \gamma^0 \\ &= \gamma^0 (c_V^\nu - c_A^\nu \gamma^5)^\dagger (\gamma^\nu)^\dagger \gamma^0. \end{aligned} \quad (3.41)$$

Since,  $(\gamma^5)^\dagger = \gamma^5$  and  $\{\gamma^\mu, \gamma^5\} = 0$  we get,

$$\begin{aligned}\bar{\Gamma}_2 &= (c_V^\nu + c_A^\nu \gamma^5) \gamma^0 (\gamma^\nu)^\dagger \gamma^0, \\ \bar{\Gamma}_2 &= (c_V^\nu + c_A^\nu \gamma^5) \gamma^\nu,\end{aligned}\tag{3.42}$$

where we have used the property  $\gamma^0 (\gamma^\nu)^\dagger \gamma^0 = \gamma^\nu$ .

Similarly for  $\bar{\Gamma}_4$ , we find;

$$\bar{\Gamma}_4 = (c_V^e + c_A^e \gamma^5) \gamma_\nu.\tag{3.43}$$

Using Equations (3.42) and (3.43), Equation (3.38) turns out to be,

$$\begin{aligned}\sum_{spins} |\mathcal{M}|^2 &= \frac{g_z^4}{16m_Z^4} \overbrace{Tr[\gamma^\mu (c_V^\nu - c_A^\nu \gamma^5) (\not{p}_1 + m_1) (c_V^\nu + c_A^\nu \gamma^5) \gamma^\nu (\not{p}_3 + m_3)]}^{T_1} \\ &\quad \times \underbrace{Tr[\gamma_\mu (c_V^e - c_A^e \gamma^5) (\not{p}_2 + m_2)] (c_V^e + c_A^e \gamma^5) \gamma_\nu (\not{p}_4 + m_4)}_{T_2}\end{aligned}\tag{3.44}$$

First, let us evaluate the following trace that we denoted as  $T_1$ ,

$$T_1 = Tr[\gamma^\mu (c_V^\nu - c_A^\nu \gamma^5) (\not{p}_1 + m_1) (c_V^\nu + c_A^\nu \gamma^5) \gamma^\nu (\not{p}_3 + m_3)].\tag{3.45}$$

Once we expand Equation (3.45) and use the identity  $Tr(A + B) = Tr(A) + Tr(B)$ , we get,

$$T_1 = Tr[\gamma^\mu (c_V^\nu - c_A^\nu \gamma^5) \not{p}_1 (c_V^\nu + c_A^\nu \gamma^5) \gamma^\nu \not{p}_3]\tag{3.46a}$$

$$+ m_1 Tr[\gamma^\mu (c_V^\nu - c_A^\nu \gamma^5) (c_V^\nu + c_A^\nu \gamma^5) \gamma^\nu \not{p}_3]\tag{3.46b}$$

$$+ m_3 Tr[\gamma^\mu (c_V^\nu - c_A^\nu \gamma^5) \not{p}_1 (c_V^\nu + c_A^\nu \gamma^5) \gamma^\nu]\tag{3.46c}$$

$$+ m_1 m_3 Tr[\gamma^\mu (c_V^\nu - c_A^\nu \gamma^5) (c_V^\nu + c_A^\nu \gamma^5) \gamma^\nu]\tag{3.46d}$$

Moreover, to make it easy to show the calculations in details let us split  $T_1$  as;

$$T_1 = T_{11} + T_{12} + T_{13} + T_{14},\tag{3.47}$$

where

$$\begin{aligned}T_{11} &= Tr[\gamma^\mu (c_V^\nu - c_A^\nu \gamma^5) \not{p}_1 (c_V^\nu + c_A^\nu \gamma^5) \gamma^\nu \not{p}_3], \\ T_{12} &= m_1 Tr[\gamma^\mu (c_V^\nu - c_A^\nu \gamma^5) (c_V^\nu + c_A^\nu \gamma^5) \gamma^\nu \not{p}_3], \\ T_{13} &= m_3 Tr[\gamma^\mu (c_V^\nu - c_A^\nu \gamma^5) \not{p}_1 (c_V^\nu + c_A^\nu \gamma^5) \gamma^\nu], \\ T_{14} &= m_1 m_3 Tr[\gamma^\mu (c_V^\nu - c_A^\nu \gamma^5) (c_V^\nu + c_A^\nu \gamma^5) \gamma^\nu].\end{aligned}\tag{3.48}$$

Let us evaluate  $T_{11}$  first.

$$\begin{aligned}
T_{11} &= Tr[\gamma^\mu (c_V^\nu - c_A^\nu \gamma^5) \not{p}_1 (c_V^\nu + c_A^\nu \gamma^5) \gamma^\nu \not{p}_3] \\
&= Tr[\gamma^\mu (c_V^\nu - c_A^\nu \gamma^5) (c_V^\nu - c_A^\nu \gamma^5) \not{p}_1 \gamma^\nu \not{p}_3] \\
&= Tr[\gamma^\mu ((c_V^\nu)^2 - 2c_V^\nu c_A^\nu \gamma^5 + (c_A^\nu)^2) \not{p}_1 \gamma^\nu \not{p}_3] \\
&= ((c_V^\nu)^2 + (c_A^\nu)^2) Tr[\gamma^\mu \not{p}_1 \gamma^\nu \not{p}_3] - 2c_V^\nu c_A^\nu Tr[\gamma^\mu \gamma^5 \not{p}_1 \gamma^\nu \not{p}_3]
\end{aligned} \tag{3.49}$$

With the help of following trace identities,

$$Tr[\gamma^\mu \not{p}_1 \gamma^\nu \not{p}_3] = 4[p_1^\mu p_3^\nu + p_1^\nu p_3^\mu - (p_1 \cdot p_3) g^{\mu\nu}] . \tag{3.50}$$

$$\begin{aligned}
Tr[\gamma^5 \gamma^\mu \gamma^\alpha p_{1\alpha} \gamma^\nu \gamma^\beta p_{3\beta}] &= p_{1\alpha} p_{3\beta} Tr[\gamma^5 \gamma^\mu \gamma^\alpha \gamma^\nu \gamma^\beta] \\
&= 4i\epsilon^{\mu\alpha\nu\beta} p_{1\alpha} p_{3\beta} = -4i\epsilon^{\mu\nu\alpha\beta} p_{1\alpha} p_{3\beta} ,
\end{aligned} \tag{3.51}$$

$T_{11}$  becomes as;

$$T_{11} = 4((c_V^\nu)^2 + (c_A^\nu)^2)(p_1^\mu p_3^\nu + p_1^\nu p_3^\mu - (p_1 \cdot p_3) g^{\mu\nu}) - 8c_A^\nu c_V^\nu i\epsilon^{\mu\nu\alpha\beta} p_{1\alpha} p_{3\beta} . \tag{3.52}$$

For  $T_{12}$  we get

$$\begin{aligned}
T_{12} &= m_1 Tr[\gamma^\mu (c_V^\nu - c_A^\nu \gamma^5) (c_V^\nu + c_A^\nu \gamma^5) \gamma^\nu \not{p}_3] \\
&= m_1 ((c_V^\nu)^2 - (c_A^\nu)^2) Tr[\gamma^\mu \gamma^\nu \not{p}_3] = 0
\end{aligned} \tag{3.53}$$

where we have used the fact that the trace of odd number gamma matrices is zero.

Similarly for  $T_{13}$ ,

$$\begin{aligned}
T_{13} &= m_3 Tr[\gamma^\mu (c_V^\nu - c_A^\nu \gamma^5) \not{p}_1 (c_V^\nu + c_A^\nu \gamma^5) \gamma^\nu] \\
&= m_3 Tr[\gamma^\mu (c_V^\nu - c_A^\nu \gamma^5) (c_V^\nu - c_A^\nu \gamma^5) \not{p}_1 \gamma^\nu] \\
&= m_3 Tr[\gamma^\mu ((c_V^\nu)^2 + (c_A^\nu)^2 - 2c_V^\nu c_A^\nu \gamma^5) \not{p}_1 \gamma^\nu] \\
&= m_3 ((c_V^\nu)^2 + (c_A^\nu)^2) Tr[\gamma^\mu \not{p}_1 \gamma^\nu] - 2m_3 c_V^\nu c_A^\nu Tr[\gamma^\mu \gamma^5 \not{p}_1 \gamma^\nu] \\
&= 0 .
\end{aligned} \tag{3.54}$$

For  $T_{14}$  we find,

$$\begin{aligned}
T_{14} &= m_1 m_3 Tr[\gamma^\mu (c_V^\nu - c_A^\nu \gamma^5) (c_V^\nu + c_A^\nu \gamma^5) \gamma^\nu] \\
&= m_1 m_3 ((c_V^\nu)^2 - (c_A^\nu)^2) Tr[\gamma^\mu \gamma^\nu] \\
&= m_1 m_3 ((c_V^\nu)^2 - (c_A^\nu)^2) 4g^{\mu\nu}
\end{aligned} \tag{3.55}$$

Hence, putting Equations (3.52) to (3.55),  $T_1$  turns out to be equal to

$$\begin{aligned}
T_1 &= Tr[\gamma^\mu (c_V^\nu - c_A^\nu \gamma^5)(\not{p}_1 + m_1)(c_V^\nu + c_A^\nu \gamma^5)\gamma^\nu(\not{p}_3 + m_3)] \\
&= T_{11} + T_{12} + T_{13} + T_{14} \\
&= 4((c_V^\nu)^2 + (c_A^\nu)^2)(p_1^\mu p_3^\nu + p_1^\nu p_3^\mu - (p_1 \cdot p_3)g^{\mu\nu}) - 8c_A^\nu c_V^\nu i\epsilon^{\mu\nu\alpha\beta} p_{1\alpha} p_{3\beta} \\
&\quad + m_1 m_3 ((c_V^\nu)^2 - (c_A^\nu)^2) 4g^{\mu\nu} .
\end{aligned} \tag{3.56}$$

Now let us calculate the second term in Equation (3.44).

$$T_2 = Tr[\gamma_\mu (c_V^e - c_A^e \gamma^5)(\not{p}_2 + m_2)](c_V^e + c_A^e \gamma^5)\gamma_\nu(\not{p}_4 + m_4) . \tag{3.57}$$

We observe that  $T_2$  is in the same form with  $T_1$  (Equation (3.45)). One can easily see that, the expressions for  $T_2$  can be obtained from  $T_1$  with the help of following replacements.

$$\begin{aligned}
c_V^\nu &\rightarrow c_V^e, \quad c_A^\nu \rightarrow c_A^e \\
m_3 &\rightarrow m_4, \quad m_1 \rightarrow m_2 \\
\not{p}_1 &\rightarrow \not{p}_2, \quad \not{p}_3 \rightarrow \not{p}_4
\end{aligned} \tag{3.58}$$

With these replacements we obtain  $T_2$ ,

$$\begin{aligned}
T_2 &= Tr[\gamma_\mu (c_V^e - c_A^e \gamma^5)(\not{p}_2 + m_2)](c_V^e + c_A^e \gamma^5)\gamma_\nu(\not{p}_4 + m_4) \\
&= 4((c_V^e)^2 + (c_A^e)^2)(p_{2\mu} p_{4\nu} + p_{2\nu} p_{4\mu} - (p_2 \cdot p_4)g_{\mu\nu}) - 8c_A^e c_V^e i\epsilon_{\mu\nu}^{\alpha\beta} p_{2\alpha} p_{4\beta} \\
&\quad + 4m_2 m_4 ((c_V^e)^2 - (c_A^e)^2) g_{\mu\nu} .
\end{aligned} \tag{3.59}$$

In order to find  $|\mathcal{M}|^2$ , we need to multiply  $T_1$  and  $T_2$  and contract all the terms.

The multiplication  $T_1 T_2$  can be written as;

$$T_1 T_2 = (A_1^{\mu\nu} - A_2^{\mu\nu} + A_3^{\mu\nu})(B_{1\mu\nu} - B_{2\mu\nu} + B_{3\mu\nu}) \tag{3.60}$$

where

$$\begin{aligned}
A_1^{\mu\nu} &= 4((c_V^\nu)^2 + (c_A^\nu)^2)(p_1^\mu p_3^\nu + p_1^\nu p_3^\mu - (p_1 \cdot p_3)g^{\mu\nu}) , \\
A_2^{\mu\nu} &= 8c_A^\nu c_V^\nu i\epsilon^{\mu\nu\alpha\beta} p_{1\alpha} p_{3\beta} , \\
A_3^{\mu\nu} &= 4m_1 m_3 ((c_V^\nu)^2 - (c_A^\nu)^2) g^{\mu\nu} , \\
B_{1\mu\nu} &= 4((c_V^e)^2 + (c_A^e)^2)(p_{2\mu} p_{4\nu} + p_{2\nu} p_{4\mu} - (p_2 \cdot p_4)g_{\mu\nu}) , \\
B_{2\mu\nu} &= 8c_A^e c_V^e i\epsilon_{\mu\nu}^{\alpha\beta} p_{2\alpha} p_{4\beta} , \\
B_{3\mu\nu} &= 4m_2 m_4 ((c_V^e)^2 - (c_A^e)^2) g_{\mu\nu} .
\end{aligned} \tag{3.61}$$

Note that,  $A_1^{\mu\nu}$ ,  $A_3^{\mu\nu}$ ,  $B_{1\mu\nu}$  and  $B_{3\mu\nu}$  are symmetric while  $A_2^{\mu\nu}$  and  $B_{2\mu\nu}$  are anti symmetric with respect to  $\mu, \nu$  indices.

Once we expand Equation (3.60) we get,

$$\begin{aligned} T_1 T_2 &= A_1^{\mu\nu} B_{1\mu\nu} - \cancel{A_1^{\mu\nu} B_{2\mu\nu}} + A_1^{\mu\nu} B_{3\mu\nu} \\ &\quad - \cancel{A_2^{\mu\nu} B_{1\mu\nu}} + A_2^{\mu\nu} B_{2\mu\nu} - \cancel{A_2^{\mu\nu} B_{3\mu\nu}} \\ &\quad + A_3^{\mu\nu} B_{1\mu\nu} - \cancel{A_3^{\mu\nu} B_{2\mu\nu}} + A_3^{\mu\nu} B_{3\mu\nu}. \end{aligned} \quad (3.62)$$

Notice that,  $A_1^{\mu\nu} B_{2\mu\nu}$ ,  $A_3^{\mu\nu} B_{2\mu\nu}$ ,  $A_2^{\mu\nu} B_{1\mu\nu}$  and  $A_2^{\mu\nu} B_{3\mu\nu}$  terms are zero due to multiplication of symmetric and anti-symmetric tensors.

Next, we will evaluate the remaining terms in Equation (3.62) term by term.

For  $A_1^{\mu\nu} B_{1\mu\nu}$  we get,

$$\begin{aligned} A_1^{\mu\nu} B_{1\mu\nu} &= [4((c_V^\nu)^2 + (c_A^\nu)^2)(p_1^\mu p_3^\nu + p_1^\nu p_3^\mu - (p_1 \cdot p_3)g^{\mu\nu})] \\ &\quad \times [4((c_V^e)^2 + (c_A^e)^2)(p_{2\mu} p_{4\nu} + p_{2\nu} p_{4\mu} - (p_2 \cdot p_4)g_{\mu\nu})] \\ &= 16((c_V^\nu)^2 + (c_A^\nu)^2)((c_V^e)^2 + (c_A^e)^2) \\ &\quad \times [p_1^\mu p_3^\nu p_{2\mu} p_{4\nu} + p_1^\mu p_3^\nu p_{2\nu} p_{4\mu} - p_1^\mu p_3^\nu (p_2 \cdot p_4)g_{\mu\nu} \\ &\quad + p_1^\nu p_3^\mu p_{2\mu} p_{4\nu} + p_1^\nu p_3^\mu p_{2\nu} p_{4\mu} - p_1^\nu p_3^\mu (p_2 \cdot p_4)g_{\mu\nu} \\ &\quad - (p_1 \cdot p_3)g^{\mu\nu} p_{2\mu} p_{4\nu} - (p_1 \cdot p_3)p_{2\nu} p_{4\mu} g^{\mu\nu} \\ &\quad + (p_1 \cdot p_3)g^{\mu\nu} (p_2 \cdot p_4)g_{\mu\nu}]. \end{aligned} \quad (3.63)$$

In a compact form we can write

$$\begin{aligned} A_1^{\mu\nu} B_{1\mu\nu} &= 16((c_V^\nu)^2 + (c_A^\nu)^2)((c_V^e)^2 + (c_A^e)^2) \\ &\quad \times [(p_1 \cdot p_2)(p_3 \cdot p_4) + (p_1 \cdot p_4)(p_2 \cdot p_3) \\ &\quad - (p_1 \cdot p_3)(p_2 \cdot p_4) + (p_1 \cdot p_4)(p_2 \cdot p_3) + (p_1 \cdot p_2)(p_3 \cdot p_4) - (p_1 \cdot p_3)(p_2 \cdot p_4) \\ &\quad - (p_1 \cdot p_3)(p_2 \cdot p_4) - (p_1 \cdot p_3)(p_2 \cdot p_4) + 4(p_1 \cdot p_3)(p_2 \cdot p_4)] \\ &= 32((c_V^\nu)^2 + (c_A^\nu)^2)((c_V^e)^2 + (c_A^e)^2) [(p_1 \cdot p_2)(p_3 \cdot p_4) + (p_1 \cdot p_4)(p_2 \cdot p_3)]. \end{aligned} \quad (3.64)$$



For  $A_1^{\mu\nu} B_{3\mu\nu}$  we obtain

$$\begin{aligned}
A_1^{\mu\nu} B_{3\mu\nu} &= 4((c_V^\nu)^2 + (c_A^\nu)^2)(p_1^\mu p_3^\nu + p_1^\nu p_3^\mu - (p_1 \cdot p_3)g^{\mu\nu})4m_2 m_4((c_V^e)^2 - (c_A^e)^2)g_{\mu\nu} \\
&= 16m_2 m_4((c_V^\nu)^2 + (c_A^\nu)^2)((c_V^e)^2 - (c_A^e)^2)(p_1 \cdot p_3 + p_1 \cdot p_3 - 4p_1 \cdot p_3) \\
&= -32m_2 m_4((c_V^\nu)^2 + (c_A^\nu)^2)((c_V^e)^2 - (c_A^e)^2)(p_1 \cdot p_3) .
\end{aligned} \tag{3.65}$$

For  $A_2^{\mu\nu} B_{2\mu\nu}$  we find;

$$\begin{aligned}
A_2^{\mu\nu} B_{2\mu\nu} &= 8c_A^\nu c_V^\nu i \epsilon^{\mu\nu\alpha\beta} p_{1\alpha} p_{3\beta} 8c_A^e c_V^e i \epsilon_{\mu\nu}^{\alpha\beta} p_{2\alpha} p_{4\beta} \\
&= -64c_A^\nu c_V^\nu c_A^e c_V^e p_{1\alpha} p_{3\beta} p_{2\alpha} p_{4\beta} \epsilon^{\mu\nu\alpha\beta} \epsilon_{\mu\nu}^{\alpha\beta} \\
&= -64c_A^\nu c_V^\nu c_A^e c_V^e p_{1\alpha} p_{3\beta} p_{2\alpha} p_{4\beta} g^{\alpha\sigma} g^{\alpha\rho} \epsilon^{\mu\nu\alpha\beta} \epsilon_{\mu\nu\sigma\rho} \\
&= -64c_A^\nu c_V^\nu c_A^e c_V^e p_{1\alpha} p_{3\beta} p_{2\alpha} p_{4\beta} g^{\alpha\sigma} g^{\alpha\rho} (-2)(\delta_\sigma^\alpha \delta_\rho^\beta - \delta_\rho^\alpha \delta_\sigma^\beta) \\
&= 128c_A^\nu c_V^\nu c_A^e c_V^e (p_{1\alpha} p_{3\beta} p_{2\alpha} p_{4\beta} g^{\alpha\sigma} g^{\alpha\rho} \delta_\sigma^\alpha \delta_\rho^\beta - p_{1\alpha} p_{3\beta} p_{2\alpha} p_{4\beta} g^{\alpha\sigma} g^{\alpha\rho} \delta_\rho^\alpha \delta_\sigma^\beta) \\
&= 128c_A^\nu c_V^\nu c_A^e c_V^e ((p_1 \cdot p_2)(p_3 \cdot p_4) - (p_1 \cdot p_4)(p_2 \cdot p_3)) .
\end{aligned} \tag{3.66}$$

For  $A_3^{\mu\nu} B_{1\mu\nu}$  we get;

$$\begin{aligned}
A_3^{\mu\nu} B_{1\mu\nu} &= 4m_1 m_3((c_V^\nu)^2 - (c_A^\nu)^2)g^{\mu\nu} 4((c_V^e)^2 + (c_A^e)^2) \\
&\quad \times (p_{2\mu} p_{4\nu} + p_{2\nu} p_{4\mu} - (p_2 \cdot p_4)g_{\mu\nu}) \\
&= 16m_1 m_3((c_V^\nu)^2 - (c_A^\nu)^2)((c_V^e)^2 + (c_A^e)^2)(p_2 \cdot p_4 + p_2 \cdot p_4 - 4p_2 \cdot p_4) \\
&= -32m_1 m_3((c_V^\nu)^2 - (c_A^\nu)^2)((c_V^e)^2 + (c_A^e)^2)p_2 \cdot p_4 .
\end{aligned} \tag{3.67}$$

Finally for  $A_3^{\mu\nu} B_{3\mu\nu}$  we get;

$$\begin{aligned}
A_3^{\mu\nu} B_{3\mu\nu} &= 4m_1 m_3((c_V^\nu)^2 - (c_A^\nu)^2)g^{\mu\nu} 4m_2 m_4((c_V^e)^2 - (c_A^e)^2)g_{\mu\nu} \\
&= 16m_1 m_2 m_3 m_4((c_V^\nu)^2 - (c_A^\nu)^2)((c_V^e)^2 - (c_A^e)^2)g^{\mu\nu} g_{\mu\nu} \\
&= 64m_1 m_2 m_3 m_4((c_V^\nu)^2 - (c_A^\nu)^2)((c_V^e)^2 - (c_A^e)^2) .
\end{aligned} \tag{3.68}$$

Once we put these findings into Equation (3.62), we get the final result for  $T_1 T_2$  as,

$$\begin{aligned}
T_1 T_2 = & 32((c_V^\nu)^2 + (c_A^\nu)^2)((c_V^e)^2 + (c_A^e)^2)[(p_1 \cdot p_2)(p_3 \cdot p_4) + (p_1 \cdot p_4)(p_2 \cdot p_3)] \\
& - 32m_2 m_4((c_V^\nu)^2 + (c_A^\nu)^2)((c_V^e)^2 - (c_A^e)^2)(p_1 \cdot p_3) \\
& + 128c_A^\nu c_V^\nu c_A^e c_V^e((p_1 \cdot p_2)(p_3 \cdot p_4) - (p_1 \cdot p_4)(p_2 \cdot p_3)) \\
& - 32m_1 m_3((c_V^\nu)^2 - (c_A^\nu)^2)((c_V^e)^2 + (c_A^e)^2)p_2 \cdot p_4 \\
& + 64m_1 m_2 m_3 m_4((c_V^\nu)^2 - (c_A^\nu)^2)((c_V^e)^2 - (c_A^e)^2) .
\end{aligned} \tag{3.69}$$

Note that, the averaging over initial spins leads to a  $1/2$  factor instead of  $1/4$ , even though neutrinos are spin  $1/2$  particles. Since neutrinos come in a unique helicity state, i.e. helicity =  $-1$ , there will be no factor due to spin averaging of neutrinos. The  $1/2$  factor is due to spin of the electron only. Thus, we can write the result for spin averaged amplitude square as;

$$\begin{aligned}
\langle |\mathcal{M}|^2 \rangle_{\nu_\mu - e^-} = & \frac{1}{2} \frac{g_z^4}{16m_Z^4} [ \\
& 32((c_V^\nu)^2 + (c_A^\nu)^2)((c_V^e)^2 + (c_A^e)^2)[(p_1 \cdot p_2)(p_3 \cdot p_4) + (p_1 \cdot p_4)(p_2 \cdot p_3)] \\
& - 32m_2 m_4((c_V^\nu)^2 + (c_A^\nu)^2)((c_V^e)^2 - (c_A^e)^2)(p_1 \cdot p_3) \\
& + 128c_A^\nu c_V^\nu c_A^e c_V^e((p_1 \cdot p_2)(p_3 \cdot p_4) - (p_1 \cdot p_4)(p_2 \cdot p_3)) \\
& - 32m_1 m_3((c_V^\nu)^2 - (c_A^\nu)^2)((c_V^e)^2 + (c_A^e)^2)p_2 \cdot p_4 \\
& + 64m_1 m_2 m_3 m_4((c_V^\nu)^2 - (c_A^\nu)^2)((c_V^e)^2 - (c_A^e)^2)] .
\end{aligned} \tag{3.70}$$

This is the general result for the neutrino electron scattering via  $Z$  boson exchange. Coupling constants differ depending on the neutrino types. The values for  $c_V^e$ ,  $c_V^\nu$ ,  $c_A^e$  and  $c_A^\nu$  are shown in Table (3.1). Using the relevant values for the  $\nu_\mu - e^-$  scattering as  $c_V^\nu = \frac{1}{2}$  and  $c_A^\nu = \frac{1}{2}$  in  $\langle |\mathcal{M}|^2 \rangle_{\nu_\mu - e^-}$ , the last two terms in the above equation cancel as follows.

$$\begin{aligned}
\langle |\mathcal{M}|^2 \rangle_{\nu_\mu - e^-} &= \frac{1}{2} \frac{g_z^4}{16m_Z^4} 32 \left[ \right. \\
&\quad \underbrace{\left( (c_V^\nu)^2 + (c_A^\nu)^2 \right)}_{1/2} \left( (c_V^e)^2 + (c_A^e)^2 \right) \left[ (p_1 \cdot p_2)(p_3 \cdot p_4) + (p_1 \cdot p_4)(p_2 \cdot p_3) \right] \\
&\quad - m_2 m_4 \underbrace{\left( (c_V^\nu)^2 + (c_A^\nu)^2 \right)}_{1/2} \left( (c_V^e)^2 - (c_A^e)^2 \right) (p_1 \cdot p_3) \\
&\quad + 4 \underbrace{c_A^\nu c_V^\nu}_{1/4} c_A^e c_V^e \left( (p_1 \cdot p_2)(p_3 \cdot p_4) - (p_1 \cdot p_4)(p_2 \cdot p_3) \right) \\
&\quad - m_1 m_3 \left( (c_V^\nu)^2 - (c_A^\nu)^2 \right) \left( (c_V^e)^2 + (c_A^e)^2 \right) p_2 \cdot p_4 \\
&\quad \left. + 2m_1 m_2 m_3 m_4 \left( (c_V^\nu)^2 - (c_A^\nu)^2 \right) \left( (c_V^e)^2 - (c_A^e)^2 \right) \right].
\end{aligned} \tag{3.71}$$

In a more compact form, one gets

$$\begin{aligned}
\langle |\mathcal{M}|^2 \rangle_{\nu_\mu - e^-} &= \frac{1}{2} \frac{g_z^4}{16m_Z^4} 32 \frac{1}{2} \left[ \right. \\
&\quad \left. \left( (c_V^e)^2 + (c_A^e)^2 \right) \left[ (p_1 \cdot p_2)(p_3 \cdot p_4) + (p_1 \cdot p_4)(p_2 \cdot p_3) \right] \right. \\
&\quad - m_2 m_4 \left( (c_V^e)^2 - (c_A^e)^2 \right) (p_1 \cdot p_3) \\
&\quad \left. + 2c_A^e c_V^e \left( (p_1 \cdot p_2)(p_3 \cdot p_4) - (p_1 \cdot p_4)(p_2 \cdot p_3) \right) \right].
\end{aligned} \tag{3.72}$$

If we reorder the terms, we get,

$$\begin{aligned}
\langle |\mathcal{M}|^2 \rangle_{\nu_\mu - e^-} &= \frac{1}{2} \frac{g_z^4}{16m_Z^4} 32 \frac{1}{2} \left[ \right. \\
&\quad (p_1 \cdot p_2)(p_3 \cdot p_4) \underbrace{\left( (c_A^e)^2 + (c_V^e)^2 + 2c_A^e c_V^e \right)}_{(c_A^e + c_V^e)^2} \\
&\quad + (p_1 \cdot p_4)(p_2 \cdot p_3) \underbrace{\left( (c_A^e)^2 + (c_V^e)^2 - 2c_A^e c_V^e \right)}_{(c_A^e - c_V^e)^2} \\
&\quad \left. - m_2 m_4 \left( (c_V^e)^2 - (c_A^e)^2 \right) (p_1 \cdot p_3) \right].
\end{aligned} \tag{3.73}$$

Finally, the amplitude square for the  $\nu_\mu - e$  scattering turns out to be equal to;

$$\begin{aligned}
\langle |\mathcal{M}|^2 \rangle_{\nu_\mu - e^-} &= \frac{1}{2} \frac{g_z^4}{m_Z^4} \left[ \right. \\
&\quad \left. (c_A^e + c_V^e)^2 (p_1 \cdot p_2)(p_3 \cdot p_4) + (c_A^e - c_V^e)^2 (p_1 \cdot p_4)(p_2 \cdot p_3) \right. \\
&\quad \left. - m_2 m_4 \left( (c_V^e)^2 - (c_A^e)^2 \right) (p_1 \cdot p_3) \right],
\end{aligned}$$

(3.74)

Table3.1: The values of vector and axial couplings of fermions in the SM is shown.

$f$	$c_V$	$c_A$
$\nu_e, \nu_\mu, \nu_\tau$	$\frac{1}{2}$	$\frac{1}{2}$
$e, \mu, \tau$	$-\frac{1}{2} + 2 \sin^2 \theta_w$	$-\frac{1}{2}$
$u, c, t$	$\frac{1}{2} - \frac{4}{3} \sin^2 \theta_w$	$\frac{1}{2}$
$d, s, b$	$-\frac{1}{2} + \frac{2}{3} \sin^2 \theta_w$	$-\frac{1}{2}$

where  $m_2 = m_4 = m_e$  and  $m_1 = m_3 = m_\nu$ .

Notice that this result is also valid for the  $\nu_\tau - e^-$  scattering which takes place only via  $Z$  boson exchange.

### 3.2.2 The $\bar{\nu}_\mu - e^-$ Scattering

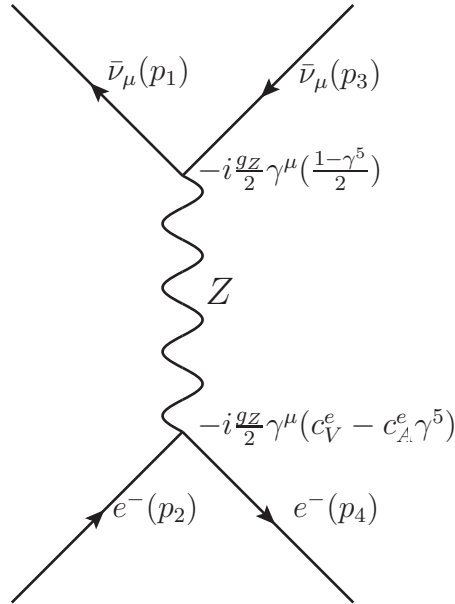


Figure 3.4: The Feynman diagram of the  $\bar{\nu}_\mu - e^-$  scattering. The interaction takes place via the exchange of  $Z$  boson.

The relevant Feynman diagram for the  $\bar{\nu}_\mu - e^-$  scattering is shown in Figure (3.4). Following the Feynman rules, the amplitude for the  $\bar{\nu}_\mu - e^-$  scattering can be written

as follows.

$$-i\mathcal{M}_{\bar{\nu}_\mu - e^-} = [\bar{\nu}(p_1) \frac{-ig_z}{2} \gamma^\mu (c_V^\nu - c_A^\nu \gamma^5) \nu(p_3)] \frac{ig_{\mu\nu}}{m_Z^2} [\bar{u}(p_4) \frac{-ig_z}{2} \gamma^\nu (c_V^e - c_A^e \gamma^5) u(p_2)] \quad (3.75)$$

Once we simplify, we get  $\mathcal{M}_{\bar{\nu}_\mu - e^-}$  as;

$$\mathcal{M}_{\bar{\nu}_\mu - e^-} = \frac{g_z^2}{4m_Z^2} [\bar{\nu}(p_1) \gamma^\mu (c_V^\nu - c_A^\nu \gamma^5) \nu(p_3)] [\bar{u}(p_4) \gamma_\mu (c_V^e - c_A^e \gamma^5) u(p_2)] . \quad (3.76)$$

However, since  $\bar{\nu}(p_1) = \bar{u}(-p_1)$  and  $\nu(p_3) = u(-p_3)$  amplitude can also be written in the following form;

$$\mathcal{M}_{\bar{\nu}_\mu - e^-} = \frac{g_z^2}{4m_Z^2} [\bar{u}(-p_1) \gamma^\mu (c_V^\nu - c_A^\nu \gamma^5) u(-p_3)] [\bar{u}(p_4) \gamma_\mu (c_V^e - c_A^e \gamma^5) u(p_2)] . \quad (3.77)$$

Remember that for the  $\nu_\mu - e^-$  scattering we found the amplitude as given in Equation (3.36);

$$\mathcal{M}_{\nu_\mu - e^-} = \frac{g_z^2}{4m_Z^2} [\bar{u}(p_3) \gamma^\mu (c_V^\nu - c_A^\nu \gamma^5) u(p_1)] [\bar{u}(p_4) \gamma_\mu (c_V^e - c_A^e \gamma^5) u(p_2)] . \quad (3.78)$$

However, if we compare the amplitudes for the  $\nu_\mu - e^-$  and  $\bar{\nu}_\mu - e^-$  (Equation (3.78) and Equation (3.77)) we figure out that once we replace  $p_1 \rightarrow -p_3$  and  $p_3 \rightarrow -p_1$  in the  $\nu_\mu - e^-$  scattering, we can find  $\langle |\mathcal{M}|^2 \rangle_{\bar{\nu}_\mu - e^-}$  for the  $\bar{\nu}_\mu - e^-$  scattering.

Note that we already found  $|\mathcal{M}|_{\nu_\mu - e^-}^2$  in Equation (3.74) as;

$$\begin{aligned} \langle |\mathcal{M}|^2 \rangle_{\nu_\mu - e^-} &= \frac{1}{2} \frac{g_z^4}{m_Z^4} [ \\ &\quad (c_A^e + c_V^e)^2 (p_1 \cdot p_2)(p_3 \cdot p_4) + (c_A^e - c_V^e)^2 (p_1 \cdot p_4)(p_2 \cdot p_3) \\ &\quad - m_2 m_4 ((c_V^e)^2 - (c_A^e)^2) (p_1 \cdot p_3) ] . \end{aligned} \quad (3.79)$$

Replacing  $p_1 \rightarrow -p_3$  and  $p_3 \rightarrow -p_1$  in Equation (3.79), we get  $|\mathcal{M}|_{\bar{\nu}_\mu - e^-}^2$  for the  $\bar{\nu}_\mu - e^-$  scattering as;

$$\begin{aligned} \langle |\mathcal{M}|^2 \rangle_{\bar{\nu}_\mu - e^-} &= \frac{1}{2} \frac{g_z^4}{m_Z^4} [ \\ &\quad (c_A^e + c_V^e)^2 ((-p_3) \cdot p_2)((-p_1) \cdot p_4) + (c_A^e - c_V^e)^2 ((-p_3) \cdot p_4)(p_2 \cdot (-p_1)) \\ &\quad - m_2 m_4 ((c_V^e)^2 - (c_A^e)^2) ((-p_3) \cdot (-p_1)) ] , \end{aligned} \quad (3.80)$$

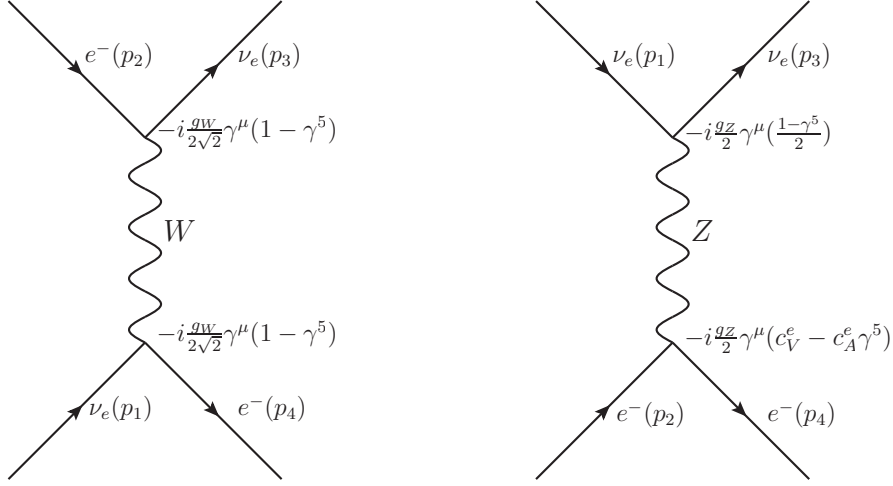


Figure 3.5: The  $\nu_e - e^-$  scattering takes place via the charged current ( $W$  boson) as well as the neutral current ( $Z$  boson) exchange.

which can further be simplified to

$$\langle |\mathcal{M}|^2 \rangle_{\bar{\nu}_\mu - e^-} = \frac{1}{2} \frac{g_z^4}{m_z^4} \left[ \begin{aligned} & (c_A^e + c_V^e)^2 (p_2 \cdot p_3)(p_1 \cdot p_4) + (c_A^e - c_V^e)^2 (p_3 \cdot p_4)(p_1 \cdot p_2) \\ & - m_2 m_4 ((c_V^e)^2 - (c_A^e)^2) (p_1 \cdot p_3) \end{aligned} \right]. \quad (3.81)$$

Once we compare Equation (3.79) and Equation (3.81) we figure out that the coefficients of  $(c_A^e + c_V^e)^2$  and  $(c_V^e - c_A^e)^2$  are exchanged while converting  $\nu_\mu - e^-$  to  $\bar{\nu}_\mu - e^-$  scattering.

### 3.2.3 The $\nu_e - e^-$ Scattering

On the contrary of the  $\nu_\mu - e^-$  scattering, the  $\nu_e - e^-$  scattering occurs via neutral  $Z$  boson as well as the charged  $W$  boson exchange diagrams as shown in Figure (3.5). The amplitude for the process can be written as,

$$\mathcal{M}_{\nu_e - e^-} = \mathcal{M}_{\nu_e - e^-}^{NC} - \mathcal{M}_{\nu_e - e^-}^{CC} \quad (3.82)$$

where the "-" sign is due to the crossing symmetry and  $NC$ ,  $CC$  corresponds to neutral and charged current respectively.

Using the Feynman rules, we can write the amplitude for the  $\nu_e - e^-$  scattering due to the neutral current as,

$$-i\mathcal{M}_{\nu_e - e^-}^{NC} = [\bar{u}(p_3) \frac{-ig_z}{2} \gamma^\mu (c_V^\nu - c_A^\nu \gamma^5) u(p_1)] \frac{ig_{\mu\nu}}{m_Z^2} [\bar{u}(p_4) \frac{-ig_z}{2} \gamma^\nu (c_V^e - c_A^e \gamma^5) u(p_2)] \quad (3.83)$$

and then can simplify it as;

$$\mathcal{M}_{\nu_e - e^-}^{NC} = \frac{g_z^2}{4m_Z^2} [\bar{u}(p_3) \gamma^\mu (c_V^\nu - c_A^\nu \gamma^5) u(p_1)] [\bar{u}(p_4) \gamma_\mu (c_V^e - c_A^e \gamma^5) u(p_2)]. \quad (3.84)$$

This matrix element is same with the amplitude for the  $\nu_\mu - e^-$  scattering as expected.

On the other hand, for the charged current interaction, following the Feynman rules we can construct the amplitude as;

$$-i\mathcal{M}_{\nu_e - e^-}^{CC} = [\bar{u}(p_4) \frac{-ig_w}{2\sqrt{2}} \gamma^\mu (1 - \gamma^5) u(p_1)] \frac{ig_{\mu\nu}}{m_W^2} [\bar{u}(p_3) \frac{-ig_w}{2\sqrt{2}} \gamma^\nu (1 - \gamma^5) u(p_2)] \quad (3.85)$$

and this can be simplified into

$$\mathcal{M}_{\nu_e - e^-}^{CC} = \frac{g_w^2}{8m_W^2} [\bar{u}(p_4) \gamma^\mu (1 - \gamma^5) u(p_1)] [\bar{u}(p_3) \gamma_\mu (1 - \gamma^5) u(p_2)]. \quad (3.86)$$

Once we use the Fierz reordering (as derived in the Appendix A) we can replace  $\bar{u}(p_4)$  and  $\bar{u}(p_3)$  so that this amplitude resembles to the amplitude of  $\nu_\mu - e^-$  scattering. Thus, we can find  $|\mathcal{M}_{\nu_e - e^-}|^2$  without performing any lengthy calculations. After the Fierz reordering (using the Equation (A.44)), we can write Equation (3.86) as,

$$\mathcal{M}_{\nu_e - e^-}^{CC} = -\frac{g_w^2}{8m_W^2} [\bar{u}(p_3) \gamma^\mu (1 - \gamma^5) u(p_1)] [\bar{u}(p_4) \gamma_\mu (1 - \gamma^5) u(p_2)]. \quad (3.87)$$

Since the parameters  $g_w$  and  $g_z$  are related with the Fermi coupling constant as shown in Equation (3.32), we can rewrite the  $CC$  and  $NC$  contributions in terms of the Fermi coupling constant ( $G_F$ ) as;

$$\mathcal{M}_{\nu_e - e^-}^{NC} = \frac{\sqrt{2}G_F}{2} [\bar{u}(p_3) \gamma^\mu (1 - \gamma^5) u(p_1)] [\bar{u}(p_4) \gamma_\mu (c_V^e - c_A^e \gamma^5) u(p_2)], \quad (3.88)$$

where we plugged the numeric values of  $c_V^\nu$  and  $c_A^\nu$  as depicted in Table (3.1). And the amplitude for the charge current can be written in terms of  $G_F$  as,

$$\mathcal{M}_{\nu_e - e^-}^{CC} = -\frac{\sqrt{2}G_F}{2} [\bar{u}(p_3) \gamma^\mu (1 - \gamma^5) u(p_1)] [\bar{u}(p_4) \gamma_\mu (1 - \gamma^5) u(p_2)]. \quad (3.89)$$

Now, we can write  $\mathcal{M}_{\nu_e - e^-}$

$$\begin{aligned}
\mathcal{M}_{\nu_e - e^-} &= \mathcal{M}_{\nu_e - e^-}^{NC} - \mathcal{M}_{\nu_e - e^-}^{CC} \\
&= \frac{\sqrt{2}G_F}{2} [\bar{u}(p_3)\gamma^\mu(1 - \gamma^5)u(p_1)] \\
&\quad \times ([\bar{u}(p_4)\gamma^\nu(c_V^e - c_A^e\gamma^5)u(p_2)] + [\bar{u}(p_4)\gamma_\mu(1 - \gamma^5)u(p_2)]) \\
&= \frac{\sqrt{2}G_F}{2} [\bar{u}(p_3)\gamma^\mu(1 - \gamma^5)u(p_1)][\bar{u}(p_4)\gamma_\mu((c_V^e + 1) - (c_A^e + 1)\gamma^5)u(p_2)].
\end{aligned} \tag{3.90}$$

Remember that we already found the matrix element,  $\mathcal{M}$ , for the  $\nu_\mu - e^-$  scattering which can be written in terms of  $G_F$  as;

$$\mathcal{M}_{\nu_\mu - e^-} = \frac{\sqrt{2}G_F}{2} [\bar{u}(p_3)\gamma^\mu(1 - \gamma^5)u(p_1)][\bar{u}(p_4)\gamma_\mu(c_V^e - c_A^e\gamma^5)u(p_2)], \tag{3.91}$$

where we used the numerical values for  $c_V^e$  and  $c_A^e$  couplings and which is obviously same with Equation (3.90).

Thus, once we compare Equation (3.90) with Equation (3.91), we realize that by replacing  $c_V^e$  to  $c_V^e + 1$  and  $c_A^e$  to  $c_A^e + 1$  in the  $\nu_\mu - e^-$  scattering, we can find  $\mathcal{M}_{\nu_e - e^-}$  for the  $\nu_e - e^-$  scattering.

Remember that, for the  $\nu_\mu - e^-$  scattering  $\langle |\mathcal{M}|^2 \rangle_{\nu_\mu - e^-}$  is given by Equation (3.74) as;

$$\begin{aligned}
\langle |\mathcal{M}|^2 \rangle_{\nu_\mu - e^-} &= \frac{1}{2} \frac{g_z^4}{m_Z^4} [ \\
&\quad (c_A^e + c_V^e)^2 (p_1 \cdot p_2)(p_3 \cdot p_4) + (c_A^e - c_V^e)^2 (p_1 \cdot p_4)(p_2 \cdot p_3) \\
&\quad - m_2 m_4 ((c_V^e)^2 - (c_A^e)^2)(p_1 \cdot p_3)].
\end{aligned} \tag{3.92}$$

Moreover if we express this in terms of  $G_F$  we get;

$$\begin{aligned}
\langle |\mathcal{M}|^2 \rangle_{\nu_\mu - e^-} &= 16G_F^2 [ \\
&\quad (c_A^e + c_V^e)^2 (p_1 \cdot p_2)(p_3 \cdot p_4) + (c_A^e - c_V^e)^2 (p_1 \cdot p_4)(p_2 \cdot p_3) \\
&\quad - m_2 m_4 ((c_V^e)^2 - (c_A^e)^2)(p_1 \cdot p_3)].
\end{aligned} \tag{3.93}$$

Replacing  $c_V^e \rightarrow c_V^e + 1$  and  $c_A^e \rightarrow c_A^e + 1$  in Equation (3.93) we get the  $\langle |\mathcal{M}|^2 \rangle$  for



the  $\nu_e - e^-$  scattering;

$$\begin{aligned}
\langle |\mathcal{M}|^2 \rangle_{\nu_e - e^-} &= 16G_F^2 [ \\
&\quad ((c_A^e + 1) + (c_V^e + 1))^2 (p_1 \cdot p_2)(p_3 \cdot p_4) \\
&\quad + ((c_A^e + 1) - (c_V^e + 1))^2 (p_1 \cdot p_4)(p_2 \cdot p_3) \\
&\quad - m_2 m_4 ((c_V^e + 1)^2 - (c_A^e + 1)^2) (p_1 \cdot p_3) ]
\end{aligned} \tag{3.94}$$

and this can be simplified as;

$$\begin{aligned}
\langle |\mathcal{M}|^2 \rangle_{\nu_e - e^-} &= \frac{1}{2} \frac{g_z^4}{m_Z^4} [ ((c_A^e + 1) + (c_V^e + 1))^2 (p_1 \cdot p_2)(p_3 \cdot p_4) \\
&\quad + (c_A^e - c_V^e)^2 (p_1 \cdot p_4)(p_2 \cdot p_3) \\
&\quad - m_2 m_4 ((c_V^e + 1)^2 - (c_A^e + 1)^2) (p_1 \cdot p_3) ] .
\end{aligned} \tag{3.95}$$

### 3.2.4 The $\bar{\nu}_e - e^-$ Scattering

The Feynman diagram of the interaction for the  $\bar{\nu}_e - e^-$  scattering is shown in Figure (3.6). Different from the  $\nu_e - e^-$  scattering, the charged current interaction occurs in the s-channel.

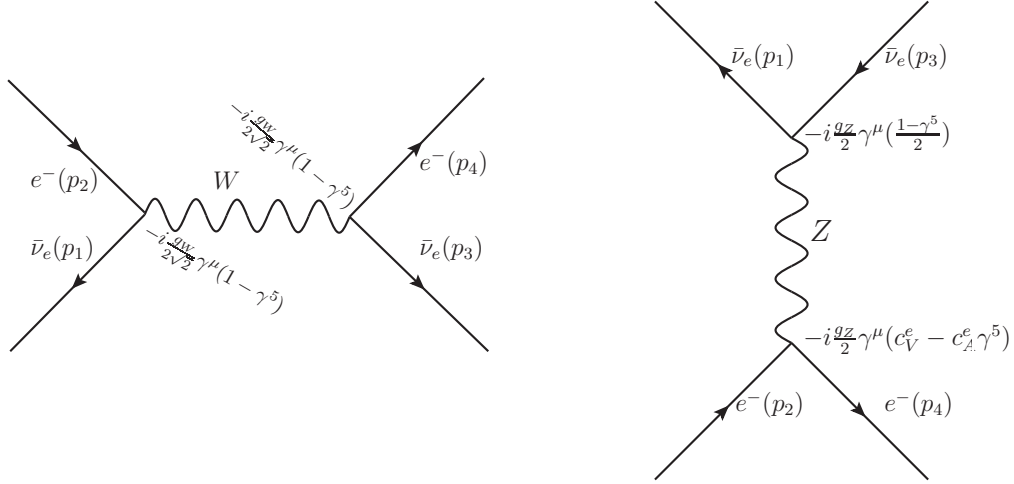


Figure 3.6: The  $\bar{\nu}_e - e^-$  scattering takes place via the charged current as well as the neutral current. However, the interaction with  $W$  boson takes place in the s-channel unlike the  $\nu_e - e^-$  scattering.

Following the Feynman rules for the  $Z$  boson exchange diagram in Figure (3.6), we

can write the amplitude

$$-i\mathcal{M}_{\bar{\nu}_e - e^-}^{NC} = [\bar{\nu}(p_1) \frac{-ig_z}{2} \gamma^\mu (c_V^\nu - c_A^\nu \gamma^5) \nu(p_3)] \frac{ig_{\mu\nu}}{m_Z^2} [\bar{u}(p_4) \frac{-ig_z}{2} \gamma^\nu (c_V^e - c_A^e \gamma^5) u(p_2)]. \quad (3.96)$$

Once we simplify, we can write the above equation as;

$$\mathcal{M}_{\bar{\nu}_e - e^-}^{NC} = \frac{g_z^2}{4m_Z^2} [\bar{\nu}(p_1) \gamma_\mu (c_V^\nu - c_A^\nu \gamma^5) \nu(p_3)] [\bar{u}(p_4) \gamma^\mu (c_V^e - c_A^e \gamma^5) u(p_2)]. \quad (3.97)$$

Using the values of  $c_V^\nu$  and  $c_A^\nu$  given in Table (3.1) and denoting the amplitude in terms of the Fermi coupling constant ( $G_F$ ), we get

$$\mathcal{M}_{\bar{\nu}_e - e^-}^{NC} = \frac{\sqrt{2}G_F}{2} [\bar{\nu}(p_1) \gamma_\mu (1 - \gamma^5) \nu(p_3)] [\bar{u}(p_4) \gamma^\mu (c_V^e - c_A^e \gamma^5) u(p_2)]. \quad (3.98)$$

Similarly, for the charged current interaction we can write  $\mathcal{M}_{\bar{\nu}_e - e^-}^{CC}$  in terms of  $G_F$  as;

$$\begin{aligned} \mathcal{M}_{\bar{\nu}_e - e^-}^{CC} &= \frac{g_W^2}{8m_W^2} [\bar{u}(p_4) \gamma_\mu (1 - \gamma^5) \nu(p_3)] [\bar{\nu}(p_1) \gamma^\mu (1 - \gamma^5) u(p_2)] \\ &= \frac{\sqrt{2}G_F}{2} [\bar{u}(p_4) \gamma_\mu (1 - \gamma^5) \nu(p_3)] [\bar{\nu}(p_1) \gamma^\mu (1 - \gamma^5) u(p_2)]. \end{aligned} \quad (3.99)$$

Using the Fierz transformation one can replace the order of  $\bar{u}(p_4)$  and  $\bar{\nu}(p_1)$  as before;

$$\mathcal{M}_{\bar{\nu}_e - e^-}^{CC} = -\frac{\sqrt{2}G_F}{2} [\bar{\nu}(p_1) \gamma_\mu (1 - \gamma^5) \nu(p_3)] [\bar{u}(p_4) \gamma^\mu (1 - \gamma^5) u(p_2)] (1 - \gamma^5) u(p_2) \quad (3.100)$$

Note that, the minus sign is due to the Fierz transformation as explained in Appendix A.

Since  $\mathcal{M}_{\bar{\nu}_e - e^-} = \mathcal{M}_{\bar{\nu}_e - e^-}^{NC} - \mathcal{M}_{\bar{\nu}_e - e^-}^{CC}$ , we can write the amplitude as;

$$\begin{aligned} \mathcal{M}_{\bar{\nu}_e - e^-} &= \frac{\sqrt{2}G_F}{2} [\bar{\nu}(p_1) \gamma_\mu (1 - \gamma^5) \nu(p_3)] \\ &\quad \times \left( [\bar{u}(p_4) \gamma^\mu ((c_V^e - c_A^e) \gamma^5) u(p_2)] + [\bar{u}(p_4) \gamma^\mu (1 - \gamma^5) u(p_2)] \right) \end{aligned} \quad (3.101)$$

and this can be simplified into;

$$\mathcal{M}_{\bar{\nu}_e - e^-} = \frac{\sqrt{2}G_F}{2} [\bar{\nu}(p_1) \gamma_\mu (1 - \gamma^5) \nu(p_3)] [\bar{u}(p_4) ((c_V^e + 1) - (c_A^e + 1) \gamma^5) u(p_2)]. \quad (3.102)$$

Moreover, since  $\bar{\nu}(p_1) = \bar{u}(-p_1)$  and  $\nu(p_3) = u(-p_3)$  Equation (3.102) can be written as;

$$\mathcal{M}_{\bar{\nu}_e - e^-} = \frac{\sqrt{2}G_F}{2} [\bar{u}(-p_1)\gamma_\mu(1-\gamma^5)u(-p_3)][\bar{u}(p_4)((c_V^e+1)-(c_A^e+1)\gamma^5)u(p_2)]. \quad (3.103)$$

With the replacements of  $p_1 \rightarrow -p_3$  and  $p_3 \rightarrow -p_1$ , this equation turns out to be same with  $\mathcal{M}_{\nu_e - e^-}$  as shown in Equation (3.90). Hence once we replace,  $p_3 \rightarrow -p_1$  and  $p_1 \rightarrow -p_3$  in  $\langle |\mathcal{M}_{\nu_e - e^-}|^2 \rangle$  in Equation (3.95), we find  $\langle |\mathcal{M}_{\bar{\nu}_e - e^-}|^2 \rangle$  as;

$$\begin{aligned} \langle |\mathcal{M}_{\bar{\nu}_e - e^-}|^2 \rangle &= \frac{1}{2} \frac{g_z^4}{m_Z^4} [((c_A^e+1) + (c_V^e+1))^2 ((-p_3) \cdot p_2)((-p_1) \cdot p_4) \\ &\quad + (c_A^e - c_V^e)^2 ((-p_3) \cdot p_4)(p_2 \cdot (-p_1)) \\ &\quad - m_2 m_4 ((c_V^e+1)^2 - (c_A^e+1)^2)((-p_3) \cdot (-p_1))] . \end{aligned} \quad (3.104)$$

After simplifications we obtain,

$$\begin{aligned} \langle |\mathcal{M}_{\bar{\nu}_e - e^-}|^2 \rangle &= \frac{1}{2} \frac{g_z^4}{m_Z^4} [((c_A^e+1) + (c_V^e+1))^2 (p_2 \cdot p_3)(p_4 \cdot p_1) \\ &\quad + (c_A^e - c_V^e)^2 (p_4 \cdot p_3)(p_2 \cdot p_1) \\ &\quad - m_2 m_4 ((c_V^e+1)^2 - (c_A^e+1)^2)(p_1 \cdot p_3)] . \end{aligned} \quad (3.105)$$

Thus, we realize that as in the comparison of the  $\bar{\nu}_\mu - e^-$  scattering with the  $\nu_\mu - e^-$  scattering, only  $(c_A^e+1 + c_V^e+1) \leftrightarrow (c_A^e - c_V^e)^2$  replacement is needed when we compared the amplitude squares for the  $\bar{\nu}_e - e^-$  scattering with the  $\nu_e - e^-$  scattering.

As a result, we have derived  $\langle |\mathcal{M}_{\nu_\alpha - e^-}|^2 \rangle$  for all types of neutrinos and it is useful to summarize our results for the neutrino electron scattering in terms of  $G_F$  for later convenience:

$$\begin{aligned}
\langle |\mathcal{M}|^2 \rangle_{\nu_{\mu(\tau)}-e^-} &= 16G_F^2 [(c_A^e + c_V^e)^2 (p_1 \cdot p_2)(p_3 \cdot p_4) \\
&\quad + (c_A^e - c_V^e)^2 (p_1 \cdot p_4)(p_2 \cdot p_3) - m_2 m_4 ((c_V^e)^2 - (c_A^e)^2)(p_1 \cdot p_3)] , \\
\langle |\mathcal{M}|^2 \rangle_{\bar{\nu}_{\mu(\tau)}-e^-} &= 16G_F^2 [(c_A^e + c_V^e)^2 (p_2 \cdot p_3)(p_1 \cdot p_4) \\
&\quad + (c_A^e - c_V^e)^2 (p_3 \cdot p_4)(p_1 \cdot p_2) - m_2 m_4 ((c_V^e)^2 - (c_A^e)^2)(p_1 \cdot -p_3)] , \\
\langle |\mathcal{M}|^2 \rangle_{\nu_e-e^-} &= 16G_f^2 [((c_A^e + 1) + (c_V^e + 1))^2 (p_1 \cdot p_2)(p_3 \cdot p_4) \\
&\quad + (c_V^e - c_A^e)^2 (p_1 \cdot p_4)(p_2 \cdot p_3) \\
&\quad - m_2 m_4 ((c_V^e + 1)^2 - (c_A^e + 1)^2)(p_1 \cdot p_3)] , \\
\langle |\mathcal{M}|^2 \rangle_{\bar{\nu}_e-e^-} &= 16G_f^2 [((c_A^e + 1) + (c_V^e + 1))^2 (p_1 \cdot p_4)(p_2 \cdot p_3) \\
&\quad + (c_V^e - c_A^e)^2 (p_1 \cdot p_2)(p_3 \cdot p_4) \\
&\quad - m_2 m_4 ((c_V^e + 1)^2 - (c_A^e + 1)^2)(p_1 \cdot p_3)] .
\end{aligned}
\tag{3.106}$$

### 3.3 The Differential Cross Section for the $\nu - e$ Scatterings

Before delving into the derivation of the cross-section formulas in terms of the recoil energy of the target particle for the neutrino electron scattering, since  $|\mathcal{M}|^2$  contains terms like  $p_1 \cdot p_2$ ,  $p_1 \cdot p_4$ ,  $p_1 \cdot p_4$ ,  $p_2 \cdot p_3$  and  $p_1 \cdot p_3$  first it is better to express these terms in terms of the recoil energy in the rest frame of initial electron. The detailed calculations are shown in Appendix B, the obtained results are summarized below.

$$\begin{aligned}
p_1 \cdot p_3 &= m_\nu^2 + m_e T \\
(p_1 \cdot p_4)(p_2 \cdot p_3) &= m_e^2 (E_1 - T)^2 \\
(p_1 \cdot p_2)(p_3 \cdot p_4) &= E_1^2 m_e^2
\end{aligned}
\tag{3.107}$$

Using these relations in Equation (3.106), we find  $\langle |\mathcal{M}|^2 \rangle$  in terms of the recoil energy

of the electron in the lab frame as follows.

$$\begin{aligned}
\langle |\mathcal{M}|^2 \rangle_{\nu_\mu - e^-} &= 16G_F^2 [ \\
&\quad (c_A^e + c_V^e)^2 E_1^2 m_e^2 + (c_A^e - c_V^e)^2 m_e^2 (E_1 - T)^2 \\
&\quad - m_e^2 ((c_V^e)^2 - (c_A^e)^2) (m_\nu^2 + m_e T) ] \\
\langle |\mathcal{M}|^2 \rangle_{\bar{\nu}_\mu - e^-} &= 16G_F^2 [ \\
&\quad (c_A^e + c_V^e)^2 m_e^2 (E_1 - T)^2 + (c_A^e - c_V^e)^2 E_1^2 m_e^2 \\
&\quad - m_e^2 ((c_V^e)^2 - (c_A^e)^2) (m_\nu^2 + m_e T) ] \\
\langle |\mathcal{M}|^2 \rangle_{\nu_e - e^-} &= 16G_f^2 [ \\
&\quad ((c_A^e + 1) + (c_V^e + 1))^2 E_1^2 m_e^2 + (c_V^e - c_A^e)^2 m_e^2 (E_1 - T)^2 \\
&\quad - m_e^2 ((c_V^e + 1)^2 - (c_A^e + 1)^2) (m_\nu^2 + m_e T) ] \\
\langle |\mathcal{M}|^2 \rangle_{\bar{\nu}_e - e^-} &= 16G_f^2 [ \\
&\quad ((c_A^e + 1) + (c_V^e + 1))^2 m_e^2 (E_1 - T)^2 + (c_V^e - c_A^e)^2 m_e^2 E_1^2 \\
&\quad - m_e^2 ((c_V^e + 1)^2 - (c_A^e + 1)^2) (m_\nu^2 + m_e T) ]
\end{aligned} \tag{3.108}$$

Remember that in the rest frame of the electron we already derived the differential cross section with respect to the recoil energy of the electron in Equation (3.29) as

$$\frac{d\sigma}{dT} = |\mathcal{M}|^2 \frac{1}{32\pi m_e |\vec{p}_1|^2} \tag{3.109}$$

and when we neglect the mass of neutrino then  $E_1 = |\vec{p}_1|$  and we have;

$$\frac{d\sigma}{dT} = |\mathcal{M}|^2 \frac{1}{32\pi m_e E_1^2} . \tag{3.110}$$

Once we put  $|\mathcal{M}|^2$  from Equation (3.108) into Equation (3.110), we find the differential cross section with respect to the recoil energy ( $\frac{d\sigma}{dT}$ ) for the neutrino electron scattering as;

$$\begin{aligned}
\left(\frac{d\sigma}{dT}\right)_{\nu_\mu - e^-} &= |\mathcal{M}|^2 \frac{1}{32\pi m_e E_1^2} \\
&= \frac{G_F^2 m_e}{2\pi} \times \\
&\quad \left[ (c_A^e + c_V^e)^2 + (c_A^e - c_V^e)^2 \left(1 - \frac{T}{E_1}\right)^2 - ((c_V^e)^2 - (c_A^e)^2) \frac{m_e T}{E_1^2} \right],
\end{aligned} \tag{3.111}$$

$$\begin{aligned}
\left(\frac{d\sigma}{dT}\right)_{\bar{\nu}_\mu - e^-} &= |\mathcal{M}|^2 \frac{1}{32\pi m_e E_1^2} \\
&= \frac{G_F^2 m_e}{2\pi} \times \\
&\quad \left[ (c_A^e + c_V^e)^2 \left(1 - \frac{T}{E_1}\right)^2 + (c_A^e - c_V^e)^2 - ((c_V^e)^2 - (c_A^e)^2) \left(\frac{m_e T}{E_1^2}\right) \right],
\end{aligned} \tag{3.112}$$

$$\begin{aligned}
\left(\frac{d\sigma}{dT}\right)_{\nu_e - e^-} &= |\mathcal{M}|^2 \frac{1}{32\pi m_e E_1^2} \\
&= \frac{G_F^2 m_e}{2\pi} \left[ ((c_A^e + 1) + (c_V^e + 1))^2 + (c_V^e - c_A^e)^2 \left(1 - \frac{T}{E_1}\right)^2 \right. \\
&\quad \left. - ((c_V^e + 1)^2 - (c_A^e + 1)^2) \left(\frac{m_e T}{E_1^2}\right) \right],
\end{aligned} \tag{3.113}$$

$$\begin{aligned}
\left(\frac{d\sigma}{dT}\right)_{\bar{\nu}_e - e^-} &= |\mathcal{M}|^2 \frac{1}{32\pi m_e E_1^2} \\
&= \frac{G_F^2 m_e}{2\pi} \left[ ((c_A^e + 1) + (c_V^e + 1))^2 \left(1 - \frac{T}{E_1}\right)^2 + (c_V^e - c_A^e)^2 \right. \\
&\quad \left. - ((c_V^e + 1)^2 - (c_A^e + 1)^2) \left(\frac{m_e T}{E_1^2}\right) \right].
\end{aligned} \tag{3.114}$$

Expressing  $c_V^e, c_A^e$  in terms of the Weinberg angle ( $\sin^2\theta_W$ ) and using the values shown in Table (3.1), we can collect all these cross-section formulas in more compact form with the following redefinitions;

$$\begin{aligned}
a &= \frac{c_V^e + c_A^e}{2} = \sin^2\theta_W - \frac{1}{2}, \\
b &= \frac{c_V^e - c_A^e}{2} = \sin^2\theta_W.
\end{aligned} \tag{3.115}$$

Table3.2: The parameters  $a$  and  $b$  in the SM cross section expression in Equation (3.116).  $\alpha$  corresponds to  $\mu$  or  $\tau$ .

Process	$a$	$b$
$\nu_e - e^- \rightarrow \nu_e - e^-$	$\sin^2 \theta_w + \frac{1}{2}$	$\sin^2 \theta_w$
$\bar{\nu}_e - e^- \rightarrow \bar{\nu}_e - e^-$	$\sin^2 \theta_w$	$\sin^2 \theta_w + \frac{1}{2}$
$\nu_\alpha e^- \rightarrow \nu_\alpha e^-$	$\sin^2 \theta_w - \frac{1}{2}$	$\sin^2 \theta_w$
$\bar{\nu}_\alpha e^- \rightarrow \bar{\nu}_\alpha e^-$	$\sin^2 \theta_w$	$\sin^2 \theta_w - \frac{1}{2}$

Hence, the cross-sections for the  $\nu - e^-$  scatterings can be expressed as,

$$\left[ \frac{d\sigma}{dT}(\nu e^- \rightarrow \nu e^-) \right]_{\text{SM}} = \frac{2G_F^2 m_e}{\pi E_\nu^2} \left( a^2 E_\nu^2 + b^2 (E_\nu - T)^2 - ab m_e T \right) \quad (3.116)$$

where the values of  $a$  and  $b$  are shown in Table (3.2).

The recoil energy of the electron depends on the energy of the incoming neutrino and gets its maximum value when the neutrino scatters in backward direction, which means the angle between  $\vec{p}_3$  and  $\vec{p}_4$  is  $180^\circ$  in Figure (3.1). The maximum recoil energy is found as (See Appendix C for detailed calculations.)

$$T_{\text{max}} = \frac{2E_1^2}{m_e + 2E_1} . \quad (3.117)$$

In addition, once we solve this equation for  $E_1$ , we find the minimum energy of neutrino necessary to give the electron a recoil energy  $T$ .

$$E_{\nu_{\text{min}}} = \frac{T + \sqrt{T^2 + 2Tm_e}}{2} . \quad (3.118)$$

The plot for  $T_{\text{max}}$  vs  $E_\nu$  is shown in Figure (3.7). The diagram shows that as  $E_\nu \gg m_e$  then maximum recoil energy equals to the energy of the incoming neutrino ( $T_{\text{max}} \cong E_\nu$ ). However for low energy neutrinos, the difference between  $E_\nu$  and  $T_{\text{max}}$  becomes so apparent.

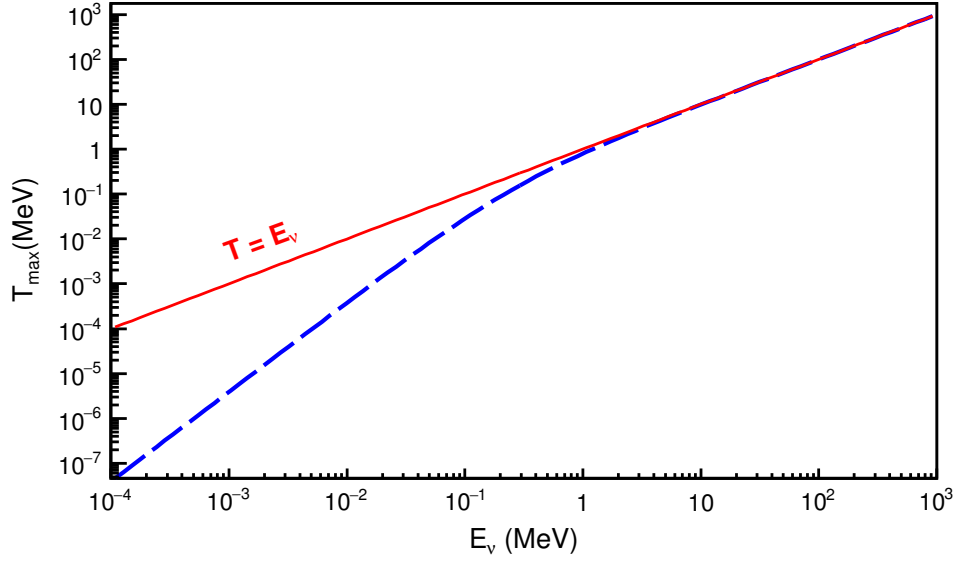


Figure 3.7: Dependence of the maximum recoil energy of the electron with respect to the incoming neutrino energy is demonstrated.

For fixed incoming neutrino energy  $E_\nu = 10$  MeV, spectrum of the recoil energy for each type of neutrinos are shown in Figure (3.8) by taking into account the limiting values mentioned above. The tough part of a neutrino experiment is always reducing the background. It is not possible to have the chance to measure the all range of the recoil energy of electron. Every experiment has its own threshold energy for which signal can be discriminated from the background. Depending on the purpose of the physics program and experimental set-up, each experiment has its own threshold energy some of which are explained in the following chapter.

In order to measure the total cross section, we need to integrate Equation (3.116) over the recoil energy from the threshold energy ( $T_{th}$ ) to the maximum recoil energy ( $T_{max}$ ). As a result, we obtain;

$$\begin{aligned}
\sigma(\nu e^- \rightarrow \nu e^-) &= \int_{T_{th}}^{T_{max}} \frac{2G_F^2 m_e}{\pi E_\nu^2} \left( a^2 E_\nu^2 + b^2 (E_\nu - T)^2 - ab m_e T \right) dT \\
&= \frac{2G_F^2 m_e}{\pi E_\nu^2} \left[ a^2 E_\nu^2 T - b^2 \frac{(E_\nu - T)^3}{3} - \frac{ab m_e T^2}{2} \right]_{T_{th}}^{T_{max}} \\
&= \frac{2G_F^2 m_e}{\pi E_\nu^2} \left( a^2 E_\nu^2 (T_{max} - T_{th}) - \frac{b^2}{3} \left( (E_\nu - T_{max})^3 - (E_\nu - T_{th})^3 \right) \right. \\
&\quad \left. - \frac{ab m_e}{2} (T_{max}^2 - T_{th}^2) \right),
\end{aligned} \tag{3.119}$$



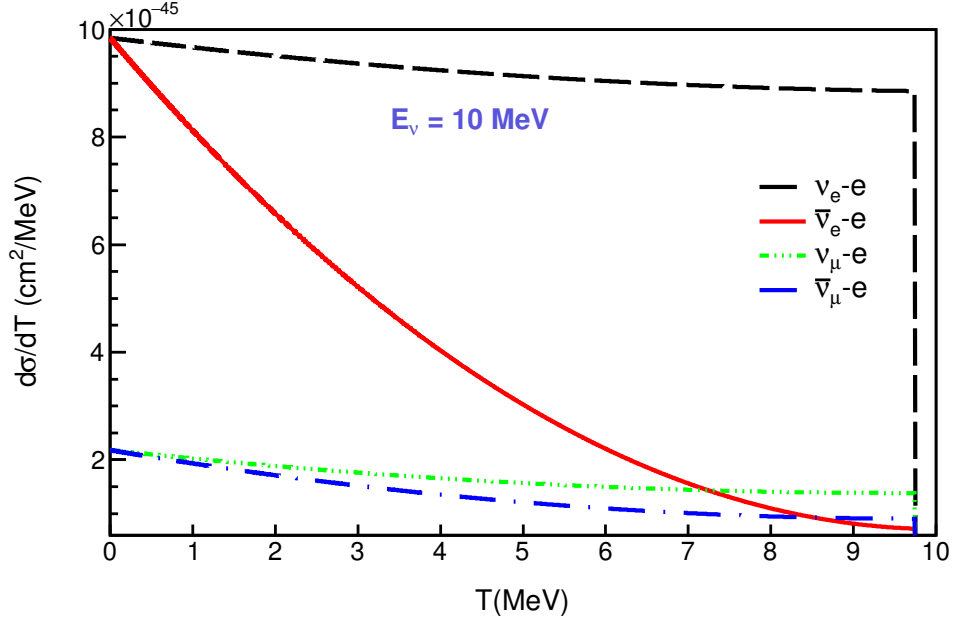


Figure 3.8: The recoil energy spectra of the  $\nu - e$  scattering for the incident neutrino energy  $E_\nu = 10$  MeV is shown.

where  $T_{max}$  is given in Equation (3.117). Let us simplify the above expression. Since,

$$\begin{aligned} (E_\nu - T_{max})^3 &= E_\nu^3 - 3E_\nu^2 T_{max} + 3E_\nu T_{max}^2 - T_{max}^3 \\ (E_\nu - T_{th})^3 &= E_\nu^3 - 3E_\nu^2 T_{th} + 3E_\nu T_{th}^2 - T_{th}^3 \end{aligned} \quad (3.120)$$

we can write,

$$(E_\nu - T_{max})^3 - (E_\nu - T_{th})^3 = -3E_\nu^2(T_{max} - T_{th}) + 3E_\nu(T_{max}^2 - T_{th}^2) - (T_{max}^3 - T_{th}^3). \quad (3.121)$$

Putting Equation (3.121) into Equation (3.119) we get for the total cross-section for the neutrino-electron scattering equals to

$$\begin{aligned} \sigma(\nu e^- \rightarrow \nu e^-) &= \frac{2G_F^2 m_e}{\pi E_\nu^2} \left( a^2 E_\nu^2 (T_{max} - T_{th}) - \frac{b^2}{3} (-3E_\nu^2 (T_{max} - T_{th}) \right. \\ &\quad \left. + 3E_\nu (T_{max}^2 - T_{th}^2) - (T_{max}^3 - T_{th}^3)) - \frac{abm_e}{2} (T_{max}^2 - T_{th}^2) \right). \end{aligned} \quad (3.122)$$

And this can be put into more compact form as;

$$\boxed{\sigma(\nu e^- \rightarrow \nu e^-) = \frac{2G_F^2 m_e}{\pi} \left( (a^2 + b^2)(T_{max} - T_{th}) - \left( b^2 + \frac{abm_e}{2E_\nu} \right) \frac{(T_{max}^2 - T_{th}^2)}{E_\nu} + \frac{b^2}{3} \frac{(T_{max}^3 - T_{th}^3)}{E_\nu^2} \right). \quad (3.123)$$

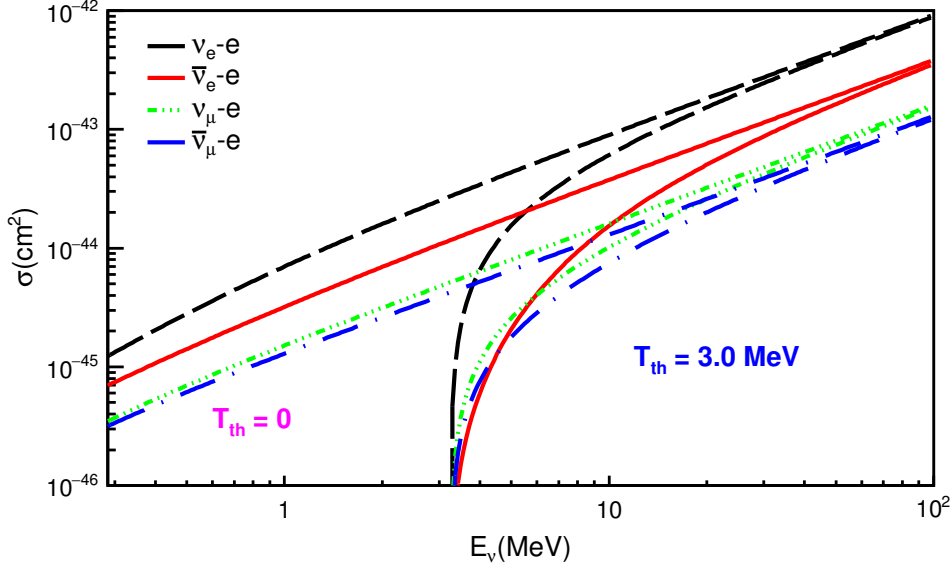


Figure 3.9: The neutrino electron scattering with respect to the incoming neutrino energy,  $E_\nu$  is shown for two cases. In the first case, we neglected the threshold value, i.e.  $T_{th} = 0$ , which is practically impossible (left side of the Figure). In the second case 3 MeV threshold value is used, which is generally the range for the reactor neutrino experiments (right side of the Figure).

One needs to take into account of the threshold values of each experiment for comparison of the Standard Model prediction with the data. The cross-section values with respect to the energy of incoming neutrinos are shown in Figure (3.9) for  $T_{th} = 0$  and  $T_{th} = 3 \text{ MeV}$ .

### 3.4 Neutrino Electron Scattering for High Energy Neutrinos

For high energetic neutrinos, ( $E_\nu \gg m_e$ ) the differential cross section is in general denoted in terms of inelasticity parameter,  $y = \frac{T}{E_\nu}$  (which is also called as the Bjorken variable). With the replacements of  $y = \frac{T}{E_\nu}$  and hence,  $dT = E_\nu dy$ , Equation (3.116) can be written as;

$$\left[ \frac{d\sigma}{dy} (\nu e^- \rightarrow \nu e^-) \right]_{\text{SM}} = \frac{2G_F^2 m_e E_\nu}{\pi} \left( a^2 + b^2(1-y)^2 - ab \frac{m_e}{E_\nu} y \right). \quad (3.124)$$

Note that for high energetic neutrinos ( $E_\nu \gg m_e$ ), from Equation (3.117) we deduce that  $T_{\text{max}} \simeq E_\nu$  and thus,  $y$  can take values in the range  $0 \leq y \leq 1$ . Moreover, for

high energy neutrinos the last term in Equation (3.124) ( $ab\frac{m_e}{E_\nu}y$ ) can be neglected and we can write the neutrino-electron scattering cross section in terms of the Bjorken variable  $y$  as;

$$\boxed{\left[\frac{d\sigma}{dy}(\nu e^- \rightarrow \nu e^-)\right]_{\text{SM}} = \frac{2G_F^2 m_e E_\nu}{\pi} (a^2 + b^2(1-y)^2)}. \quad (3.125)$$

Especially for the accelerator neutrinos this approximation works well.

Integrating Equation (3.125) we can obtain the total cross section

$$\begin{aligned} \left[\sigma(E_\nu)(\nu e^- \rightarrow \nu e^-)\right]_{\text{SM}} &= \int_0^1 \frac{2G_F^2 m_e E_\nu}{\pi} (a^2 + b^2(1-y)^2) dy \\ &= \frac{2G_F^2 m_e E_\nu}{\pi} \left[ a^2 y + b^2 \left( y - y^2 + \frac{y^3}{3} \right) \right]_0^1 \\ &= \frac{2G_F^2 m_e E_\nu}{\pi} \left( a^2 + \frac{1}{3} b^2 \right). \end{aligned} \quad (3.126)$$

Let us denote the overall constant  $\frac{2G_F^2 m_e}{\pi}$  as  $\sigma_0$ .

$$\sigma_0 = \frac{2G_F^2 m_e}{\pi} = 1.72 \times 10^{-44} \text{ cm}^2/\text{MeV} \quad (3.127)$$

With this notation Equation (3.126) becomes

$$\left[\sigma(E_\nu)(\nu e^- \rightarrow \nu e^-)\right]_{\text{SM}} = \sigma_0 E_\nu \left( a^2 + \frac{1}{3} b^2 \right). \quad (3.128)$$

Since the cross section (for  $E_\nu \gg m_e$ ) depends on the energy of incoming neutrino explicitly, we can find the numerical value for the total cross sections in terms of the incoming neutrino energy once we use the numerical values for  $a$  and  $b$  from Table (3.2) as;

$$\boxed{\begin{aligned} \sigma_{\nu_e - e^-} &= 9.27 \times 10^{-45} (E_\nu/\text{MeV}) \text{ cm}^2, \\ \sigma_{\bar{\nu}_e - e^-} &= 3.84 \times 10^{-45} (E_\nu/\text{MeV}) \text{ cm}^2, \\ \sigma_{\nu_\mu - e^-} &= 1.61 \times 10^{-45} (E_\nu/\text{MeV}) \text{ cm}^2, \\ \sigma_{\bar{\nu}_\mu - e^-} &= 1.29 \times 10^{-45} (E_\nu/\text{MeV}) \text{ cm}^2. \end{aligned}} \quad (3.129)$$

Note that, we used  $\sin^2 \theta_w = 0.2223$  to obtain the above results and the cross-section value for  $\nu_\tau - e^-$  scattering is same with the  $\nu_\mu - e^-$ .

### 3.5 The Neutrino Electron Scattering With Respect to the Scattering Angle of Electron

The scattering angle of the electrons can also be measured in experiments. In this case relevant quantity becomes the differential cross-section over the scattering angle, i.e.  $\frac{d\sigma}{d\cos\theta}$ . Relating the electron recoil energy with the scattering angle, we can find  $\frac{d\sigma}{d\cos\theta}$  as follows.

Using the energy momentum conservation for the scattering process (see Figure (3.1)) we obtain

$$\begin{aligned} p_1 - p_4 &= p_3 - p_2 \\ (p_1 - p_4)^2 &= (p_3 - p_2)^2 . \end{aligned} \quad (3.130)$$

Since  $m_1 = m_3 = m_\nu$  and  $m_2 = m_4 = m_e$  we find

$$\begin{aligned} p_1^2 + p_4^2 + 2p_1 \cdot p_4 &= p_3^2 + p_2^2 + 2p_3 \cdot p_2 \\ m_1^2 + m_4^2 + 2p_1 \cdot p_4 &= m_3^2 + m_2^2 + 2p_3 \cdot p_2 \\ 2p_1 \cdot p_4 &= 2p_3 \cdot p_2 \\ p_1 \cdot p_4 &= p_3 \cdot p_2 \end{aligned} \quad (3.131)$$

In the rest frame of the electron, (we can take it as also the lab frame since the energy of target electrons are so small that we can assume they are at rest in the lab frame) we have;  $E_2 = m_e$  and  $\vec{p}_2 = 0$ . Then we get;

$$\begin{aligned} E_1 E_4 - \vec{p}_1 \cdot \vec{p}_4 &= E_3 \underbrace{E_2}_{m_e} - \vec{p}_3 \cdot \vec{p}_2 \\ E_1 E_4 - |\vec{p}_1| |\vec{p}_4| \cos \theta &= E_3 m_e \\ E_1 E_4 - E_1 |\vec{p}_4| \cos \theta &= E_3 m_e \end{aligned} \quad (3.132)$$

Note that, once we neglect the mass of neutrinos then;  $E_\nu = |\vec{p}_1|$ . We can write the energy of the electron after the interaction in terms of the recoil energy ( $T$ ) as  $E_4 = m_e + T$ . Moreover,  $E_3$  can be written in terms of the recoil energy (see Equation (3.23)).

$$E_3 = E_1 - T . \quad (3.133)$$

Furthermore, we can write  $|\vec{p}_4|$  in terms of  $T$  using the dispersion relation as follows.

$$\begin{aligned}
|\vec{p}_4|^2 &= E_4^2 - m_4^2 \\
|\vec{p}_4|^2 &= (E_4 - m_e)(E_4 + m_e) \\
|\vec{p}_4|^2 &= T(T + 2m_e) \\
|\vec{p}_4| &= \sqrt{T(T + 2m_e)}.
\end{aligned} \tag{3.134}$$

Hence, once we put Equations (3.133) and (3.134) into Equation (3.132), we obtain

$$\begin{aligned}
E_1 E_4 - E_1 |\vec{p}_4| \cos \theta &= E_3 m_e \\
E_1(T + m_e) - E_1 \sqrt{T(T + 2m_e)} \cos \theta &= (E_1 - T)m_e \\
E_1 T + m_e E_1 - E_1 \cos \theta \sqrt{T(T + 2m_e)} &= m_e E_1 - m_e T \\
T(E_1 + m_e) &= E_1 \cos \theta \sqrt{T(T + 2m_e)}
\end{aligned} \tag{3.135}$$

Now let us square both sides to find  $T$  in terms of  $\cos \theta$ .

$$\begin{aligned}
T^2(E_1 + m_e)^2 &= E_1^2 \cos^2 \theta T(T + 2m_e) \\
T(E_1 + m_e)^2 &= E_1^2 \cos^2 \theta (T + 2m_e) \\
T(E_1 + m_e)^2 &= E_1^2 T \cos^2 \theta + 2m_e E_1^2 \cos^2 \theta \\
T((E_1 + m_e)^2 - E_1^2 \cos^2 \theta) &= 2m_e E_1^2 \cos^2 \theta \\
T &= \frac{2m_e E_1^2 \cos^2 \theta}{(E_1 + m_e)^2 - E_1^2 \cos^2 \theta},
\end{aligned} \tag{3.136}$$

where  $\theta$  is the scattering angle of the electron as shown in Figure (3.1). Note that for the maximum recoil energy,  $\theta = 180$ . If we put this into Equation (3.136) we get

$$\begin{aligned}
T_{max} &= \frac{2m_e E_1^2}{(E_1 + m_e)^2 - E_1^2} \\
&= \frac{2m_e E_1^2}{m_e(m_e + 2E_\nu)} \\
&= \frac{2E_1^2}{(m_e + 2E_\nu)}.
\end{aligned} \tag{3.137}$$

as we already derived in the Appendix (see Equation (C.9)). From Equation (3.136)

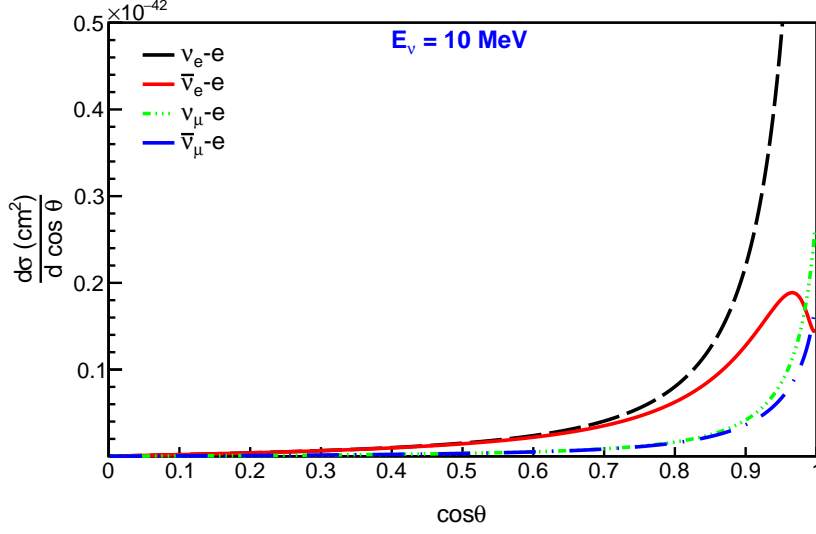


Figure 3.10: The differential cross section for the neutrino electron scattering with respect to the scattering angle of the electron is shown for all neutrino flavors as well as anti-neutrinos.

we can find  $dT$  as;

$$\begin{aligned}
 T &= \frac{2m_e E_1^2 \cos^2 \theta}{(E_1 + m_e)^2 - E_1^2 \cos^2 \theta} \\
 dT &= 2m_e E_1^2 \left( \frac{2 \cos \theta d(\cos \theta) ((E_1 + m_e)^2 - E_1^2 \cos^2 \theta) - (-2E_1^2 \cos \theta d(\cos \theta)) (\cos^2 \theta)}{((E_1 + m_e)^2 - E_1^2 \cos^2 \theta)^2} \right) \\
 dT &= \frac{4m_e E_1^2 \left( (E_1 + m_e)^2 - E_1^2 \cos^2 \theta + E_1^2 \cos^2 \theta \right)}{((E_1 + m_e)^2 - E_1^2 \cos^2 \theta)^2} \cos \theta d(\cos \theta) \\
 dT &= \frac{4m_e E_1^2 (E_1 + m_e)^2}{((E_1 + m_e)^2 - E_1^2 \cos^2 \theta)^2} \cos \theta d(\cos \theta)
 \end{aligned} \tag{3.138}$$

Once we put Equations (3.136) and (3.138) into Equation (3.116) we can transform the cross section  $\frac{d\sigma}{dT}$  to  $\frac{d\sigma}{d \cos \theta}$  as following;

$$\begin{aligned}
 \left[ \frac{d\sigma}{dT} (\nu e^- \rightarrow \nu e^-) \right]_{\text{SM}} &= \frac{2G_F^2 m_e}{\pi E_\nu^2} \left( a^2 E_\nu^2 + b^2 (E_\nu - T)^2 - ab m_e T \right), \\
 \frac{d\sigma}{d \cos \theta} &= \frac{4m_e E_\nu^2 (E_\nu + m_e)^2}{((E_\nu + m_e)^2 - E_\nu^2 \cos^2 \theta)^2} \cos \theta \frac{2G_F^2 m_e}{\pi E_\nu^2} \left( \right. \\
 &\quad \left. a^2 E_\nu^2 + b^2 \left( E_\nu - \frac{2m_e E_\nu^2 \cos^2 \theta}{(E_\nu + m_e)^2 - E_\nu^2 \cos^2 \theta} \right)^2 - ab m_e \frac{2m_e E_\nu^2 \cos^2 \theta}{(E_\nu + m_e)^2 - E_\nu^2 \cos^2 \theta} \right).
 \end{aligned} \tag{3.139}$$

This can be simplified into;

$$\frac{d\sigma}{d\cos\theta} = \frac{8G_F^2 m_e^2}{\pi} \frac{(E_\nu + m_e)^2 \cos\theta}{((E_\nu + m_e)^2 - E_\nu^2 \cos^2\theta)^2} \left( a^2 E_\nu^2 + b^2 \left( E_\nu - \frac{2m_e E_\nu^2 \cos^2\theta}{(E_\nu + m_e)^2 - E_\nu^2 \cos^2\theta} \right)^2 - ab \frac{2m_e^2 E_\nu^2 \cos^2\theta}{(E_\nu + m_e)^2 - E_\nu^2 \cos^2\theta} \right). \quad (3.140)$$

Cross section with respect to the scattering angle of the electron is depicted in Figure (3.10). We can infer that most of the electrons are scattered in the forward direction.





## CHAPTER 4

### $\nu - e$ SCATTERING EXPERIMENTS

For searching the dark photon effects as well as for the tracks of non-commutative space effects in neutrino interactions, we preferred analyzing data of several experiments; TEXONO and GEMMA, which are reactor neutrino experiments, BOREXINO, which is a solar neutrino experiment and LSND and CHARM II, in which neutrinos are produced at accelerators. This choice was due to the different energy ranges of neutrinos as well as characteristic threshold energies for the recoil electrons in each experiment.

Since, we are going to search the new physics effects in these experiments, a brief information about the characteristic properties of the experiments would be useful and in this chapter they are summarized.

#### 4.1 TEXONO

TEXONO (Taiwan Experiment On Neutrino) collaboration was initiated in 1997 to conduct experiments at low energy neutrino as well as astrophysics. Collaboration consists of institutes from Taiwan, China, India and Turkey. The main focus of the collaboration is searching the interactions of neutrinos in low energy regime with high-Z nuclei detectors such as solid state devices and scintillating crystals [61].

Kuo-Sheng Neutrino Laboratory is established 28m far from one of the two cores of the Kuo-Sheng Nuclear Power Station (KSNPS). For a schematic view of the station see Figure (4.1). The nuclear reactor has a 2.9 GW nominal thermal output and the

## Kuo-Sheng Nuclear Power Station : Reactor Building

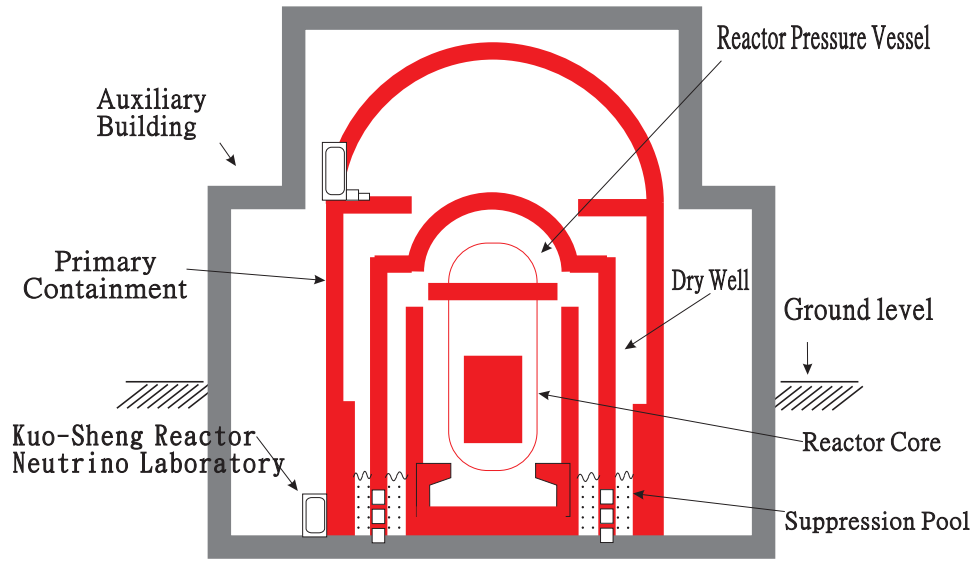


Figure 4.1: The schematic view of the KSNPS is shown (Figure is adapted from [62]).

laboratory is located 10 meter below the ground level with an overburden of 30 m.w.e (meter water equivalent).

The volume of  $100\text{ cm} \times 80\text{ cm} \times 75\text{ cm}$  is used as multi-purpose inner target detector space. Two different detectors are located in this space and data is taken simultaneously with these different detectors (See Figure (4.2)). The space is shielded with a 50 ton material as depicted in Figure (4.3). The 2.5 cm thick plastic scintillators are established in the outer part of the shielding material with photo-multiplier tubes in order to veto cosmic-ray events. From outside to inside, 15cm thick lead, 5cm thick steel, 25 cm polyethylene with boron-loaded and 5 cm of OFHC copper is used as the shielding material which enables the attenuation of the gamma-ray background as well as the ambient neutron.

The source of the neutrinos are the beta decay of radioactive nuclei hence, the neutrinos are  $\bar{\nu}_e$ . Average flux of  $\bar{\nu}_e$  from KSNPS is  $6.4 \times 10^{12}\text{cm}^{-2}\text{ s}^{-1}$  and the spectrum of  $\bar{\nu}_e$  for a typical nuclear power station is depicted in Figure (4.4). The vast amount of anti-neutrinos are due to fission of  $^{235}\text{U}$ ,  $^{238}\text{U}$ ,  $^{239}\text{Pu}$  and  $^{241}\text{Pu}$  which are the major elements in the reactor fuel. In addition to these major fission decays, hundreds of daughter nuclei whose properties are not well known are involved in the process also

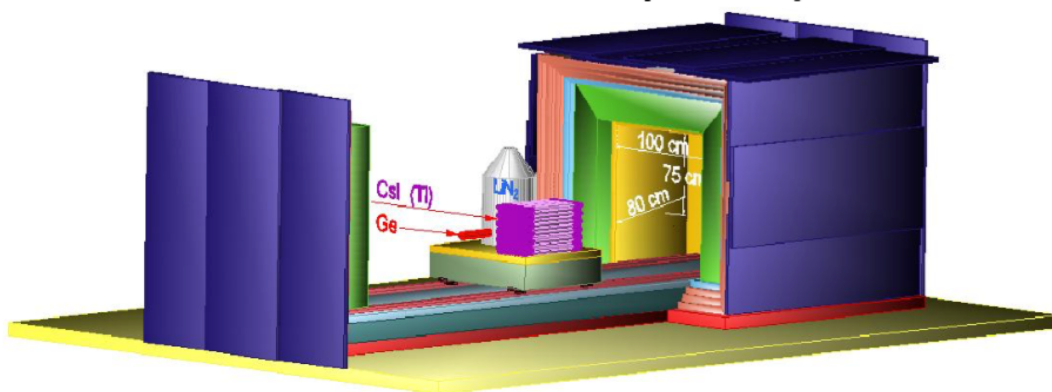


Figure 4.2: Two different detectors are placed in the shielded space (Figure is adapted from [62]).

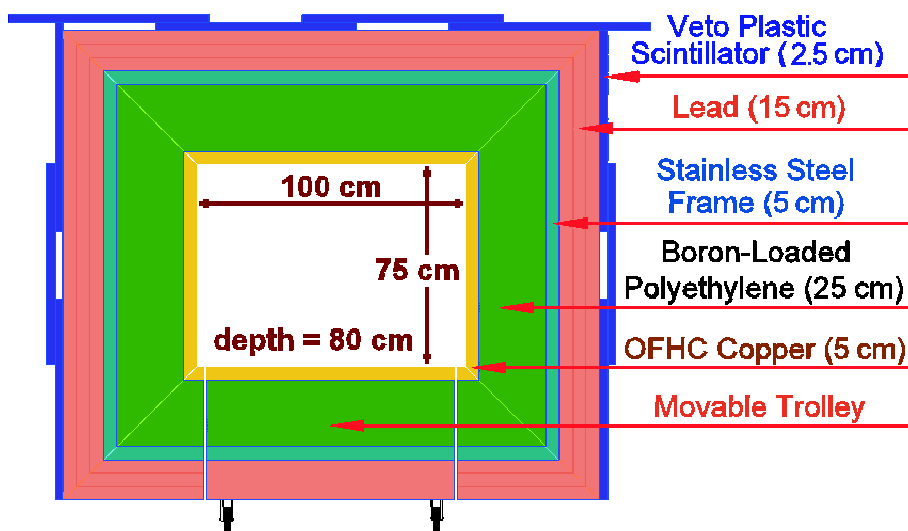


Figure 4.3: The schematic view of the shielding design of the TEXONO collaboration (Figure is adapted from [62]).

and this makes it difficult to calculate the flux of anti-neutrinos emitted from nuclear reactors accurately. There is still debate of the discrepancy between measured and calculated flux of neutrinos which would mimic existence of sterile neutrinos [63, 64, 65]. The uncertainties in spectrum of neutrinos limit the cross-section measurements of neutrino electron scatterings [66].

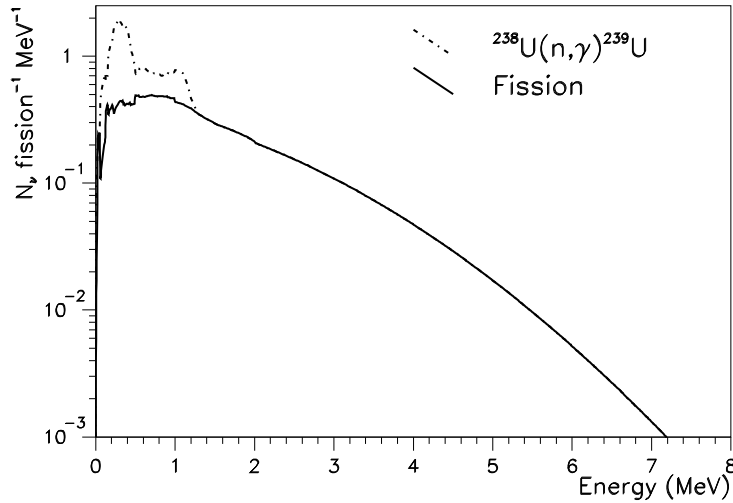


Figure 4.4: Typical  $\bar{\nu}_e$  spectrum for reactor neutrinos is shown (Figure is adapted from [62]).

Reactor is off almost for 50 days in every 18 months for cleaning and refueling and this time is very crucial for measuring the background signals. Three different data sets of the Texono collaboration is used for this thesis and a brief information is given below for these experiments.

### 1. CsI(Tl) Scintillating Crystal Array:

Neutrino interactions are rare, hence large-target mass detectors are needed for detection. However, as the mass of the target material increases it becomes difficult to search low energy region due to background issues. Studies reveal that, crystal scintillators can be used at the keV-MeV range for low background experiments [67].

Collaboration used CsI(Tl) scintillating crystals (with % 0.15 admixture of Tl) as both the target and the detector. The crystals are packed in an array with a total mass of 187 kg as shown in Figure (4.5). The crystals are in hexagonal shape with 2 cm side and 40 cm length so that there is not any space left and the

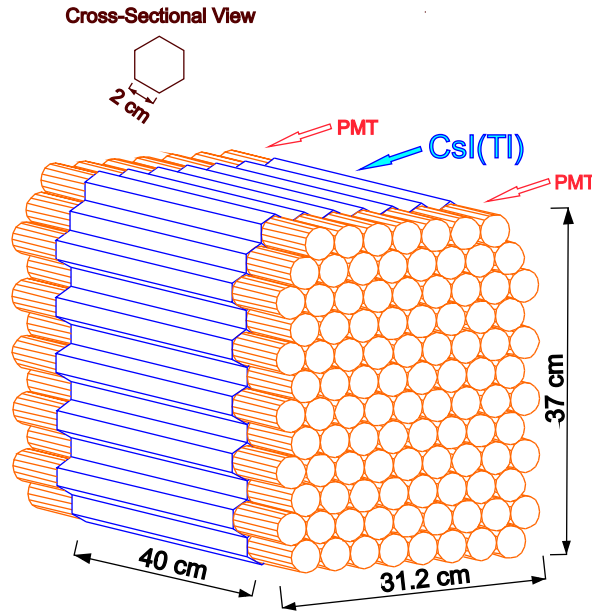


Figure 4.5: The schematic view for the scintillating crystals are shown. The signals are recorded with PMTs at both ends (Figure is adapted from [62]).

detector is compact. Using the information recorded by PMTs at the end of the crystals, the energy and the position of the event can be measured.

With this experimental set up, total of 29882 kg-day collected-data when reactor was on and 7369 kg-day recorded-data when reactor was in off position combined to search neutrino interactions. The measured quantity is the recoil energy of the electrons and the achieved analysis recoil energy range of the electrons are 3 – 8 MeV with CsI(Tl) scintillating crystals. The measured spectrum in terms of event rate ( $\text{day}^{-1} \text{kg}^{-1} \text{MeV}^{-1}$ ) vs recoil energy of the electron (T) is shown in Figure (4.6). With this data, TEXONO measured the Weinberg angle and put constraints for the magnetic moment of neutrinos as well as the charge radius square of the neutrino [62].

## 2. High-Purity Germanium Detector (HPGe)

In order to search for the magnetic moment of neutrinos, the low recoil energy region should be investigated due to the characteristic form of the cross section. As shown in Figure (4.7), the cross-section increases as the recoil energies are lowered. For this purpose, scintillating crystal detectors can not be used since the measured quantity is two back-scattering photons and therefore the threshold energy is around MeV. On the other hand, high purity germanium detectors

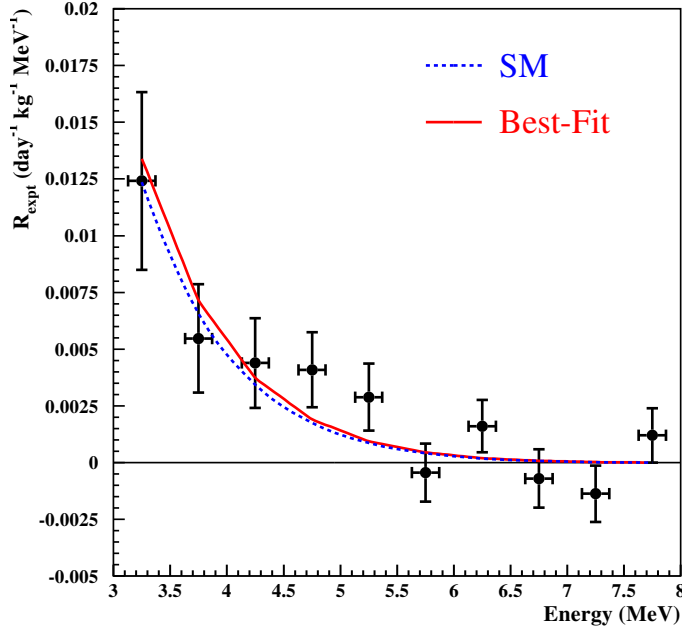


Figure 4.6: Measured event rate with respect to the recoil energy is shown with the SM prediction is fitted (Figure is adapted from [62]).

(HPGe) having excellent energy resolution makes it a good choice to search low recoil energy region and hence the neutrino magnetic moment [68].

The schematic view of the detector set-up is shown in Figure (4.8). 1.06 kg of HPGe is surrounded by detector system named as anti-compton veto (ACV) which comprises of three parts. 5 cm thickness of NaI(Tl) detector is located under 7 cm thick of CsI(Tl) which is directly connected to PMTs as active light guide consists of the first part. The second part is consisted of 5 cm thickness of ring detector located at the joint of the cryostat and 4 cm thick of CsI comprises the third part as a base detector. This whole set-up is located in the same volume with the CsI(Tl) scintillating crystal arrays as shown in Figure (4.2).

Analyzing 570.7 days Reactor ON and 127.8 days Reactor OFF data, the spectrum for the  $\bar{\nu}_e - e$  shown in Figure (4.9) is acquired with analysis threshold 12 keV. With this data, a direct limit is set for the magnetic moment of  $\bar{\nu}_e$  as  $\mu_{\bar{\nu}_e} < 7.4 \times 10^{-11} \mu_B$  at 90% C.L. [69].

### 3. N-type Point Contact Germanium Detector (NPCGe) :

Another detector used by the collaboration to search neutrino properties is the n-type point contact Ge detector (NPCGe). Using germanium detectors, the

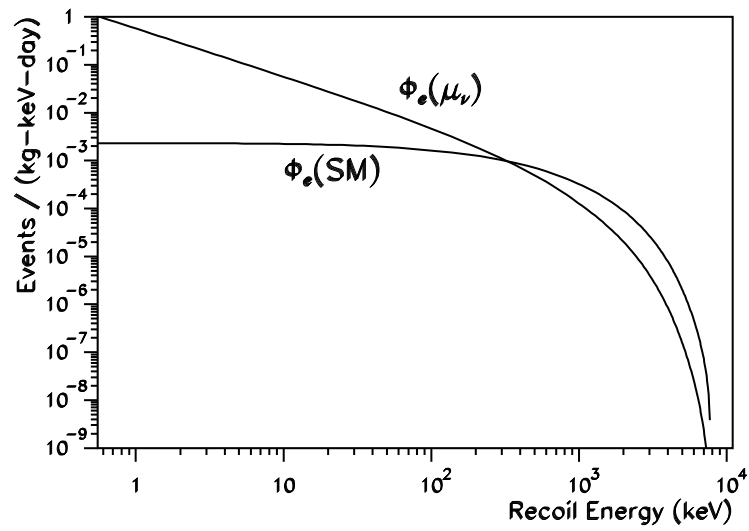


Figure 4.7: The spectrum for a  $\bar{\nu}_e = 10^{13} \text{ cm}^{-2} \text{ s}^{-1}$  is shown with SM and magnetic moments at  $\mu_\nu = 10^{-10} \mu_B$  (Figure is adapted from [69]).

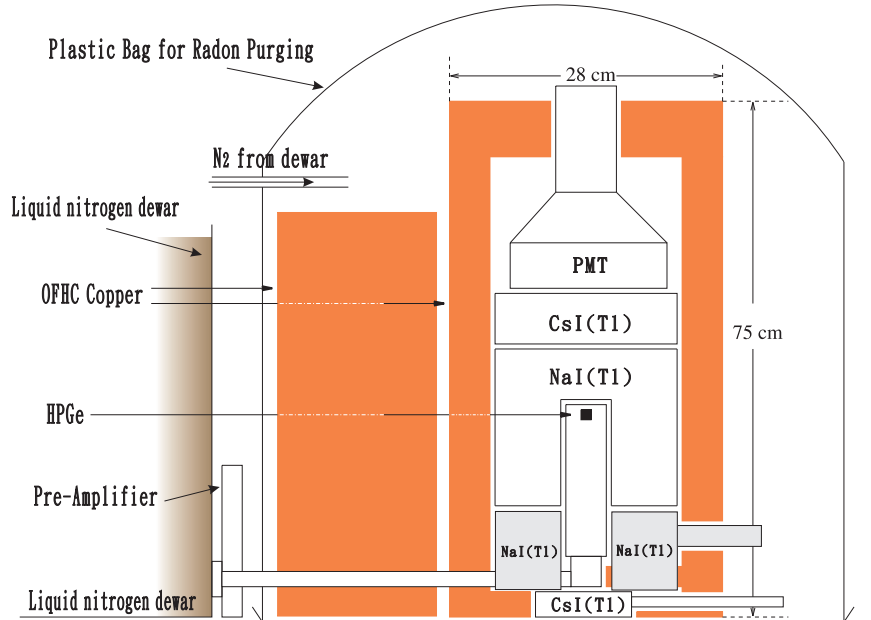


Figure 4.8: The schematic view of the experiment with its inner shieldings is shown for HPGe detector (Figure is adapted from [69]).

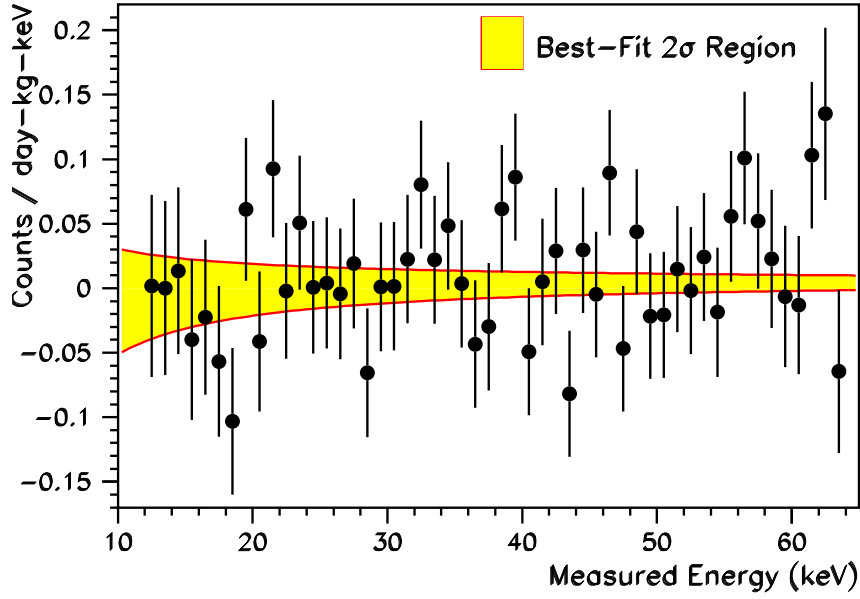


Figure 4.9: The residual spectrum is depicted with respect to recoil energy (Figure is adapted from [69]).

analysis threshold is aimed to be lowered ( $\mathcal{O} \sim 100$  eV) to search the dark matter as well as the neutrino magnetic moment and neutrino nucleus coherent scattering [70]. The experimental set-up is shown in Figure (4.10). With this set-up 300 eV analysis threshold is achieved with 500 g fiducial mass NPCGe detector. With 124.2 days Reactor ON and 70.3 days Reactor OFF data, bounds are set for neutrino mili-charge as  $|\delta_Q| < 1.0 \times 10^{-12}$  [71].

Table4.1: Key parameters of the TEXONO experiments are summarized.

Experiments	$\sin^2\theta_W$	$\mu_\nu$ ( $\mu_B$ ) (90% C.L. upper limit)	Reactor ON/OFF (kg-days)	Analysis Range
CsI(Tl)	$0.251 \pm 0.039$	$2.2 \times 10^{-10}$	29882/7369	3 – 8 MeV
HPGe	-	$7.4 \times 10^{-11}$	570.7/127.8	12 – 65 keV
NPCGe	-	$2.6 \times 10^{-10}$	124.2/70.3	0.3 – 12.4 keV



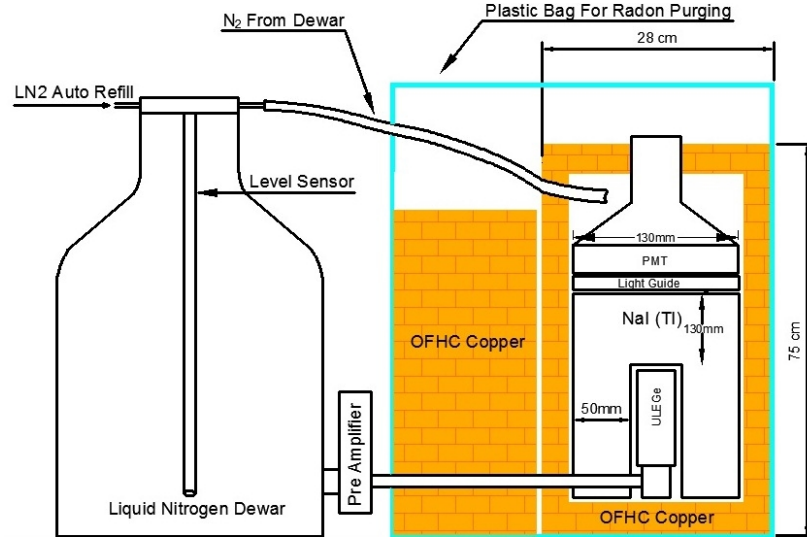


Figure 4.10: The schematic view of the experimental set-up for the NPCGe is shown with its shielding structure (Figure is adapted from [72]).

## 4.2 GEMMA

GEMMA (**G**ermanium **E**xperiment for measurement of **M**agnetic **M**oment Antineutrino) collaboration aimed to measure the magnetic moment of neutrino using high-purity Ge detectors as the TEXONO collaboration. The experiment is located near the Kalinin Nuclear Power Plant (KNPP), located about 200 km north west of Moscow. The core of the reactor has 3 GW power and anti-neutrino flux produced is  $2.7 \times 10^{13} \text{ cm}^{-2}\text{s}^{-1}$ . 1.5 kg HPGe with its shielding materials are located at a distance of 13.9 m from the reactor core with an overburden of 70 m.w.e as shown in Figure (4.12). To reduce the background, germanium detector is located inside NaI crystals which are covered by 14 cm thick walls and which is also surrounded by electrolytic copper and lead with 15 cm thick. This experimental design (active & passive shielding) enables to reduce the external  $\gamma$  background.

GEMMA collaboration has been taking data since 2005 and using 755.6 days Reactor ON and 187 days Reactor OFF data, bound on the neutrino magnetic moment at 90% CL is set as [75],

$$\mu_\nu < 2.9 \times 10^{-11} \mu_B,$$

which is the world best upper limit for the magnetic moment of neutrinos [76]. The

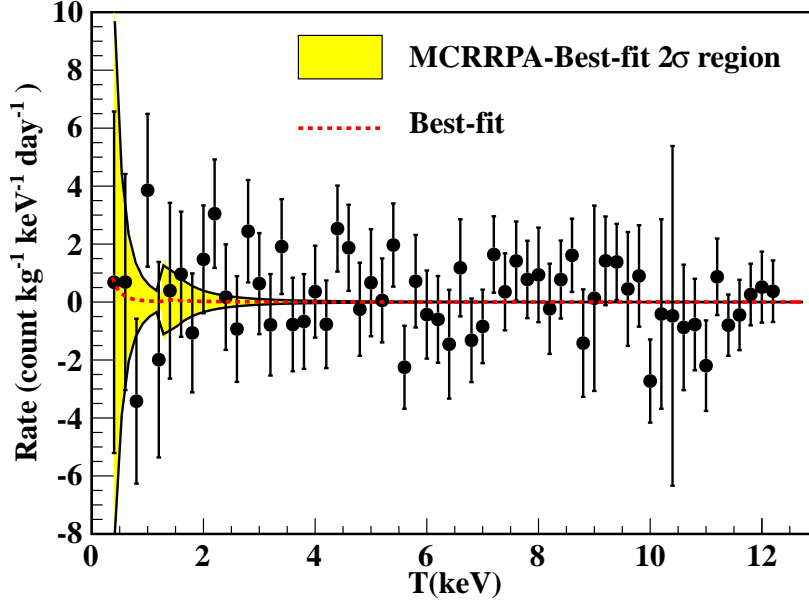


Figure 4.11: The Reactor ON-OFF data taken by NPCGe detector is shown with respect to recoil energy. The fitted region is for the analysis of  $\bar{\nu}_e$  millicharge (Figure is adapted from [73]).

analysis range of the recoil energy of the electron is 2.8 keV – 55 keV.

### 4.3 LSND

LSND (**L**iquid **S**ciintillator **N**eutrino **D**etector) is located at Los Alamos National Laboratory (LANL) and operated between 1993-1998. Even though the main scientific direction of the LSND collaboration was searching for neutrino oscillation ( $\bar{\nu}_\mu \rightarrow \bar{\nu}_e$ ), using the advantage of the experimental set-up, the measurement of electroweak parameters are also done once the cross-section of neutrino-electron elastic scattering ( $\nu_e + e^- \rightarrow \nu_e + e^-$ ) is measured.

LSND can be considered as an accelerator experiment since the neutrinos are produced at Los Alamos Meson Physics Facility (LAMPF). Protons with an energy of 800 MeV impinged on a beam dump and mesons, mostly pions ( $\pi^+$ ), are produced. These stopped pions decay into muons and muon-neutrinos ( $\pi^+ \rightarrow \mu^+ + \nu_\mu$ ). Moreover, produced muons stop and decay into electron and neutrinos too ( $\mu^+ \rightarrow e^+ + \nu_e + \bar{\nu}_\mu$ ). Thus, the neutrino beam consists of three kinds,  $\nu_\mu$ ,  $\bar{\nu}_\mu$  and  $\nu_e$ . The energy of the

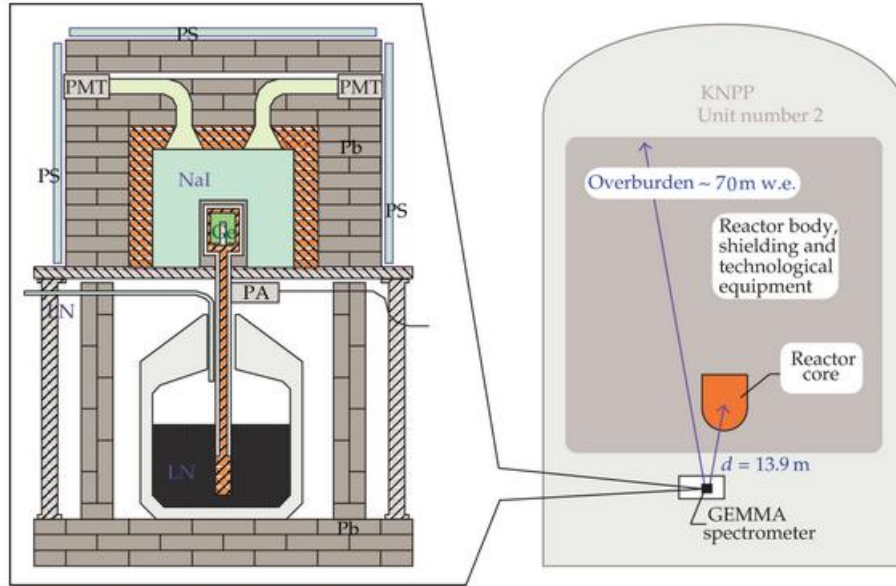


Figure 4.12: The schematic view of the GEMMA Experiment with its shielding structure is shown (Figure is adapted from [74]).

produced neutrinos are in the range of 20 – 55 MeV.

On the other hand, when protons hit on the targets,  $\pi^-$  mesons are also produced and decays into muons as well. In this case  $\bar{\nu}_e$  is produced from the decay of muon ( $\mu^- \rightarrow e^- + \bar{\nu}_e + \nu_\mu$ ). However,  $\pi^-$  and  $\mu^-$  are absorbed in the beam stop materials before they decay, hence the  $\bar{\nu}_e$  background is highly suppressed which is very crucial to detect oscillation.

The produced neutrinos are detected by a cylindrical detector filled with 167 tons of mineral oil and surrounded by 1220 phototubes (See Figure (4.14)). This detector was located 30 meter far from the beam dumb as depicted in Figure (4.15). The observation of  $\bar{\nu}_e + p \rightarrow e^+ + n$  would mean the oscillation of anti-muon neutrinos into anti-electron neutrinos. The detector signal is expected to be the Cherenkov and scintillation light due to positron first and later on due to neutron capture process ( $n + p \rightarrow d + \gamma$ ). The energy of the emitted  $\gamma$  is expected to be 2.2 MeV. LSND collaboration observed  $87.9 \pm 22.4 \pm 6.0$  excess  $\bar{\nu}_e$  events over the background and consistent with the  $\bar{\nu}_e + p \rightarrow e^+ + n$  interactions [77, 78]. This observation does not fit with the oscillation model with three neutrino flavours and called as LSND anomaly in literature and to explain

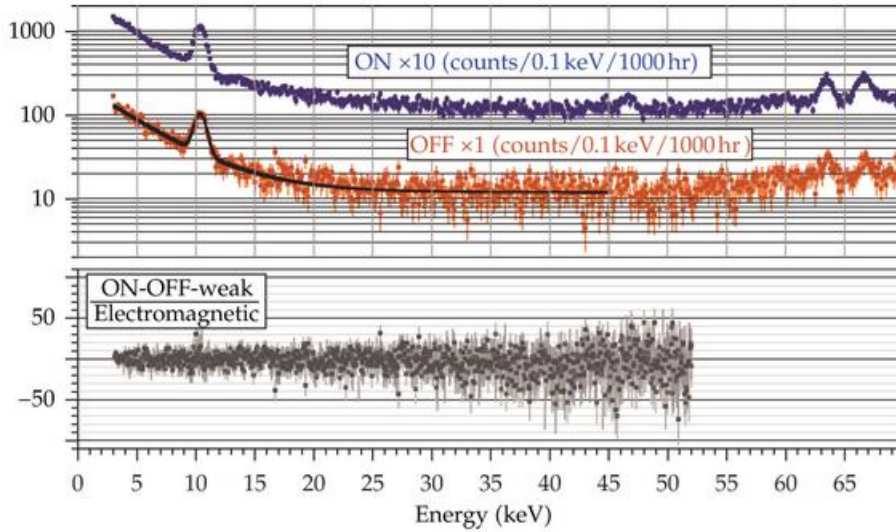


Figure 4.13: The spectra of Reactor ON and OFF as well as ON-OFF is shown with respect to the recoil energy of electron. The analysis threshold achieved is 2.8 keV (Figure is adapted from [74]).

this anomaly existence of sterile neutrinos have been argued [79].

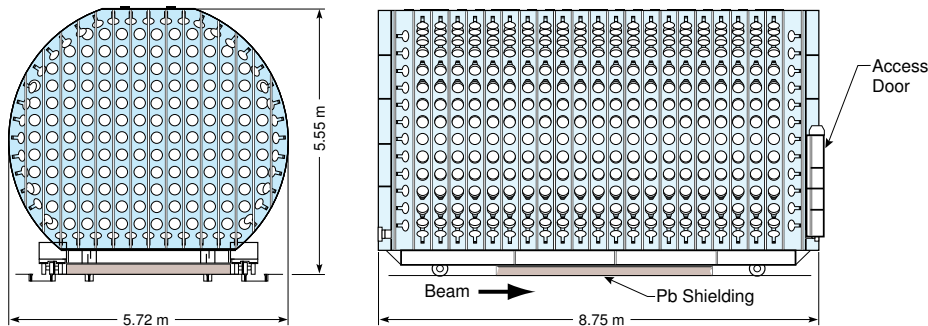


Figure 4.14: The schematic view of the LSND detector is depicted (Figure is adapted from [80]).

The advantage of accelerator neutrinos over reactor neutrinos is that the flux of neutrinos can be determined so accurately. This advantage could be used to measure the Weinberg angle via measuring the cross-section of the neutrino-electron scattering  $\nu_e + e^- \rightarrow \nu_e + e^-$ . The source of  $\nu_e$  used for this measurement is again due to decay at rest of stopped  $\pi^+$  and  $\mu^+$ . The flux of  $\nu_e$ ,  $\bar{\nu}_\mu$  and  $\nu_\mu$  are shown in Figure (4.16).

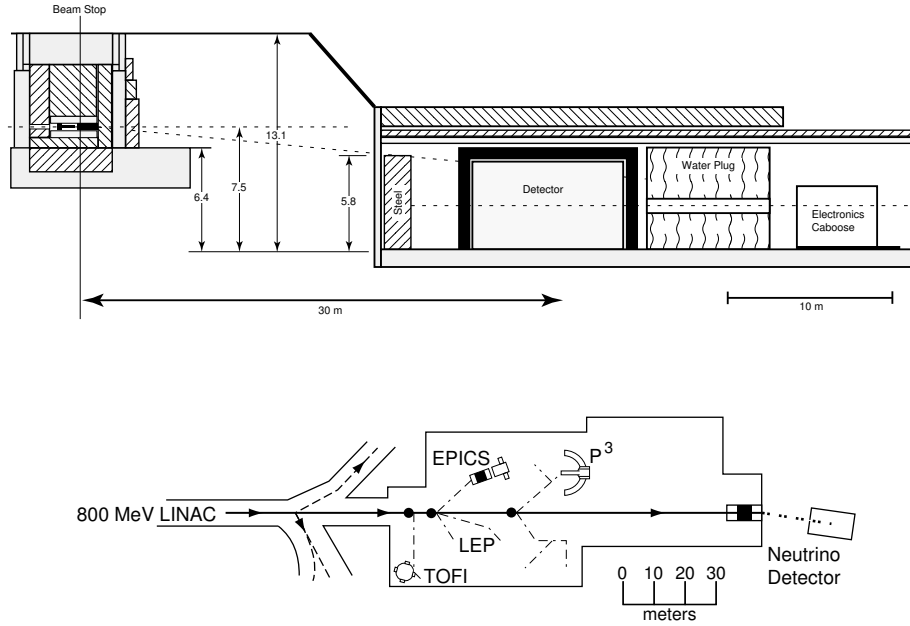


Figure 4.15: The schematic view of the target area and detector enclosure (top) as well as the experimental area is shown (bottom) (Figure is adapted from [78]).

Since  $\nu_\mu$  are produced only due to decay of pion, which is a two body decay, the energy of muon-neutrinos is constant. On the other hand, the intensities of  $\nu_e$  and  $\bar{\nu}_\mu$  are almost similar.

The data used for the cross-section measurement was collected between the years 1994-1998. The flux of  $\nu_e$  is  $11.76 \times 10^{13} \text{ cm}^{-2}$ . With an observed  $191 \pm 22$  events, the cross-section is measured with explicit incoming energy as;

$$\sigma_{\nu_e e^-} = (10.1 \pm 1.1(\text{stat}) \pm 1.0(\text{syst})) \times E_\nu(\text{MeV}) \times 10^{-45} \text{ cm}^{-2} . \quad (4.1)$$

With this result, the Weinberg angle is also determined as [81],

$$\sin^2 \theta_W = 0.248 \pm 0.051 . \quad (4.2)$$

In addition to this, bounds on neutrino magnetic moment and the neutrino charge radius squared are also set with this data [81].

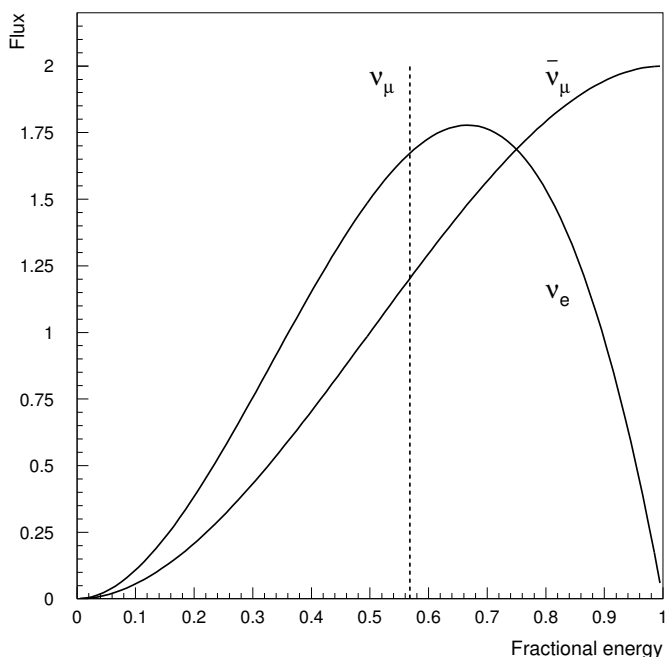


Figure 4.16: The shape of the flux for neutrinos in LSND experiment is shown. The flux values are normalized (Figure is adapted from [81]).

#### 4.4 CHARM II

The main aim of the CHARM II (Cern-**H**Amburg-**R**ome-**M**oscow) collaboration was to measure the Weinberg angle ( $\sin^2\theta_W$ ) with a precision,  $\Delta\sin^2\theta_W = \pm 0.005$ , in order to test grounds of the Standard Model at the one-loop level. Deviation from the calculated corrections would indicate existence of the new physics [82]. In order to achieve that high precision level, collaboration planned to measure the neutrino electron ( $\nu_\mu - e^-$ ) and antineutrino electron ( $\bar{\nu}_\mu - e^-$ ) scattering, since the ratio of these cross-sections is directly related with the Weinberg angle as follows [83];

$$R = \frac{\sigma(\nu_\mu e)/E_\nu}{\sigma(\bar{\nu}_\mu e)/E_{\bar{\nu}}} = 3 \frac{1 - 4 \sin^2 \theta_W + 16/3 \sin^4 \theta_W}{1 - 4 \sin^2 \theta_W + 16 \sin^4 \theta_W}. \quad (4.3)$$

This ratio can also be expressed in terms of the observed events ( $N$ ) as;

$$R = \frac{N(\nu_\mu e) \int \Phi_{\bar{\nu}} E_{\bar{\nu}} dE_{\bar{\nu}}}{N(\bar{\nu}_\mu e) \int \Phi_{\nu} E_{\nu} dE_{\nu}} \quad (4.4)$$

where  $\Phi$  corresponds to neutrino flux and  $E$  is the energy of the neutrinos. The errors for the flux of accelerator neutrinos are small. Moreover, with this method, the

systematic uncertainties in the neutrino fluxes and detection efficiencies almost cancel and accuracy of the Weinberg angle measurement would increase [83].

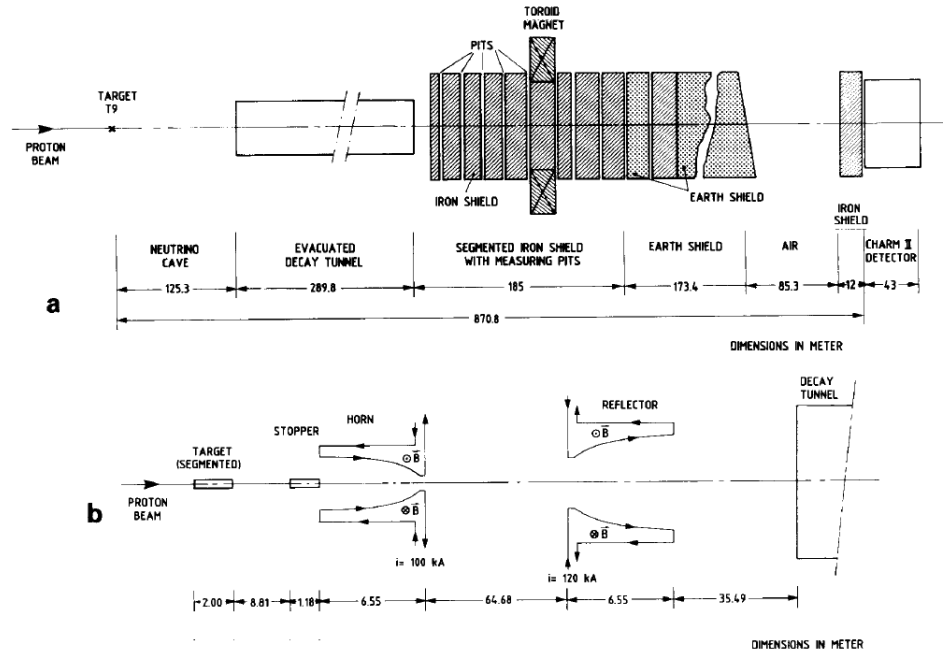


Figure 4.17: Schematic view of the neutrino beam of CHARM II experiment is shown. While in (a), general view is shown, in (b) neutrino cave area is shown schematically (Figure is adapted from [84]).

The neutrinos are produced with wide-band neutrino beam of the CERN SPS (Super Proton Synchrotron). Protons are accelerated up to 450 GeV with SPS. The typical intensities of the beam are at the order of  $10^{13}$  protons on target. Proton beams are hit on Beryllium (Be) targets and hadrons, which comprise mostly pions and kaons, are produced. The sign of the hadrons going through the evacuation channel can be determined using the magnetic lenses called as “horns” and “reflectors”. With this mechanism the signs of the mesons, hence type of the neutrinos are determined [82] (See Figure (4.17)). While positively selected hadrons produce  $\nu_\mu$  beam, negatively selected hadrons result in with  $\bar{\nu}_\mu$  beam. The energies of the hadrons produced with 450 GeV protons hitting on target could be up to 70 GeV which also produce neutrino energies up to 40 GeV.

Some of the hadrons produced after proton hitting on target, decay in the evacuation tube and remaining hadrons are stopped in the iron shield. The muons produced due to decay of hadrons are swept out with the toroidal magnet. With this method all

particles except the neutrinos are excluded from the beam.

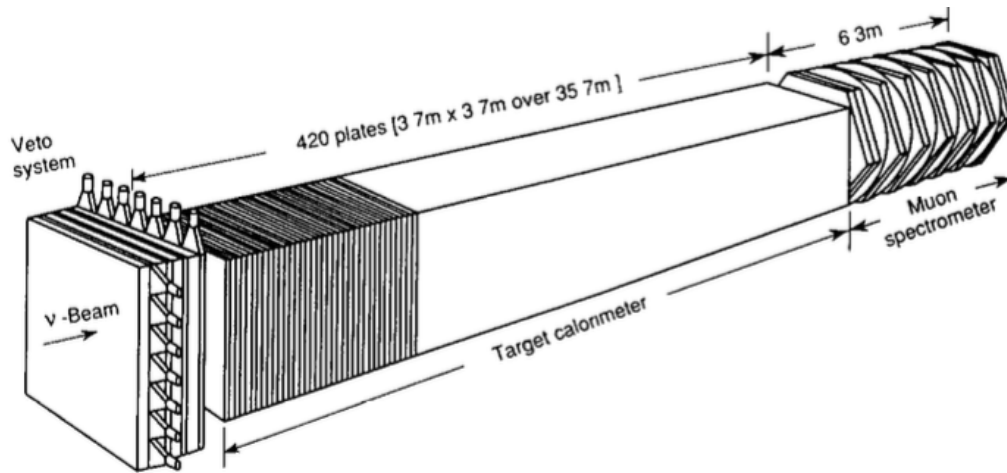


Figure 4.18: The schematic view of the CHARM II detector is depicted (Figure is adapted from [82]).

Schematic layout of the detector is showed in Figure (4.18). The detector with a length of 37.5 m consists of a target calorimeter which is made of 692 t glass and magnetic spectrometer module is added to the end of the calorimeter to determine the momentum of the muons produced via charged current interactions. The calorimeter makes it possible to measure the direction of the produced particle showers as well as their energy. Hence, different type of neutrino interactions could be detected with this experimental set-up.

The flux of the neutrino beam is  $1.3 \times 10^{10} \text{ m}^{-2}$  which corresponds to  $10^{13}$  protons on target. However, for the anti-neutrino beam the flux is around 50% percent less than the neutrino flux. Moreover, the average energy for the neutrino beam is 24 GeV whereas 20 GeV for the anti neutrino beam.

With the data collected between the years 1987-1991, a total of  $2677 \pm 82$  the  $\nu_\mu - e^-$  scattering events and  $2752 \pm 88$   $\bar{\nu}_\mu - e^-$  events are observed. With the ratio of these two observations the Weinberg angle is measured with high precision as [85];

$$\sin^2\theta_W = 0.2324 \pm 0.0083 . \tag{4.5}$$



## 4.5 BOREXINO

Borexino (**BORon EXperiment**) collaboration has been under operation since 2007 and is located underground in Laboratori Nazionali del Gran Sasso (LNGS), Italy. The collaboration aimed to make a real-time measurement of the mono-energetic neutrinos emitted from the electron capture of Beryllium, during the proton-proton (pp cycle) chain in the sun [86]. The Standard Solar Model predicts the energy of the neutrinos emitted from the reaction,  ${}^7\text{Be} + e^- \rightarrow {}^7\text{Li} + \nu_e$ , as 862 keV, hence detecting these mono-energetic neutrinos is crucial to test the SSM. Moreover, with this detection, the solar neutrino oscillation in low energy regime, hence MSW-LMA theory, will have been tested for the first time also. These neutrinos are planned to be detected via observation of neutrino electron scattering events using ultra-pure liquid scintillator.

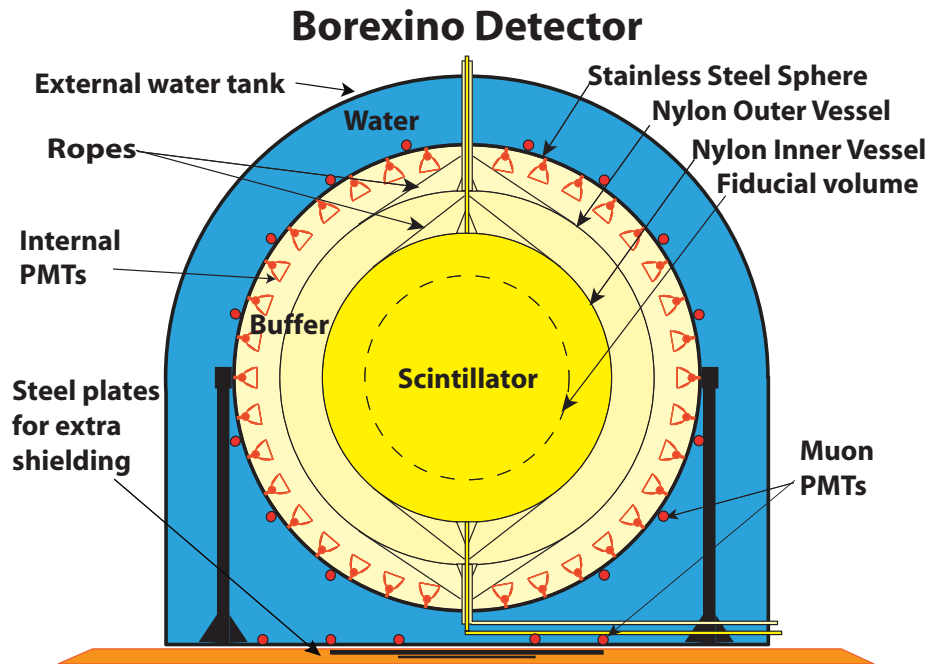


Figure 4.19: The schematic view of the Borexino detector is shown (Figure is adapted from [87]).

Collaboration also extended their search for measuring the solar neutrinos from the CNO, pep cycle and possibly pp and  ${}^8\text{B}$  chain [88], once they found out that the observed background is much lower than the expected one. Furthermore, the anti-neutrinos from the earth core named as geoneutrinos [89] are also observed. In addi-

tion to the solar and geo-neutrino search, supernova neutrinos, the magnetic moment of the neutrinos, the electron decay [90] or the nucleon decay into invisible particles [91] are also in the research program of the collaboration.

Borexino detector is capable of measuring all type of neutrino flavours via the  $\nu_x + e^- \rightarrow \nu_x + e^-$  neutrino electron scattering. The recoil energy of the electron is converted into scintillation light and collected by PMTs. The mean free path for the scattered electron is at most a few centimeters in the scintillator, hence scattered electron looks like a point light source. Thus, the direction of the neutrinos could not be determined with this setup. On the other hand, for the antineutrinos, the signal is due to the inverse beta decay on protons or carbon nuclei. In this case, the recoil energy of the positron is detected with the scintillation detector.

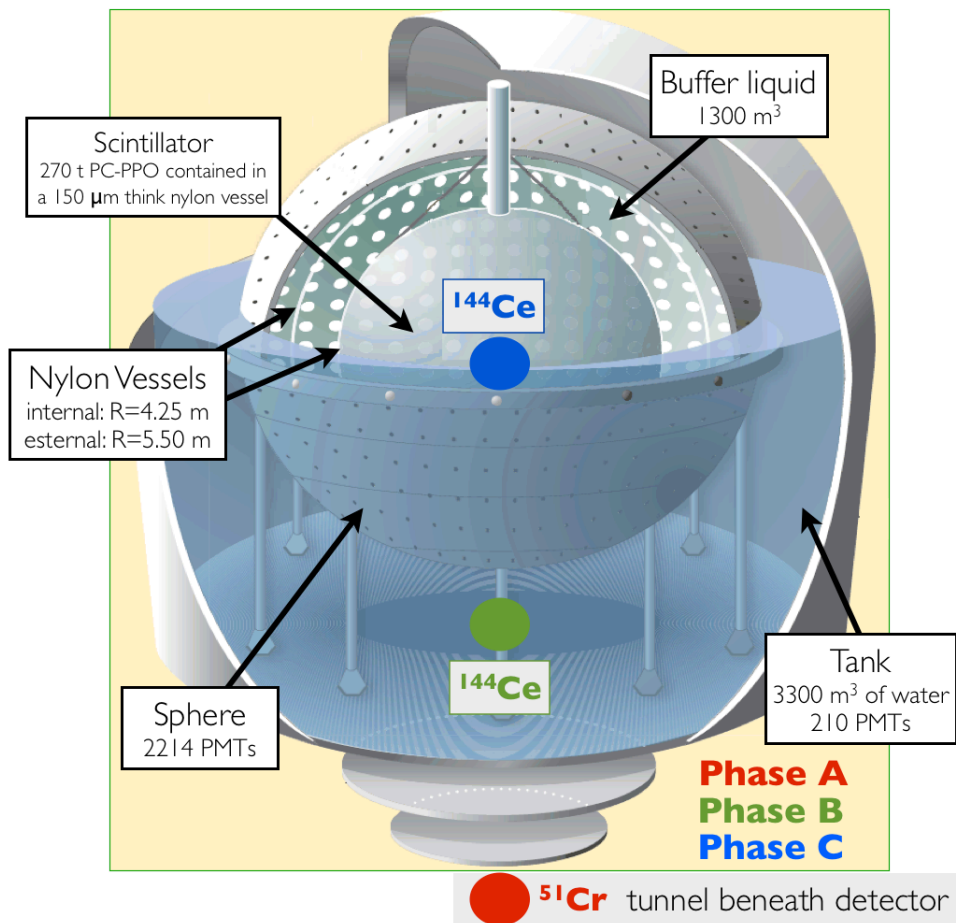


Figure 4.20: The schematic drawing of the Borexino detector is shown (Figure is adapted from [92]).

In order to measure the spectrum of sub-MeV solar neutrinos, the background sup-

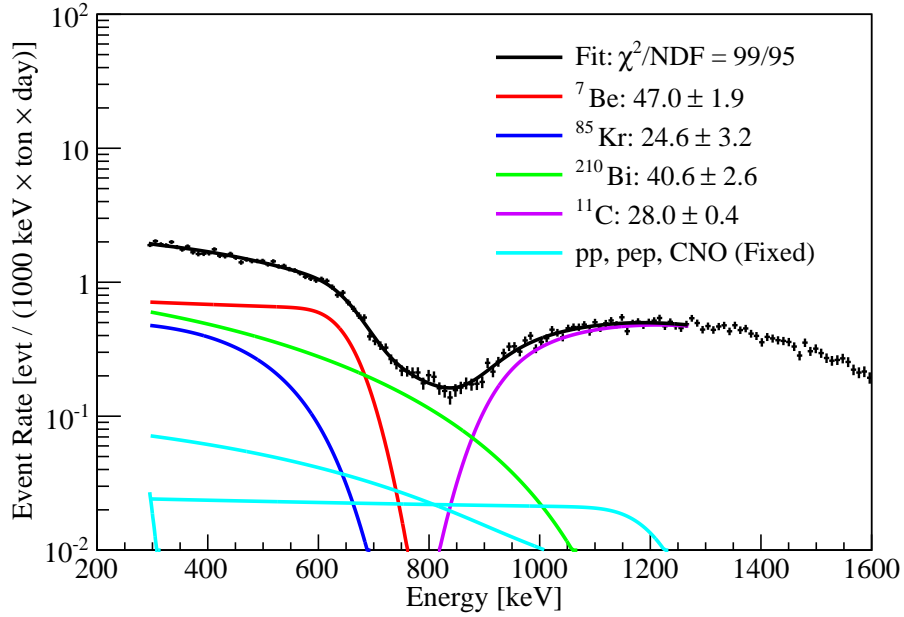


Figure 4.21: Observed neutrino spectrum with an analytic fit over the 290 – 1270 keV range is shown (Figure is adapted from [93]).

pression plays a crucial role. To reduce the background, the detector is located in deep underground with an 3800 m.w.e in LNGS, in which the flux of cosmic muons are suppressed by a factor of  $10^6$  [87].

The schematic view of the detector is shown in Figure (4.19). 300 tons of ultra low-background liquid scintillators are surrounded by 8.5 m and 11 m diameter nylon vessels each of which are filled with different chemical solutions. 2212 photo multiplier tubes are hinged on the inner surface of the stainless steel sphere with a diameter of 13.7 m, which comprises the outer part of the detector. Non-scintillating buffer oil is filled between the inner nylon vessel and stainless steel sphere as a last shielding for external backgrounds. This whole setup is located inside a tank filled with ultra-pure water, which plays the role of shielding against  $\gamma$  rays and neutrons from the tank as well as being used as a Cherenkov muon counter and muon tracker (See Figure (4.20)).

One of the big difficulties for trying to measure low energy solar neutrinos is the energy of natural radiactivities from the decay chains of  $^{235}\text{U}$  and  $^{232}\text{Th}$  as well as decay of  $^{40}\text{K}$  is being similar with the neutrinos from  $^7\text{Be}$  and pep cycle. These elements emit  $\gamma$  rays with energies below 2.7 MeV and interfere with the neutrino signals. However,

Borexino collaboration achieved to measure the neutrino signals by getting rid of the contamination of these radioactive materials as much as possible.

The obtained neutrino spectrum by the collaboration is depicted with various backgrounds in Figure (4.21). The rate of neutrino-elastic scattering from  ${}^7\text{Be}$  solar neutrinos from 862 keV is measured as,

$$46.0 \pm 1.5(\text{stat})_{1.6}^{+1.5}(\text{syst}) \text{ counts}/(\text{day}\cdot 100 \text{ ton}) .$$

This result is acquired with analysis of 740.7 live-days data taken during 2010-2013, which correspond to a 153.6 ton.yr fiducial exposure [93]. Note that, since it is a two body decay, the energy of the  ${}^7\text{Be}$  neutrinos are expected to be fixed. However, the observed spectrum has a sharp maximum edge at  $T = 660$  keV and have a smooth behaviour which is due to the Compton scattering of the recoil electrons.

## CHAPTER 5

### NONCOMMUTATIVE SPACE

Noncommutativity not only appears in quantum mechanics but also in classical physics as well. For instance, we realize that, we cannot get the same position of the solid, when apply the following rotations in order in  $3D$  (See Figure (5.1));

1. Rotation  $90^\circ$  about x axes ( $R_x(\pi/2)$ ) first and then rotation  $90^\circ$  about y axes ( $R_y(\pi/2)$ ).
2. Rotation  $90^\circ$  about y axes ( $R_y(\pi/2)$ ) first and then rotation  $90^\circ$  about x axes ( $R_x(\pi/2)$ ).

Hence, we infer that rotations in  $3D$  do not commute,

$$R_x(\phi)R_y(\phi) - R_y(\phi)R_x(\phi) \neq 0 .$$

Thus, we find out that the noncommutativity arises in the classical physics when the rotations in  $3D$  are considered. Moreover, it is well known that the noncommutativity appears in quantum theory. Indeed, any pair of conjugate variables like position and momentum components do not commute.

$$[x^i, p^j] = i\hbar\delta^{ij} . \quad (5.1)$$

This noncommutativity leads to the Heisenberg uncertainty relation as;

$$(\Delta x^i)(\Delta p^j) \geq \frac{\hbar}{2}\delta^{ij} . \quad (5.2)$$

Here, the Planck constant,  $\hbar$ , defines the tiniest observable phase space in quantum mechanics. The notion of a “point” has been replaced in phase space with the smallest area,  $\hbar$ , called as the “Planck Cell”.

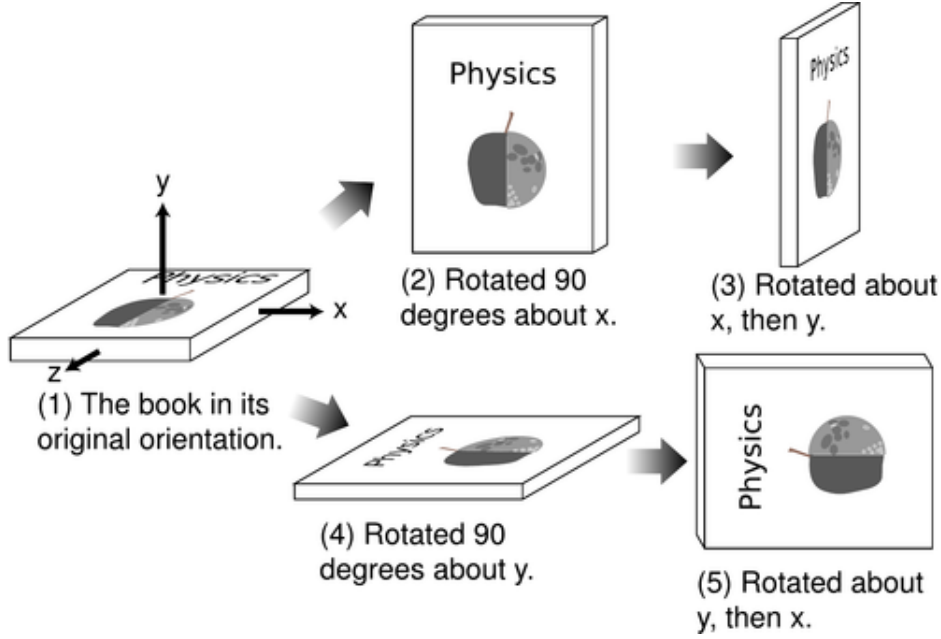


Figure 5.1: An example of noncommutativity of finite rotations is shown.

In a similar manner with the quantum phase space, can we consider that position measurements fail to commute? Assume that the space is noncommutative and let us state this by replacing the space-time coordinates  $x^\mu$  with the Hermitian operators  $\hat{x}^\mu$ <sup>1</sup> as;

$$[\hat{x}^\mu, \hat{x}^\nu] = i\theta^{\mu\nu}, \quad (5.3)$$

where  $\theta^{\mu\nu}$  is a constant, real-valued anti-symmetric  $4 \times 4$  matrix. The dimension of  $|\theta|$  is length squared, which means the smallest area that one can talk about in the  $\mu - \nu$  plane which is analogous to  $\hbar$  in the quantum phase space.

The noncommutative relation of space coordinates above leads to the uncertainty relation as ;

$$\Delta\hat{x}^\mu \Delta\hat{x}^\nu \geq \frac{1}{2}i|\theta^{\mu\nu}|. \quad (5.4)$$

Below the scale  $\sqrt{|\theta|}$  space-time coordinates become incoherent, hence, this kind of space-time is called as “fuzzy” in general [94]. The notion of a point loses its meaning in this fuzzy space. This kind of topology without mentioning points is studied by John von Neumann and named this study as the “pointless topology” [95].

The first thing that comes to mind about the scale of  $\sqrt{|\theta|}$ , especially by the hunters

<sup>1</sup> Note that, the coordinates with hat will represent the noncommutative ones from now on.

of the unifying of quantum theory with the gravity is the Planck length as;

$$\ell_p = \sqrt{\frac{\hbar G}{c^3}} \simeq 1.6 \times 10^{-35} m . \quad (5.5)$$

where  $G$  is the gravitational constant. However if that scale is so low then it becomes nearly impossible to observe such noncommutativity. There is an expectation among scientists who study on quantum gravity that existence of large extra dimensions [96] or Randall-Sundrum [97] models may shift that scale to observable range.

Apart from the motivation of unifying theories, in fact, there is not any theoretical constraints on the non-commutative scale, it can only be bounded by the experiments.

## 5.1 The Landau Problem

Surprisingly, we also come up with non-commuting coordinates in the realm of quantum mechanics. The motion of a non-relativistic charged particle under a strong magnetic field can be considered as if it is moving in a quantum space-time and this problem is known as the ‘‘Landau problem’’ since Landau was the first to find the energy levels of the charged particle under the electromagnetic field. In this section, let us show how the non-commuting coordinates arise in this problem.

Lagrangian of a charged particle under the electromagnetic field can be written as ;

$$\mathcal{L} = \frac{1}{2}m(\dot{x}^2 + \dot{y}^2 + \dot{z}^2) - q\phi + \frac{q}{c}(\dot{x}A_x + \dot{y}A_y + \dot{z}A_z) , \quad (5.6)$$

where  $\vec{A}$  and  $\phi$  are the vector and scalar potential respectively.

Once we solve for the equation of motion using this Lagrangian, we get the Lorentz force as expected;

$$\vec{F} = q(\vec{E} + \vec{v} \times \vec{B}) . \quad (5.7)$$

Canonical momentum can be found from Lagrangian

$$p_i = \frac{\partial L}{\partial \dot{q}_i} . \quad (5.8)$$

Thus, for the particle in electromagnetic field, canonical momentum can be written as;

$$\vec{p} = m\vec{v} + \frac{e}{c}\vec{A} . \quad (5.9)$$

Moreover, Hamiltonian of this particle can easily be obtained and it is equal to

$$H = \frac{1}{2m} \left( \vec{p} - \frac{e}{c} \vec{A} \right)^2. \quad (5.10)$$

Notice that, when we put Equation (5.9) into Equation (5.10), we see that  $H = \frac{1}{2m} \vec{v}^2$  which is essentially independent of the magnetic field as expected, since the magnetic field does not do work.

Assume that we want to solve for the energy eigenvalues and eigenstates of a charged particle. Consider that the particle is confined in the  $(x - y)$  plane and exposed to a constant magnetic field  $\vec{B} = B\hat{k}$  in  $\hat{z}$  direction.

For this orientation, we can choose the vector potential as;

$$\vec{A} = xB\hat{y} \quad (5.11)$$

so that  $\vec{\nabla} \times \vec{A} = \vec{B}$  is satisfied.

Substituting the vector potential into Equation (5.10), we find the Hamiltonian as ;

$$H = \frac{1}{2m} \left[ p_x^2 + \left( p_y - \frac{exB}{c} \right)^2 \right]. \quad (5.12)$$

Since Hamiltonian commutes with  $p_y$ ;

$$[H, p_y] = 0,$$

then  $H$  and  $p_y$  can be represented with the same eigenstates. We can write the eigenvalue equation for  $p_y$  easily as;

$$p_y |\psi\rangle = \hbar k_y |\psi\rangle. \quad (5.13)$$

Once we use these eigenvalues in Equation (5.12), we can write the Hamiltonian as;

$$\begin{aligned} H &= \frac{1}{2m} \left[ p_x^2 + \left( \hbar k_y - \frac{exB}{c} \right)^2 \right] \\ &= \frac{1}{2m} \left[ p_x^2 + \left( \frac{eB}{c} \right)^2 \left( x - \frac{c\hbar k_y}{eB} \right)^2 \right]. \end{aligned} \quad (5.14)$$

In addition, introducing  $\frac{eB}{c} = m\omega$ , Hamiltonian takes the form;

$$H = \frac{p_x^2}{2m} + \frac{1}{2} m\omega^2 \left( x - \frac{c\hbar k_y}{eB} \right)^2. \quad (5.15)$$



This Hamiltonian resembles to the one dimensional linear harmonic oscillator, oscillating with frequency of  $\omega$  about the point  $x = \frac{c\hbar k_y}{eB}$ . Thus, we can write the energy eigenvalues as;

$$\begin{aligned} E_n &= \hbar\omega\left(n + \frac{1}{2}\right) \\ &= \hbar\frac{eB}{mc}\left(n + \frac{1}{2}\right). \end{aligned} \quad (5.16)$$

These energy eigenvalues are called as the ‘‘Landau levels’’ which depend on  $n$  but not on  $k_y$ . We can represent the eigenstates as  $|n, k_y\rangle$ . Therefore, for each energy there are infinitely degenerate states as  $k_y$  runs up to infinity.

The energy difference between two closest states can be found as;

$$\begin{aligned} \Delta E &= \Delta_{E_{n+1}} - \Delta_{E_n} \\ &= \hbar\frac{eB}{mc}. \end{aligned} \quad (5.17)$$

Moreover, the eigenfunctions in the coordinate space can be found as;

$$\langle x, y | n, k_y \rangle = \frac{1}{\sqrt{2\pi\hbar}} e^{ik_y y} \phi_n\left(x - \frac{c\hbar k_y}{eB}\right). \quad (5.18)$$

If the magnetic field is strong enough, electron resides in the lowest Landau level, since the energy difference between the Landau levels are at the order of  $\mathcal{O}(B/m)$  and the higher states decouple to infinity. On the other hand, we can infer that the large magnetic field in some sense is similar to the small mass for the charged particle once we consider the energy difference between the Landau levels.

Thus, to show the situation for the strong magnetic field, instead, let us consider the very small mass of the particle and write the Lagrangian by neglecting the mass of the charged particle from Equation (5.6) as;

$$\mathcal{L} = \frac{e}{c} B x \dot{y}. \quad (5.19)$$

With this Lagrangian we calculate canonical momentum

$$p_y = \frac{\partial L}{\partial \dot{y}} = \frac{eBx}{c}.$$

Moreover, since Lagrangian is in the form of  $\mathcal{L} = \dot{q}p - H$ , we easily deduce that  $p_y = \frac{eBx}{c}$  and  $y$  are the canonical conjugates. Thus, we can write the commutation relation for the conjugate coordinates as;

$$[p_y, y] = \left[ \frac{eB}{c}x, y \right] = -i\hbar, \quad (5.20)$$

$$\boxed{[x, y] = -i \frac{\hbar c}{eB} .}$$

Hence, we obtained that under the strong magnetic field (or if the mass of the particle is very small) the energy levels are projected to the first Landau level and the other states decouple to infinity. In this case, the coordinates do not commute as opposed to Heisenberg algebra and this is called as the ‘‘Peierls’’ substitution [98]. Thus we find out that space noncommutativity arises for this specific gauge of the Landau problem.

However, note that, in this problem if we have chosen symmetric gauge as;

$$\vec{A} = \frac{B}{2}(-y\hat{x} + x\hat{y}),$$

the  $\vec{\nabla} \times \vec{A} = \vec{B}$  is again satisfied and in this case the coordinates would commute. Let us show this briefly.

Using Equation (5.10) we can write the Hamiltonian for the symmetric gauge chosen above as;

$$H = \frac{1}{2m} \left( p_x + \frac{eB}{2c}y \right)^2 + \frac{1}{2m} \left( p_y - \frac{eB}{2c}x \right)^2$$

$$= \underbrace{\frac{1}{2m}p_x^2 + \frac{1}{2}mw_1^2x^2 + \frac{1}{2m}p_y^2 + \frac{1}{2}mw_1^2y^2}_{\text{Hamiltonian of } 2D \text{ harmonic oscillator}} + w_1(y p_x - p_y x), \quad (5.21)$$

where  $w_1 = \frac{eB}{2mc}$ .

Notice that, this Hamiltonian resembles the 2D harmonic oscillator with an additional term  $w_1(y p_x - x p_y)$ . It is well known that algebraic approach in quantum mechanics with introducing creation and annihilation operators is very powerful for solving the harmonic oscillator problem. Let us define them with their dagger operators as;

$$\begin{aligned}
a &= \frac{1}{2} \sqrt{\frac{m\omega_1}{\hbar}} (x - iy) + \frac{i}{2} \sqrt{\frac{1}{m\omega_1\hbar}} (p_x - ip_y) , \\
b &= \frac{1}{2} \sqrt{\frac{m\omega_1}{\hbar}} (x + iy) + \frac{i}{2} \sqrt{\frac{1}{m\omega_1\hbar}} (p_x + ip_y) , \\
a^\dagger &= \frac{1}{2} \sqrt{\frac{m\omega_1}{\hbar}} (x + iy) - \frac{i}{2} \sqrt{\frac{1}{m\omega_1\hbar}} (p_x + ip_y) , \\
b^\dagger &= \frac{1}{2} \sqrt{\frac{m\omega_1}{\hbar}} (x - iy) - \frac{i}{2} \sqrt{\frac{1}{m\omega_1\hbar}} (p_x - ip_y) .
\end{aligned} \tag{5.22}$$

Note that, these operators satisfy the following commutation relations;

$$\begin{aligned}
[a, a^\dagger] &= 1 , \\
[b, b^\dagger] &= 1 ,
\end{aligned} \tag{5.23}$$

and the other commutators vanish and also remark that  $(a, a^\dagger)$  and  $(b, b^\dagger)$  are two independent harmonic oscillator operators.

The additional term in Hamiltonian (Equation (5.21)), can be written in terms of these operators as;

$$w_1(y p_x - x p_y) = \hbar w_1(b^\dagger b - a^\dagger a) . \tag{5.24}$$

Hence, Hamiltonian can be written in terms of these operators as;

$$\begin{aligned}
H &= \hbar w_1(a^\dagger a + b^\dagger b + 1) + \hbar w_1(b^\dagger b - a^\dagger a) \\
&= \hbar w_1(2b^\dagger b + 1) \\
&= 2\hbar w_1(b^\dagger b + \frac{1}{2}) .
\end{aligned} \tag{5.25}$$

We can describe the eigenstates of the Hamiltonian in terms of the quanta of the oscillator  $a$  and  $b$  as follow;

$$\begin{aligned}
a^\dagger a |n, j\rangle &= j |n, j\rangle , \\
b^\dagger b |n, j\rangle &= n |n, j\rangle ,
\end{aligned} \tag{5.26}$$

where  $j$  and  $n$  correspond to quanta of the oscillator  $a$  and  $b$ , respectively. However only  $n$  contributes to the energy, therefore there exist infinitely degenerate states in  $j$  for each Landau levels ( $n$ ).

With the symmetric gauge chosen, to calculate the commutation relation of the coordinates,  $[x, y]$ , let us express coordinates in terms of the ladder operators as well. For this purpose, first note that;

$$\begin{aligned} a + a^\dagger &= \sqrt{\frac{mw_1}{\hbar}}x + \sqrt{\frac{1}{mw_1\hbar}}p_y, \\ b + b^\dagger &= \sqrt{\frac{mw_1}{\hbar}}x - \sqrt{\frac{1}{mw_1\hbar}}p_y, \end{aligned} \tag{5.27}$$

$$\begin{aligned} a - a^\dagger &= -i\sqrt{\frac{mw_1}{\hbar}}y + i\sqrt{\frac{1}{mw_1\hbar}}p_x, \\ b - b^\dagger &= i\sqrt{\frac{mw_1}{\hbar}}y + i\sqrt{\frac{1}{mw_1\hbar}}p_x. \end{aligned}$$

With these relations, we can easily find  $x$  and  $y$  in terms of the operators as follow;

$$\begin{aligned} x &= \sqrt{\frac{\hbar}{4mw_1}}(a + a^\dagger + b + b^\dagger), \\ y &= i\sqrt{\frac{\hbar}{4mw_1}}(a - a^\dagger - b + b^\dagger). \end{aligned} \tag{5.28}$$

Then, we can calculate the commutation relation as;

$$\begin{aligned} [x, y] &= \frac{i\hbar}{4mw_1}[a + a^\dagger + b + b^\dagger, a - a^\dagger - b + b^\dagger] \\ &= -\frac{i\hbar}{4mw_1}([a, a] - \underbrace{[a, a^\dagger]}_1 - [a, b] + [a, b^\dagger] \\ &\quad + \underbrace{[a^\dagger, a]}_{-1} - [a^\dagger, a^\dagger] - [a^\dagger, b] + [a^\dagger, b^\dagger] \\ &\quad + [b, a] - [b, a^\dagger] - [b, b] + \underbrace{[b, b^\dagger]}_1 \\ &\quad + [b^\dagger, a] - [b^\dagger, a^\dagger] - \underbrace{[b^\dagger, b]}_{-1} + [b^\dagger, b^\dagger]) \\ &= 0. \end{aligned} \tag{5.29}$$

Hence, we showed that the coordinates commute once the symmetric gauge for vector potential  $\vec{A}$  is chosen. For more details about the Landau problem in the noncommutative-space see [99, 100, 101].

In the String theory, with a similar concept of this Landau problem, non-commuting coordinates are seen when the strong background magnetic like field is considered [102] and studies of noncommutativity of space coordinates have increased heavily then on.

## 5.2 A Brief History of the Non-commutative Space

The idea of non-commutative space goes back to 1940s before the renormalization concept was introduced. To get rid of the divergences in Quantum Field theory, Heisenberg proposed noncommuting space coordinates in a letter to Peierls [103]. Oppenheimer was informed by Pauli about the idea and H. S. Snyder, who was a student of Oppenheimer, conducted a detailed analysis of integrating noncommuting coordinates to quantum theory [104]. The paper was evaluated by Pauli and even though he was fond of the idea in the sense of mathematics, he rejected the paper for physics concerns [105].

The noncommutativity scale is defined as;

$$\Lambda_{NC} = \frac{1}{\sqrt{|\theta|}}, \quad (5.30)$$

which has the dimension of energy. Thus, this will define an ultraviolet cut-off scale  $\Lambda_{NC}$  on the momentum space integration to evaluate the Feynman diagrams. However, once the renormalization theory was constructed, the idea of non-commutative space had been ignored for a long time. In 1990s when the notion is used in the String theory [106] the idea became popular once again.

It is possible to write the noncommutativity relation in terms of the  $\Lambda_{NC}$  scale as;

$$[\hat{x}^\mu, \hat{x}^\nu] = i\theta^{\mu\nu} = i \frac{C^{\mu\nu}}{\Lambda_{NC}^2}, \quad (5.31)$$

where the anti-symmetric matrix,  $C^{\mu\nu}$ , is dimensionless coefficient of order unity. Sometimes in the literature using an analogy with the electromagnetic field strength tensor,  $C^{\mu\nu}$  is parameterized as;

$$C^{\mu\nu} = \begin{bmatrix} 0 & -E^1 & -E^2 & -E^3 \\ E^1 & 0 & -B^3 & B^2 \\ E^2 & B^3 & 0 & -B^1 \\ E^3 & -B^2 & B^1 & 0 \end{bmatrix}. \quad (5.32)$$

Note that it is generally assumed that  $\theta_{0i} = 0$  due to getting rid of the unitarity and causality problems [107, 108, 109]. With this assumption, instead of following the

notation above, we represent  $C_{\mu\nu} = \theta_{\mu\nu}$  via using anti-symmetric property of matrix as;

$$C_{\mu\nu} = \theta^{\mu\nu} = \begin{bmatrix} 0 & 0 & 0 & 0 \\ 0 & 0 & \theta_{12} & \theta_{13} \\ 0 & -\theta_{12} & 0 & \theta_{23} \\ 0 & -\theta_{13} & -\theta_{23} & 0 \end{bmatrix} \quad (5.33)$$

### 5.3 Weyl-Moyal Product

Since we are accustomed to do algebra in the commuting space, it seems cumbersome to deal with multiplications in the non-commutative space. However, there exists a very useful way of handling non-commutative algebra which is mapping the non-commutative coordinates to the usual coordinates via “\*” (Weyl-Moyal) product of functions of commuting coordinates. The Weyl-Moyal product of two functions is defined as following;

$$f(\hat{x})g(\hat{x}) \rightarrow f(x) * g(x) = \exp\left(\frac{i}{2}\theta_{\mu\nu}\frac{\partial}{\partial x_\mu}\frac{\partial}{\partial y_\nu}\right)f(x)g(y)|_{x=y}, \quad (5.34)$$

where the coordinate with a hat,  $\hat{\phantom{x}}$ , represents that it is in non-commutative space.

We can expand this equation up to the first order in  $\theta$  as;

$$f(x) * g(x) = f(x)g(x) + \frac{i}{2}\theta_{\mu\nu}\frac{\partial f(x)}{\partial x^\mu}\frac{\partial g(x)}{\partial x^\nu} + \mathcal{O}(\theta^2). \quad (5.35)$$

Now let us show that with this expression commutation relation,  $[\hat{x}^\mu, \hat{x}^\nu] = i\theta^{\mu\nu}$  is satisfied.

For instance, if we choose  $f(x) = x^\mu$  and  $g(x) = x^\nu$  then we get;

$$\begin{aligned} x^\mu * x^\nu &= x^\mu x^\nu + \frac{i}{2}\theta^{\mu\nu}\frac{\partial x^\mu}{\partial x^\mu}\frac{\partial x^\nu}{\partial x^\nu} \\ &= x^\mu x^\nu + \frac{i}{2}\theta^{\mu\nu}. \end{aligned} \quad (5.36)$$

However if  $f(x) = x^\nu$  and  $g(x) = x^\mu$  then we get;

$$\begin{aligned} x^\nu * x^\mu &= x^\nu x^\mu + \frac{i}{2}\theta^{\nu\mu}\frac{\partial x^\nu}{\partial x^\nu}\frac{\partial x^\mu}{\partial x^\mu} \\ &= x^\nu x^\mu + \frac{i}{2}\theta^{\nu\mu} \\ &= x^\nu x^\mu - \frac{i}{2}\theta^{\mu\nu}. \end{aligned} \quad (5.37)$$

where the last step is due to  $\theta^{\mu\nu}$  being anti-symmetric. Once we calculate the commutation relation as;

$$\begin{aligned}
[\hat{x}^\mu, \hat{x}^\nu] &= x^\mu * x^\nu - x^\nu * x^\mu \\
&= (x^\mu x^\nu + \frac{i}{2}\theta^{\mu\nu}) - (x^\nu x^\mu - \frac{i}{2}\theta^{\mu\nu}) \\
&= i\theta^{\mu\nu} .
\end{aligned} \tag{5.38}$$

Hence, we verified that commutation relation is satisfied using the  $*$  product.

## 5.4 Non-commutative QED

The easy recipe for doing field theory in the non-commutative space is as follows;

- Using the Seiberg-Witten maps, transform the fields in the NC space to the commutative ones
- Using the Weyl-Moyal product, transform all the multiplication in the NC space via the  $*$ -product to the ordinary space

The Seiberg-Witten maps for the non-commutative vector and fermion fields up to first order in  $\theta$  are given as [110];

$$\begin{aligned}
\hat{A}_\mu(A) &= A_\mu + e\theta^{\rho\nu} A_\nu(\partial_\rho A_\mu - \frac{1}{2}\partial_\mu A_\rho) + \mathcal{O}(\theta^2) , \\
\hat{\psi}(\psi, A) &= \psi + e\theta^{\nu\rho} A_\rho \partial_\nu \psi + \mathcal{O}(\theta^2) .
\end{aligned} \tag{5.39}$$

Notice that, replacing the usual products with the Weyl-Moyal correspondence causes an ambiguity in the order of the gauge and fermion fields like,  $eA_\mu * \psi$ ,  $e\psi * A_\mu$  or  $e(A_\mu * \psi - \psi * A_\mu)$ . While the first two couplings are the charge conjugations of each other, the charge conjugation of the third coupling is itself [111, 112, 113]. Hence, a neutral particle can have the third coupling which leads to interactions like photon self-coupling,  $Z\gamma\gamma$  and neutrino photon interactions with the definition of covariant derivative as;

$$\hat{D}_\mu \hat{\psi} = \partial_\mu \hat{\psi} - ie(\hat{A}_\mu * \hat{\psi} - \hat{\psi} * \hat{A}_\mu) . \tag{5.40}$$

Let us convert this equation into the usual product with Equation (5.35). We can write for the  $*$  products as;

$$\hat{A}_\mu * \hat{\psi} = \hat{A}_\mu \hat{\psi} + \frac{i}{2} \theta^{\nu\rho} \partial_\nu \hat{A}_\mu \partial_\rho \hat{\psi} \quad (5.41)$$

and for

$$\begin{aligned} \hat{\psi} * \hat{A}_\mu &= \hat{\psi} \hat{A}_\mu + \frac{i}{2} \theta^{\nu\rho} \partial_\nu \hat{\psi} \partial_\rho \hat{A}_\mu \\ &= \hat{\psi} \hat{A}_\mu + \frac{i}{2} \underbrace{\theta^{\rho\nu}}_{-\theta^{\nu\rho}} \partial_\rho \hat{\psi} \partial_\nu \hat{A}_\mu \\ &= \hat{\psi} \hat{A}_\mu - \frac{i}{2} \theta^{\nu\rho} \partial_\rho \hat{\psi} \partial_\nu \hat{A}_\mu . \end{aligned} \quad (5.42)$$

Hence, using Equations (5.41) and (5.42) we can write;

$$\begin{aligned} \hat{A}_\mu * \hat{\psi} - \hat{\psi} * \hat{A}_\mu &= (\cancel{\hat{A}_\mu} \hat{\psi} + \frac{i}{2} \theta^{\nu\rho} \partial_\nu \hat{A}_\mu \partial_\rho \hat{\psi}) - (\hat{\psi} \cancel{\hat{A}_\mu} - \frac{i}{2} \theta^{\nu\rho} \partial_\rho \hat{\psi} \partial_\nu \hat{A}_\mu) \\ &= i \theta^{\nu\rho} \partial_\rho \hat{\psi} \partial_\nu \hat{A}_\mu . \end{aligned} \quad (5.43)$$

Hence the covariant derivative, Equation (5.40), turns out to be equal to;

$$\hat{D}_\mu \hat{\psi} = \partial_\mu \hat{\psi} + e \theta^{\nu\rho} (\partial_\rho \hat{\psi}) (\partial_\nu \hat{A}_\mu) . \quad (5.44)$$

Let us now try to construct the noncommutative QED (NCQED) action.

The action for the quantum electrodynamics for a neutral, spin 1/2 particle can be written as;

$$S = \int d^4x [\bar{\psi} (i \not{D} - m) \psi] , \quad (5.45)$$

where  $D_\mu$  is the covariant derivative as  $D_\mu = \partial_\mu + ieA_\mu$ .

Following the recipe, replacing all the products with the  $*$  product, we get the action in the non-commutative space as following;

$$\hat{S} = \int d^4x [\bar{\hat{\psi}} * (i \gamma^\mu \hat{D}_\mu) - m] * \hat{\psi} . \quad (5.46)$$

In the action above, replacing the fields using the Seiberg-Witten map in Equations (5.39) and (5.44) and expand the Weyl-Moyal product up to the first order in  $\theta$ , we can transform the action to the ordinary space that we are familiar to do the algebra. For this purpose let us evaluate each term one by one.



$$\begin{aligned}
\bar{\psi} * i\gamma^\mu \hat{D}_\mu \hat{\psi} &= \bar{\psi} * i\gamma^\mu \overbrace{(\partial_\mu \hat{\psi} + e\theta^{\nu\rho} (\partial_\rho \hat{\psi})(\partial_\nu \hat{A}_\mu))}^{\hat{D}_\mu} \\
&= \underbrace{\bar{\psi} * i\gamma^\mu \partial_\mu \hat{\psi}}_I + \underbrace{\bar{\psi} * ie\gamma^\mu \theta^{\nu\rho} (\partial_\rho \hat{\psi})(\partial_\nu \hat{A}_\mu)}_{II} .
\end{aligned} \tag{5.47}$$

Let us evaluate  $I$  first.

$$\begin{aligned}
I &= \overbrace{(\bar{\psi} + e\theta^{\nu\rho} A_\rho \partial_\nu \bar{\psi})}^{\bar{\psi}} * i\gamma^\mu \partial_\mu \overbrace{(\psi + e\theta^{\nu\rho} A_\rho \partial_\nu \psi)}^{\psi} \\
&= \underbrace{\hat{\psi} * i\gamma^\mu \partial_\mu \psi}_{B_1} + \underbrace{\hat{\psi} * i\gamma^\mu \partial_\mu (e\theta^{\nu\rho} A_\rho \partial_\nu \psi)}_{B_2} + \underbrace{e\theta^{\nu\rho} A_\rho (\partial_\nu \bar{\psi}) * i\gamma^\mu \partial_\mu \psi}_{B_3} + \mathcal{O}(\theta^2) .
\end{aligned} \tag{5.48}$$

Let us now transform the each term above via the  $*$ -product. Using Equation (5.35) we can write each term in the ordinary product up to  $\theta$  as;

$$\begin{aligned}
B_1 &= \hat{\psi} * i\gamma^\mu \partial_\mu \psi \\
&= \underbrace{\bar{\psi} i\gamma^\mu \partial_\mu \psi}_{B_{11}} + \underbrace{\frac{i}{2} \theta^{\nu\rho} (\partial_\nu \hat{\psi}) \partial_\rho (i\gamma^\mu \partial_\mu \psi)}_{B_{12}} .
\end{aligned} \tag{5.49}$$

Once we perform the integration  $B_{12}$  term, we see that the result is zero since surface term goes to zero as follow;

$$\begin{aligned}
\int d^4x B_{12} &= \int d^4x \frac{-1}{2} \theta^{\nu\rho} \underbrace{(\partial_\rho (\partial_\nu \hat{\psi} \gamma^\mu \partial_\mu \psi) - (\partial_\rho (\partial_\nu \bar{\psi})) \gamma^\mu \partial_\mu \psi)}_{(\partial_\nu \hat{\psi}) \partial_\rho (\gamma^\mu \partial_\mu \psi)} \\
&= -\frac{1}{2} \left( \int d^4x \theta^{\nu\rho} \underbrace{\partial_\rho (\partial_\nu \hat{\psi} \gamma^\mu \partial_\mu \psi)}_{\text{surface term}} - \int d^4x \underbrace{\theta^{\nu\rho}}_{AS} \underbrace{\partial_\rho (\partial_\nu \bar{\psi}) \gamma^\mu \partial_\mu \psi}_S \right) \\
&= 0
\end{aligned} \tag{5.50}$$

since the last term contains multiplication of symmetric (S) and anti-symmetric (AS) matrices. Hence  $B_1$  equals to;

$$\boxed{B_1 = \bar{\psi} i\gamma^\mu \partial_\mu \psi} . \tag{5.51}$$

For  $B_2$ , we get up to first order in  $\theta$  as;

$$\begin{aligned}
B_2 &= \hat{\psi} * i\gamma^\mu \partial_\mu (e\theta^{\nu\rho} A_\rho \partial_\nu \psi) \\
&= \hat{\psi} i\gamma^\mu e\theta^{\nu\rho} \partial_\mu (A_\rho \partial_\nu \psi) + \mathcal{O}(\theta^2) \\
&= ie\gamma^\mu \theta^{\nu\rho} \gamma^\mu \underbrace{\left( \partial_\mu (\bar{\psi} A_\rho \partial_\nu \psi) - (\partial_\mu \bar{\psi}) A_\rho \partial_\nu \psi \right)}_{\text{surface term}}, \tag{5.52} \\
\boxed{B_2} &= -ie\theta^{\nu\rho} (\partial_\mu \bar{\psi}) A_\rho \gamma^\mu \partial_\nu \psi.
\end{aligned}$$

Realize that we again omitted the surface term due to the integration in mind.

For  $B_3$  we obtain;

$$\begin{aligned}
B_3 &= e\theta^{\nu\rho} A_\rho \partial_\nu \bar{\psi} * i\gamma^\mu \partial_\mu \psi, \\
\boxed{B_3} &= e\theta^{\nu\rho} A_\rho (\partial_\nu \bar{\psi}) i\gamma^\mu \partial_\mu \psi + \mathcal{O}(\theta^2). \tag{5.53}
\end{aligned}$$

With these findings, we can write  $I$  (Equation (5.48)) using the Equations (5.51) to (5.53) as;

$$\begin{aligned}
I &= B_1 + B_2 + B_3, \\
\boxed{I} &= \bar{\psi} i\gamma^\mu \partial_\mu \psi + ie\theta^{\nu\rho} (A_\rho (\partial_\nu \bar{\psi}) i\gamma^\mu \partial_\mu \psi - (\partial_\mu \bar{\psi}) A_\rho \gamma^\mu \partial_\nu \psi). \tag{5.54}
\end{aligned}$$

Let us evaluate  $II$  in Equation (5.47).

$$\begin{aligned}
II &= \bar{\hat{\psi}} * ie\gamma^\mu \theta^{\nu\rho} (\partial_\rho \hat{\psi}) (\partial_\nu \hat{A}_\mu) \\
&= \bar{\hat{\psi}} * ie\gamma^\mu \theta^{\nu\rho} (\partial_\nu A_\mu) (\partial_\rho \psi) + \mathcal{O}(\theta^2) \\
&= \underbrace{(\bar{\psi} + e\theta^{\nu\rho} A_\rho \partial_\nu \bar{\psi})}_{\hat{\bar{\psi}}} * ie\gamma^\mu \theta^{\nu\rho} (\partial_\nu A_\mu) (\partial_\rho \psi) + \mathcal{O}(\theta^2), \tag{5.55} \\
\boxed{II} &= \bar{\psi} i\gamma^\mu e\theta^{\nu\rho} (\partial_\nu A_\mu) (\partial_\rho \psi) + \mathcal{O}(\theta^2).
\end{aligned}$$

Hence, Equation (5.47) equals to;

$$\begin{aligned}
\bar{\hat{\psi}} * i\gamma^\mu \hat{D}_\mu \hat{\psi} &= I + II \\
&= \bar{\psi} i\gamma^\mu \partial_\mu \psi \\
&\quad + ie\theta^{\nu\rho} ((\partial_\nu \bar{\psi}) A_\rho \gamma^\mu (\partial_\mu \psi) - (\partial_\mu \bar{\psi}) A_\rho \gamma^\mu (\partial_\nu \psi) + \bar{\psi} (\partial_\nu A_\mu) \gamma^\mu (\partial_\rho \psi)). \tag{5.56}
\end{aligned}$$

Now evaluate the second term in Equation (5.46) using the  $*$ -product and the Seiberg-Witten (SW) map. First, using the SW map, we obtain;

$$\begin{aligned}\tilde{\psi} * \hat{\psi} &= (\bar{\psi} + e\theta^{\nu\rho} A_\rho \partial_\nu \bar{\psi}) * (\psi + e\theta^{\nu\rho} A_\rho \partial_\nu \psi) \\ &= \bar{\psi} * \psi + \bar{\psi} * (e\theta^{\nu\rho} A_\rho \partial_\nu \psi) + (e\theta^{\nu\rho} A_\rho \partial_\nu \bar{\psi}) * \psi + \mathcal{O}(\theta^2) .\end{aligned}\quad (5.57)$$

Now, let us convert each term to the ordinary product up to first order in  $\theta$  using the  $*$ -product.

$$\begin{aligned}\bar{\psi} * \psi &= \bar{\psi}\psi + \frac{i}{2}\theta^{\mu\nu} \underbrace{(\partial_\mu \bar{\psi})(\partial_\nu \psi)}_{\partial_\mu(\bar{\psi}\partial_\nu\psi) - \bar{\psi}\partial_\mu\partial_\nu\psi} \\ &= \bar{\psi}\psi + \frac{i}{2}\theta^{\mu\nu} \underbrace{\partial_\mu(\bar{\psi}\partial_\nu\psi)}_{\text{surface term}} - \frac{i}{2}\underbrace{\theta^{\mu\nu}}_{AS} \bar{\psi} \underbrace{\partial_\mu\partial_\nu\psi}_S \\ &= \bar{\psi}\psi ,\end{aligned}\quad (5.58)$$

in which the surface term vanishes once we perform the integration.

For the second term in Equation (5.57) we obtain;

$$\bar{\psi} * (e\theta^{\nu\rho} A_\rho \partial_\nu \psi) = e\theta^{\nu\rho} \bar{\psi} A_\rho \partial_\nu \psi + \mathcal{O}(\theta^2) ,\quad (5.59)$$

and for the third term in Equation (5.57) we get;

$$e\theta^{\nu\rho} A_\rho \partial_\nu \bar{\psi} * \psi = e\theta^{\nu\rho} A_\rho (\partial_\nu \bar{\psi}) \psi + \mathcal{O}(\theta^2) .\quad (5.60)$$

Collecting these terms, we can write  $\tilde{\psi} * \hat{\psi}$  as

$$\begin{aligned}\tilde{\psi} * \hat{\psi} &= \bar{\psi}\psi + e\theta^{\nu\rho} A_\rho \underbrace{(\bar{\psi}\partial_\nu\psi + (\partial_\nu\bar{\psi})\psi)}_{\partial_\nu(\bar{\psi}\psi)} \\ &= \bar{\psi}\psi + e\theta^{\nu\rho} A_\rho \partial_\nu(\bar{\psi}\psi) \\ &= \bar{\psi}\psi + e\theta^{\nu\rho} \underbrace{\left( \overbrace{\partial_\nu(A_\rho\bar{\psi}\psi)}^{A_\rho\partial_\nu(\bar{\psi}\psi)} - (\partial_\nu A_\rho)\bar{\psi}\psi \right)}_{\text{surface term}} .\end{aligned}\quad (5.61)$$

Once we omit the surface term, then  $\tilde{\psi} * \hat{\psi}$  equals to,

$$\begin{aligned}
\hat{\bar{\psi}} * \hat{\psi} &= \bar{\psi}\psi - e\theta^{\nu\rho}(\partial_\nu A_\rho)\bar{\psi}\psi \\
&= \bar{\psi}\psi(1 - e\theta^{\nu\rho}(\partial_\nu A_\rho)) \\
&= \bar{\psi}\psi(1 - e\underbrace{\frac{1}{2}(\theta^{\nu\rho} - \theta^{\rho\nu})}_{\theta^{\nu\rho}}(\partial_\nu A_\rho)) \\
&= \bar{\psi}\psi(1 - \frac{e}{2}\theta^{\nu\rho}(\partial_\nu A_\rho) + \frac{e}{2}\theta^{\rho\nu}(\partial_\nu A_\rho)) \\
&= \bar{\psi}\psi(1 - \frac{e}{2}\theta^{\rho\nu}(\partial_\rho A_\nu) + \frac{e}{2}\theta^{\rho\nu}(\partial_\nu A_\rho)) \\
&= \bar{\psi}\psi(1 + \frac{e}{2}\theta^{\rho\nu}(\underbrace{\partial_\nu A_\rho - \partial_\rho A_\nu}_{F_{\nu\rho}})) \\
&= \bar{\psi}\psi(1 + \frac{e}{2}\theta^{\rho\nu}F_{\nu\rho}) \\
\boxed{\hat{\bar{\psi}} * \hat{\psi} = \bar{\psi}\psi(1 - \frac{e}{2}\theta^{\nu\rho}F_{\nu\rho})} .
\end{aligned} \tag{5.62}$$

Using the Equations (5.56) and (5.62), the NCQED action in Equation (5.46) can be written as;

$$\begin{aligned}
S &= \int d^4x \{ \bar{\psi}i\gamma^\mu\partial_\mu\psi \\
&\quad + ie\theta^{\nu\rho}((\partial_\nu\bar{\psi})A_\rho\gamma^\mu(\partial_\mu\psi) - (\partial_\mu\bar{\psi})A_\rho\gamma^\mu(\partial_\nu\psi) + \bar{\psi}(\partial_\nu A_\mu)\gamma^\mu(\partial_\rho\psi)) \\
&\quad - m\bar{\psi}\psi(1 - \frac{e}{2}\theta^{\nu\rho}F_{\nu\rho}) \} \\
&= \int d^4x \{ \bar{\psi}[i\gamma^\mu\partial_\mu - m(1 - \frac{e}{2}\theta^{\nu\rho}F_{\nu\rho})]\psi \\
&\quad + ie\theta^{\nu\rho}[(\partial_\nu\bar{\psi})A_\rho\gamma^\mu(\partial_\mu\psi) - (\partial_\mu\bar{\psi})A_\rho\gamma^\mu(\partial_\nu\psi) + \bar{\psi}(\partial_\nu A_\mu)\gamma^\mu(\partial_\rho\psi)] \} .
\end{aligned} \tag{5.63}$$

Now, let us rewrite the above equation in terms of the electromagnetic field tensor. For this purpose let us perform integration by part. However, before we move on it is useful to evaluate the following terms that we are going to need for the integration.

$$\begin{aligned}
(\partial_\nu\bar{\psi})A_\rho(\partial_\mu\psi) &= \underbrace{\partial_\nu[\bar{\psi}A_\rho(\partial_\mu\psi)]}_{\text{surface term}} - \bar{\psi}(\partial_\nu A_\rho)(\partial_\mu\psi) - \bar{\psi}A_\rho\partial_\nu\partial_\mu\psi , \\
(\partial_\mu\bar{\psi})A_\rho(\partial_\nu\psi) &= \underbrace{\partial_\mu[\bar{\psi}A_\rho(\partial_\nu\psi)]}_{\text{surface term}} - \bar{\psi}(\partial_\mu A_\rho)(\partial_\nu\psi) - \bar{\psi}A_\rho\partial_\mu\partial_\nu\psi ,
\end{aligned} \tag{5.64}$$

and if we subtract the two equations above side by side and neglect the surface terms since they will be equal to zero after integration, we get;

$$\boxed{(\partial_\nu\bar{\psi})A_\rho(\partial_\mu\psi) - (\partial_\mu\bar{\psi})A_\rho(\partial_\nu\psi) = \bar{\psi}(\partial_\mu A_\rho)(\partial_\nu\psi) - \bar{\psi}(\partial_\nu A_\rho)(\partial_\mu\psi)} . \tag{5.65}$$

Let us write the second integration term in Equation (5.63) denoting as  $S_2$ ;

$$\begin{aligned}
S_2 &= \int d^4x \{ ie\theta^{\nu\rho}\gamma^\mu [(\partial_\nu\bar{\psi})A_\rho(\partial_\mu\psi) - (\partial_\mu\bar{\psi})A_\rho(\partial_\nu\psi) + \bar{\psi}(\partial_\nu A_\mu)(\partial_\rho\psi)] \} \\
&= \int d^4x \{ ie\gamma^\mu\theta^{\nu\rho} \{ \bar{\psi}(\partial_\mu A_\rho)(\partial_\nu\psi) - \bar{\psi}(\partial_\nu A_\rho)(\partial_\mu\psi) + \bar{\psi}(\partial_\nu A_\mu)(\partial_\rho\psi) \} \}
\end{aligned} \tag{5.66}$$

where we used Equation (5.65).

Notice that using the antisymmetric property of  $\theta^{\nu\rho}$ , we can write for the second term in Equation (5.66);

$$\begin{aligned}
\theta^{\nu\rho}(\partial_\nu A_\rho)(\partial_\mu\psi) &= \frac{1}{2}(\theta^{\nu\rho} - \theta^{\rho\nu})(\partial_\nu A_\rho)(\partial_\mu\psi) \\
&= \frac{1}{2}[\theta^{\nu\rho}(\partial_\nu A_\rho)(\partial_\mu\psi) - \theta^{\rho\nu}(\partial_\nu A_\rho)(\partial_\mu\psi)] \\
&= \frac{1}{2}[\theta^{\nu\rho}(\partial_\nu A_\rho)(\partial_\mu\psi) - \theta^{\nu\rho}(\partial_\rho A_\nu)(\partial_\mu\psi)] \\
&= \frac{1}{2}\theta^{\nu\rho} \underbrace{[(\partial_\nu A_\rho) - (\partial_\rho A_\nu)]}_{F_{\nu\rho}}(\partial_\mu\psi) .
\end{aligned} \tag{5.67}$$

Moreover, for the others once we reorder the terms we can write;

$$\begin{aligned}
\theta^{\nu\rho}[(\partial_\mu A_\rho)(\partial_\nu\psi) + (\partial_\nu A_\mu)(\partial_\rho\psi)] &= \frac{1}{2}(\theta^{\nu\rho} - \theta^{\rho\nu})[(\partial_\mu A_\rho)(\partial_\nu\psi) + (\partial_\nu A_\mu)(\partial_\rho\psi)] \\
&= \frac{1}{2} \left\{ \theta^{\nu\rho}(\partial_\mu A_\rho)(\partial_\nu\psi) - \underbrace{\theta^{\rho\nu}(\partial_\mu A_\rho)(\partial_\nu\psi)}_{\theta^{\nu\rho}(\partial_\mu A_\nu)(\partial_\rho\psi)} \right. \\
&\quad \left. + \theta^{\nu\rho}(\partial_\nu A_\mu)(\partial_\rho\psi) - \underbrace{\theta^{\rho\nu}(\partial_\nu A_\mu)(\partial_\rho\psi)}_{\theta^{\nu\rho}(\partial_\rho A_\mu)(\partial_\nu\psi)} \right\} \\
&= \frac{1}{2}\theta^{\nu\rho} \left\{ \underbrace{(\partial_\mu A_\rho - \partial_\rho A_\mu)}_{F_{\mu\rho}} \partial_\nu\psi + \underbrace{(\partial_\nu A_\mu - \partial_\mu A_\nu)}_{F_{\nu\mu}} \partial_\rho\psi \right\} \\
\boxed{\theta^{\nu\rho}[(\partial_\mu A_\rho)(\partial_\nu\psi) + (\partial_\nu A_\mu)(\partial_\rho\psi)]} &= \frac{1}{2}\theta^{\nu\rho} [F_{\mu\rho}\partial_\nu + F_{\nu\mu}\partial_\rho] \psi .
\end{aligned} \tag{5.68}$$

Hence using Equations (5.67) and (5.68),  $S_2$  turns out to be equal to;

$$\begin{aligned}
S_2 &= \int d^4x \ ie\theta^{\nu\rho}\gamma^\mu [\bar{\psi}((\partial_\mu A_\rho)(\partial_\nu\psi) - (\partial_\nu A_\rho)(\partial_\mu\psi) + (\partial_\nu A_\mu)(\partial_\rho\psi))] \\
&= \int d^4x \ \frac{ie}{2}\theta^{\nu\rho}\gamma^\mu [F_{\mu\rho}\partial_\nu + F_{\nu\mu}\partial_\rho - F_{\nu\rho}\partial_\mu] \psi .
\end{aligned} \tag{5.69}$$

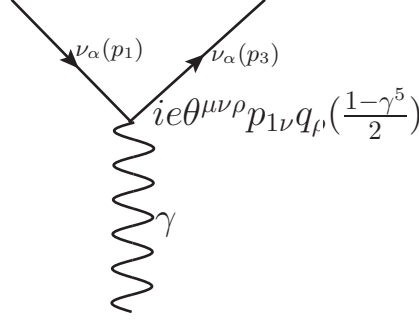


Figure 5.2: Coupling of neutral particles to photons is allowed in NCQED.

With this result Equation (5.63) can be written in the following form

$$S = \int d^4x \left\{ \bar{\psi} \left[ (i\gamma^\mu \partial_\mu - m) + \frac{e}{2} \theta^{\nu\rho} \left( i\gamma^\mu (F_{\mu\rho} \partial_\nu + F_{\nu\mu} \partial_\rho - F_{\nu\rho} \partial_\mu) + m F_{\nu\rho} \right) \right] \psi \right\}. \quad (5.70)$$

Once we define

$$\theta^{\mu\nu\rho} = \theta^{\mu\nu} \gamma^\rho + \theta^{\nu\rho} \gamma^\mu + \theta^{\rho\mu} \gamma^\nu \quad (5.71)$$

then we can write the above action in the following compact form.

$$S = \int d^4x \bar{\psi} \left[ (i\gamma^\mu \partial_\mu - m) - \frac{e}{2} F_{\mu\nu} (i\theta^{\mu\nu\rho} \partial_\rho - \theta^{\mu\nu} m) \right] \psi. \quad (5.72)$$

This action describes a tree-level interaction of photons and neutrinos on the non-commutative space with the following vertex factor as shown in Figure (5.2).

Once we neglect mass of the neutrinos, the vertex factor for the  $\nu\nu\gamma$  interaction can be found from the action as [110]

$$\Gamma^\mu(\nu\bar{\nu}\gamma) = ie \frac{1}{2} (1 - \gamma^5) \theta^{\mu\nu\rho} (p_1)_\nu q_\rho, \quad (5.73)$$

which is absent in the SM.

#### 5.4.1 Neutrino-electron Scattering in Non-Commutative Space

We showed that in the non-commutative space, neutrinos can couple with photons. Thus, in addition to the weak bosons exchange, the neutrino electron scattering can

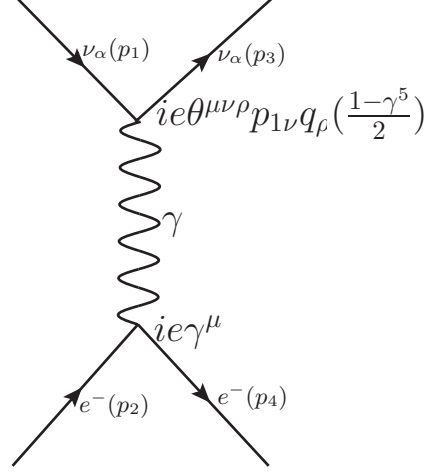


Figure 5.3: Feynman Diagram of  $\nu - e^-$  scattering in non-commutative space is displayed. Even though neutrinos are neutral they can still interact with photons.

take place via the photon exchange also. The Feynman diagram of the relevant interaction with vertex factors up to the first order of  $\theta$  is given in Figure (5.3). So let us evaluate the contribution of this new diagram to the cross-section of the neutrino-electron scattering.

Following the Feynman rules for the diagram in Figure (5.3), we can write the amplitude as;

$$-i\mathcal{M}_{NC} = [\bar{u}(p_4)(ie)\gamma^\mu u(p_2)] \left(\frac{-ig_{\mu\nu}}{q^2}\right) [\bar{u}(p_3)(ie\theta^{\nu\sigma\rho} p_{1\sigma} q_\rho \frac{1-\gamma^5}{2})u(p_1)] \quad (5.74)$$

where  $q$  is the momentum transfer,  $q = p_1 - p_3$  and  $\theta^{\mu\nu\rho} = \theta^{\mu\nu}\gamma^\rho + \theta^{\nu\rho}\gamma^\mu + \theta^{\rho\mu}\gamma^\nu$ .

Once we simplify the above equation, we get;

$$\mathcal{M}_{NC} = \frac{e^2}{2q^2} [\bar{u}(p_4)\gamma^\mu u(p_2)] [\bar{u}(p_3)\theta_\mu^{\sigma\rho} p_{1\sigma} q_\rho (1-\gamma^5)u(p_1)]. \quad (5.75)$$

Let us calculate  $|\mathcal{M}_{NC}|^2$ .

$$|\mathcal{M}_{NC}|^2 = \frac{e^4}{4q^4} [\bar{u}(p_4) \underbrace{\gamma^\mu}_{\Gamma_1} u(p_2)] [\bar{u}(p_4) \underbrace{\gamma^\alpha}_{\Gamma_2} u(p_2)]^\dagger \quad (5.76)$$

$$[\bar{u}(p_3) \underbrace{\theta_\mu^{\sigma\rho} p_{1\sigma} q_\rho (1-\gamma^5)}_{\Gamma_3} u(p_1)] [\bar{u}(p_3) \underbrace{\theta_\alpha^{\beta\eta} p_{1\beta} q_\eta (1-\gamma^5)}_{\Gamma_4} u(p_1)]^\dagger .$$

Performing summation over the possible final spin states and apply the Casimir iden-

tities we get;

$$\begin{aligned} \sum_{spin} |\mathcal{M}_{NC}|^2 &= \frac{e^4}{4q^4} Tr[\Gamma_1(p_2 + m_2)\bar{\Gamma}_2(p_4 + m_4)] \\ &\times Tr[\Gamma_3(p_1 + m_1)\bar{\Gamma}_4(p_3 + m_3)], \end{aligned} \quad (5.77)$$

where

$$\bar{\Gamma} = \gamma^0 \Gamma^\dagger \gamma^0. \quad (5.78)$$

Moreover, note that  $m_2 = m_4 = m_e$  and  $m_1 = m_3 = m_\nu$ . We can write the Equation (5.76) once we sum over final spin states as;

$$\begin{aligned} \sum_{spin} |\mathcal{M}_{NC}|^2 &= \frac{e^4}{4q^4} Tr[\gamma^\mu(p_2 + m_e)\gamma^\alpha(p_4 + m_e)] \\ &\times p_{1\sigma} p_{1\beta} q_\rho q_\eta Tr[\theta_\mu^{\sigma\rho}(1 - \gamma^5)(p_1 + m_1)\theta_\alpha^{\beta\eta}(1 - \gamma^5)(p_3 + m_3)]. \end{aligned} \quad (5.79)$$

Let us define the each trace terms in Equation (5.79) as;

$$A^{\mu\alpha} = Tr[\gamma^\mu(p_2 + m_e)\gamma^\alpha(p_4 + m_e)], \quad (5.80)$$

$$B_{\mu\alpha} = p_{1\sigma} p_{1\beta} q_\rho q_\eta Tr[\theta_\mu^{\sigma\rho}(1 - \gamma^5)(p_1 + m_1)\theta_\alpha^{\beta\eta}(1 - \gamma^5)(p_3 + m_3)] \quad (5.81)$$

so that we can write amplitude square as;

$$\sum_{spin} |\mathcal{M}_{NC}|^2 = A^{\mu\alpha} B_{\mu\alpha}. \quad (5.82)$$

Now, let us evaluate each trace separately.

$$\begin{aligned} A^{\mu\alpha} &= Tr[\gamma^\mu p_2^\alpha p_4^\alpha] + m_e \cancel{Tr[\gamma^\mu p_2^\alpha \gamma^\alpha]} \\ &+ m_e \cancel{Tr[\gamma^\mu \gamma^\alpha p_4^\alpha]} + m_e^2 Tr[\gamma^\mu \gamma^\alpha] \end{aligned} \quad (5.83)$$

Notice that the second and third terms give zero since the trace of odd number of gamma matrices is equal to zero.

For the first term we get;

$$Tr[\gamma^\mu p_2^\alpha p_4^\alpha] = 4(p_2^\mu p_4^\alpha + p_2^\alpha p_4^\mu - (p_2 \cdot p_4)g^{\mu\alpha}). \quad (5.84)$$



And for the last term;

$$Tr[\gamma^\mu \gamma^\alpha] = 4g^{\mu\alpha} . \quad (5.85)$$

Thus, with these results Equation (5.80) turns out to be;

$$A^{\mu\alpha} = 4(p_2^\mu p_4^\alpha + p_2^\alpha p_4^\mu - (p_2 \cdot p_4)g^{\mu\alpha} + g^{\mu\alpha} m e^2) . \quad (5.86)$$

Let us evaluate  $B_{\mu\alpha}$  (Equation (5.81)).

$$\begin{aligned} B_{\mu\alpha} &= p_{1\sigma} p_{1\beta} q_\rho q_\eta \left( Tr[\theta_\mu^{\sigma\rho} (1 - \gamma^5) \not{p}_1 \theta_\alpha^{\beta\eta} (1 - \gamma^5) \not{p}_3] \right. \\ &\quad + m_3 Tr[\theta_\mu^{\sigma\rho} (1 - \gamma^5) \not{p}_1 \theta_\alpha^{\beta\eta} (1 - \gamma^5)] \\ &\quad + m_1 Tr[\theta_\mu^{\sigma\rho} (1 - \gamma^5) \theta_\alpha^{\beta\eta} (1 - \gamma^5) \not{p}_3] \\ &\quad \left. + m_1 m_3 Tr[\theta_\mu^{\sigma\rho} (1 - \gamma^5) \theta_\alpha^{\beta\eta} (1 - \gamma^5)] \right) . \end{aligned} \quad (5.87)$$

Notice that the second term is zero due to the odd number of  $\gamma$  matrices. For the third term we get;

$$\begin{aligned} m_1 Tr[\theta_\mu^{\sigma\rho} (1 - \gamma^5) \theta_\alpha^{\beta\eta} (1 - \gamma^5) \not{p}_3] &= m_1 Tr[\theta_\mu^{\sigma\rho} (1 - \gamma^5) (1 + \gamma^5) \theta_\alpha^{\beta\eta} \not{p}_3] \\ &= 0 \end{aligned} \quad (5.88)$$

since  $(1 - \gamma^5)(1 + \gamma^5) = 0$ .

Similar to the third term, the last term also equals to zero since

$$\begin{aligned} m_1 m_3 Tr[\theta_\mu^{\sigma\rho} (1 - \gamma^5) \theta_\alpha^{\beta\eta} (1 - \gamma^5)] &= m_1 m_3 Tr[\theta_\mu^{\sigma\rho} \underbrace{(1 - \gamma^5)(1 + \gamma^5)}_0 \theta_\alpha^{\beta\eta}] \\ &= 0 . \end{aligned} \quad (5.89)$$

With these calculations, we can write Equation (5.81) as;

$$\begin{aligned} B_{\mu\alpha} &= p_{1\sigma} p_{1\beta} q_\rho q_\eta Tr[\theta_\mu^{\sigma\rho} (1 - \gamma^5) \not{p}_1 \theta_\alpha^{\beta\eta} (1 - \gamma^5) \not{p}_3] \\ &= p_{1\sigma} p_{1\beta} q_\rho q_\eta Tr[\theta_\mu^{\sigma\rho} (1 - \gamma^5) (1 - \gamma^5) \not{p}_1 \theta_\alpha^{\beta\eta} \not{p}_3] \\ &= 2p_{1\sigma} p_{1\beta} q_\rho q_\eta Tr[\theta_\mu^{\sigma\rho} (1 - \gamma^5) \not{p}_1 \theta_\alpha^{\beta\eta} \not{p}_3] \\ &= 2p_{1\sigma} p_{1\beta} q_\rho q_\eta (Tr[\theta_\mu^{\sigma\rho} \not{p}_1 \theta_\alpha^{\beta\eta} \not{p}_3] - Tr[\theta_\mu^{\sigma\rho} \gamma^5 \not{p}_1 \theta_\alpha^{\beta\eta} \not{p}_3]) \end{aligned} \quad (5.90)$$

by using  $(1 - \gamma^5)(1 - \gamma^5) = 2(1 - \gamma^5)$ .

Let us define;

$$\begin{aligned} B_1 &= Tr[\theta_\mu^{\sigma\rho} \not{p}_1 \theta_\alpha^{\beta\eta} \not{p}_3] , \\ B_2 &= Tr[\theta_\mu^{\sigma\rho} \gamma^5 \not{p}_1 \theta_\alpha^{\beta\eta} \not{p}_3] \end{aligned} \quad (5.91)$$

so that

$$B_{\mu\alpha} = 2p_{1\sigma}p_{1\beta}q_\rho q_\eta (B_1 - B_2). \quad (5.92)$$

Let us evaluate  $B_1$  first;

Since

$$\begin{aligned} \theta_\mu^{\sigma\rho} &= \theta_\mu^\sigma \gamma^\rho + \theta^{\sigma\rho} \gamma_\mu + \theta_\mu^\rho \gamma^\sigma \\ \theta_\alpha^{\beta\eta} &= \theta_\alpha^\beta \gamma^\eta + \theta^{\beta\eta} \gamma_\alpha + \theta_\alpha^\eta \gamma^\beta \end{aligned} \quad (5.93)$$

$B_1$  can be written as ;

$$B_1 = Tr[(\theta_\mu^\sigma \gamma^\rho + \theta^{\sigma\rho} \gamma_\mu + \theta_\mu^\rho \gamma^\sigma) \not{p}_1 (\theta_\alpha^\beta \gamma^\eta + \theta^{\beta\eta} \gamma_\alpha + \theta_\alpha^\eta \gamma^\beta) \not{p}_3]. \quad (5.94)$$

Once we expand each term we get;

$$\begin{aligned} B_1 &= \theta_\mu^\sigma \theta_\alpha^\beta Tr[\gamma^\rho \not{p}_1 \gamma^\eta \not{p}_3] + \theta_\mu^\sigma \theta^{\beta\eta} Tr[\gamma^\rho \not{p}_1 \gamma_\alpha \not{p}_3] + \theta_\mu^\sigma \theta_\alpha^\eta Tr[\gamma^\rho \not{p}_1 \gamma^\beta \not{p}_3] \\ &+ \theta^{\sigma\rho} \theta_\alpha^\beta Tr[\gamma_\mu \not{p}_1 \gamma^\eta \not{p}_3] + \theta^{\sigma\rho} \theta^{\beta\eta} Tr[\gamma_\mu \not{p}_1 \gamma_\alpha \not{p}_3] + \theta^{\sigma\rho} \theta_\alpha^\eta Tr[\gamma_\mu \not{p}_1 \gamma^\beta \not{p}_3] \\ &+ \theta_\mu^\rho \theta_\alpha^\beta Tr[\gamma^\sigma \not{p}_1 \gamma^\eta \not{p}_3] + \theta_\mu^\rho \theta^{\beta\eta} Tr[\gamma^\sigma \not{p}_1 \gamma_\alpha \not{p}_3] + \theta_\mu^\rho \theta_\alpha^\eta Tr[\gamma^\sigma \not{p}_1 \gamma^\beta \not{p}_3]. \end{aligned} \quad (5.95)$$

We can evaluate one of the trace terms as;

$$Tr[\gamma^\alpha \not{p}_1 \gamma^\beta \not{p}_2] = 4(p_1^\alpha p_2^\beta + p_1^\beta p_2^\alpha - (p_1 \cdot p_2) g^{\alpha\beta}). \quad (5.96)$$

Notice that all the other trace terms are in same form and can be evaluated easily.

Hence,  $B_1$  equals to;

$$\begin{aligned} B_1 &= 4 \left( \theta_\mu^\sigma \theta_\alpha^\beta (p_1^\rho p_3^\eta + p_1^\eta p_3^\rho - (p_1 \cdot p_3) g^{\rho\eta}) + \theta_\mu^\sigma \theta^{\beta\eta} (p_1^\rho p_{3\alpha} + p_{1\alpha} p_3^\rho - (p_1 \cdot p_3) g_\alpha^\rho) \right. \\ &+ \theta_\mu^\sigma \theta_\alpha^\eta (p_1^\rho p_3^\beta + p_1^\beta p_3^\rho - (p_1 \cdot p_3) g^{\rho\beta}) + \theta^{\sigma\rho} \theta_\alpha^\beta (p_{1\mu} p_3^\eta + p_1^\eta p_{3\mu} - (p_1 \cdot p_3) g_\mu^\eta) \\ &+ \theta^{\sigma\rho} \theta^{\beta\eta} (p_{1\mu} p_{3\alpha} + p_{1\alpha} p_{3\mu} - (p_1 \cdot p_3) g_{\mu\alpha}) + \theta^{\sigma\rho} \theta_\alpha^\eta (p_{1\mu} p_3^\beta + p_1^\beta p_{3\mu} - (p_1 \cdot p_3) g_\mu^\beta) \\ &+ \theta_\mu^\rho \theta_\alpha^\beta (p_1^\sigma p_3^\eta + p_1^\eta p_3^\sigma - (p_1 \cdot p_3) g^{\sigma\eta}) + \theta_\mu^\rho \theta^{\beta\eta} (p_1^\sigma p_{3\alpha} + p_{1\alpha} p_3^\sigma - (p_1 \cdot p_3) g_\alpha^\sigma) \\ &\left. + \theta_\mu^\rho \theta_\alpha^\eta (p_1^\sigma p_3^\beta + p_1^\beta p_3^\sigma - (p_1 \cdot p_3) g^{\sigma\beta}) \right). \end{aligned} \quad (5.97)$$

Now let us evaluate  $B_2$  ;

$$\begin{aligned} B_2 &= Tr[\theta_\mu^{\sigma\rho} \gamma^5 \not{p}_1 \theta_\alpha^{\beta\eta} \not{p}_3] \\ &= Tr[(\theta_\mu^\sigma \gamma^\rho + \theta^{\sigma\rho} \gamma_\mu + \theta_\mu^\rho \gamma^\sigma) \gamma^5 \not{p}_1 (\theta_\alpha^\beta \gamma^\eta + \theta^{\beta\eta} \gamma_\alpha + \theta_\alpha^\eta \gamma^\beta) \not{p}_3]. \end{aligned} \quad (5.98)$$

Once we expand the terms we get;

$$\begin{aligned}
B_2 = & \theta_\mu^\sigma \theta_\alpha^\beta Tr[\gamma^\rho \gamma^5 p_1 \gamma^\eta p_3] + \theta_\mu^\sigma \theta^{\beta\eta} Tr[\gamma^\rho \gamma^5 p_1 \gamma_\alpha p_3] + \theta_\mu^\sigma \theta_\alpha^\eta Tr[\gamma^\rho \gamma^5 p_1 \gamma^\beta p_3] \\
& + \theta^{\sigma\rho} \theta_\alpha^\beta Tr[\gamma_\mu \gamma^5 p_1 \gamma^\eta p_3] + \theta^{\sigma\rho} \theta^{\beta\eta} Tr[\gamma_\mu \gamma^5 p_1 \gamma_\alpha p_3] + \theta^{\sigma\rho} \theta_\alpha^\eta Tr[\gamma^\mu \gamma^5 p_1 p_3] \\
& + \theta_\mu^\rho \theta_\alpha^\beta Tr[\gamma^\sigma \gamma^5 p_1 \gamma^\eta p_3] + \theta_\mu^\rho \theta^{\beta\eta} Tr[\gamma^\sigma \gamma^5 p_1 \gamma_\alpha p_3] + \theta_\mu^\rho \theta_\alpha^\eta Tr[\gamma^\sigma \gamma^5 p_1 \gamma^\beta p_3] .
\end{aligned} \tag{5.99}$$

All the terms are in the same form with different indices. Hence let us evaluate one of the terms and the others are trivial.

$$\begin{aligned}
Tr[\gamma^\mu \gamma^5 p_1 \gamma^\nu p_2] &= p_{1\alpha} p_{2\beta} Tr[\gamma^\mu \gamma^5 \gamma^\alpha \gamma^\nu \gamma^\beta] \\
&= -p_{1\alpha} p_{2\beta} Tr[\gamma^5 \gamma^\mu \gamma^\alpha \gamma^\nu \gamma^\beta] \\
&= -p_{1\alpha} p_{2\beta} 4i \epsilon^{\mu\alpha\nu\beta} \\
&= 4ip_{1\alpha} p_{2\beta} \epsilon^{\mu\nu\alpha\beta} .
\end{aligned} \tag{5.100}$$

Thus, with the result of this trace we can write  $B_2$  as;

$$\begin{aligned}
B_2 = & 4ip_{1a} p_{3b} \left( \theta_\mu^\sigma \theta_\alpha^\beta \epsilon^{\rho\eta ab} + \theta_\mu^\sigma \theta^{\beta\eta} g_{\alpha\xi} \epsilon^{\rho\xi ab} + \theta_\mu^\sigma \theta_\alpha^\eta \epsilon^{\rho\beta ab} \right. \\
& + \theta^{\sigma\rho} \theta_\alpha^\beta g_{\mu\xi} \epsilon^{\xi\eta ab} + \theta^{\sigma\rho} \theta^{\beta\eta} g_{\mu\xi_1} g_{\mu\xi_2} \epsilon^{\xi_1 \xi_2 ab} + \theta^{\sigma\rho} \theta_\alpha^\eta g_{\mu\xi} \epsilon^{\xi\beta ab} \\
& \left. + \theta_\mu^\rho \theta_\alpha^\beta \epsilon^{\sigma\eta ab} + \theta_\mu^\rho \theta^{\beta\eta} g_{\xi\alpha} \epsilon^{\sigma\xi ab} + \theta_\mu^\rho \theta_\alpha^\eta \epsilon^{\sigma\beta ab} \right) .
\end{aligned} \tag{5.101}$$

We evaluated all the traces. Now, let us contract the terms for  $A^{\mu\alpha} B_{\mu\alpha}$ .

$$\begin{aligned}
A^{\mu\alpha} B_{\mu\alpha} &= 4 \overbrace{(p_2^\mu p_4^\alpha + p_2^\alpha p_4^\mu - (p_2 \cdot p_4) g^{\mu\alpha} + g^{\mu\alpha} m e^2)}^{A^{\mu\alpha}} \overbrace{(2p_{1\sigma} p_{1\beta} q_\rho q_\eta (B_1 - B_2))}^{B_{\mu\alpha}} \\
&= 8p_{1\sigma} p_{1\beta} q_\rho q_\eta (p_2^\mu p_4^\alpha + p_2^\alpha p_4^\mu - (p_2 \cdot p_4) g^{\mu\alpha} + g^{\mu\alpha} m e^2) (B_1 - B_2) \\
&= 8p_{1\sigma} p_{1\beta} q_\rho q_\eta (p_2^\mu p_4^\alpha + p_2^\alpha p_4^\mu - (p_2 \cdot p_4) g^{\mu\alpha} + g^{\mu\alpha} m e^2) B_1 \\
&\quad - 8p_{1\sigma} p_{1\beta} q_\rho q_\eta (p_2^\mu p_4^\alpha + p_2^\alpha p_4^\mu - (p_2 \cdot p_4) g^{\mu\alpha} + g^{\mu\alpha} m e^2) B_2
\end{aligned} \tag{5.102}$$

where  $B_1$  and  $B_2$  are given by Equations (5.97) and (5.101), respectively.

For clarity let us define;

$$\begin{aligned}
C_1 &= 8p_{1\sigma} p_{1\beta} q_\rho q_\eta (p_2^\mu p_4^\alpha + p_2^\alpha p_4^\mu - (p_2 \cdot p_4) g^{\mu\alpha} + g^{\mu\alpha} m e^2) B_1 , \\
C_2 &= 8p_{1\sigma} p_{1\beta} q_\rho q_\eta (p_2^\mu p_4^\alpha + p_2^\alpha p_4^\mu - (p_2 \cdot p_4) g^{\mu\alpha} + g^{\mu\alpha} m e^2) B_2
\end{aligned} \tag{5.103}$$

so that we can write Equation (5.102) as;

$$A^{\mu\alpha}B_{\mu\alpha} = C_1 - C_2 . \quad (5.104)$$

Let us first evaluate  $C_2$ . Once we use Equation (5.101) for  $B_2$  then  $C_2$  can be written as;

$$\begin{aligned} C_2 = & 32ip_{1a}p_{3b}p_{1\sigma}p_{1\beta}q_{\rho}q_{\eta}(p_2^{\mu}p_4^{\alpha} + p_2^{\alpha}p_4^{\mu} - (p_2 \cdot p_4)g^{\mu\alpha} + g^{\mu\alpha}me^2) \\ & \times (\theta_{\mu}^{\sigma}\theta_{\alpha}^{\beta}\epsilon^{\rho\eta ab} + \theta_{\mu}^{\sigma}\theta^{\beta\eta}g_{\alpha\xi}\epsilon^{\rho\xi ab} + \theta_{\mu}^{\sigma}\theta_{\alpha}^{\eta}\epsilon^{\rho\beta ab} + \theta^{\sigma\rho}\theta_{\alpha}^{\beta}g_{\mu\xi}\epsilon^{\xi\eta ab} \\ & + \theta^{\sigma\rho}\theta^{\beta\eta}g_{\mu\xi_1}g_{\mu\xi_2}\epsilon^{\xi_1\xi_2 ab} + \theta^{\sigma\rho}\theta_{\alpha}^{\eta}g_{\mu\xi}\epsilon^{\xi\beta ab} + \theta_{\mu}^{\rho}\theta_{\alpha}^{\beta}\epsilon^{\sigma\eta ab} + \theta_{\mu}^{\rho}\theta^{\beta\eta}g_{\xi\alpha}\epsilon^{\sigma\xi ab} + \theta_{\mu}^{\rho}\theta_{\alpha}^{\eta}\epsilon^{\sigma\beta ab}) . \end{aligned} \quad (5.105)$$

Let us expand each product and evaluate them term by term for a neater calculation. By decomposing  $C_2$ , we can write;

$$C_2 = C_{21} + C_{22} + C_{23} + C_{24} + C_{25} + C_{26} + C_{27} + C_{28} + C_{29} . \quad (5.106)$$

For  $C_{21}$ , we perform the calculation as;

$$\begin{aligned} C_{21} = & 32ip_{1a}p_{3b}p_{1\sigma}p_{1\beta} \underbrace{q_{\rho}q_{\eta}}_S (p_2^{\mu}p_4^{\alpha} + p_2^{\alpha}p_4^{\mu} - (p_2 \cdot p_4)g^{\mu\alpha} + g^{\mu\alpha}me^2) \theta_{\mu}^{\sigma}\theta_{\alpha}^{\beta} \underbrace{\epsilon^{\rho\eta ab}}_{AS} \\ = & 0 \end{aligned} \quad (5.107)$$

where "S" corresponds to symmetric and "AS" corresponds to anti-symmetric terms. Since  $C_{21}$  contains symmetric times anti-symmetric components, the result is zero.

For  $C_{22}$ ;

$$C_{22} = 32ip_{1a}p_{3b}p_{1\sigma}p_{1\beta}q_{\rho}q_{\eta}(p_2^{\mu}p_4^{\alpha} + p_2^{\alpha}p_4^{\mu} - (p_2 \cdot p_4)g^{\mu\alpha} + g^{\mu\alpha}me^2)\theta_{\mu}^{\sigma}\theta^{\beta\eta}g_{\alpha\xi}\epsilon^{\rho\xi ab} . \quad (5.108)$$

Moreover, since  $q = p_1 - p_3$  we can write  $C_{22}$  as;

$$\begin{aligned}
C_{22} &= 32ip_{1a}(p_{1\rho} - p_{3\rho})\epsilon^{\rho\xi ab}p_{3b}p_{1\sigma}p_{1\beta}q_{\eta}(p_2^{\mu}p_4^{\alpha} + p_2^{\alpha}p_4^{\mu} - (p_2 \cdot p_4)g^{\mu\alpha} + g^{\mu\alpha}me^2) \\
&\quad \times \theta_{\mu}^{\sigma}\theta^{\beta\eta}g_{\alpha\xi} \\
&= 32i\underbrace{p_{1a}p_{1\rho}}_S \underbrace{\epsilon^{\rho\xi ab}}_{AS} p_{3b}p_{1\sigma}p_{1\beta}q_{\eta}(p_2^{\mu}p_4^{\alpha} + p_2^{\alpha}p_4^{\mu} - (p_2 \cdot p_4)g^{\mu\alpha} + g^{\mu\alpha}me^2)\theta_{\mu}^{\sigma}\theta^{\beta\eta}g_{\alpha\xi} \\
&\quad - 32i\underbrace{p_{1a}p_{3b}p_{3\rho}}_S \underbrace{\epsilon^{\rho\xi ab}}_{AS} p_{1\sigma}p_{1\beta}q_{\eta}(p_2^{\mu}p_4^{\alpha} + p_2^{\alpha}p_4^{\mu} - (p_2 \cdot p_4)g^{\mu\alpha} + g^{\mu\alpha}me^2)\theta_{\mu}^{\sigma}\theta^{\beta\eta}g_{\alpha\xi} \\
&= 0.
\end{aligned} \tag{5.109}$$

Similarly for  $C_{23}$ ;

$$\begin{aligned}
C_{23} &= 32ip_{1a}p_{3b}p_{1\sigma}p_{1\beta}q_{\rho}q_{\eta}(p_2^{\mu}p_4^{\alpha} + p_2^{\alpha}p_4^{\mu} - (p_2 \cdot p_4)g^{\mu\alpha} + g^{\mu\alpha}me^2)\theta_{\mu}^{\sigma}\theta_{\alpha}^{\eta}\epsilon^{\rho\beta ab} \\
&= 32ip_{1a}p_{3b}p_{1\sigma}p_{1\beta}(p_{1\rho} - p_{3\rho})\epsilon^{\rho\beta ab}q_{\eta}(p_2^{\mu}p_4^{\alpha} + p_2^{\alpha}p_4^{\mu} - (p_2 \cdot p_4)g^{\mu\alpha} + g^{\mu\alpha}me^2)\theta_{\mu}^{\sigma}\theta_{\alpha}^{\eta} \\
&= 2ip_{1a}p_{3b}p_{1\sigma}\underbrace{p_{1\beta}p_{1\rho}}_S \underbrace{\epsilon^{\rho\beta ab}}_{AS} q_{\eta}(p_2^{\mu}p_4^{\alpha} + p_2^{\alpha}p_4^{\mu} - (p_2 \cdot p_4)g^{\mu\alpha} + g^{\mu\alpha}me^2)\theta_{\mu}^{\sigma}\theta_{\alpha}^{\eta} \\
&\quad - 2ip_{1a}p_{1\sigma}p_{1\beta}\underbrace{p_{3b}p_{3\rho}}_S \underbrace{\epsilon^{\rho\beta ab}}_{AS} q_{\eta}(p_2^{\mu}p_4^{\alpha} + p_2^{\alpha}p_4^{\mu} - (p_2 \cdot p_4)g^{\mu\alpha} + g^{\mu\alpha}me^2)\theta_{\mu}^{\sigma}\theta_{\alpha}^{\eta} \\
&= 0.
\end{aligned} \tag{5.110}$$

Due to the same argument above,  $C_{24}$  is also equal to zero as follow

$$\begin{aligned}
C_{24} &= 32ip_{1a}p_{3b}p_{1\sigma}p_{1\beta}q_{\rho}q_{\eta}(p_2^{\mu}p_4^{\alpha} + p_2^{\alpha}p_4^{\mu} - (p_2 \cdot p_4)g^{\mu\alpha} + g^{\mu\alpha}me^2)\theta^{\sigma\rho}\theta_{\alpha}^{\beta}g_{\mu\xi}\epsilon^{\xi\eta ab} \\
&= 32ip_{1a}p_{3b}p_{1\sigma}p_{1\beta}q_{\rho}(p_{1\eta} - p_{3\eta})\theta^{\sigma\rho}\theta_{\alpha}^{\beta}g_{\mu\xi}\epsilon^{\xi\eta ab} \\
&\quad \times (p_2^{\mu}p_4^{\alpha} + p_2^{\alpha}p_4^{\mu} - (p_2 \cdot p_4)g^{\mu\alpha} + g^{\mu\alpha}me^2) \\
&= 32ip_{3b}p_{1\sigma}p_{1\beta}q_{\rho}\underbrace{p_{1a}p_{1\eta}}_S \underbrace{\epsilon^{\xi\eta ab}}_{AS}(p_2^{\mu}p_4^{\alpha} + p_2^{\alpha}p_4^{\mu} - (p_2 \cdot p_4)g^{\mu\alpha} + g^{\mu\alpha}me^2)\theta^{\sigma\rho}\theta_{\alpha}^{\beta}g_{\mu\xi} \\
&\quad - 32ip_{1a}p_{1\sigma}p_{1\beta}q_{\rho}\underbrace{p_{3b}p_{3\eta}}_S \underbrace{\epsilon^{\xi\eta ab}}_{AS}(p_2^{\mu}p_4^{\alpha} + p_2^{\alpha}p_4^{\mu} - (p_2 \cdot p_4)g^{\mu\alpha} + g^{\mu\alpha}me^2)\theta^{\sigma\rho}\theta_{\alpha}^{\beta}g_{\mu\xi} \\
&= 0.
\end{aligned} \tag{5.111}$$

For  $C_{25}$ ;

$$\begin{aligned}
C_{25} &= 32ip_{1a}p_{3b}p_{1\sigma}p_{1\beta}q_{\rho}q_{\eta}(p_2^{\mu}p_4^{\alpha} + p_2^{\alpha}p_4^{\mu} - (p_2 \cdot p_4)g^{\mu\alpha} + g^{\mu\alpha}me^2) \\
&\quad \times \theta^{\sigma\rho}\theta^{\beta\eta}g_{\mu\xi_1}g_{\mu\xi_2}\epsilon^{\xi_1\xi_2ab} \\
&= 32ip_{1a}p_{3b}p_{1\sigma}p_{1\beta}q_{\rho}q_{\eta} \underbrace{(p_2^{\mu}p_4^{\alpha} + p_2^{\alpha}p_4^{\mu} - (p_2 \cdot p_4)g^{\mu\alpha} + g^{\mu\alpha}me^2)}_{S \text{ in } \mu, \alpha} \underbrace{\epsilon_{\mu\alpha}^{ab}}_{AS \text{ in } \mu, \alpha} \theta^{\sigma\rho}\theta^{\beta\eta} \\
&= 0.
\end{aligned} \tag{5.112}$$

For  $C_{26}$ ;

$$\begin{aligned}
C_{26} &= 32ip_{1a}p_{3b}p_{1\sigma}p_{1\beta}q_{\rho}q_{\eta}(p_2^{\mu}p_4^{\alpha} + p_2^{\alpha}p_4^{\mu} - (p_2 \cdot p_4)g^{\mu\alpha} + g^{\mu\alpha}me^2)\theta_{\mu}^{\sigma}\theta_{\alpha}^{\eta}\epsilon^{\rho\beta ab} \\
&= 32ip_{3b}p_{1\sigma} \underbrace{p_{1a}p_{1\beta}}_S \underbrace{\epsilon^{\rho\beta ab}}_{AS} q_{\rho}q_{\eta}(p_2^{\mu}p_4^{\alpha} + p_2^{\alpha}p_4^{\mu} - (p_2 \cdot p_4)g^{\mu\alpha} + g^{\mu\alpha}me^2)\theta_{\mu}^{\sigma}\theta_{\alpha}^{\eta} \\
&= 0.
\end{aligned} \tag{5.113}$$

For  $C_{27}$ ;

$$\begin{aligned}
C_{27} &= 32ip_{1a}p_{3b}p_{1\sigma}p_{1\beta}q_{\rho}q_{\eta}(p_2^{\mu}p_4^{\alpha} + p_2^{\alpha}p_4^{\mu} - (p_2 \cdot p_4)g^{\mu\alpha} + g^{\mu\alpha}me^2)\theta_{\mu}^{\rho}\theta_{\alpha}^{\beta}\epsilon^{\sigma\eta ab} \\
&= 32ip_{3b}p_{1\beta} \underbrace{p_{1a}p_{1\sigma}}_S \underbrace{\epsilon^{\sigma\eta ab}}_{AS} q_{\rho}q_{\eta}(p_2^{\mu}p_4^{\alpha} + p_2^{\alpha}p_4^{\mu} - (p_2 \cdot p_4)g^{\mu\alpha} + g^{\mu\alpha}me^2)\theta_{\mu}^{\rho}\theta_{\alpha}^{\beta} \\
&= 0.
\end{aligned} \tag{5.114}$$

For  $C_{28}$ ;

$$\begin{aligned}
C_{28} &= 32ip_{1a}p_{3b}p_{1\sigma}p_{1\beta}q_{\rho}q_{\eta}(p_2^{\mu}p_4^{\alpha} + p_2^{\alpha}p_4^{\mu} - (p_2 \cdot p_4)g^{\mu\alpha} + g^{\mu\alpha}me^2)\theta_{\mu}^{\rho}\theta^{\beta\eta}g_{\xi\alpha}\epsilon^{\sigma\xi ab} \\
&= 32ip_{3b} \underbrace{p_{1a}p_{1\sigma}}_S \underbrace{\epsilon^{\sigma\xi ab}}_{AS} g_{\xi\alpha}p_{1\beta}q_{\rho}q_{\eta}(p_2^{\mu}p_4^{\alpha} + p_2^{\alpha}p_4^{\mu} - (p_2 \cdot p_4)g^{\mu\alpha} + g^{\mu\alpha}me^2)\theta_{\mu}^{\rho}\theta^{\beta\eta} \\
&= 0.
\end{aligned} \tag{5.115}$$

For  $C_{29}$ ;

$$\begin{aligned}
C_{29} &= 32ip_{1a}p_{3b}p_{1\sigma}p_{1\beta}q_{\rho}q_{\eta}(p_2^{\mu}p_4^{\alpha} + p_2^{\alpha}p_4^{\mu} - (p_2 \cdot p_4)g^{\mu\alpha} + g^{\mu\alpha}me^2)\theta_{\mu}^{\rho}\theta_{\alpha}^{\eta}\epsilon^{\sigma\beta ab} \\
&= 32ip_{3b} \underbrace{p_{1a}p_{1\sigma}}_S \underbrace{\epsilon^{\sigma\beta ab}}_{AS} p_{1\beta}q_{\rho}q_{\eta}(p_2^{\mu}p_4^{\alpha} + p_2^{\alpha}p_4^{\mu} - (p_2 \cdot p_4)g^{\mu\alpha} + g^{\mu\alpha}me^2)\theta_{\mu}^{\rho}\theta_{\alpha}^{\eta} \\
&= 0.
\end{aligned} \tag{5.116}$$

Finally we find  $C_2$  as;

$$\boxed{C_2 = C_{21} + C_{22} + C_{23} + C_{24} + C_{25} + C_{26} + C_{27} + C_{28} + C_{29} = 0 .} \quad (5.117)$$

Now let us evaluate  $C_1$ ;

$$\begin{aligned} C_1 &= 8p_{1\sigma}p_{1\beta}q_\rho q_\eta (p_2^\mu p_4^\alpha + p_2^\alpha p_4^\mu - (p_2 \cdot p_4)g^{\mu\alpha} + g^{\mu\alpha}m e^2) B_1 \\ &= \underbrace{8p_{1\sigma}p_{1\beta}q_\rho q_\eta p_2^\mu p_4^\alpha B_1}_{C_{11}} + \underbrace{8p_{1\sigma}p_{1\beta}q_\rho q_\eta p_2^\alpha p_4^\mu B_1}_{C_{12}} \\ &\quad - \underbrace{8p_{1\sigma}p_{1\beta}q_\rho q_\eta (p_2 \cdot p_4)g^{\mu\alpha} B_1}_{C_{13}} + \underbrace{8p_{1\sigma}p_{1\beta}q_\rho q_\eta g^{\mu\alpha} m e^2 B_1}_{C_{14}} . \end{aligned} \quad (5.118)$$

Decomposing each term for later convenience we write

$$C_1 = C_{11} + C_{12} - C_{13} + C_{14} . \quad (5.119)$$

$C_{11}$  is expressed as;

$$\begin{aligned} C_{11} &= 8p_{1\sigma}p_{1\beta}q_\rho q_\eta p_2^\mu p_4^\alpha B_1 \\ &= 32p_{1\sigma}p_{1\beta}q_\rho q_\eta p_2^\mu p_4^\alpha \left( \theta_\mu^\sigma \theta_\alpha^\beta (p_1^\rho p_3^\eta + p_1^\eta p_3^\rho - (p_1 \cdot p_3)g^{\rho\eta}) + \right. \\ &\quad \theta_\mu^\sigma \theta_\alpha^\beta (p_1^\rho p_3^\alpha + p_{1\alpha} p_3^\rho - (p_1 \cdot p_3)g_\alpha^\rho) + \theta_\mu^\sigma \theta_\alpha^\eta (p_1^\rho p_3^\beta + p_1^\beta p_3^\rho - (p_1 \cdot p_3)g^{\rho\beta}) \\ &\quad + \theta^{\sigma\rho} \theta_\alpha^\beta (p_{1\mu} p_3^\eta + p_1^\eta p_{3\mu} - (p_1 \cdot p_3)g_\mu^\eta) + \theta^{\sigma\rho} \theta^{\beta\eta} (p_{1\mu} p_{3\alpha} + p_{1\alpha} p_{3\mu} - (p_1 \cdot p_3)g_{\mu\alpha}) \\ &\quad + \theta^{\sigma\rho} \theta_\alpha^\eta (p_{1\mu} p_3^\beta + p_1^\beta p_{3\mu} - (p_1 \cdot p_3)g_\mu^\beta) + \theta_\mu^\rho \theta_\alpha^\beta (p_1^\sigma p_3^\eta + p_1^\eta p_3^\sigma - (p_1 \cdot p_3)g^{\sigma\eta}) \\ &\quad \left. + \theta_\mu^\rho \theta^{\beta\eta} (p_1^\sigma p_{3\alpha} + p_{1\alpha} p_3^\sigma - (p_1 \cdot p_3)g_\alpha^\sigma) + \theta_\mu^\rho \theta_\alpha^\eta (p_1^\sigma p_3^\beta + p_1^\beta p_3^\sigma - (p_1 \cdot p_3)g^{\sigma\beta}) \right) . \end{aligned} \quad (5.120)$$

Since it contains lengthy terms, it is better to separate each term and evaluate them one by one as before;

Let us call  $C_{111}$  as;

$$\begin{aligned} C_{111} &= 32p_{1\sigma}p_{1\beta}q_\rho q_\eta p_2^\mu p_4^\alpha \theta_\mu^\sigma \theta_\alpha^\beta (p_1^\rho p_3^\eta + p_1^\eta p_3^\rho - (p_1 \cdot p_3)g^{\rho\eta}) \\ &= 32p_{1\sigma}p_{1\beta}p_2^\mu p_4^\alpha \theta_\mu^\sigma \theta_\alpha^\beta (q_\rho q_\eta (p_1^\rho p_3^\eta + p_1^\eta p_3^\rho - (p_1 \cdot p_3)g^{\rho\eta})) \\ &= 32p_{1\sigma}p_{1\beta}p_2^\mu p_4^\alpha \theta_\mu^\sigma \theta_\alpha^\beta ((q \cdot p_1)(q \cdot p_3) + (q \cdot p_3)(q \cdot p_1) - q^2(p_1 \cdot p_3)) \\ &= 32p_{1\sigma}p_{1\beta}p_2^\mu p_4^\alpha \theta_\mu^\sigma \theta_\alpha^\beta (2(q \cdot p_1)(q \cdot p_3) - q^2(p_1 \cdot p_3)) . \end{aligned} \quad (5.121)$$

$C_{112}$  as;

$$\begin{aligned}
C_{112} &= 32p_{1\sigma}p_{1\beta}q_\rho q_\eta p_2^\mu p_4^\alpha \theta_\mu^\sigma \theta^{\beta\eta} (p_1^\rho p_{3\alpha} + p_{1\alpha} p_3^\rho - (p_1 \cdot p_3) g_\alpha^\rho) \\
&= 32p_{1\sigma}p_{1\beta}q_\eta p_2^\mu \theta_\mu^\sigma \theta^{\beta\eta} (q_\rho p_4^\alpha (p_1^\rho p_{3\alpha} + p_{1\alpha} p_3^\rho - (p_1 \cdot p_3) g_\alpha^\rho)) \\
&= 32p_{1\sigma}p_{1\beta}q_\eta p_2^\mu \theta_\mu^\sigma \theta^{\beta\eta} ((q \cdot p_1)(p_4 \cdot p_3) + (q \cdot p_3)(p_4 \cdot p_1) - (p_1 \cdot p_3)(q \cdot p_4)) .
\end{aligned} \tag{5.122}$$

$C_{113}$  as;

$$\begin{aligned}
C_{113} &= 32p_{1\sigma}p_{1\beta}q_\rho q_\eta p_2^\mu p_4^\alpha \theta_\mu^\sigma \theta_\alpha^\eta (p_1^\rho p_3^\beta + p_1^\beta p_3^\rho - (p_1 \cdot p_3) g^{\rho\beta}) \\
&= 32p_{1\sigma}q_\eta p_2^\mu p_4^\alpha \theta_\mu^\sigma \theta_\alpha^\eta (p_{1\beta} q_\rho (p_1^\rho p_3^\beta + p_1^\beta p_3^\rho - (p_1 \cdot p_3) g^{\rho\beta})) \\
&= 32p_{1\sigma}q_\eta p_2^\mu p_4^\alpha \theta_\mu^\sigma \theta_\alpha^\eta ((q \cdot p_1)(\overline{p_1 \cdot p_3}) + (q \cdot p_3)p_1^2 - \overline{(p_1 \cdot p_3)(p_1 \cdot q)}) \\
&= 32p_{1\sigma}q_\eta p_2^\mu p_4^\alpha \theta_\mu^\sigma \theta_\alpha^\eta (q \cdot p_3) p_1^2 .
\end{aligned} \tag{5.123}$$

$C_{114}$  as;

$$\begin{aligned}
C_{114} &= 32p_{1\sigma}p_{1\beta}q_\rho q_\eta p_2^\mu p_4^\alpha \theta^{\sigma\rho} \theta_\alpha^\beta (p_{1\mu} p_3^\eta + p_1^\eta p_{3\mu} - (p_1 \cdot p_3) g_\mu^\eta) \\
&= 32p_{1\sigma}p_{1\beta}q_\rho p_4^\alpha \theta^{\sigma\rho} \theta_\alpha^\beta (q_\eta p_2^\mu (p_{1\mu} p_3^\eta + p_1^\eta p_{3\mu} - (p_1 \cdot p_3) g_\mu^\eta)) \\
&= 32p_{1\sigma}p_{1\beta}q_\rho p_4^\alpha \theta^{\sigma\rho} \theta_\alpha^\beta ((q \cdot p_3)(p_2 \cdot p_1) + (q \cdot p_1)(p_2 \cdot p_3) - (p_1 \cdot p_3)(q \cdot p_2)) .
\end{aligned} \tag{5.124}$$

$C_{115}$  as;

$$\begin{aligned}
C_{115} &= 32p_{1\sigma}p_{1\beta}q_\rho q_\eta p_2^\mu p_4^\alpha \theta^{\sigma\rho} \theta^{\beta\eta} (p_{1\mu} p_{3\alpha} + p_{1\alpha} p_{3\mu} - (p_1 \cdot p_3) g_{\mu\alpha}) \\
&= 32p_{1\sigma}p_{1\beta}q_\rho q_\eta \theta^{\sigma\rho} \theta^{\beta\eta} (p_2^\mu p_4^\alpha (p_{1\mu} p_{3\alpha} + p_{1\alpha} p_{3\mu} - (p_1 \cdot p_3) g_{\mu\alpha})) \\
&= 32p_{1\sigma}p_{1\beta}q_\rho q_\eta \theta^{\sigma\rho} \theta^{\beta\eta} ((p_1 \cdot p_2)(p_3 \cdot p_4) + (p_1 \cdot p_4)(p_2 \cdot p_3) - (p_1 \cdot p_3)(p_2 \cdot p_4)) .
\end{aligned} \tag{5.125}$$

$C_{116}$  as;

$$\begin{aligned}
C_{116} &= 32p_{1\sigma}p_{1\beta}q_\rho q_\eta p_2^\mu p_4^\alpha \theta^{\sigma\rho} \theta_\alpha^\eta (p_{1\mu} p_3^\beta + p_1^\beta p_{3\mu} - (p_1 \cdot p_3) g_\mu^\beta) \\
&= 32p_{1\sigma}q_\rho q_\eta p_4^\alpha \theta^{\sigma\rho} \theta_\alpha^\eta (p_{1\beta} p_2^\mu (p_{1\mu} p_3^\beta + p_1^\beta p_{3\mu} - (p_1 \cdot p_3) g_\mu^\beta)) \\
&= 32p_{1\sigma}q_\rho q_\eta p_4^\alpha \theta^{\sigma\rho} \theta_\alpha^\eta ((\overline{p_1 \cdot p_3})(p_1 \cdot p_2) + p_1^2 (p_2 \cdot p_3) - \overline{(p_1 \cdot p_3)(p_1 \cdot p_2)}) \\
&= 32p_{1\sigma}q_\rho q_\eta p_4^\alpha \theta^{\sigma\rho} \theta_\alpha^\eta (p_1^2 (p_2 \cdot p_3)) .
\end{aligned} \tag{5.126}$$



$C_{117}$  as;

$$\begin{aligned}
C_{117} &= 32p_{1\sigma}p_{1\beta}q_\rho q_\eta p_2^\mu p_4^\alpha \theta^{\sigma\rho} \theta_\mu^\rho \theta_\alpha^\beta (p_1^\sigma p_3^\eta + p_1^\eta p_3^\sigma - (p_1 \cdot p_3)g^{\sigma\eta}) \\
&= 32p_{1\beta}q_\rho p_2^\mu p_4^\alpha \theta^{\sigma\rho} \theta_\mu^\rho \theta_\alpha^\beta (p_{1\sigma}q_\eta (p_1^\sigma p_3^\eta + p_1^\eta p_3^\sigma - (p_1 \cdot p_3)g^{\sigma\eta})) \\
&= 32p_{1\beta}q_\rho p_2^\mu p_4^\alpha \theta^{\sigma\rho} \theta_\mu^\rho \theta_\alpha^\beta (p_1^2(q \cdot p_3) + \cancel{(q \cdot p_1)(p_1 \cdot p_3)} - \cancel{(p_1 \cdot p_3)(p_1 \cdot q)}) \\
&= 32p_{1\beta}q_\rho p_2^\mu p_4^\alpha \theta^{\sigma\rho} \theta_\mu^\rho \theta_\alpha^\beta (p_1^2(q \cdot p_3)) .
\end{aligned} \tag{5.127}$$

$C_{118}$  as;

$$\begin{aligned}
C_{118} &= 32p_{1\sigma}p_{1\beta}q_\rho q_\eta p_2^\mu p_4^\alpha \theta_\mu^\rho \theta^{\beta\eta} (p_1^\sigma p_{3\alpha} + p_{1\alpha} p_3^\sigma - (p_1 \cdot p_3)g_\alpha^\sigma) \\
&= 32p_{1\beta}q_\rho q_\eta p_2^\mu \theta_\mu^\rho \theta^{\beta\eta} (p_{1\sigma}p_4^\alpha (p_1^\sigma p_{3\alpha} + p_{1\alpha} p_3^\sigma - (p_1 \cdot p_3)g_\alpha^\sigma)) \\
&= 32p_{1\beta}q_\rho q_\eta p_2^\mu \theta_\mu^\rho \theta^{\beta\eta} (p_1^2(p_3 \cdot p_4) + \cancel{(p_1 \cdot p_3)(p_1 \cdot p_4)} - \cancel{(p_1 \cdot p_3)(p_1 \cdot p_4)}) \\
&= 32p_{1\beta}q_\rho q_\eta p_2^\mu \theta_\mu^\rho \theta^{\beta\eta} (p_1^2(p_3 \cdot p_4)) .
\end{aligned} \tag{5.128}$$

$C_{119}$  as;

$$\begin{aligned}
C_{119} &= 32p_{1\sigma}p_{1\beta}q_\rho q_\eta p_2^\mu p_4^\alpha \theta_\mu^\rho \theta_\alpha^\eta (p_1^\sigma p_3^\beta + p_1^\beta p_3^\sigma - (p_1 \cdot p_3)g^{\sigma\beta}) \\
&= 32q_\rho q_\eta p_2^\mu p_4^\alpha \theta_\mu^\rho \theta_\alpha^\eta (p_{1\sigma}p_{1\beta} (p_1^\sigma p_3^\beta + p_1^\beta p_3^\sigma - (p_1 \cdot p_3)g^{\sigma\beta})) \\
&= 32q_\rho q_\eta p_2^\mu p_4^\alpha \theta_\mu^\rho \theta_\alpha^\eta (p_1^2(p_1 \cdot p_3) + \cancel{p_1^2(p_1 \cdot p_3)} - \cancel{(p_1 \cdot p_3)p_1^2}) \\
&= 32q_\rho q_\eta p_2^\mu p_4^\alpha \theta_\mu^\rho \theta_\alpha^\eta (p_1^2(p_1 \cdot p_3)) .
\end{aligned} \tag{5.129}$$

Hence, we can write  $C_1$  as;

$$\begin{aligned}
C_{11} &= C_{111} + C_{112} + C_{113} + C_{114} + C_{115} + C_{116} + C_{117} + C_{118} + C_{119} \\
&= 32p_{1\sigma}p_{1\beta}p_2^\mu p_4^\alpha \theta_\mu^\sigma \theta_\alpha^\beta (2(q \cdot p_1)(q \cdot p_3) - q^2(p_1 \cdot p_3)) \\
&\quad + 32p_{1\sigma}p_{1\beta}q_\rho q_\eta p_2^\mu \theta_\mu^\sigma \theta^{\beta\eta} ((q \cdot p_1)(p_4 \cdot p_3) + (q \cdot p_3)(p_4 \cdot p_1) - (p_1 \cdot p_3)(q \cdot p_4)) \\
&\quad + 32p_{1\sigma}q_\eta p_2^\mu p_4^\alpha \theta_\mu^\sigma \theta_\alpha^\eta (q \cdot p_3)p_1^2 \\
&\quad + 32p_{1\sigma}p_{1\beta}q_\rho p_4^\alpha \theta^{\sigma\rho} \theta_\alpha^\beta ((q \cdot p_3)(p_2 \cdot p_1) + (q \cdot p_1)(p_2 \cdot p_3) - (p_1 \cdot p_3)(q \cdot p_2)) \\
&\quad + 32p_{1\sigma}p_{1\beta}q_\rho q_\eta \theta^{\sigma\rho} \theta^{\beta\eta} ((p_1 \cdot p_2)(p_3 \cdot p_4) + (p_1 \cdot p_4)(p_2 \cdot p_3) - (p_1 \cdot p_3)(p_2 \cdot p_4)) \\
&\quad + 32p_{1\sigma}q_\rho q_\eta p_4^\alpha \theta^{\sigma\rho} \theta_\alpha^\eta (p_1^2(p_2 \cdot p_3)) + 32p_{1\beta}q_\rho p_2^\mu p_4^\alpha \theta^{\sigma\rho} \theta_\mu^\rho \theta_\alpha^\beta (p_1^2(q \cdot p_3)) \\
&\quad + 32p_{1\beta}q_\rho q_\eta p_2^\mu \theta_\mu^\rho \theta^{\beta\eta} (p_1^2(p_3 \cdot p_4)) + 32q_\rho q_\eta p_2^\mu p_4^\alpha \theta_\mu^\rho \theta_\alpha^\eta (p_1^2(p_1 \cdot p_3)) .
\end{aligned} \tag{5.130}$$

Once we neglect mass of neutrinos then  $p_1^2 = 0$  and  $p_3^2 = 0$ .  $q$  is the momentum transfer and equals to  $q = p_1 - p_3 = p_4 - p_2$ . Then, we find the following results for terms containing  $q$  in Equation (5.130).

$$\begin{aligned} q \cdot p_1 &= (p_1 - p_3) \cdot p_1 \\ &= \cancel{p_1^2} - (p_1 \cdot p_3) \end{aligned} \quad (5.131)$$

$$\boxed{q \cdot p_1 = -(p_1 \cdot p_3) .}$$

$$\begin{aligned} q \cdot p_3 &= (p_1 - p_3) \cdot p_3 \\ &= -\cancel{p_3^2} + (p_1 \cdot p_3) \end{aligned} \quad (5.132)$$

$$\boxed{q \cdot p_3 = (p_1 \cdot p_3) .}$$

$$q \cdot p_2 = (p_1 - p_3) \cdot p_2 \quad (5.133)$$

$$\boxed{q \cdot p_2 = (p_1 \cdot p_2) - (p_2 \cdot p_3) .}$$

Similarly  $q \cdot p_4$  can be written as;

$$\boxed{q \cdot p_4 = (p_1 \cdot p_4) - (p_3 \cdot p_4) .} \quad (5.134)$$

And for  $q^2$ ;

$$\begin{aligned} q^2 &= (p_1 - p_3)^2 \\ &= \cancel{p_1^2} + \cancel{p_3^2} - 2p_1 \cdot p_3 \end{aligned} \quad (5.135)$$

$$\boxed{q^2 = -(2p_1 \cdot p_3) .}$$

With these results we can write Equation (5.130) in terms of the momentums as follows.

$$\begin{aligned} C_{11} &= 32p_{1\sigma}p_{1\beta}p_2^\mu p_4^\alpha \theta_\mu^\sigma \theta_\alpha^\beta (-2\cancel{(p_1 \cdot p_3)^2} + 2\cancel{(p_1 \cdot p_3)^2}) \\ &\quad + 32p_{1\sigma}p_{1\beta}q_\eta p_2^\mu \theta_\mu^\sigma \theta^{\beta\eta} (-\cancel{(p_1 \cdot p_3)(p_4 \cdot p_3)} + \cancel{(p_1 \cdot p_3)(p_4 \cdot p_1)} - \cancel{(p_1 \cdot p_3)(p_1 \cdot p_4)} \\ &\quad + \cancel{(p_1 \cdot p_3)(p_3 \cdot p_4)}) + 32p_{1\sigma}q_\eta p_2^\mu p_4^\alpha \theta_\mu^\sigma \theta_\alpha^\eta (q \cdot p_3) \cancel{p_1^2} \\ &\quad + 32p_{1\sigma}p_{1\beta}q_\rho p_4^\alpha \theta^{\sigma\rho} \theta_\alpha^\beta ((\cancel{(p_1 \cdot p_3)(p_2 \cdot p_1)} - \cancel{(p_3 \cdot p_1)(p_2 \cdot p_3)} - \cancel{(p_1 \cdot p_3)(p_1 \cdot p_2)} \\ &\quad + \cancel{(p_1 \cdot p_3)(p_2 \cdot p_3)}) \\ &\quad + 32p_{1\sigma}p_{1\beta}q_\rho q_\eta \theta^{\sigma\rho} \theta^{\beta\eta} ((p_1 \cdot p_2)(p_3 \cdot p_4) + (p_1 \cdot p_4)(p_2 \cdot p_3) - (p_1 \cdot p_3)(p_2 \cdot p_4)) \\ &\quad + 32p_{1\sigma}q_\rho q_\eta p_4^\alpha \theta^{\sigma\rho} \theta_\alpha^\eta (\cancel{p_1^2}(p_2 \cdot p_3)) + 32p_{1\beta}q_\rho p_2^\mu p_4^\alpha \theta^{\sigma\rho} \theta_\mu^\beta (\cancel{p_1^2}(q \cdot p_3)) \\ &\quad + 32p_{1\beta}q_\rho q_\eta p_2^\mu \theta_\mu^\rho \theta^{\beta\eta} (\cancel{p_1^2}(p_3 \cdot p_4)) + 32q_\rho q_\eta p_2^\mu p_4^\alpha \theta_\mu^\rho \theta_\alpha^\eta (\cancel{p_1^2}(p_1 \cdot p_3)) . \end{aligned} \quad (5.136)$$

With these simplifications  $C_{11}$  becomes

$$C_{11} = 32p_{1\sigma}p_{1\beta}q_{\rho}q_{\eta}\theta^{\sigma\rho}\theta^{\beta\eta}((p_1 \cdot p_2)(p_3 \cdot p_4) + (p_1 \cdot p_4)(p_2 \cdot p_3) - (p_1 \cdot p_3)(p_2 \cdot p_4)) \quad (5.137)$$

For  $C_{12}$ ;

$$\begin{aligned} C_{12} &= 8p_{1\sigma}p_{1\beta}q_{\rho}q_{\eta}p_2^{\alpha}p_4^{\mu}B_1 \\ &= 32p_{1\sigma}p_{1\beta}q_{\rho}q_{\eta}p_2^{\alpha}p_4^{\mu} \left( \right. \\ &\quad \theta_{\mu}^{\sigma}\theta_{\alpha}^{\beta}(p_1^{\rho}p_3^{\eta} + p_1^{\eta}p_3^{\rho} - (p_1 \cdot p_3)g^{\rho\eta}) + \theta_{\mu}^{\sigma}\theta^{\beta\eta}(p_1^{\rho}p_{3\alpha} + p_{1\alpha}p_3^{\rho} - (p_1 \cdot p_3)g_{\alpha}^{\rho}) \\ &\quad + \theta_{\mu}^{\sigma}\theta_{\alpha}^{\eta}(p_1^{\rho}p_3^{\beta} + p_1^{\beta}p_3^{\rho} - (p_1 \cdot p_3)g^{\rho\beta}) + \theta^{\sigma\rho}\theta_{\alpha}^{\beta}(p_{1\mu}p_3^{\eta} + p_1^{\eta}p_{3\mu} - (p_1 \cdot p_3)g_{\mu}^{\eta}) \\ &\quad + \theta^{\sigma\rho}\theta^{\beta\eta}(p_{1\mu}p_{3\alpha} + p_{1\alpha}p_{3\mu} - (p_1 \cdot p_3)g_{\mu\alpha}) + \theta^{\sigma\rho}\theta_{\alpha}^{\eta}(p_{1\mu}p_3^{\beta} + p_1^{\beta}p_{3\mu} - (p_1 \cdot p_3)g_{\mu}^{\beta}) \\ &\quad + \theta_{\mu}^{\rho}\theta_{\alpha}^{\beta}(p_1^{\sigma}p_3^{\eta} + p_1^{\eta}p_3^{\sigma} - (p_1 \cdot p_3)g^{\sigma\eta}) + \theta_{\mu}^{\rho}\theta^{\beta\eta}(p_1^{\sigma}p_{3\alpha} + p_{1\alpha}p_3^{\sigma} - (p_1 \cdot p_3)g_{\alpha}^{\sigma}) \\ &\quad \left. + \theta_{\mu}^{\rho}\theta_{\alpha}^{\eta}(p_1^{\sigma}p_3^{\beta} + p_1^{\beta}p_3^{\sigma} - (p_1 \cdot p_3)g^{\sigma\beta}) \right). \end{aligned} \quad (5.138)$$

If we compare the terms containing  $C_{11}$  and  $C_{12}$  (Equation (5.130) and Equation (5.138)) we realize that once we replace  $p_2 \leftrightarrow p_4$  in  $C_{11}$ , then we can find the result for  $C_{12}$  easily. Hence from Equation (5.137) we can write  $C_{12}$  as;

$$C_{12} = 32p_{1\sigma}p_{1\beta}q_{\rho}q_{\eta}\theta^{\sigma\rho}\theta^{\beta\eta}((p_1 \cdot p_4)(p_3 \cdot p_2) + (p_1 \cdot p_2)(p_4 \cdot p_3) - (p_1 \cdot p_3)(p_4 \cdot p_2)) \quad (5.139)$$

Once we compare Equation (5.137) and Equation (5.139) we identify that;

$$C_{11} = C_{12}. \quad (5.140)$$

For  $C_{13}$ ;

$$\begin{aligned} C_{13} &= 8p_{1\sigma}p_{1\beta}q_{\rho}q_{\eta}(p_2 \cdot p_4)g^{\mu\alpha}B_1 \\ &= 32p_{1\sigma}p_{1\beta}q_{\rho}q_{\eta}(p_2 \cdot p_4)g^{\mu\alpha} \\ &\quad \left( \theta_{\mu}^{\sigma}\theta_{\alpha}^{\beta}(p_1^{\rho}p_3^{\eta} + p_1^{\eta}p_3^{\rho} - (p_1 \cdot p_3)g^{\rho\eta}) + \theta_{\mu}^{\sigma}\theta^{\beta\eta}(p_1^{\rho}p_{3\alpha} + p_{1\alpha}p_3^{\rho} - (p_1 \cdot p_3)g_{\alpha}^{\rho}) \right. \\ &\quad + \theta_{\mu}^{\sigma}\theta_{\alpha}^{\eta}(p_1^{\rho}p_3^{\beta} + p_1^{\beta}p_3^{\rho} - (p_1 \cdot p_3)g^{\rho\beta}) + \theta^{\sigma\rho}\theta_{\alpha}^{\beta}(p_{1\mu}p_3^{\eta} + p_1^{\eta}p_{3\mu} - (p_1 \cdot p_3)g_{\mu}^{\eta}) \\ &\quad + \theta^{\sigma\rho}\theta^{\beta\eta}(p_{1\mu}p_{3\alpha} + p_{1\alpha}p_{3\mu} - (p_1 \cdot p_3)g_{\mu\alpha}) + \theta^{\sigma\rho}\theta_{\alpha}^{\eta}(p_{1\mu}p_3^{\beta} + p_1^{\beta}p_{3\mu} - (p_1 \cdot p_3)g_{\mu}^{\beta}) \\ &\quad + \theta_{\mu}^{\rho}\theta_{\alpha}^{\beta}(p_1^{\sigma}p_3^{\eta} + p_1^{\eta}p_3^{\sigma} - (p_1 \cdot p_3)g^{\sigma\eta}) + \theta_{\mu}^{\rho}\theta^{\beta\eta}(p_1^{\sigma}p_{3\alpha} + p_{1\alpha}p_3^{\sigma} - (p_1 \cdot p_3)g_{\alpha}^{\sigma}) \\ &\quad \left. + \theta_{\mu}^{\rho}\theta_{\alpha}^{\eta}(p_1^{\sigma}p_3^{\beta} + p_1^{\beta}p_3^{\sigma} - (p_1 \cdot p_3)g^{\sigma\beta}) \right). \end{aligned} \quad (5.141)$$

Let us again evaluate each term one by one. Let us define  $C_{131}$  as,

$$\begin{aligned}
C_{131} &= 32p_{1\sigma}p_{1\beta}q_{\rho}q_{\eta}(p_2 \cdot p_4)g^{\mu\alpha}\theta_{\mu}^{\sigma}\theta_{\alpha}^{\beta}(p_1^{\rho}p_3^{\eta} + p_1^{\eta}p_3^{\rho} - (p_1 \cdot p_3)g^{\rho\eta}) \\
&= 32p_{1\sigma}p_{1\beta}(p_2 \cdot p_4)g^{\mu\alpha}\theta_{\mu}^{\sigma}\theta_{\alpha}^{\beta}(q_{\rho}q_{\eta}(p_1^{\rho}p_3^{\eta} + p_1^{\eta}p_3^{\rho} - (p_1 \cdot p_3)g^{\rho\eta})) \quad (5.142) \\
&= 32p_{1\sigma}p_{1\beta}(p_2 \cdot p_4)g^{\mu\alpha}\theta_{\mu}^{\sigma}\theta_{\alpha}^{\beta}(2(q \cdot p_1)(q \cdot p_3) - q^2(p_1 \cdot p_3)) .
\end{aligned}$$

$C_{132}$  as;

$$\begin{aligned}
C_{132} &= 32p_{1\sigma}p_{1\beta}q_{\rho}q_{\eta}(p_2 \cdot p_4)g^{\mu\alpha}(\theta_{\mu}^{\sigma}\theta^{\beta\eta}(p_1^{\rho}p_{3\alpha} + p_{1\alpha}p_3^{\rho} - (p_1 \cdot p_3)g_{\alpha}^{\rho}) \\
&= 32p_{1\sigma}p_{1\beta}q_{\eta}(p_2 \cdot p_4)\theta_{\mu}^{\sigma}\theta^{\beta\eta}g^{\mu\alpha}(q_{\rho}(p_1^{\rho}p_{3\alpha} + p_{1\alpha}p_3^{\rho} - (p_1 \cdot p_3)g_{\alpha}^{\rho})) \\
&= 32p_{1\sigma}p_{1\beta}q_{\eta}(p_2 \cdot p_4)\theta_{\mu}^{\sigma}\theta^{\beta\eta}g^{\mu\alpha}((q \cdot p_1)p_{3\alpha} + (q \cdot p_3)p_{1\alpha} - (p_1 \cdot p_3)q_{\alpha}) . \quad (5.143)
\end{aligned}$$

$C_{133}$  as;

$$\begin{aligned}
C_{133} &= 32p_{1\sigma}p_{1\beta}q_{\rho}q_{\eta}(p_2 \cdot p_4)g^{\mu\alpha}(\theta_{\mu}^{\sigma}\theta_{\alpha}^{\eta}(p_1^{\rho}p_3^{\beta} + p_1^{\beta}p_3^{\rho} - (p_1 \cdot p_3)g^{\rho\beta})) \\
&= 32p_{1\sigma}q_{\eta}(p_2 \cdot p_4)g^{\mu\alpha}\theta_{\mu}^{\sigma}\theta_{\alpha}^{\eta}(p_{1\beta}q_{\rho}(p_1^{\rho}p_3^{\beta} + p_1^{\beta}p_3^{\rho} - (p_1 \cdot p_3)g^{\rho\beta})) \\
&= 32p_{1\sigma}q_{\eta}(p_2 \cdot p_4)g^{\mu\alpha}\theta_{\mu}^{\sigma}\theta_{\alpha}^{\eta}(\cancel{(p_1 \cdot p_3)}(q \cdot p_1) + p_1^2(q \cdot p_3) - \cancel{(p_1 \cdot p_3)}(p_1 \cdot q)) . \quad (5.144)
\end{aligned}$$

$C_{134}$  as;

$$\begin{aligned}
C_{134} &= 32p_{1\sigma}p_{1\beta}q_{\rho}q_{\eta}(p_2 \cdot p_4)g^{\mu\alpha}(\theta^{\sigma\rho}\theta_{\alpha}^{\beta}(p_{1\mu}p_3^{\eta} + p_1^{\eta}p_{3\mu} - (p_1 \cdot p_3)g_{\mu}^{\eta})) \\
&= 32p_{1\sigma}p_{1\beta}q_{\rho}(p_2 \cdot p_4)g^{\mu\alpha}\theta^{\sigma\rho}\theta_{\alpha}^{\beta}(q_{\eta}(p_{1\mu}p_3^{\eta} + p_1^{\eta}p_{3\mu} - (p_1 \cdot p_3)g_{\mu}^{\eta})) \\
&= 32p_{1\sigma}p_{1\beta}q_{\rho}(p_2 \cdot p_4)g^{\mu\alpha}\theta^{\sigma\rho}\theta_{\alpha}^{\beta}(p_{1\mu}(q \cdot p_3) + p_{3\mu}(q \cdot p_1) - q_{\mu}(p_1 \cdot p_3)) . \quad (5.145)
\end{aligned}$$

$C_{135}$  as;

$$\begin{aligned}
C_{135} &= 32p_{1\sigma}p_{1\beta}q_{\rho}q_{\eta}(p_2 \cdot p_4)g^{\mu\alpha}(\theta^{\sigma\rho}\theta^{\beta\eta}(p_{1\mu}p_{3\alpha} + p_{1\alpha}p_{3\mu} - (p_1 \cdot p_3)g_{\mu\alpha})) \\
&= 32p_{1\sigma}p_{1\beta}q_{\rho}q_{\eta}(p_2 \cdot p_4)\theta^{\sigma\rho}\theta^{\beta\eta}(g^{\mu\alpha}(p_{1\mu}p_{3\alpha} + p_{1\alpha}p_{3\mu} - (p_1 \cdot p_3)g_{\mu\alpha})) \quad (5.146) \\
&= 32p_{1\sigma}p_{1\beta}q_{\rho}q_{\eta}(p_2 \cdot p_4)\theta^{\sigma\rho}\theta^{\beta\eta}((p_1 \cdot p_3) + (p_1 \cdot p_3) - 4(p_1 \cdot p_3)) \\
&= 32p_{1\sigma}p_{1\beta}q_{\rho}q_{\eta}(p_2 \cdot p_4)\theta^{\sigma\rho}\theta^{\beta\eta}(-2(p_1 \cdot p_3)) .
\end{aligned}$$

$C_{136}$  as;

$$\begin{aligned}
C_{136} &= 32p_{1\sigma}p_{1\beta}q_\rho q_\eta(p_2 \cdot p_4)g^{\mu\alpha}(\theta^{\sigma\rho}\theta_\alpha^\eta(p_{1\mu}p_3^\beta + p_1^\beta p_{3\mu} - (p_1 \cdot p_3)g_\mu^\beta)) \\
&= 32p_{1\sigma}q_\rho q_\eta(p_2 \cdot p_4)g^{\mu\alpha}\theta^{\sigma\rho}\theta_\alpha^\eta(p_{1\beta}(p_{1\mu}p_3^\beta + p_1^\beta p_{3\mu} - (p_1 \cdot p_3)g_\mu^\beta)) \\
&= 32p_{1\sigma}q_\rho q_\eta(p_2 \cdot p_4)g^{\mu\alpha}\theta^{\sigma\rho}\theta_\alpha^\eta(\cancel{p_{1\mu}(p_1 \cdot p_3)} + p_{3\mu}p_1^2 - \cancel{p_{1\mu}(p_1 \cdot p_3)}) \\
&= 32p_{1\sigma}q_\rho q_\eta(p_2 \cdot p_4)g^{\mu\alpha}\theta^{\sigma\rho}\theta_\alpha^\eta(p_{3\mu}p_1^2) .
\end{aligned} \tag{5.147}$$

$C_{137}$  as;

$$\begin{aligned}
C_{137} &= 32p_{1\sigma}p_{1\beta}q_\rho q_\eta(p_2 \cdot p_4)g^{\mu\alpha}(\theta_\mu^\rho\theta_\alpha^\beta(p_1^\sigma p_3^\eta + p_1^\eta p_3^\sigma - (p_1 \cdot p_3)g^{\sigma\eta})) \\
&= 32p_{1\beta}q_\rho(p_2 \cdot p_4)g^{\mu\alpha}\theta_\mu^\rho\theta_\alpha^\beta(p_{1\sigma}q_\eta(p_1^\sigma p_3^\eta + p_1^\eta p_3^\sigma - (p_1 \cdot p_3)g^{\sigma\eta})) \\
&= 32p_{1\beta}q_\rho(p_2 \cdot p_4)g^{\mu\alpha}\theta_\mu^\rho\theta_\alpha^\beta(p_1^2(q \cdot p_3) + \cancel{(q \cdot p_1)(p_1 \cdot p_3)} - \cancel{(p_1 \cdot p_3)(q \cdot p_1)}) \\
&= 32p_{1\beta}q_\rho(p_2 \cdot p_4)g^{\mu\alpha}\theta_\mu^\rho\theta_\alpha^\beta(p_1^2(q \cdot p_3)) .
\end{aligned} \tag{5.148}$$

$C_{138}$  as;

$$\begin{aligned}
C_{138} &= 32p_{1\sigma}p_{1\beta}q_\rho q_\eta(p_2 \cdot p_4)g^{\mu\alpha}(\theta_\mu^\rho\theta^{\beta\eta}(p_1^\sigma p_{3\alpha} + p_{1\alpha}p_3^\sigma - (p_1 \cdot p_3)g_\alpha^\sigma)) \\
&= 32p_{1\beta}q_\rho q_\eta(p_2 \cdot p_4)g^{\mu\alpha}\theta_\mu^\rho\theta^{\beta\eta}(p_{1\sigma}(p_1^\sigma p_{3\alpha} + p_{1\alpha}p_3^\sigma - (p_1 \cdot p_3)g_\alpha^\sigma)) \\
&= 32p_{1\beta}q_\rho q_\eta(p_2 \cdot p_4)g^{\mu\alpha}\theta_\mu^\rho\theta^{\beta\eta}(p_1^2 p_{3\alpha} + \cancel{p_{1\alpha}(p_1 \cdot p_3)} - \cancel{(p_1 \cdot p_3)p_{1\alpha}}) \\
&= 32p_{1\beta}q_\rho q_\eta(p_2 \cdot p_4)g^{\mu\alpha}\theta_\mu^\rho\theta^{\beta\eta}(p_1^2 p_{3\alpha}) .
\end{aligned} \tag{5.149}$$

$C_{139}$  as;

$$\begin{aligned}
C_{139} &= 32p_{1\sigma}p_{1\beta}q_\rho q_\eta(p_2 \cdot p_4)g^{\mu\alpha}(\theta_\mu^\rho\theta_\alpha^\eta(p_1^\sigma p_3^\beta + p_1^\beta p_3^\sigma - (p_1 \cdot p_3)g^{\sigma\beta})) \\
&= 32q_\rho q_\eta(p_2 \cdot p_4)g^{\mu\alpha}\theta_\mu^\rho\theta_\alpha^\eta(p_{1\sigma}p_{1\beta}(p_1^\sigma p_3^\beta + p_1^\beta p_3^\sigma - (p_1 \cdot p_3)g^{\sigma\beta})) \\
&= 32q_\rho q_\eta(p_2 \cdot p_4)g^{\mu\alpha}\theta_\mu^\rho\theta_\alpha^\eta(p_1^2(p_1 \cdot p_3)) .
\end{aligned} \tag{5.150}$$

With these findings  $C_{13}$  turns out to be;

$$\begin{aligned}
C_{13} = & 32p_{1\sigma}p_{1\beta}(p_2 \cdot p_4)g^{\mu\alpha}\theta_\mu^\sigma\theta_\alpha^\beta(2(q \cdot p_1)(q \cdot p_3) - q^2(p_1 \cdot p_3)) \\
& + 32p_{1\sigma}p_{1\beta}q_\eta(p_2 \cdot p_4)\theta_\mu^\sigma\theta^{\beta\eta}g^{\mu\alpha}((q \cdot p_1)p_{3\alpha} + (q \cdot p_3)p_{1\alpha} - (p_1 \cdot p_3)q_\alpha) \\
& + 32p_{1\sigma}q_\eta(p_2 \cdot p_4)g^{\mu\alpha}\theta_\mu^\sigma\theta_\alpha^\eta(p_1^2(q \cdot p_3)) \\
& + 32p_{1\sigma}p_{1\beta}q_\rho(p_2 \cdot p_4)g^{\mu\alpha}\theta^{\sigma\rho}\theta_\alpha^\beta(p_{1\mu}(q \cdot p_3) + p_{3\mu}(q \cdot p_1) - q_\mu(p_1 \cdot p_3)) \\
& + 32p_{1\sigma}p_{1\beta}q_\rho q_\eta(p_2 \cdot p_4)\theta^{\sigma\rho}\theta^{\beta\eta}(-2(p_1 \cdot p_3)) + 32p_{1\sigma}q_\rho q_\eta(p_2 \cdot p_4)g^{\mu\alpha}\theta^{\sigma\rho}\theta_\alpha^\eta(p_{3\mu}p_1^2) \\
& + 32p_{1\beta}q_\rho(p_2 \cdot p_4)g^{\mu\alpha}\theta_\mu^\rho\theta_\alpha^\beta(p_1^2(q \cdot p_3)) + 32p_{1\beta}q_\rho q_\eta(p_2 \cdot p_4)g^{\mu\alpha}\theta_\mu^\rho\theta^{\beta\eta}(p_1^2 p_{3\alpha}) \\
& + 32q_\rho q_\eta(p_2 \cdot p_4)g^{\mu\alpha}\theta_\mu^\rho\theta_\alpha^\eta(p_1^2(p_1 \cdot p_3)) .
\end{aligned} \tag{5.151}$$

Neglecting the mass of neutrinos we get,

$$\begin{aligned}
C_{13} = & 32p_{1\sigma}p_{1\beta}(p_2 \cdot p_4)g^{\mu\alpha}\theta_\mu^\sigma\theta_\alpha^\beta(\overline{-2(p_1 \cdot p_3)(p_1 \cdot p_3)} + \overline{2(p_1 \cdot p_3)(p_1 \cdot p_3)}) \\
& + 32p_{1\sigma}p_{1\beta}q_\eta(p_2 \cdot p_4)\theta_\mu^\sigma\theta^{\beta\eta}g^{\mu\alpha} \\
& \times (\overline{-(p_1 \cdot p_3)p_{3\alpha}} + \overline{(p_1 \cdot p_3)p_{1\alpha}} - \overline{(p_1 \cdot p_3)p_{1\alpha}} + \overline{p_{3\alpha}(p_1 \cdot p_3)}) \\
& + 32p_{1\sigma}q_\eta(p_2 \cdot p_4)g^{\mu\alpha}\theta_\mu^\sigma\theta_\alpha^\eta(\overline{p_1^2(q \cdot p_3)}) + 32p_{1\sigma}p_{1\beta}q_\rho(p_2 \cdot p_4)g^{\mu\alpha}\theta^{\sigma\rho}\theta_\alpha^\beta \\
& \times (\overline{p_{1\mu}(p_1 \cdot p_3)} - \overline{p_{3\mu}(p_3 \cdot p_1)} - \overline{p_{1\mu}(p_1 \cdot p_3)} + \overline{p_{3\mu}(p_1 \cdot p_3)}) \\
& + 32p_{1\sigma}p_{1\beta}q_\rho q_\eta(p_2 \cdot p_4)\theta^{\sigma\rho}\theta^{\beta\eta}(-2(p_1 \cdot p_3)) + 32p_{1\sigma}q_\rho q_\eta(p_2 \cdot p_4)g^{\mu\alpha}\theta^{\sigma\rho}\theta_\alpha^\eta(\overline{p_{3\mu}p_1^2}) \\
& + 32p_{1\beta}q_\rho(p_2 \cdot p_4)g^{\mu\alpha}\theta_\mu^\rho\theta_\alpha^\beta(\overline{p_1^2(q \cdot p_3)}) + 32p_{1\beta}q_\rho q_\eta(p_2 \cdot p_4)g^{\mu\alpha}\theta_\mu^\rho\theta^{\beta\eta}(\overline{p_1^2 p_{3\alpha}}) \\
& + 32q_\rho q_\eta(p_2 \cdot p_4)g^{\mu\alpha}\theta_\mu^\rho\theta_\alpha^\eta(\overline{p_1^2(p_1 \cdot p_3)}) ,
\end{aligned} \tag{5.152}$$

where we also used the relations Equations (5.131) to (5.134). Hence  $C_{13}$  simplifies to;

$$\boxed{C_{13} = -64p_{1\sigma}p_{1\beta}q_\rho q_\eta(p_2 \cdot p_4)\theta^{\sigma\rho}\theta^{\beta\eta}(p_1 \cdot p_3) .} \tag{5.153}$$

We can state  $C_{14}$  as;

$$C_{14} = p_{1\sigma}p_{1\beta}q_\rho q_\eta g^{\mu\alpha} m_e^2 B_1 . \tag{5.154}$$

However, we realize that  $C_{14}$  can be acquired by just replacing  $(p_2 \cdot p_4) \rightarrow m_e^2$  in  $C_{13}$ .

Hence, we find  $C_{14}$  easily as;

$$\boxed{C_{14} = -64p_{1\sigma}p_{1\beta}q_\rho q_\eta m_e^2 \theta^{\sigma\rho}\theta^{\beta\eta}(p_1 \cdot p_3) .} \tag{5.155}$$

Finally,  $C_1$  can be written as;

$$\begin{aligned}
C_1 &= C_{11} + C_{12} - C_{13} + C_{14} \\
&= 32p_{1\sigma}p_{1\beta}q_\rho q_\eta \theta^{\sigma\rho} \theta^{\beta\eta} \left( (p_1 \cdot p_2)(p_3 \cdot p_4) + (p_1 \cdot p_4)(p_2 \cdot p_3) - (p_1 \cdot p_3)(p_2 \cdot p_4) \right) \\
&\quad + 32p_{1\sigma}p_{1\beta}q_\rho q_\eta \theta^{\sigma\rho} \theta^{\beta\eta} \left( (p_1 \cdot p_4)(p_3 \cdot p_2) + (p_1 \cdot p_2)(p_4 \cdot p_3) - (p_1 \cdot p_3)(p_4 \cdot p_2) \right) \\
&\quad + 64p_{1\sigma}p_{1\beta}q_\rho q_\eta \theta^{\sigma\rho} \theta^{\beta\eta} (p_2 \cdot p_4)(p_1 \cdot p_3) - 64p_{1\sigma}p_{1\beta}q_\rho q_\eta m_e^2 \theta^{\sigma\rho} \theta^{\beta\eta} (p_1 \cdot p_3) .
\end{aligned} \tag{5.156}$$

Moreover, the terms can be collected as;

$$\begin{aligned}
C_1 &= 64p_{1\sigma}p_{1\beta}q_\rho q_\eta \theta^{\sigma\rho} \theta^{\beta\eta} \\
&\quad \times \left( (p_1 \cdot p_4)(p_3 \cdot p_2) + (p_1 \cdot p_2)(p_4 \cdot p_3) - \cancel{(p_1 \cdot p_3)(p_4 \cdot p_2)} + \cancel{(p_2 \cdot p_4)(p_1 \cdot p_3)} \right. \\
&\quad \left. - m_e^2(p_1 \cdot p_3) \right) .
\end{aligned} \tag{5.157}$$

Furthermore, this can be simplified into;

$$\boxed{C_1 = 64p_{1\sigma}p_{1\beta}q_\rho q_\eta \theta^{\sigma\rho} \theta^{\beta\eta} \left( (p_1 \cdot p_4)(p_3 \cdot p_2) + (p_1 \cdot p_2)(p_4 \cdot p_3) - m_e^2(p_1 \cdot p_3) \right) .} \tag{5.158}$$

Remember from Equation (5.104) we denoted  $A^{\mu\alpha} B_{\mu\alpha}$  as;

$$\begin{aligned}
A^{\mu\alpha} B_{\mu\alpha} &= C_1 - C_2 = C_1 \\
&= 64p_{1\sigma}p_{1\beta}q_\rho q_\eta \theta^{\sigma\rho} \theta^{\beta\eta} \left( (p_1 \cdot p_4)(p_3 \cdot p_2) + (p_1 \cdot p_2)(p_4 \cdot p_3) - m_e^2(p_1 \cdot p_3) \right) .
\end{aligned} \tag{5.159}$$

Hence we can write the amplitude square as;

$$\boxed{\begin{aligned}
\sum_{spin} |\mathcal{M}_{NC}|^2 &= \frac{e^4}{4q^4} A^{\mu\alpha} B_{\mu\alpha} \\
&= \frac{e^4}{4q^4} 64p_{1\sigma}p_{1\beta}q_\rho q_\eta \theta^{\sigma\rho} \theta^{\beta\eta} \\
&\quad \times \left( (p_1 \cdot p_4)(p_3 \cdot p_2) + (p_1 \cdot p_2)(p_4 \cdot p_3) - m_e^2(p_1 \cdot p_3) \right) .
\end{aligned}} \tag{5.160}$$

Once we average over initial spin states we need to multiply with  $\frac{1}{2}$  due to neutrinos

fixed helicity states. Hence, we obtain

$$\begin{aligned}
\langle |\mathcal{M}_{NC}|^2 \rangle &= \frac{e^4}{4q^4} A^{\mu\alpha} B_{\mu\alpha} \\
&= \frac{8e^4}{q^4} p_{1\sigma} p_{1\beta} q_\rho q_\eta \theta^{\sigma\rho} \theta^{\beta\eta} \\
&\quad \times \left( (p_1 \cdot p_4)(p_3 \cdot p_2) + (p_1 \cdot p_2)(p_4 \cdot p_3) - m_e^2(p_1 \cdot p_3) \right).
\end{aligned} \tag{5.161}$$

Let us evaluate  $p_{1\sigma} p_{1\beta} q_\rho q_\eta \theta^{\sigma\rho} \theta^{\beta\eta}$  by expanding  $q$  in terms of momentums as  $q = p_1 - p_3$ .

$$\begin{aligned}
p_{1\sigma} p_{1\beta} q_\rho q_\eta \theta^{\sigma\rho} \theta^{\beta\eta} &= p_{1\sigma} p_{1\beta} (p_{1\rho} - p_{3\rho})(p_{1\eta} - p_{3\eta}) \theta^{\sigma\rho} \theta^{\beta\eta} \\
&= \underbrace{p_{1\sigma} p_{1\rho}}_S \underbrace{p_{1\beta} p_{1\eta}}_S \underbrace{\theta^{\sigma\rho}}_{AS} \underbrace{\theta^{\beta\eta}}_{AS} \\
&\quad - \underbrace{p_{1\sigma} p_{1\rho}}_S \underbrace{p_{1\beta} p_{3\eta}}_{AS} \theta^{\sigma\rho} \theta^{\beta\eta} \\
&\quad - p_{1\sigma} p_{3\rho} \underbrace{p_{1\beta} p_{1\eta}}_S \theta^{\sigma\rho} \underbrace{\theta^{\beta\eta}}_{AS} \\
&\quad + p_{1\sigma} p_{1\beta} p_{3\rho} p_{3\eta} \theta^{\sigma\rho} \theta^{\beta\eta}
\end{aligned} \tag{5.162}$$

Symmetric times anti-symmetric terms vanish and we get

$$p_{1\sigma} p_{1\beta} q_\rho q_\eta \theta^{\sigma\rho} \theta^{\beta\eta} = p_{1\sigma} p_{1\beta} p_{3\rho} p_{3\eta} \theta^{\sigma\rho} \theta^{\beta\eta} . \tag{5.163}$$

Finally, once we put Equation (5.163) into Equation (5.161) we find the amplitude square as follows.

$$\begin{aligned}
\langle |\mathcal{M}_{NC}|^2 \rangle &= \frac{e^4}{8q^4} A^{\mu\alpha} B_{\mu\alpha} \\
&= \frac{8e^4}{q^4} p_{1\sigma} p_{3\rho} \theta^{\sigma\rho} p_{1\beta} p_{3\eta} \theta^{\beta\eta} \\
&\quad \times \left( (p_1 \cdot p_4)(p_3 \cdot p_2) + (p_1 \cdot p_2)(p_4 \cdot p_3) - m_e^2(p_1 \cdot p_3) \right).
\end{aligned}$$

(5.164)

For unitarity conditions to be satisfied we choose  $\theta_{0i} = 0$  and  $\theta_{ij} \neq 0$  as in Equation (5.33). Using this choice we have,



$$\begin{aligned}
p_{1\sigma}p_{3\rho}\theta^{\sigma\rho} &= (p_1)_0((p_3)_0\theta^{00} + (p_3)_1\theta^{01} + (p_3)_2\theta^{02} + (p_3)_3\theta^{03}) \\
&+ (p_1)_1((p_3)_0\theta^{10} + (p_3)_1\theta^{11} + (p_3)_2\theta^{12} + (p_3)_3\theta^{13}) \\
&+ (p_1)_2((p_3)_0\theta^{20} + (p_3)_1\theta^{21} + (p_3)_2\theta^{22} + (p_3)_3\theta^{23}) \\
&+ (p_1)_3((p_3)_0\theta^{30} + (p_3)_1\theta^{31} + (p_3)_2\theta^{32} + (p_3)_3\theta^{33}) .
\end{aligned} \tag{5.165}$$

Since  $\theta^{\mu\nu}$  is anti-symmetric then  $\theta^{\mu\nu} = -\theta^{\nu\mu}$  and Equation (5.165) turns out to be;

$$\begin{aligned}
p_{1\sigma}p_{3\rho}\theta^{\sigma\rho} &= (p_1)_1((p_3)_2\theta^{12} + (p_3)_3\theta^{13}) + (p_1)_2(- (p_3)_1\theta^{12} + (p_3)_3\theta^{23}) \\
&+ (p_1)_3(- (p_3)_1\theta^{13} - (p_3)_2\theta^{23}) .
\end{aligned} \tag{5.166}$$

Once we collect the terms, this equation can be simplified into;

$$\begin{aligned}
p_{1\sigma}p_{3\rho}\theta^{\sigma\rho} &= ((p_1)_1(p_3)_2 - (p_1)_2(p_3)_1)\theta^{12} + ((p_1)_1(p_3)_3 - (p_1)_3(p_3)_1)\theta^{13} \\
&+ ((p_1)_2(p_3)_3 - (p_1)_3(p_3)_2)\theta^{23} .
\end{aligned} \tag{5.167}$$

To express this term in a more compact form let us define  $\vec{\theta}$  vector as;

$$\vec{\theta} = (\theta^{23}, \theta^{31}, \theta^{12}) \tag{5.168}$$

so that we can write Equation (5.167) as

$$p_{1\sigma}p_{3\rho}\theta^{\sigma\rho} = (\vec{p}_1 \times \vec{p}_3) \cdot \vec{\theta} \tag{5.169}$$

We can now write amplitude square (Equation (5.164)) as;

$$\begin{aligned}
\langle |\mathcal{M}_{NC}|^2 \rangle &= \frac{8e^4}{q^4} ((\vec{p}_1 \times \vec{p}_3) \cdot \vec{\theta})^2 \\
&\times ((p_1 \cdot p_4)(p_3 \cdot p_2) + (p_1 \cdot p_2)(p_4 \cdot p_3) - m_e^2(p_1 \cdot p_3)) .
\end{aligned} \tag{5.170}$$

In order to calculate  $(\vec{p}_1 \times \vec{p}_3) \cdot \vec{\theta}$  we need to choose a coordinate system for the rest frame of the electron. Let us choose the following frame;

$$\begin{aligned}
p_1 &= (E_1, 0, 0, |\vec{p}_1|) , \\
p_2 &= (m_e, 0, 0, 0) , \\
p_3 &= (E_3, -|\vec{p}_4| \sin \alpha \cos \phi, -|\vec{p}_4| \sin \alpha \sin \phi, |\vec{p}_1| - |\vec{p}_4| \cos \alpha) , \\
p_4 &= (E_4, |\vec{p}_4| \sin \alpha \cos \phi, |\vec{p}_4| \sin \alpha \sin \phi, |\vec{p}_4| \cos \alpha) , \\
\vec{\theta} &= (|\vec{\theta}| \sin \lambda, 0, |\vec{\theta}| \sin \lambda) ,
\end{aligned} \tag{5.171}$$

where  $|\vec{p}_1| = E_1$ , once we neglect the mass of neutrinos. We prefer to express all factors in terms of recoil energy of the electron which is the measured quantity in the experiments.

We know that  $\cos \alpha$  is related to the recoil energy ( $T$ ) of the electron and one way to find this angle in terms of  $T$  is by using the condition  $p_3^2 = 0$  in the above chosen coordinates.

$$\begin{aligned}
p_3^2 &= E_3^2 - (|\vec{p}_4|^2 \sin^2 \alpha \cos^2 \phi + |\vec{p}_4|^2 \sin^2 \alpha \sin^2 \phi + (|\vec{p}_1| - |\vec{p}_4| \cos \alpha)^2) \\
&= (E_1 + \underbrace{m_e}_{E_2} - \underbrace{(T + m_e)}_{E_4})^2 - \underbrace{(|\vec{p}_4|^2 \sin^2 \alpha (\cos^2 \phi + \sin^2 \phi) + |\vec{p}_4|^2 \cos^2 \alpha}_{p_4^2} + |\vec{p}_1|^2 - 2|\vec{p}_1||\vec{p}_4|) \\
&= (E_1 - T)^2 - |\vec{p}_4|^2 - E_1^2 - 2E_1|\vec{p}_4| \cos \alpha \\
&= \cancel{E_1^2} + T^2 - 2E_1T - |\vec{p}_4|^2 - \cancel{E_1^2} + 2E_1|\vec{p}_4| \cos \alpha \\
&= T^2 - 2E_1T - T(T + 2m_e) + 2E_1|\vec{p}_4| \cos \alpha \\
&= \cancel{T^2} - 2E_1T - \cancel{T^2} - 2m_eT + 2E_1|\vec{p}_4| \cos \alpha \\
&= -2T(E_1 + m_e) + 2E_1|\vec{p}_4| \cos \alpha = 0 \\
\Rightarrow \boxed{\cos \alpha = \frac{T(E_1 + m_e)}{E_1|\vec{p}_4|}}.
\end{aligned} \tag{5.172}$$

With this orientation, we find  $\vec{p}_1 \times \vec{p}_3$  as;

$$\vec{p}_1 \times \vec{p}_3 = |\vec{p}_1||\vec{p}_3| \sin \alpha \sin \phi \hat{x} - |\vec{p}_3| \sin \alpha \cos \phi |\vec{p}_1| \hat{y}. \tag{5.173}$$

Hence  $\vec{\theta} \cdot (\vec{p}_1 \times \vec{p}_3)$  term can be found in this frame using Equation (5.168) as;

$$\vec{\theta} \cdot (\vec{p}_1 \times \vec{p}_3) = |\vec{\theta}| \sin(\lambda) |\vec{p}_1| |\vec{p}_3| \sin \alpha \sin \phi. \tag{5.174}$$

In Appendix B, we already found out the following kinematic relations in the rest frame of electrons (neglecting the mass of neutrinos)

$$\begin{aligned}
(p_1 \cdot p_2)(p_3 \cdot p_4) &= m_e^2 E_1^2 \\
(p_1 \cdot p_4)(p_2 \cdot p_3) &= m_e^2 (E_1 - (E_4 - m_e))^2 = m_e^2 (E_1 - T)^2 \\
(p_1 \cdot p_3) &= m_e (E_4 - m_e) = m_e T,
\end{aligned} \tag{5.175}$$

where  $T$  is the recoil energy of the electron ( $T = E_4 - m_e$ ). Thus, we find;

$$\boxed{(p_1 \cdot p_2)(p_3 \cdot p_4) + (p_1 \cdot p_4)(p_2 \cdot p_3) - m_e^2(p_1 \cdot p_3) = m_e^2 E_1^2 \left(1 + \left(1 - \frac{T}{E_1}\right)^2 - \frac{m_e T}{E_1^2}\right)} \quad (5.176)$$

Using Equation (5.176) and Equation (5.174), we can write the amplitude square (Equation (5.170)) in the following form.

$$\begin{aligned} \langle |\mathcal{M}_{NC}|^2 \rangle &= \frac{8e^4}{q^4} |\vec{\theta}|^2 \sin^2(\lambda) |\vec{p}_1|^2 |\vec{p}_3|^2 \sin^2 \alpha \sin^2 \phi m_e^2 (E_1^2 + (E_1 - T)^2 - m_e T) \\ &= \frac{8e^4}{4(p_1 \cdot p_3)^2} |\vec{\theta}|^2 \sin^2(\lambda) E_1^2 |\vec{p}_4|^2 \sin^2 \alpha \sin^2 \phi m_e^2 \\ &\quad \times (E_1^2 + (E_1 - T)^2 - m_e T) \\ &= \frac{2e^4}{m_e^2 T^2} |\vec{\theta}|^2 \sin^2(\lambda) E_1^2 |\vec{p}_4|^2 \underbrace{(1 - \cos^2 \alpha)}_{\sin^2 \alpha} \sin^2 \phi m_e^2 \\ &\quad (E_1^2 + (E_1 - T)^2 - m_e T) \\ &= \frac{2e^4}{m_e^2 T^2} |\vec{\theta}|^2 \sin^2(\lambda) E_1^2 |\vec{p}_4|^2 \sin^2 \alpha \sin^2 \phi m_e^2 (E_1^2 + (E_1 - T)^2 - m_e T) \end{aligned} \quad (5.177)$$

in which  $q^4 = 4(p_1 \cdot p_3)^2$ ,  $|p_1| = E_1$  once we neglect mass of the neutrinos.

Moreover,  $\sin^2 \alpha$  can be described in terms of the recoil energy of the electron and incoming energy of the neutrino using Equation (5.172) as;

$$\begin{aligned} \sin^2 \alpha &= 1 - \cos^2 \alpha \\ &= 1 - \left(\frac{T(E_1 + m_e)}{E_1 |\vec{p}_4|}\right)^2 \\ &= \frac{E_1^2 |\vec{p}_4|^2 - T^2 (E_1 + m_e)^2}{E_1^2 |\vec{p}_4|^2} \\ &= \frac{E_1^2 T(T + 2m_e) - T^2 (E_1^2 + 2m_e E_1 + m_e^2)}{E_1^2 |\vec{p}_4|^2} \\ &= \frac{\cancel{E_1^2 T^2} + 2m_e E_1^2 T - \cancel{T^2 E_1^2} - 2m_e E_1 T^2 - m_e^2 T^2}{E_1^2 |\vec{p}_4|^2} \\ &= \frac{2m_e E_1 T (E_1 - T) - m_e^2 T^2}{E_1^2 |\vec{p}_4|^2}. \end{aligned} \quad (5.178)$$

Hence, once we put the above equation into Equation (5.177), we can write the amplitude square in terms of the recoil energy of the electron as;

$$\begin{aligned}
\langle |\mathcal{M}_{NC}|^2 \rangle &= \frac{2e^4}{m_e^2 T^2} |\vec{\theta}|^2 \sin^2(\lambda) \sin^2 \phi \frac{E_1^2 |\vec{p}_4|^2 m_e^2}{E_1^2 |\vec{p}_4|^2} \left( \frac{2m_e E_1 T (E_1 - T) - m_e^2 T^2}{E_1^2 |\vec{p}_4|^2} \right) \\
&\quad \times (E_1^2 + (E_1 - T)^2 - m_e T) , \\
\langle |\mathcal{M}_{NC}|^2 \rangle &= \frac{2}{T^2} e^4 |\vec{\theta}|^2 \sin^2(\lambda) \sin^2 \phi (2m_e E_1 T (E_1 - T) - m_e^2 T^2) \\
&\quad \times (E_1^2 + (E_1 - T)^2 - m_e T) .
\end{aligned} \tag{5.179}$$

Notice that we used Equation (5.172) so that the amplitude square is in terms of the recoil energy of the electron only.

From Equation (3.18) , once we rule out the  $\phi$  integral we can write  $d\sigma/dT$  as;

$$\frac{d\sigma}{dT} = \frac{S |\mathcal{M}_{NC}|^2}{64\pi^2 m_e E_1^2} d\phi . \tag{5.180}$$

Since in the experiments we can not measure the recoil angle of the electrons it is not possible to constrain the  $\lambda$  term, instead we average over  $\lambda$ . From Equation (5.177) once we average over angle  $\lambda$  we get;

$$\frac{1}{2\pi} \int_0^{2\pi} \sin^2 \lambda d\lambda = \frac{1}{2} . \tag{5.181}$$

Moreover, when we evaluate  $\phi$  integral we find;

$$\int_0^{2\pi} \sin^2 \phi d\phi = \pi . \tag{5.182}$$

Hence, we can write the differential cross-section using Equation (5.179) as;

$$\begin{aligned}
\frac{d\sigma}{dT} &= \frac{\pi}{2} \frac{2 e^4 |\vec{\theta}|^2 (2m_e E_1 T (E_1 - T) - m_e^2 T^2) (E_1^2 + (E_1 - T)^2 - m_e T)}{64\pi^2 m_e E_1^2} \\
&= \frac{e^4 |\vec{\theta}|^2 m_e T (2E_1 (E_1 - T) - m_e T) (E_1^2 + (E_1 - T)^2 - m_e T)}{64\pi m_e E_1^2 T^2} \\
&= \frac{e^4 |\vec{\theta}|^2 (2E_1 (E_1 - T) - m_e T) (E_1^2 + (E_1 - T)^2 - m_e T)}{64\pi E_1^2 T} .
\end{aligned} \tag{5.183}$$

In order to see the dependence of the cross section to the incoming energy and the recoil energy of the electron, let us try to write the cross section in a neater form as;

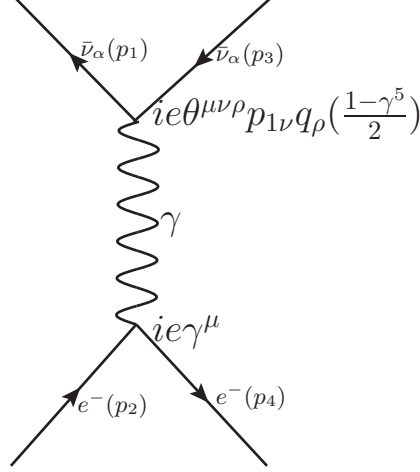


Figure 5.4: Feynman Diagram of  $\bar{\nu} - e^-$  scattering in non-commutative space is displayed. Even though neutrinos are chargeless they can still interact with photons.

$$\frac{d\sigma}{dT} = \frac{e^4 |\vec{\theta}|^2 E_1^2}{16\pi} \left( \frac{1}{T} - \frac{2}{E_1} + \frac{3T - 2m_e}{2E_1^2} - \frac{T^2 - 2m_e T}{2E_1^3} - \frac{m_e T^2}{4E_1^4} \left(1 - \frac{m_e}{T}\right) \right). \quad (5.184)$$

Finally, since  $e = \sqrt{4\pi\alpha}$  we can write the cross section

$$\boxed{\begin{aligned} \frac{d\sigma}{dT} &= |\vec{\theta}|^2 \pi \alpha^2 E_1^2 \left( \frac{1}{T} - \frac{2}{E_1} + \frac{3T - 2m_e}{2E_1^2} - \frac{T^2 - 2m_e T}{2E_1^3} - \frac{m_e T^2}{4E_1^4} \left(1 - \frac{m_e}{T}\right) \right) \\ &= \frac{\pi \alpha^2}{\Lambda_{NC}^4} E_1^2 \left( \frac{1}{T} - \frac{2}{E_1} + \frac{3T - 2m_e}{2E_1^2} - \frac{T^2 - 2m_e T}{2E_1^3} - \frac{m_e T^2}{4E_1^4} \left(1 - \frac{m_e}{T}\right) \right) \end{aligned}} \quad (5.185)$$

where we used  $|\vec{\theta}| = \frac{1}{\Lambda_{NC}^2}$ .

#### 5.4.2 Anti-neutrino Electron Scattering In Non-commutative Space

The amplitude for the  $\bar{\nu} - e^-$  interaction in the non-commutative space can be written using the Feynman diagram shown in Figure (5.4) as;

$$\mathcal{M}_{\bar{\nu}-e} = \frac{e^2}{q^2} [\bar{u}(p_4) \gamma^\mu u(p_2)] [\bar{\nu}(p_1) \theta_\mu^{\sigma\rho} p_{1\sigma} q_\rho (1 - \gamma^5) \nu(p_3)]. \quad (5.186)$$

Since  $\nu(p) = u(-p)$ , we can also write the amplitude as;

$$\mathcal{M}_{\bar{\nu}-e} = \frac{e^2}{q^2} [\bar{u}(p_4) \gamma^\mu u(p_2)] [\bar{u}(-p_1) \theta_\mu^{\sigma\rho} p_{1\sigma} q_\rho (1 - \gamma^5) u(-p_3)]. \quad (5.187)$$

Once we compare this amplitude with Equation (5.75), amplitude for the  $\nu - e^-$  scattering in the non-commutative space, we realize that if we replace  $p_1 \rightarrow -p_3$  and  $p_3 \rightarrow -p_1$ , we get the same amplitude. Hence, instead of recalculating for the amplitude square, we can easily do the replacements in Equation (5.164).

Remember that we found the amplitude square for the  $\nu - e^-$  scattering in Equation (5.164) as;

$$\boxed{\langle |\mathcal{M}_{NC}|_{\nu-e^-}^2 \rangle = \frac{8e^4}{q^4} p_{1\sigma} p_{3\rho} \theta^{\sigma\rho} p_{1\beta} p_{3\eta} \theta^{\beta\eta} \times \left( (p_1 \cdot p_4)(p_3 \cdot p_2) + (p_1 \cdot p_2)(p_4 \cdot p_3) - m_e^2(p_1 \cdot p_3) \right)} \quad (5.188)$$

Once we do the following replacements;

$$\begin{aligned} p_1 &\rightarrow -p_3 \\ p_3 &\rightarrow -p_1 \end{aligned} \quad (5.189)$$

we get;

$$\begin{aligned} \langle |\mathcal{M}_{NC}|_{\nu-e^-}^2 \rangle &= \frac{8e^4}{q^4} (-p_{3\sigma})(-p_{1\rho})\theta^{\sigma\rho}(-p_{3\beta})(-p_{1\eta})\theta^{\beta\eta} \\ &\times \left( ((-p_3) \cdot p_4)((-p_1) \cdot p_2) + ((-p_3) \cdot p_2)(p_4 \cdot (-p_1)) \right. \\ &\quad \left. - m_e^2((-p_3) \cdot (-p_1)) \right) \\ &= \frac{8e^4}{q^4} p_{3\sigma} p_{1\rho} \theta^{\sigma\rho} p_{3\beta} p_{1\eta} \theta^{\beta\eta} \\ &\times \left( (p_3 \cdot p_4)(p_1 \cdot p_2) + (p_3 \cdot p_2)(p_4 \cdot p_1) - m_e^2(p_3 \cdot p_1) \right) \\ &= \frac{8e^4}{q^4} p_{1\sigma} p_{3\rho} \theta^{\sigma\rho} p_{1\beta} p_{3\eta} \theta^{\beta\eta} \\ &\times \left( (p_3 \cdot p_4)(p_1 \cdot p_2) + (p_3 \cdot p_2)(p_4 \cdot p_1) - m_e^2(p_3 \cdot p_1) \right). \end{aligned} \quad (5.190)$$

Note that once we change the dummy indices as  $\sigma \leftrightarrow \beta$   $\rho \leftrightarrow \eta$  then we realize that the following terms are equal;

$$p_{1\sigma} p_{3\rho} \theta^{\sigma\rho} p_{1\beta} p_{3\eta} \theta^{\beta\eta} = p_{1\beta} p_{3\eta} \theta^{\beta\eta} p_{1\sigma} p_{3\rho} \theta^{\sigma\rho} .$$

When we compare Equation (5.190) with Equation (5.164), we easily see that we get the same amplitude square. Hence we deduce that the cross-section for the neutrino-electron scattering in the non-commutative space is the same for the neutrinos and anti-neutrinos as well as being the same for all neutrino flavors.

The interference of photon exchange diagram in NC space with the electroweak diagrams in the SM is zero [113]. The calculation of the interference term for  $\nu_\mu - e^-$  scattering is done in detail in Appendix D.

## 5.5 Analysis & Results

Having derived the cross-section for the  $\nu - e^-$  scattering in the non-commutative (NC) space, we can compare these new physics predictions with the data to search the existence of new signals which deviate from the SM prediction in order to get information about the NC space.

When we analyzed the form of the cross-section formula (Equation (5.185)), we realize that  $1/T$  and  $E_\nu^2$  dependencies are significantly different from the SM expression given in Equation (3.116). The first term in Equation (5.185) implies that the cross-section increases for the low recoil energy of the electrons. Hence, it is expected that, TEXONO like low recoil energy experiments would have better sensitivity for searching the NC space effects in the  $\nu - e^-$  scattering. On the other hand, the cross section is proportional to  $E_\nu^2$  which makes high energy neutrino experiments advantageous. In order to test this situation, we decided to analyze three different data sets of neutrino experiments depending on the energy range as mentioned in Chapter 4. For the low recoil energies we analyzed the data sets of TEXONO collaboration, for the middle energy neutrinos, LSND experiment was suitable and for the high energy neutrinos, data collected by CHARM II collaboration is preferred. The key parameters of these experiments such as the mean energy of neutrinos are also shown in Table 5.1.

Moreover, to figure out the sensitivity of the recoil energy to new physics effects in a quantitative way, it is better to plot the differential cross section with respect to the recoil energy. For the each data sets of the collaborations,  $d\sigma/dT$  vs  $T$  diagram is plotted by fixing the value of non-commutative scale,  $\Lambda_{NC}$ . The results are shown

in Figure (5.6). We realize from those plots that either low recoil energies or high incoming neutrino energies would be expected to give more stringent bounds for  $\Lambda_{NC}$ . Note also that neutrino spectra are normalized to unity for plotting the spectrum.

For constraining  $\Lambda_{NC}$ , we need to compare the data with the NC space contributions as well as SM. We consider that any difference between the experiment and the standard model prediction is due to “new physics”, for this case which is the existence of NC space. We need to evaluate the number of events of the model prediction since the data is recorded in that way. Since the incoming neutrinos do not have fixed energy, to find the number of events we need to integrate over the flux of neutrinos.

$$R_X = t\rho_e \int_T \int_{E_\nu} \left[ \left( \frac{d\sigma}{dT}(E_\nu, T) \right)_X \frac{d\phi_\nu(E_\nu)}{dE_\nu} \right] dE_\nu \quad (5.191)$$

where  $R$  corresponds to measured event rate,  $\rho_e$  is the electron number density per kg of target material,  $t$  is the data taking period,  $\phi_\nu(E_\nu)$  is the neutrino flux<sup>2</sup> and  $X$  corresponds to either SM or new physics (NP) contribution.

For each data set of the collaborations there is slight difference in performing the analysis, hence let us mention them one by one.<sup>3</sup>

### 5.5.1 TEXONO

For searching the signatures of the  $\nu - e$  interaction via the photon exchange in the NC space, two of the data sets of the TEXONO Collaboration (HPGe and CsI(Tl) scintillating crystal detector) are analyzed.

Data taken by HPGe detector is used to search for the neutrino magnetic moment and the data is published in terms of per kg per keV as shown in 4.9. Analysis range is  $T \sim 12 - 60$  keV and note that as the threshold energy decreases, it becomes difficult to discriminate the signal over the background hence, errors become larger as seen in Figure (4.9).

On the other hand, the cross-section and hence, the Weinberg angle is measured with

---

<sup>2</sup> The neutrino spectrum is normalized to 1 ( $\int \phi(E_\nu) dE_\nu = 1$ ) throughout this study.

<sup>3</sup> See Chapter 4 for more information about the experiments.



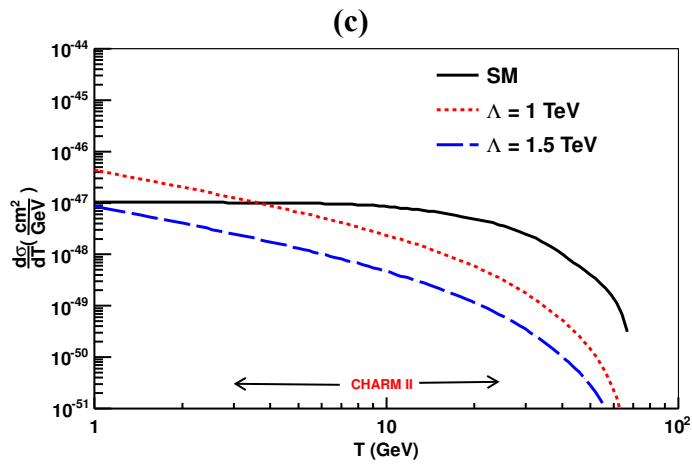
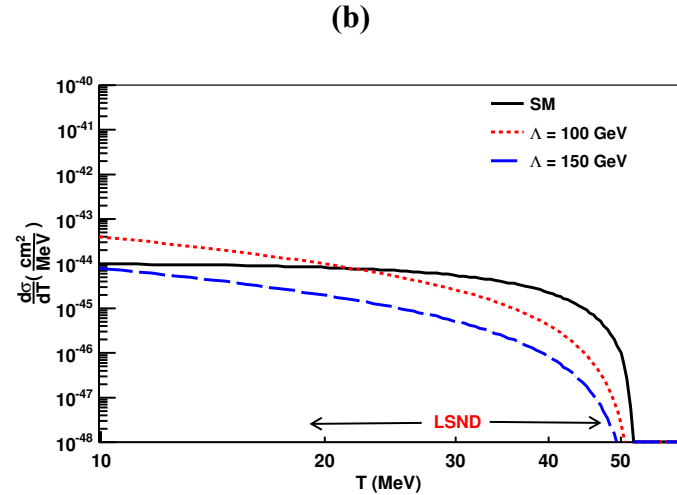
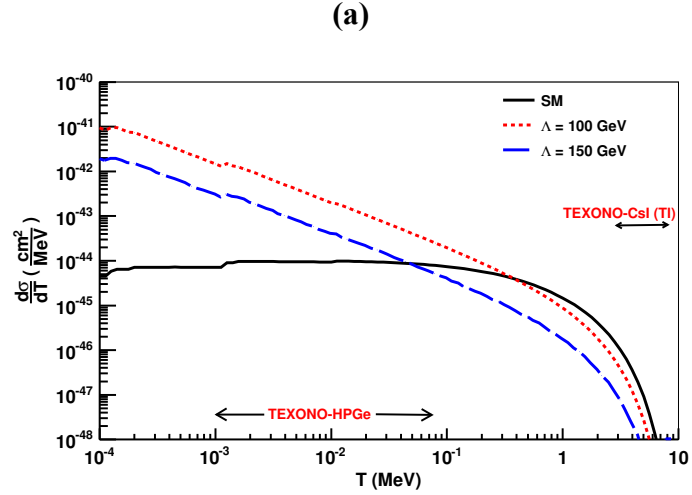


Figure 5.5: The differential cross-sections as a function of the recoil energy is depicted for (a) Top: TEXONO experiment with reactor  $\bar{\nu}_e$  [62, 69, 68], (b) Middle: LSND experiment with  $\nu_\mu$  from stopped-pion [81], and (c) Bottom: CHARM-II experiment with accelerator  $\nu_\mu(\bar{\nu}_\mu)$  [114, 85]. Both SM and NC contributions are displayed. (Figure is adapted from [115].)

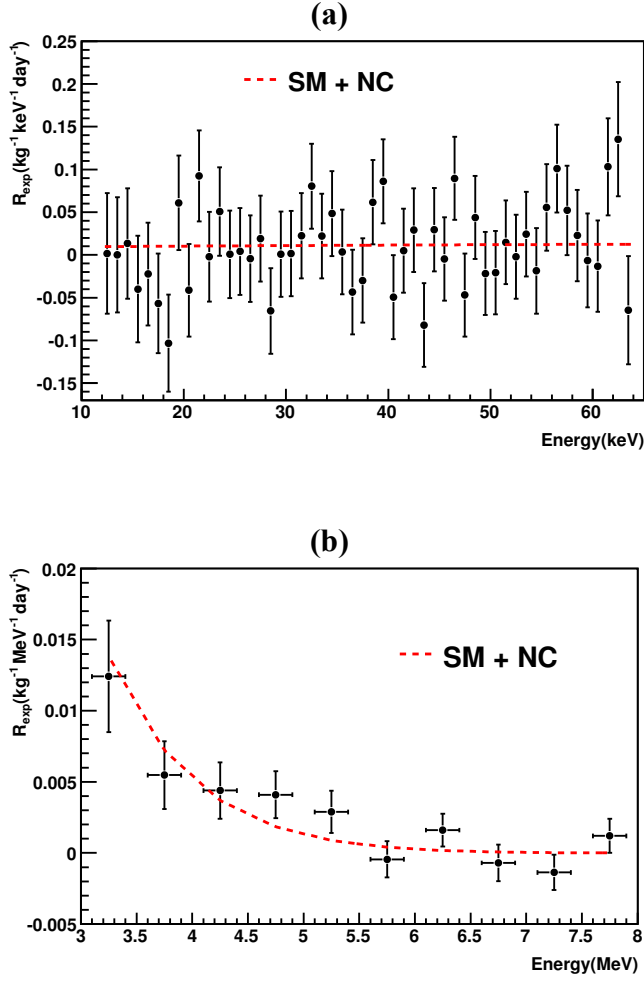


Figure 5.6: Data sets of TEXONO adapted for the noncommutative analysis. SM+NC effects are fitted to data.

the data collected using CsI(Tl) scintillating crystal arrays by TEXONO. The measured recoil energy spectrum is depicted in terms of per kg, per MeV per day and the recoil energy range is 3 – 8 MeV as shown in 4.6. Key parameters of the experiments are also summarized in Table 5.1.

For each data set, we calculated the Standard Model prediction and new physics effect in terms of the published data for the HPGe and CsI target separately for each related energy bins using Equation (5.191). Then, we applied a  $\chi^2$  fit as;

$$\chi^2 = \sum_{i=1} \left[ \frac{R_{exp}(i) - [R_{SM}(i) + R_X(i)]}{\Delta_{stat}(i)} \right]^2. \quad (5.192)$$

where  $R_{exp}(i)$  and  $\Delta_{stat}(i)$  are the measured rates and uncertainties on the  $i^{th}$  data bin, respectively.

With  $\chi^2$  fit (See Figure (5.6)), the mean value of the  $|\theta|^2$  is determined and bounds are transformed into 95 % C.L. for the NC scale,  $\Lambda_{NC}$ , using Feldman-Cousins method [116]. The obtained bounds are shown in Table 5.1.

### 5.5.2 LSND

LSND collaboration reported the cross-section measurement in terms of explicit incoming energy of neutrino as given in Equation (5.193);

$$\sigma_{\nu_e e^-} = (10.1 \pm 1.1(stat) \pm 1.0(syst)) \times E_\nu(\text{MeV}) \times 10^{-45} \text{ cm}^{-2} \quad (5.193)$$

Moreover, we derived in Section 3.5 (See Equation (3.126)) that for high energetic neutrinos the SM cross-section turns out to be equal to

$$\sigma_{\nu_e - e^-} = 9.27 \times 10^{-45} (E_\nu/\text{MeV}) \text{ cm}^2 .$$

However, we can not use these SM prediction and measured value to constrain  $\Lambda_{NC}$ , since we can not extract the  $E_\nu$  explicitly for the additional neutrino-photon interaction as calculated in Equation (5.185). Hence, instead of pure cross-section measurement we preferred to choose flux averaged cross-section that LSND measured as [81];

$$\langle \sigma \rangle = (3.19 \pm 0.35 \pm 0.33) \times 10^{-43} \text{ cm}^2 \quad (5.194)$$

In order to compare data with SM and new physics predictions we need to calculate the flux averaged cross-sections hence we need neutrino spectrum. For that reason, the flux shown in Figure (4.16) is used via normalizing to unity, since the exact values of the spectrum had not been presented in the paper.

Using

$$\langle \sigma \rangle = \int_T \int_{E_\nu} \left[ \frac{d\sigma}{dT}(E_\nu, T) \right]_X \frac{d\phi_\nu(E_\nu)}{dE_\nu} dE_\nu \quad (5.195)$$

we calculate the SM and NC contributions first. And to get the deviation of the measured flux average value with the SM prediction we compared the Weinberg angle measurement of LSND with the value published in PDG [13]. With this method we put constraint at 95% CL on the parameter  $\Lambda_{NC}$  as depicted in Table 5.1.

Note that since the Weinberg angle depends on the  $Q^2$  value, then PDG value of the relevant Weinberg angle must be used. (See Figure (5.7)).

### 5.5.3 CHARM II

On the contrary to LSND collaboration, CHARM II published their results in terms of number of events observed for the  $\nu_\mu - e^-$  and the  $\bar{\nu}_\mu - e^-$  scattering as  $2677 \pm 82$  and  $2752 \pm 88$  respectively as mentioned in Section 4.4. Moreover the Weinberg angle is measured as  $0.2324 \pm 0.0083$  by CHARM II. This analysis is similar to LSND but in this case number of events must be calculated using the neutrino flux recorded with CHARM II.

It is important to note that while calculating the SM prediction, the relevant Weinberg angle value must be used since the Weinberg angle varies with respect to energy as presented in Figure (5.7) [13]. The neutrino flux is normalized to unity as in LSND and bounds are set for  $|\theta|^2$  and hence  $\Lambda_{NC}$  as shown in Table 5.1.

Table5.1: The key parameters of the TEXONO, LSND and CHARM-II measurements on the  $\nu - e$  scattering, and the derived bounds on NC physics. The best-fit values in  $\Theta^2$  and the 95% CL lower limits on  $\Lambda_{NC}$  are shown.

Experiment	$\nu$	$\langle E_\nu \rangle$	$T$	Measured $\sin^2\theta_W$	Best-Fit on $\Theta^2$ (MeV <sup>-4</sup> )	$\Lambda_{NC}$ (95% CL)
TEXONO-HPGe [69, 68]	$\bar{\nu}_e$	1–2 MeV	12–60 keV	–	$(9.27 \pm 6.65) \times 10^{-22}$	> 145 GeV
TEXONO-CsI(Tl) [62]	$\bar{\nu}_e$	1–2 MeV	3–8 MeV	$0.251 \pm 0.039$	$(0.81 \pm 5.74) \times 10^{-21}$	> 95 GeV
LSND [81]	$\nu_e$	36 MeV	18–50 MeV	$0.248 \pm 0.051$	$(0.38 \pm 2.06) \times 10^{-21}$	> 123 GeV
CHARM-II [114, 85]	$\nu_\mu$	23.7 GeV	3-24 GeV	} $0.2324 \pm 0.0083$	$(0.20 \pm 1.03) \times 10^{-26}$	> 2.6 TeV
	$\bar{\nu}_\mu$	19.1 GeV	3-24 GeV		$(-0.92 \pm 4.77) \times 10^{-27}$	> 3.3 TeV

### 5.5.4 Bounds from Other Channels

Since  $\theta$  contains the directional information, it is possible to measure the components of  $\theta$  and for this case one needs to consider the motion of the lab frame in which the measurement is done [117]. However, in most of the phenomenological studies,  $|\vec{\theta}|$  (we will mention it as  $\theta$ ) is defined as the average magnitude of  $\theta_{\mu\nu}$ . In addition to this,  $\theta$  is related with the energy scale as  $1/\sqrt{\theta} = \Lambda_{NC}$ , which mimics that the deformation of the space time is observable above that scale. Hence, most of the bounds are given in terms of  $\Lambda_{NC}$  in the literature. It is believed that effects of the non-commutative scale may seem much below the  $\Lambda_{NC}$  in which effective theories with small parameter

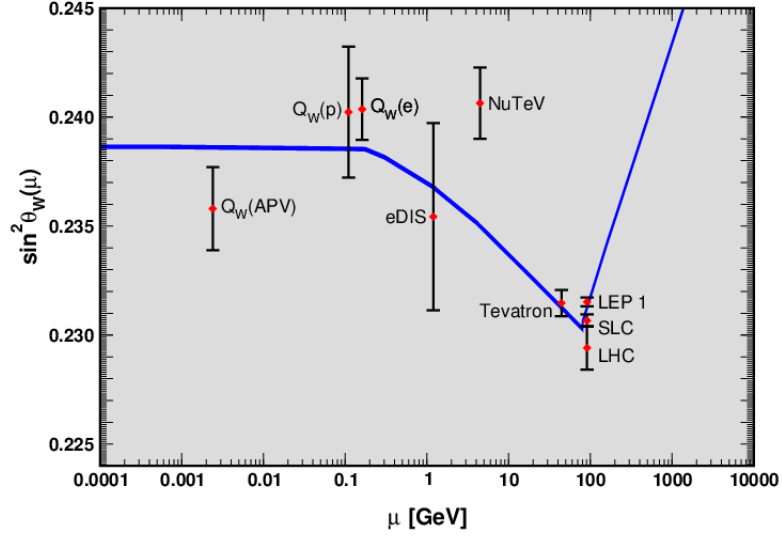


Figure 5.7: Weinberg angle measurements are shown with respect to energy. For more details See [13].

$\theta$  expansion is reasonable.

The Standard Model in the non-commutative space (NCSM) is studied extensively. With the expectation of observing the effects of NC space much below the Planck scale, the possible effects are searched in many channels. In general noncommutative studies can be categorized into three groups as; High energy collider experiments, low energy precision experiments and astrophysics and cosmology. A nice review of the bounds are shown in [118] and these bounds are summarized in Table 5.2.

High energy collider experiments can search the direct effects of noncommutative physics since the energy scale is comparable with the expected non-commutative energy scale. LEP-OPAL experiment constrained as  $\Lambda_{NC} > 141$  GeV [119] via searching NC-QED induced signatures in the  $e^- + e^+ \rightarrow \gamma\gamma$  process. Moreover, Tevatron experiment put more stringent bound as  $\Lambda_{NC}$  when  $W$ -boson polarization is analyzed in top quark decays [120]. Future prospected colliders are expected to probe  $\Lambda_{NC}$  up to 10 TeV.

On the other hand, low energy-high precision experiments can search the indirect effects of noncommutative physics. Noncommutative effects are quadratically suppressed as  $\sim E^2\theta$ , hence, in order to search the rare effects, high precision should have been reached in the experiments. Indirect bounds are obtained from atomic transitions,

magnetic moments of electron and muon, CP violating effects and atomic clock measurements. Even though the bounds derived from dipole moment and atomic clock experiments are so tight, it is important to note that their interpretations are model independent [118].

Furthermore, the indirect signals are also searched in astrophysics and cosmology in many channels in which the bounds are at the order of TeV. However, in high energy regime many new particles such as supersymmetric particles are hoping to be discovered. Therefore, searching for the NC effect only in high energy regime may not give reliable results. For this reason, searches in the electroweak regime is important in the sense that it can give precise results.

The stringent bounds that we acquired from the neutrino electron scattering experiment is  $\Lambda_{NC} > 3.3$  TeV with the CHARM II experiment. This improves the bounds from OPAL experiment and comparable with the bounds obtained from the collider experiments. Moreover, our results verify the proposal that either low recoil energy or incoming neutrinos with high energies would improve the bounds on the non-commutative scale. For instance, the limit we get from HPGe is more stringent than the LSND bounds as shown in Table 5.1. However, the bounds from CHARM II experiment show that, neutrinos with energies at the order of GeV or higher would be expected to give more stringent bounds among neutrino experiments once we contemplated that lowering the recoil energies at the order of eV is not practically possible. With this deduction we can infer that the ultra high energy neutrinos that Ice-cube experiment [121] observed recently could put more stringent bounds to the non-commutative scale.

Although the bounds from accelerator or neutrino experiments are much lower than the astrophysical and high-precision experiments, this should not mean that these studies are not necessary. It is possible that  $\theta_{\mu\nu}$  is not a constant but more complicated function, even energy-momentum dependent for higher order operators [122]. In that case, the noncommutative signals would reveal itself at higher energies and hence model independent studies are required [123].

It is important to note that the cross section is independent of the neutrino flavor as we showed. It is possible to consider flavor changing interactions like  $\nu_\alpha + e^- \rightarrow$

Table 5.2: Summary of experimental constraints on the NC energy scale  $\Lambda_{NC}$ . The quoted bounds for the direct experiments on scattering processes at colliders are at 95% C.L. These are complemented by order-of-magnitude estimates for the model-dependent bounds with the atomic, hadronic and astrophysical systems. The projected sensitivities from current and future collider experiments are also listed. (Table is adapted from [115].)

Experiments	Direct Scattering Channels	$\Lambda_{NC}$
<b>High Energy Collider Experiments</b>		
<b>Current Bounds</b>		
LEP-OPAL	$e^- + e^+ \rightarrow \gamma + \gamma$ [119].	> 141 GeV
LEP	$e^- + e^+ \rightarrow Z \rightarrow \gamma + \gamma$ [124]	> 110 GeV
Tevatron	$t \rightarrow W + b$ [120]	> 624 GeV
	$t \rightarrow W_R + b$ [120]	> 1.5 TeV
<b>Projected Sensitivities</b>		
LHC	$Z \rightarrow \gamma + \gamma$ [125]	> 1 TeV
	$p + p \rightarrow Z + \gamma \rightarrow l^+ + l^- + \gamma$ [126, 127]	> 1 TeV
	$p + p \rightarrow W^+ + W^-$ [128]	> 840 GeV
Linear Collider	$e + \gamma \rightarrow e + \gamma$ [129]	> 900 GeV
	$e^- + e^- \rightarrow e^- + e^-$ [130]	> 1.7 TeV
	$e^- + e^+ \rightarrow \gamma + \gamma$ [130]	> 740 GeV
	$\gamma + \gamma \rightarrow \gamma + \gamma$ [130]	> 700 GeV
	$e^- + e^+ \rightarrow \gamma + \gamma \rightarrow Z$ [131]	> 4 TeV
	$e^- + e^+ \rightarrow Z + \gamma \rightarrow e^+ + e^- + \gamma$ [126, 127]	> 6 TeV
	$e^- + e^+ \rightarrow W^+ + W^-$ [128]	> 10 TeV
	$\gamma + \gamma \rightarrow l^+ + l^-$ [132]	> 700 GeV
Photon Collider	$\gamma + \gamma \rightarrow f + \bar{f}$ [133]	> 1 TeV
<b>Low Energy and Precision Experiments</b>		
	Atom Spectrum of Helium [134]	> 30 GeV
	Lamb Shift in Hydrogen [135]	> 10 TeV
	Electric Dipole Moment of Electron [136, 137]	> 100 TeV
	Atomic Clock Measurements [138]	> $10^8$ TeV
	CP Violating Effects in $K^0$ System [139]	> 2 TeV
	C Violating Effects in $\pi^0 \rightarrow \gamma + \gamma + \gamma$ [140]	> 1 TeV
	Magnetic Moment of Muon [141, 142, 143]	> 1 TeV
<b>Astrophysics and Cosmology Bounds</b>		
	Energy Loss via $\gamma \rightarrow \nu\bar{\nu}$ in Stellar Clusters [110]	> 80 GeV
	Cooling of SN1987A via $\gamma \rightarrow \nu\bar{\nu}$ [144]	> 4 TeV
	Effects of $\gamma \rightarrow \nu\bar{\nu}$ in Primordial Nucleosynthesis [145]	> 3 TeV
	Ultra High Energy Astrophysical Neutrinos [146]	> 200 TeV

$\nu_\beta + e^-$  in the noncommutative space. With an additional flavor dependent parameter  $\lambda_{\alpha\beta}$ , noncommutative induced effects could be searched as an alternative to neutrino oscillations and bounds could be set for  $(\Lambda_{NC}$  and  $\lambda_{\alpha\beta})$  in the high precision neutrino oscillation experiments. This analysis would be analogous to searching non-standard neutrino interactions especially in the neutrino oscillation experiments [147, 148].



## CHAPTER 6

### DARK PHOTON

With the discovery of the long-sought particle, Higgs boson [45, 46], the “particle-content puzzle” for the SM have been completed. Even though the Standard Model can be considered as a very successful theory in explaining the data observed at the electroweak scale, it is still reasonable to contemplate the SM as an effective theory of another more fundamental theory, therefore searching for new symmetries in law of nature has been going on. Moreover, another motivation for the new physics searches is the anomalies that the SM lacks to explain.

Dark matter, which is believed as candidate for the missing mass in the universe, is one of the big mystery that the SM can not resolve. Including new particles that feebly interact with the ordinary matter is thought widely as a necessary ingredient to have an explanation for dark matter.

The observation of excess number of positrons in the cosmic rays without the anti-proton abundance first observed by ATIC [149] and later verified by PAMELA [150], FERMI [151] and AMS [152] collaborations also cannot be explained within the SM. One of the struggles to explain this anomaly is the idea of dark matter annihilation via a mediator to the SM particles. Another puzzle is the excess number of events observed by DAMA/LIBRA [153] as well as COGENT [154] experiments as an annual oscillation in the signal. One of the alternatives as a remedy for this puzzle is the interaction of WIMPS (weakly interacting massive particles), which are also considered as dark matter candidates, with an expected mass of  $\mathcal{O}(5 \text{ GeV})$  [155]. Another idea proposed to explain this phenomenon is the interaction of dark matter particles with the ordinary matter taking place via a new gauge boson with an arbitrary mass [156].

Apart from these recent anomalies having been observed in the dark matter experiments, another unexplained phenomenon waiting to be understood for a long time is the discrepancy between the measured and calculated value of the magnetic moment of the muon. The magnetic moment of the muon is predicted by the Dirac equation with a gyromagnetic ratio  $g_\mu = 2$ ,

$$\vec{M} = g_\mu \frac{e}{2m_\mu} \vec{S}. \quad (6.1)$$

However, when the loop contributions are taken into account, a deviation from the gyromagnetic ratio is expected. This deviation is parameterized by the anomalous magnetic moment as;

$$a_\mu = \frac{g_\mu - 2}{2}. \quad (6.2)$$

The theoretical and experimental values of the anomalous magnetic moment are [13];

$$\begin{aligned} a_\mu^{SM} &= 116591803(1)(42)(26) \times 10^{-11}, \\ a_\mu^{exp} &= 116592091(54)(33) \times 10^{-11}, \end{aligned} \quad (6.3)$$

where the errors in the SM calculation are due to the electroweak, the lowest-order and higher order hadronic contributions, respectively, and the errors in measurement correspond to statistical and systematical uncertainties. The difference between the calculation and measurement is;

$$\Delta a_\mu = a_\mu^{exp} - a_\mu^{SM} = 288(63)(49) \times 10^{-11}, \quad (6.4)$$

which corresponds to a  $3.6\sigma$  discrepancy. This anomaly was also tried to be enlightened with a hypothetical vector boson with a mass range  $M_V \sim 10 - 100$  MeV [13].

To enlighten the anomalies that the SM can not solve, many ideas under the name of “new physics” or “physics beyond the standard model” are proposed. In general, new physics contributions can be categorized as a combination of the ultraviolet (UV), and infrared (IR) terms added to the SM Lagrangian as;

$$\begin{aligned} \mathcal{L} &= \mathcal{L}_{SM} + \mathcal{L}_{NP}, \\ \mathcal{L}_{NP} &= \mathcal{L}_{UV} + \mathcal{L}_{IR}. \end{aligned} \quad (6.5)$$

Ultraviolet terms are related with the new massive particles and suppressed by the UV cut-off scale ( $\Lambda_{UV}$ ). On the other hand, IR region can be considered as a low energy extension of the SM.

One of the common expectation is the discovery of new particles with a large mass corresponding to new symmetries at LHC. However, any signal that is responsible for physics beyond the standard model has not been observed at the collider experiments yet. On the other hand, it is important to note that the anomalies mentioned above do not necessitate the existence of new heavy particles. For instance, these anomalies can be resolved if there exists the interaction of new states which are almost decoupled from the SM, called as “Hidden Sector”. Also, the mass scale of the hidden sector can take any value depending on the interaction strength with the SM particles.

In the following section, brief information about the hidden sector will be given and focusing on the vector portals, which may shed light on the anomalies mentioned above if the free parameters of the model are in the expected range, the  $\nu - e^-$  scattering under  $U(1)_{(B-L)}$  will be studied and the parameter space of the model will be investigated.

## 6.1 Hidden Sector

The hidden sector is also named as “Dark” or “Secluded” sector since this sector is assumed to be comprised of particles that interact very weakly with the SM particles. The communication between the SM and the hidden sector particles are usually believed to be supplied by mediators which are assumed to carry quantum numbers of both the SM and dark sector. Depending on the models, the mediator particles either can interact directly or indirectly through mixing or loop diagrams with the SM particles.

In the literature, there are only a few well-motivated interactions which lead to a “portal” from the SM to the dark sector. These portals depending on the spin and parity of the mediator can be categorized into four as follow [157].

- **Neutrino Portal:** Neutrino mass mechanism is one of the phenomena that the SM comes short to explain. Debates about the sterile neutrinos have continued from the anomalous result of the LSND experiment [77]. With an addition of the Yukawa term to the Lagrangian, sterile neutrinos are introduced as a standard model singlet. The neutrino portal is better to be searched in the neutrino

Table6.1: Various hidden sector models are summarized.

Portal	Particles	Operators
Neutrino	Sterile Neutrinos	$y_N L H N$
Higgs	Dark Scalars	$(\mu S + \lambda S^2) H^\dagger H$
Axion	Pseudoscalars	$\frac{a}{f_a} F_{\mu\nu} \tilde{F}^{\mu\nu}, \frac{a}{f_a} G_{i\mu\nu} \tilde{G}_i^{\mu\nu}$
Vector	Dark Photons	$-\frac{\epsilon}{2 \cos \theta_W} B_{\mu\nu} F'^{\mu\nu}$

facilities especially in the reactor neutrinos.

- **Higgs Portal:** With the additions of the third and fourth order operators to the Lagrangian, it is possible to implement an additional scalar particle through its interactions with the Higgs boson as shown in Table 6.1. Since the interactions involve Higgs boson, it is better to search the effects in the high energy colliders.
- **Axion Portal:** The axions are one of the powerful candidates to explain the so called the “strong CP problem”. It is a very well known fact that CP is violated in the weak interactions. On the other hand, even though the Quantum Chromodynamics (QCD) includes a CP-violating term for non-zero quark masses in the Lagrangian as;

$$\mathcal{L} \sim \frac{\theta}{32\pi^2} G_{\mu\nu} \tilde{G}^{\mu\nu}, \quad (6.6)$$

where  $G_{\mu\nu}$  is the gluon field strength and  $\theta$  is a free parameter to be determined experimentally, no such effect has been observed. This anomaly is generally related to the probe of the electric dipole moment of neutron, which is expected to be;

$$|d_n| \sim \frac{e}{m_n} \left( \frac{m_q}{m_n} \right) |\theta| \sim 10^{-16} |\bar{\theta}| \text{ e cm}, \quad (6.7)$$

where  $m_n(m_q)$  is the neutron (quark) mass and  $\bar{\theta}$  is the effective physical CP violating parameter in the SM. However, the experimental upper bound on the dipole moment of neutron is recorded as [13];

$$|d_n| < 2.9 \times 10^{-26} \text{ e cm}, \quad (6.8)$$

which can be converted the bound on  $\bar{\theta}$  as;

$$|\bar{\theta}| \leq 10^{-10}. \quad (6.9)$$

Unnaturally the smallness of this parameter can not be explained in the standard model and referred as the “strong CP problem”.

Axions, which arise as the pseudo-Nambu-Goldstone boson (PNGB) from a spontaneous symmetry breaking of the Peccei-Quinn (PQ)  $U(1)$  approximate global symmetry at a scale of  $f_a$ , are the most popular candidate for solving this problem. Possible interactions of the axions with the SM particles are depicted in Table 6.1 depending on the specific models.

The mass and coupling constant of the axions depend on the scale parameter  $f_a$ . However, in principle it is possible to propose new interactions in which the mass and coupling constants are free of them. The particles of this model are named as Axion Like Particles (ALPs) in the literature and hence, couplings of the ALPS to the SM particles are arbitrary.

Axions are also proposed in the string theory with the scale parameter  $f_a$  varying between  $10^9 - 10^{17}$  GeV [157, 158, 159, 160, 161, 162, 163]. Effects of axions are searched in a wide range phenomenologically from cosmology to the laser experiments [155, 157].

- **Vector Portal:** The mediator of the vector portal is generally named as dark photon ( $A'$ ) (also as the U-boson, hidden sector photon, heavy photon, para-photon or secluded photon), which is neutral. The interaction of the standard model fermions, with dark photon is mostly defined via the following term;

$$\mathcal{L} \sim g' q_f \bar{\psi}_f \gamma^\mu \psi_f A'_\mu, \quad (6.10)$$

where  $q_f$  corresponds to the charge of the SM fermions and  $g'$  is the coupling constant of the new interaction. Free parameters of the models are the mass of the gauge boson and the coupling constant which should be determined experimentally.

Many extensions of the interaction of this neutral particle with the SM particles are in the market, in which all can be grouped under the name of dark photon models. Since these models do not require the ultraviolet scale, it is better to search dark photons at the high intensity and low energy facilities as well as at the colliders. Let us first give brief information about the commonly used vector-boson models.

### A) Kinetic Mixing Model

Widely studied model for the dark photon is the possibility of the mixing between the gauge boson of  $U(1)_D$  group with the ordinary photon via the interaction term;

$$\mathcal{L} \sim \frac{-1}{2} \epsilon F^{\mu\nu} F'^{\mu\nu}, \quad (6.11)$$

where  $\epsilon$  is the kinetic mixing parameter. Breaking of the electroweak symmetry leads to the interaction of fermions with the dark photon as;

$$\mathcal{L} \sim \epsilon e \bar{\psi} \gamma^\mu \psi A'_\mu, \quad (6.12)$$

where  $e$  is the electromagnetic charge of fermions.

Depending on the specific model at hand, dark photons are considered as either massive or massless. Massless models imply the existence of millicharged particles [164].

Kinetic mixing model is studied extensively in the literature. One reason is that the model contains only two free parameters (the kinetic mixing parameter  $\epsilon$  as well as the mass of the dark photon  $M'_{A'}$ ) hence, it becomes easy to pin down the signatures for the model.

Dark photons can also interact with the dark fermions,  $\chi$ , which are assumed to be as dark matter candidates. In a simple manner the interaction of the dark photon with the dark fermions can be described similar to QED as;

$$\mathcal{L}_D \sim \sqrt{4\pi\alpha_D} \bar{\chi} \gamma^\mu \chi A'_\mu, \quad (6.13)$$

where  $\alpha_D$  corresponds to the coupling constant of the  $U(1)_D$  gauge group in the secluded sector. It is possible that, this coupling constant is much larger than the kinetic mixing parameter ( $\alpha_D \gg \alpha\epsilon^2$ ). These models are generally named as “*non-minimal kinetic mixing*” models. In this model, the branching ratio of  $A' \rightarrow \chi\chi$  is much larger than the  $A'$  decaying into the SM particles if  $m_{A'} > 2m_\chi$ . Hence, the dark fermions from  $A'$  decay will not be detected and it becomes difficult to observe the effects of  $A'$ . On the other hand, in this scenario it is possible to observe the effects of dark fermions indirectly via the scattering of electrons through  $A - A'$  mixing.

The cross section of the interaction is calculated as in [165];

$$\frac{d\sigma_{e\chi \rightarrow e\chi}}{dT} = \frac{\alpha_D \epsilon^2}{\alpha} \frac{8\pi \alpha^2 m_e (1 - T/E)}{(M_A'^2 + 2m_e T)^2}, \quad (6.14)$$

where  $T$  is the recoil energy of the electron.

There are also many models proposing “-phobic” [166, 167] and “-philic” [168, 169] interactions from the hidden sector to the SM sector to explain the anomalies that the SM lacks to explain.

However, in this thesis, we will concentrate on the  $U(1)_{(B-L)}$  model and modifications for the neutrino-electron scattering will be studied under this model.

### B) $U(1)_{B-L}$ :

Another prevailing model connecting the dark sector with the SM is through  $U(1)$  gauging, like  $U(1)_{B-L}$ , where  $B-L$  corresponds to Baryon - Lepton number. Under this  $B-L$  symmetry, the corresponding  $U(1)_{B-L}$  gauge boson, named as the dark photon,  $A'$  can interact with any SM particle with a non-zero  $B-L$  number at tree level.

In principle, it is also possible to consider both the kinetic mixing with the hypercharge  $U(1)_Y$  and  $B-L$  coupling. The interaction can be defined for this case with the following Lagrangian;

$$\begin{aligned} \mathcal{L} \sim & -\frac{1}{4} B_{\mu\nu}'^2 - \frac{1}{4} F_{\mu\nu}''^2 + \frac{1}{2} \epsilon' B_{\mu\nu}' F''^{\mu\nu} + \frac{1}{2} M_{A'}^2 A_{\mu}''^2 \\ & + g_Y j_B^\mu B_\mu' + g_{B-L} j_{B-L}^\mu A_\mu'', \dots, \end{aligned} \quad (6.15)$$

where  $A_\mu''$  and  $B_\mu'$  corresponds to the  $U(1)_{B-L}$  and  $U(1)_Y$  gauge groups, respectively. The currents for these gauge groups are defined as;

$$\begin{aligned} j_{B-L}^\mu &= (B-L) \bar{f} \gamma^\mu f = -\bar{\ell} \gamma^\mu \ell - \bar{\nu}_\ell \gamma^\mu \nu_\ell + \frac{1}{3} \bar{q} \gamma^\mu q \\ j_B^\mu &= \frac{e}{g_Y} (\cos \theta_W j_{em}^\mu - \sin \theta_W j_Z^\mu). \end{aligned} \quad (6.16)$$

Once the fields are rotated from  $(B_\mu', A_\mu'')$  to  $(B_\mu, A_\mu')$  via the following relations in first order  $\epsilon'$ ,

$$\begin{aligned} B_\mu'' &\simeq B_\mu + \epsilon' A_\mu', \\ A_\mu'' &\simeq A_\mu', \end{aligned} \quad (6.17)$$

we get;

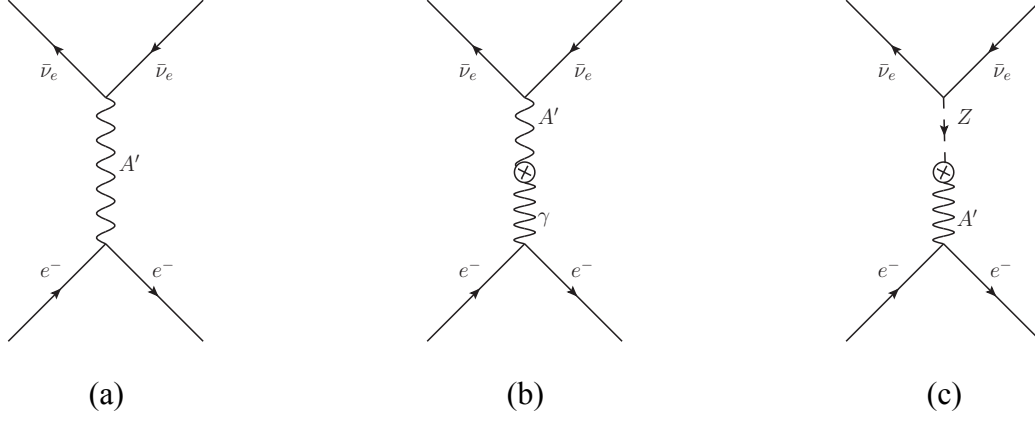


Figure 6.1: Interactions of neutrinos with electron via  $t$  channel dark photon ( $A'$ ) exchange in panel (a). The panels (b) and (c) are for the kinetic mixing between photon-dark photon and  $Z$  boson-dark photon, respectively. (Figure is adapted from [170].)

$$\mathcal{L} = -\frac{1}{4}B_{\mu\nu}^2 - \frac{1}{4}F_{\mu\nu}^{\prime 2} + \frac{1}{2}M_{A'}^2 A_{\mu}^{\prime 2} + g_Y j_B^\mu B_\mu + g_{B-L} j_{B-L}^\mu A'_\mu + e\epsilon j_{\text{em}}^\mu A'_\mu + \dots \quad (6.18)$$

where  $M_{A''} \simeq M_{A'}$  and  $\epsilon \equiv \epsilon' \cos \theta_W$ . The last term in the above equation represents the interaction of the dark photon with the charged matter field with coupling  $e\epsilon$ .

Within this model, in addition to SM contributions as shown in Figure (3.5), the neutrino-electron scattering can take place via

- interchange of dark photon  $A'$
- interchange of  $A'$  that mixes with photon
- interchange of  $A'$  that mixes with  $Z$  boson

as shown in Figure (6.1).

However, for the sake of minimalism, we will only consider the  $U(1)_{B-L}$  model and neglect any kinetic mixing model so that free parameters of the models will turn out to be just the mass of the dark photon  $M'_{A'}$  and the coupling constant  $g_{B-L}$ .



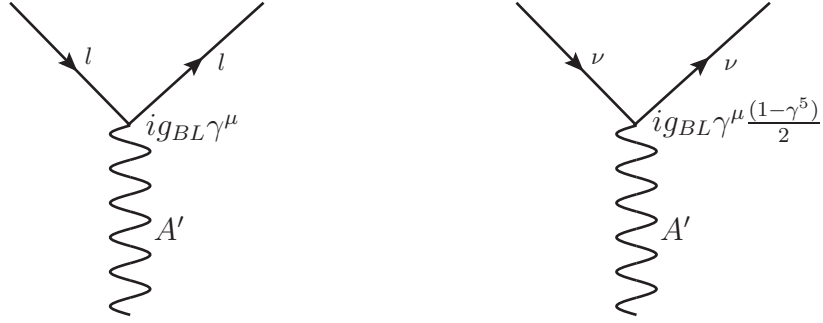


Figure 6.2: The dark photon couples to charged leptons and neutrinos in a different way. The relevant vertex factors are depicted.

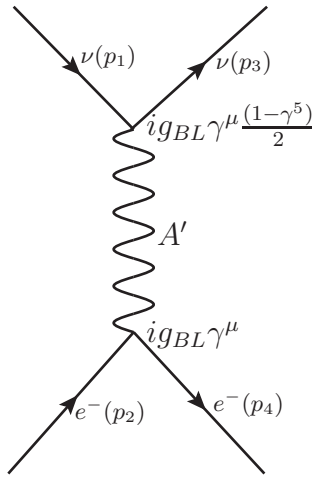


Figure 6.3: The Neutrino electron scattering can also take place via the dark photon exchange in the  $U(1)_{B-L}$  model as well as  $W$  and  $Z$  boson exchanges. The interaction is independent of the neutrino flavors.

## 6.2 The $\nu - e$ Scattering Under the $U(1)_{B-L}$ Symmetry

Interactions of dark photons with neutrinos at tree level is possible under the  $U(1)_{B-L}$  gauge (see Figure (6.2)). The Feynman diagram for the  $\nu - e$  scattering via the dark photon exchange with the relevant vertex factors are depicted in Figure (6.3). Note that the interaction is flavor blind and dark photons couple to all neutrino flavors equally.

The propagator of dark photon (spin-1) for the relevant energies can be taken in Feyn-

man gauge as

$$propagator = \frac{-ig_{\mu\nu}}{q^2 - m_{A'}^2}.$$

By following the Feynman rules, the amplitude for the interaction can be written as;

$$-i\mathcal{M}_{DP} = [\bar{u}(p_3)ig_{BL}\gamma^\mu \frac{(1 - \gamma^5)}{2} u(p_1)] \left( \frac{-ig_{\mu\nu}}{q^2 - m_{A'}^2} \right) [\bar{u}(p_4)ig_{BL}\gamma^\nu u(p_2)] \quad (6.19)$$

where  $q$  is the momentum transfer,  $q = p_1 - p_3 = p_4 - p_2$ .

After simplification the amplitude has the form,

$$\mathcal{M}_{DP} = \frac{g_{BL}^2}{2(m_{A'}^2 - q^2)} [\bar{u}(p_3)\gamma^\mu(1 - \gamma^5)u(p_1)][\bar{u}(p_4)\gamma_\mu u(p_2)]. \quad (6.20)$$

Performing summation over the final particles spin states we obtain

$$\begin{aligned} \sum_{spin} |\mathcal{M}_{DP}|^2 &= \frac{g_{BL}^4}{4(m_{A'}^2 - q^2)^2} \sum_{s_1, s_3} [\bar{u}(p_3)\gamma^\mu(1 - \gamma^5)u(p_1)][\bar{u}(p_3)\gamma^\nu(1 - \gamma^5)u(p_1)]^* \\ &\quad \times \sum_{s_2, s_4} [\bar{u}(p_4)\gamma_\mu u(p_2)][\bar{u}(p_4)\gamma_\nu u(p_2)]^* \end{aligned} \quad (6.21)$$

Once we use the Casimir's trick we can write the amplitude square in terms of traces as follow.

$$\begin{aligned} |\mathcal{M}_{DP}|^2 &= \frac{g_{BL}^4}{4(m_{A'}^2 - q^2)^2} \underbrace{Tr[\gamma^\mu(1 - \gamma^5)(\not{p}_1 + m_\nu)\gamma^\nu(1 - \gamma^5)(\not{p}_3 + m_\nu)]}_I \\ &\quad \times \underbrace{Tr[\gamma_\mu(\not{p}_2 + m_e)\gamma_\nu(\not{p}_4 + m_e)]}_{II} \end{aligned} \quad (6.22)$$

since,  $m_1 = m_3 = m_\nu$  and  $m_2 = m_4 = m_e$ .

Notice that the trace denoted with  $I$  is actually in the form of the trace that we already evaluated for calculating the  $\nu_\mu - e^-$  scattering in Equation (3.56). Once we rewrite that Equation (3.56) we get;

$$\begin{aligned} T_1 &= Tr[\gamma^\mu(c_V^\nu - c_A^\nu\gamma^5)(\not{p}_1 + m_1)(c_V^\nu + c_A^\nu\gamma^5)\gamma^\nu(\not{p}_3 + m_3)] \\ &= Tr[\gamma^\mu(c_V^\nu - c_A^\nu\gamma^5)(\not{p}_1 + m_\nu)\gamma^\nu(c_V^\nu - c_A^\nu\gamma^5)(\not{p}_3 + m_\nu)] \\ &= 4((c_V^\nu)^2 + (c_A^\nu)^2)(p_1^\mu p_3^\nu + p_1^\nu p_3^\mu - (p_1 \cdot p_3)g^{\mu\nu}) - 8c_A^\nu c_V^\nu i\epsilon^{\mu\nu\alpha\beta} p_{1\alpha} p_{3\beta} \\ &\quad + m_1 m_3 ((c_V^\nu)^2 - (c_A^\nu)^2) 4g^{\mu\nu}. \end{aligned} \quad (6.23)$$

Once we take  $c_V^\nu = 1$  and  $c_A^\nu = 1$  in the above equation we recover the trace denoted as  $I$  and hence, it can be evaluated easily as;

$$I = 4 \underbrace{\left( (c_V^\nu)^2 + (c_A^\nu)^2 \right)}_2 (p_1^\mu p_3^\nu + p_1^\nu p_3^\mu - (p_1 \cdot p_3) g^{\mu\nu}) - 8 \underbrace{c_A^\nu c_V^\nu}_1 i \epsilon^{\mu\nu\alpha\beta} p_{1\alpha} p_{3\beta} + m_1 m_3 \underbrace{\left( (c_V^\nu)^2 - (c_A^\nu)^2 \right)}_0 4g^{\mu\nu} \quad (6.24)$$

$$\boxed{I = 8(p_1^\mu p_3^\nu + p_1^\nu p_3^\mu - (p_1 \cdot p_3) g^{\mu\nu} - i \epsilon^{\mu\nu\alpha\beta} p_{1\alpha} p_{3\beta})}.$$

Now let us calculate the second trace that we denoted as  $II$ .

$$\begin{aligned} II &= Tr[\gamma_\mu (\not{p}_2 + m_e) \gamma_\nu (\not{p}_4 + m_e)] \\ &= Tr[\gamma_\mu \not{p}_2 \gamma_\nu (\not{p}_4 + m_e)] + m_e Tr[\gamma_\mu \gamma_\nu \not{p}_4 + m_e] \\ &= Tr[\gamma_\mu \not{p}_2 \gamma_\nu \not{p}_4] + m_e \cancel{Tr[\gamma_\mu \not{p}_2 \gamma_\nu]} + m_e \cancel{Tr[\gamma_\mu \gamma_\nu \not{p}_4]} + m_e^2 Tr[\gamma_\mu \gamma_\nu] \end{aligned} \quad (6.25)$$

where the canceled terms are due to the trace of odd number gamma matrix multiplication. Then the above equation turns out to be,

$$\begin{aligned} II &= Tr[\gamma_\mu \not{p}_2 \gamma_\nu \not{p}_4] + m_e^2 Tr[\gamma_\mu \gamma_\nu] \\ &= 4 \underbrace{[p_{2\mu} p_{4\nu} + p_{4\mu} p_{2\nu} - (p_2 \cdot p_4) g_{\mu\nu}]}_{Tr[\gamma_\mu \not{p}_2 \gamma_\nu \not{p}_4]} + m_e^2 \underbrace{4g_{\mu\nu}}_{Tr[\gamma_\mu \gamma_\nu]} \end{aligned} \quad (6.26)$$

$$\boxed{II = 4[p_{2\mu} p_{4\nu} + p_{4\mu} p_{2\nu} - (p_2 \cdot p_4) g_{\mu\nu} + m_e^2 g_{\mu\nu}]}.$$

Having evaluated the relevant traces, let us contract those two terms.

$$\begin{aligned} I \cdot II &= 32 [p_1^\mu p_3^\nu + p_1^\nu p_3^\mu - (p_1 \cdot p_3) g^{\mu\nu} - i \epsilon^{\mu\nu\alpha\beta} p_{1\alpha} p_{3\beta}] \\ &\quad \times [p_{2\mu} p_{4\nu} + p_{4\mu} p_{2\nu} - (p_2 \cdot p_4) g_{\mu\nu} + m_e^2 g_{\mu\nu}] \\ &= 32 \underbrace{[p_1^\mu p_3^\nu (p_{2\mu} p_{4\nu} + p_{4\mu} p_{2\nu} - (p_2 \cdot p_4) g_{\mu\nu} + m_e^2 g_{\mu\nu})]}_{A_1} \\ &\quad + \underbrace{p_3^\mu p_1^\nu (p_{2\mu} p_{4\nu} + p_{4\mu} p_{2\nu} - (p_2 \cdot p_4) g_{\mu\nu} + m_e^2 g_{\mu\nu})}_{A_2} \\ &\quad - \underbrace{(p_1 \cdot p_3) g^{\mu\nu} (p_{2\mu} p_{4\nu} + p_{4\mu} p_{2\nu} - (p_2 \cdot p_4) g_{\mu\nu} + m_e^2 g_{\mu\nu})}_{A_3} \\ &\quad - \underbrace{i \epsilon^{\mu\nu\alpha\beta} p_{1\alpha} p_{3\beta} (p_{2\mu} p_{4\nu} + p_{4\mu} p_{2\nu} - (p_2 \cdot p_4) g_{\mu\nu} + m_e^2 g_{\mu\nu})}_{A_4} \end{aligned} \quad (6.27)$$

Hence, with this notation we can write

$$I \cdot II = 32(A_1 + A_2 + A_3 + A_4). \quad (6.28)$$

Let us evaluate each term one by one via contracting the terms.

$$\begin{aligned}
A_1 &= (p_1 \cdot p_2)(p_3 \cdot p_4) + (p_1 \cdot p_4)(p_2 \cdot p_3) - (p_1 \cdot p_3)(p_2 \cdot p_4) + m_e^2(p_1 \cdot p_3) \\
A_2 &= (p_1 \cdot p_4)(p_2 \cdot p_3) + (p_1 \cdot p_2)(p_3 \cdot p_4) - (p_1 \cdot p_3)(p_2 \cdot p_4) + m_e^2(p_1 \cdot p_3) \\
A_3 &= -((p_1 \cdot p_3)(p_2 \cdot p_4) + (p_1 \cdot p_3)(p_2 \cdot p_4) - 4(p_1 \cdot p_3)(p_2 \cdot p_4) + 4m_e^2(p_1 \cdot p_3)) \\
&= 2(p_1 \cdot p_3)(p_2 \cdot p_4) - 4m_e^2(p_1 \cdot p_3) \\
A_4 &= -ip_{1\alpha}p_{3\beta} \left( \underbrace{\epsilon^{\mu\nu\alpha\beta}}_{AS(\mu,\nu)} \underbrace{(p_{2\mu}p_{4\nu} + p_{4\mu}p_{2\nu})}_{S(\mu,\nu)} - \underbrace{\epsilon^{\mu\nu\alpha\beta}}_{AS} \underbrace{g_{\mu\nu}}_S (p_2 \cdot p_4) + \underbrace{\epsilon^{\mu\nu\alpha\beta}}_{AS} \underbrace{g_{\mu\nu}}_S m_e^2 \right) \\
&= 0
\end{aligned} \tag{6.29}$$

in which multiplication of symmetric and anti-symmetric tensors cancels.

Once we add them together we get;

$$A_1 + A_2 + A_3 + A_4 = 2[(p_1 \cdot p_2)(p_3 \cdot p_4) + (p_1 \cdot p_4)(p_2 \cdot p_3) - m_e^2(p_1 \cdot p_3)] . \tag{6.30}$$

Hence we can write,

$$I \cdot II = 64[(p_1 \cdot p_2)(p_3 \cdot p_4) + (p_1 \cdot p_4)(p_2 \cdot p_3) - m_e^2(p_1 \cdot p_3)] . \tag{6.31}$$

When we put this result into Equation (6.22) and average over the initial spin states we get

$$\begin{aligned}
\langle |\mathcal{M}_{DP}|_{\nu-e^-}^2 \rangle &= \frac{1}{2} \frac{g_{BL}^4}{4(m_{A'}^2 - q^2)^2} \\
&\times 64[(p_1 \cdot p_2)(p_3 \cdot p_4) + (p_1 \cdot p_4)(p_2 \cdot p_3) - m_e^2(p_1 \cdot p_3)] .
\end{aligned} \tag{6.32}$$

Note that, once we average over initial spin states the factor equals to 2, due to helicity states of neutrinos.

In Appendix B, we already showed that in the rest frame of the electron, the following scalar products of the four-dimensional momentums can be written in terms of the recoil energy as

$$\boxed{
\begin{aligned}
p_1 \cdot p_2 &= p_3 \cdot p_4 = E_1 m_e , \\
p_1 \cdot p_3 &= m_\nu^2 + m_e T , \\
(p_1 \cdot p_4)(p_2 \cdot p_3) &= m_e^2 (E_1 - T)^2 ,
\end{aligned}
} \tag{6.33}$$

where  $T$  is the recoil energy of the electron. Moreover, the differential cross-section with respect to the recoil energy is found in Chapter 3 as; (See Equation (3.109).)

$$\frac{d\sigma}{dT} = \frac{|\mathcal{M}_{DP}|^2}{32\pi m_e |p_1|^2}. \quad (6.34)$$

Let us evaluate the amplitude square in terms of the incoming energy of neutrino and the recoil energy of the electron first. Once we denote the scalar product terms in Equation (6.32) as  $B$ , using Equation (6.33) we get,

$$\begin{aligned} B &= [(p_1 \cdot p_2)(p_3 \cdot p_4) + (p_1 \cdot p_4)(p_2 \cdot p_3) - m_e^2(p_1 \cdot p_3)] \\ &= m_e^2 E_1^2 + m_e^2 (E_1 - T)^2 - m_e^2 (m_\nu^2 + m_e T) \\ &= m_e^2 [E_1^2 + (E_1 - T)^2 - (m_\nu^2 + m_e T)] \\ &= m_e^2 [E_1^2 + E_1^2 + T^2 - 2TE_1 - m_e T - m_\nu^2] \\ &= m_e^2 [2E_1^2 - 2TE_1 + T^2 - m_e T - m_\nu^2]. \end{aligned} \quad (6.35)$$

Moreover, we need to write the momentum transfer  $q$  in terms of the recoil energy as well. Since  $q = p_1 - p_3 = p_4 - p_2$  we get

$$\begin{aligned} q^2 &= (p_4 - p_2)^2 = \underbrace{p_4^2}_{m_e^2} + \underbrace{p_2^2}_{m_e^2} - 2 \underbrace{p_2 \cdot p_4}_{m_e E_4} \\ &= 2m_e^2 - 2m_e \underbrace{E_4}_{T+m_e} \\ &= \cancel{2m_e^2} - 2m_e T - \cancel{2m_e^2} \\ &= -2m_e T. \end{aligned} \quad (6.36)$$

With these results at hand, we can write the amplitude square in terms of the incoming neutrino energy ( $E_1 = E_\nu$ ) and the recoil energy of electron,  $T$ ,

$$\langle |\mathcal{M}_{DP \rightarrow \nu - e^-}|^2 \rangle = \frac{8g_{BL}^4}{(m_{A'}^2 + 2m_e T)^2} m_e^2 [2E_\nu^2 - 2TE_\nu + T^2 - m_e T + m_\nu^2 (1 - \frac{T}{m_e})]. \quad (6.37)$$

Using Equation (6.34), the differential cross-section turns out to be equal to

$$\frac{d\sigma}{dT} = \frac{1}{4\pi} \frac{g_{BL}^4}{(m_{A'}^2 + 2m_e T)^2} \frac{m_e}{(E_\nu^2 - m_\nu^2)} [2E_\nu^2 - 2TE_\nu + T^2 - m_e T - m_\nu^2]. \quad (6.38)$$

On the other hand once we neglect the mass of neutrino, then,  $|p_1| = E_1$  and we get;

$$\left( \frac{d\sigma}{dT} \right)_{DP} = \frac{1}{4\pi} \frac{g_{BL}^4}{(m_{A'}^2 + 2m_e T)^2} \frac{m_e}{E_\nu^2} [2E_\nu^2 - 2TE_\nu + T^2 - m_e T]. \quad (6.39)$$

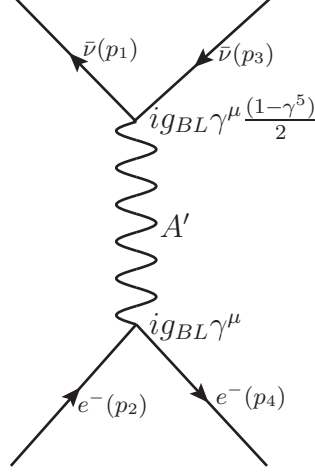


Figure 6.4: The anti-neutrino electron scattering diagram via dark photon exchange.

Thus, we have calculated the differential cross-section due to the pure dark photon exchange. Let us now elaborate the same situation for the anti-neutrino electron scattering.

### 6.3 The $\bar{\nu} - e$ Scattering Under the $U(1)_{B-L}$ Symmetry

Feynman diagram for the interaction of the  $\bar{\nu} - e^-$  scattering via the dark photon exchange is depicted in Figure (6.4). We can write the amplitude for this diagram as

$$\begin{aligned}
 -i\mathcal{M}_{DP} &= [\bar{\nu}(p_1)ig_{BL}\gamma^\mu\frac{(1-\gamma^5)}{2}\nu(p_3)]\left(\frac{-ig_{\mu\nu}}{q^2-m_{A'}^2}\right)[\bar{u}(p_4)ig_{BL}\gamma^\nu u(p_2)] \\
 \mathcal{M}_{DP_{\bar{\nu}-e^-}} &= \frac{g_{BL}^2}{2(m_{A'}^2-q^2)}[\bar{\nu}(p_1)\gamma^\mu\nu(p_3)][\bar{u}(p_4)\gamma_\mu u(p_2)].
 \end{aligned} \tag{6.40}$$

Since  $\nu(p_1) = u(-p_1)$ , we can write the amplitude above as;

$$\mathcal{M}_{DP\rightarrow\bar{\nu}-e} = \frac{g_{BL}^2}{2(m_{A'}^2-q^2)}[\bar{u}(-p_1)\gamma^\mu u(-p_3)][\bar{u}(p_4)\gamma_\mu u(p_2)]. \tag{6.41}$$

When we compare the Equation (6.41) with Equation (6.20) we realize that once we replace  $p_3 \leftrightarrow -p_1$  and  $p_1 \leftrightarrow -p_3$  in Equation (6.20), we obtain the amplitude for the  $\bar{\nu} - e$  scattering.

Remember the amplitude square we get for the  $\nu - e$  scattering (Equation (6.32))

$$\begin{aligned} \langle |\mathcal{M}_{DP}|_{\nu-e}^2 \rangle &= \frac{1}{2} \frac{g_{BL}^4}{4(m_{A'}^2 - q^2)^2} \\ &\times 64 [(p_1 \cdot p_2)(p_3 \cdot p_4) + (p_1 \cdot p_4)(p_2 \cdot p_3) - m_e^2(p_1 \cdot p_3)] . \end{aligned} \quad (6.42)$$

Hence, without doing lengthy calculations once we do the replacements we directly get,

$$\begin{aligned} \langle |\mathcal{M}_{DP}|_{\bar{\nu}-e^-}^2 \rangle &= \frac{1}{2} \frac{g_{BL}^4}{4(m_{A'}^2 - q^2)^2} \\ &64 [((-p_3) \cdot p_2)((-p_1) \cdot p_4) + ((-p_3) \cdot p_4)(p_2 \cdot (-p_1)) \\ &\quad - m_e^2((-p_3) \cdot (-p_1))] , \end{aligned} \quad (6.43)$$

$$\begin{aligned} \langle |\mathcal{M}_{DP}|_{\bar{\nu}-e^-}^2 \rangle &= \frac{1}{2} \frac{g_{BL}^4}{4(m_{A'}^2 - q^2)^2} \\ &64 [(p_3 \cdot p_2)(p_1 \cdot p_4) + (p_3 \cdot p_4)(p_2 \cdot p_1) - m_e^2(p_3 \cdot p_1)] . \end{aligned}$$

Thus, we found out that the amplitude square for pure DP contribution is the same for both neutrino and anti-neutrino scattering and so is the differential cross-section.

Note that even though the amplitude square is same for the neutrino and anti-neutrino scattering, the interference terms would be different since the SM contributions are different for the neutrino and anti-neutrino as we derived in Chapter 3.

## 6.4 Interference of Dark Photon and Standard Model Diagrams

The interference of SM diagrams with the dark photon exchange cannot be neglected and must have been taken into account. For instance, for the  $\nu_e - e^-$  scattering we need to evaluate the three diagrams via  $W$ ,  $Z$  and  $A'$  exchange as shown in Figure (6.5) and the amplitude square takes the form,

$$\begin{aligned} |\mathcal{M}_{\nu_e-e^-}|^2 &= |\mathcal{M}_W + \mathcal{M}_Z + \mathcal{M}_{A'}|^2 \\ &= \underbrace{|\mathcal{M}_W|^2 + |\mathcal{M}_Z|^2 + 2|\mathcal{M}_W||\mathcal{M}_Z|}_{\text{SM}} \\ &\quad + \underbrace{|\mathcal{M}_{A'}|^2}_{\text{Pure DP}} + \underbrace{2|\mathcal{M}_W||\mathcal{M}_{A'}| + 2|\mathcal{M}_Z||\mathcal{M}_{A'}|}_{\text{Interference}} . \end{aligned} \quad (6.44)$$

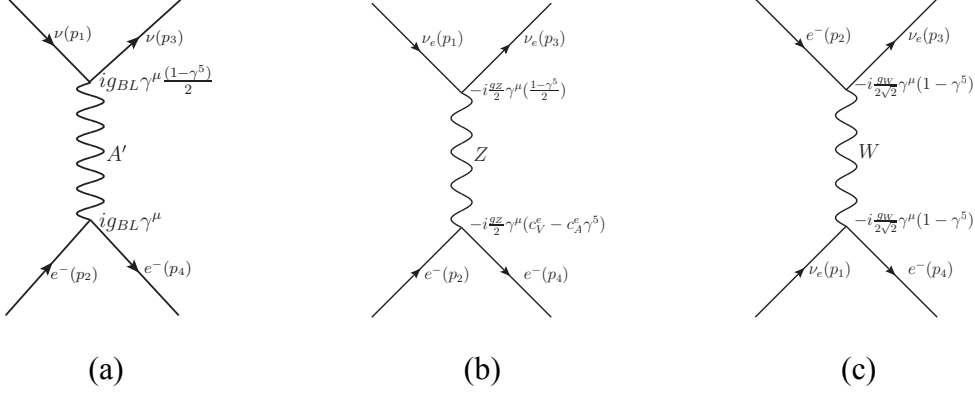


Figure 6.5: The  $\nu - e^-$  scattering takes place via the exchange of W and Z boson as well as the dark photon contribution. To calculate the interference term, all these diagrams must be considered. On the other hand for the  $\nu_\mu - e^-$  scattering one just needs to consider the diagram shown in panel (a) and (b) since W exchange is not allowed.

On the other hand, for the  $\nu_\mu - e^-$  scattering there are only two diagrams ( $Z, A'$ ) since the charge current interaction does not take place in this case and we can write,

$$\begin{aligned}
 |\mathcal{M}_{\nu_\mu - e^-}|^2 &= |\mathcal{M}_Z + \mathcal{M}_{A'}|^2 \\
 &= \underbrace{|\mathcal{M}_Z|^2}_{\text{SM}} + \underbrace{|\mathcal{M}_{A'}|^2}_{\text{Pure DP}} + \underbrace{2|\mathcal{M}_Z||\mathcal{M}_{A'}|}_{\text{Interference}}
 \end{aligned} \tag{6.45}$$

Instead of doing lengthy calculations by hand, CalcHEP package [171] with its Mathematica output is used for the evaluation of the interference terms. Moreover, the pure DP contributions as well as the SM ones calculated by hand are checked with CalcHEP also. The relevant CalcHEP model file and Mathematica files are presented in Appendix E. We obtained the following results for the interference terms.

$$\begin{aligned}
 \frac{d\sigma_{\text{INT}}(\nu_e e^-)}{dT} &= \frac{g_{B-L}^2 G_F m_e}{2\sqrt{2} E_\nu^2 \pi (M_{A'}^2 + 2mT)} \left( 2E_\nu^2 - m_e T + \beta \right), \\
 \frac{d\sigma_{\text{INT}}(\bar{\nu}_e e^-)}{dT} &= \frac{g_{B-L}^2 G_F m_e}{2\sqrt{2} E_\nu^2 \pi (M_{A'}^2 + 2mT)} \left( 2E_\nu^2 + 2T^2 - T(4E_\nu + m_e) + \beta \right), \\
 \frac{d\sigma_{\text{INT}}(\nu_\alpha e^-)}{dT} &= \frac{g_{B-L}^2 G_F m_e}{2\sqrt{2} E_\nu^2 \pi (M_{A'}^2 + 2mT)} \left( -2E_\nu^2 + m_e T + \beta \right), \\
 \frac{d\sigma_{\text{INT}}(\bar{\nu}_\alpha e^-)}{dT} &= \frac{g_{B-L}^2 G_F m_e}{2\sqrt{2} E_\nu^2 \pi (M_{A'}^2 + 2mT)} \left( -2E_\nu^2 - 2T^2 + T(4E_\nu + m_e) + \beta \right)
 \end{aligned} \tag{6.46}$$



where the parameter  $\beta$  is defined as

$$\beta = \sin^2\theta_w(8E_\nu^2 - 8E_\nu T - 4m_e T + 4T^2)$$

and the index  $\alpha$  corresponds to either muon or tau. Note that, mass of the neutrinos are neglected in these results and neutrinos we consider are Dirac-type neutrinos.

Remember that the pure dark photon contribution we derived is the same for all neutrino flavors.

$$\left[\frac{d\sigma}{dT}(\nu e^- \rightarrow \nu e^-)\right]_{DP} = \frac{g_{B-L}^4 m_e}{4\pi E_\nu^2 (M_{A'}^2 + 2m_e T)^2} (2E_\nu^2 + T^2 - 2TE_\nu - m_e T). \quad (6.47)$$

Hence the total cross section can be described as a sum of the pure DP and the SM contribution as well as the interference terms as,

$$\left[\frac{d\sigma}{dT}\right] = \left[\frac{d\sigma}{dT}\right]_{SM} + \left[\frac{d\sigma}{dT}\right]_{DP} + \left[\frac{d\sigma}{dT}\right]_{INT}. \quad (6.48)$$

## 6.5 Analysis & Results

We derived the differential cross-sections for pure DP contribution as well as the interference terms between the SM and DP diagrams in the previous section. The free parameters of the  $U(1)_{B-L}$  model are the mass of the new gauge boson ( $m_{A'}$ ) and the coupling constant ( $g_{B-L}$ ). It is important to decide the neutrino experiments that we are going to use to constrain the DP parameters wisely so that stringent bounds could be obtained. For this purpose, the differential cross-section of the DP contribution (Equation (6.47)) should be analyzed carefully.

The denominator term,  $(m_{A'}^2 + 2m_e T)^2$  in Equation (6.47) implies that as the recoil energy decreases, then, the cross-section increases unless  $m_{A'}^2 \gg 2m_e T$ . For  $T \gg m_{A'}^2$ , the dependency of  $m_{A'}$  is lost. Hence, we infer that, depending on the mass region of  $A'$ , we expect that the low recoil energy experiments as GEMMA and TEXONO would give stringent bounds for  $g_{B-L}$ . On the other hand, if  $E_\nu$  increases, then the analysis threshold for the recoil energy also increases since the background becomes large and it is difficult to discriminate the signal. In that case, the mass region of  $m_{A'}^2$  being close to the recoil energy, ( $\sim m_e T$ ), would be sensitive to determine  $g_{B-L}$ . Hence, by just looking the form of the pure DP contribution, we infer that either low

Table 6.2: The key parameters of the TEXONO, LSND, CHARM II, BOREXINO and GEMMA experiments on the  $\nu - e$  scattering is shown. (Table is adapted from [170].)

Experiment	Type of neutrino	$\langle E_\nu \rangle$	$T$	Measured $\sin^2\theta_W$
TEXONO-NPCGe [71]	$\bar{\nu}_e$	1–2 MeV	0.35–12 keV	–
TEXONO-HPGe [68, 69]	$\bar{\nu}_e$	1–2 MeV	12–60 keV	–
TEXONO-CsI(Tl) [62]	$\bar{\nu}_e$	1–2 MeV	3–8 MeV	$0.251 \pm 0.039$
LSND [81]	$\nu_e$	36 MeV	18–50 MeV	$0.248 \pm 0.051$
BOREXINO [93]	$\nu_e$	862 keV	270–665 keV	–
GEMMA [172]	$\bar{\nu}_e$	1–2 MeV	3–25 keV	–
CHARM II [114, 85]	$\nu_\mu$	23.7 GeV	3–24 GeV	} $0.2324 \pm 0.0083$
	$\bar{\nu}_\mu$	19.1 GeV	3–24 GeV	

recoil energy or neutrinos with high incoming energy experiments would be sensitive to different range of  $m_{A'}$ .

Moreover, in order to observe how the differential cross-section varies with respect to the recoil energy, we plot  $\frac{d\sigma}{dT}$  vs  $T$  diagram at a fixed value of  $g_{B-L}$  and for various  $m_{A'}$  values as demonstrated in Figure (6.6). From this figure we deduce that, as the recoil energy is lowered, the point where the curve starts being flat also shifts to the lower  $T$  values especially for smaller  $m_{A'}$  which implies that for searching low  $m_{A'}$  region, low recoil energies should be analyzed.

Furthermore, it is important to note that since there is not any theoretical constraint on the mass of  $m_{A'}$ , it can take any value. Having not been observed at LHC so far, the searches should favor low mass regions for  $A'$  and with this figure plotted we infer that low recoil energies would have much sensitivity for the low mass values of  $m_{A'}$ .

Having the comments mentioned in the previous paragraph in mind, we preferred to search the DP parameters in several  $\nu - e^-$  experiments whose key parameters are summarized in Table 6.2<sup>1</sup>.

The analysis methods are the same with the ones we used for the non-commutative space search in Chapter 5. However, note that different from the NC-space search, in the dark photon case we have two free parameters. Thus, to constrain the free

<sup>1</sup> For more information about the experiments see Chapter 4.

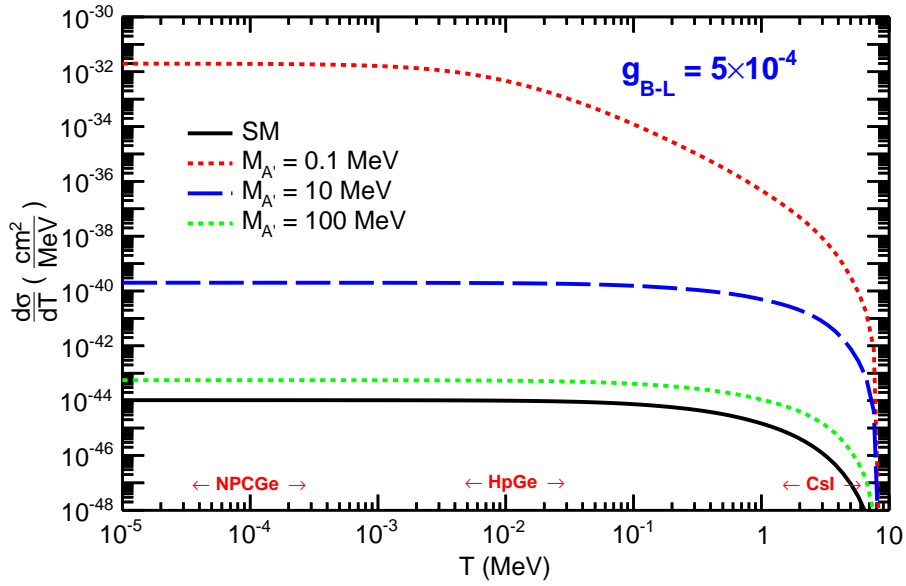


Figure 6.6: The differential cross-section spectrum is shown for various  $M_{A'}$  at a fixed arbitrarily chosen  $g_{B-L}$  over the recoil energy for the TEXONO experiment. For this plot, the neutrino flux is normalized to 1. (Figure is adapted from [170].)

parameters via the  $\nu - e^-$  scattering experiments, we applied the following method. Choosing the  $m_{A'}$  in range keV to 10 GeV, we calculated the cross-section for several values of  $m_{A'}$  in terms of  $g_{B-L}$ . Hence, comparing data with the dark photon as well as the SM predictions bounds are found for  $g_{B-L}$  at 90% CL. Finally, the obtained bounds are shown in the  $g_{B-L}$  vs  $m_{A'}$  plane. In Figure (6.7), for an arbitrary  $m_{A'}$  value the acquired fit for the parameter  $g_{B-L}$  is shown as an example for CsI and HPGe data sets of TEXONO.

Once we realized that each experiment has its own sensitive region for  $m_{A'}$ , we decided to analyze many  $\nu - e$  experiments in favor of the DP. In addition to the neutrino experiments that we used for the NC-space search, we analyzed NPCGe data of TEXONO as well as BOREXINO.

For the TEXONO data,  $\chi^2$  fit is applied as before using Equation (5.192) where  $X$  corresponds to the DP interaction in this case. For the TEXONO-NPCGe analysis, the data used is depicted in Figure (4.11). Similar to TEXONO Experiment, GEMMA collaboration also searched the magnetic moment of neutrinos via data collected over the recoil recoil energies as shown in Figure (4.13). Once similar  $\chi^2$  analysis applied

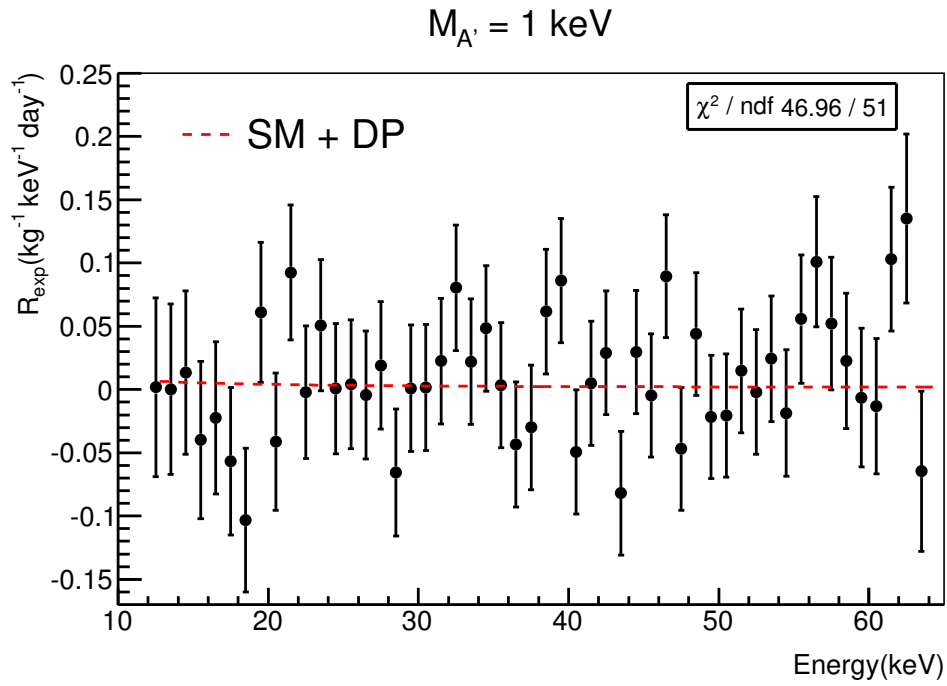
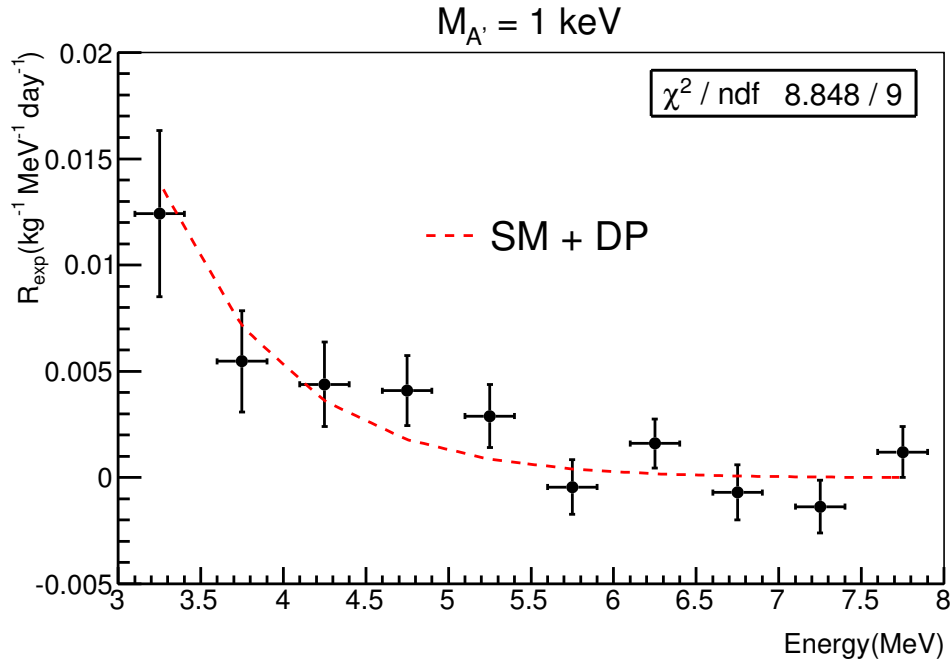


Figure 6.7: TEXONO-CsI and TEXONO-HPGe data is fitted for a fixed value of  $m_{A'} = 1 \text{ keV}$  and bounds are set for  $g_{B-L}$ . This procedure is conducted over the  $A'$  mass-range, keV to 10 GeV, so that the bounds are obtained in  $m_{A'} - g_{B-L}$  plane.

for the data of GEMMA experiment, lower bounds can be acquired in the  $g_{B-L}-m_{A'}$  plane. On the other hand, BOREXINO collaboration announced that they measured the cross-section for the  $\nu_e - e$  scattering in terms of counts/(day.100 ton) as;

$$R = 46.0 \pm 1.5(stat) + 1.5(syst) \text{ counts}/(\text{day}.100 \text{ ton}) .$$

Note that the incoming energy of neutrino is  $E_\nu = 862 \text{ keV}$  (see Chapter 4 for details). Using the relevant cross-section formulas; the SM prediction is calculated via using Equation (3.116) and the DP contribution is calculated via Equation (6.47) as well as the interference term using Equation (6.46), the expected events are calculated in terms of counts/(day 100 ton) for various  $m_{A'}$  values and bounds at 90% CL for  $g_{B-L}$  is acquired from BOREXINO data.

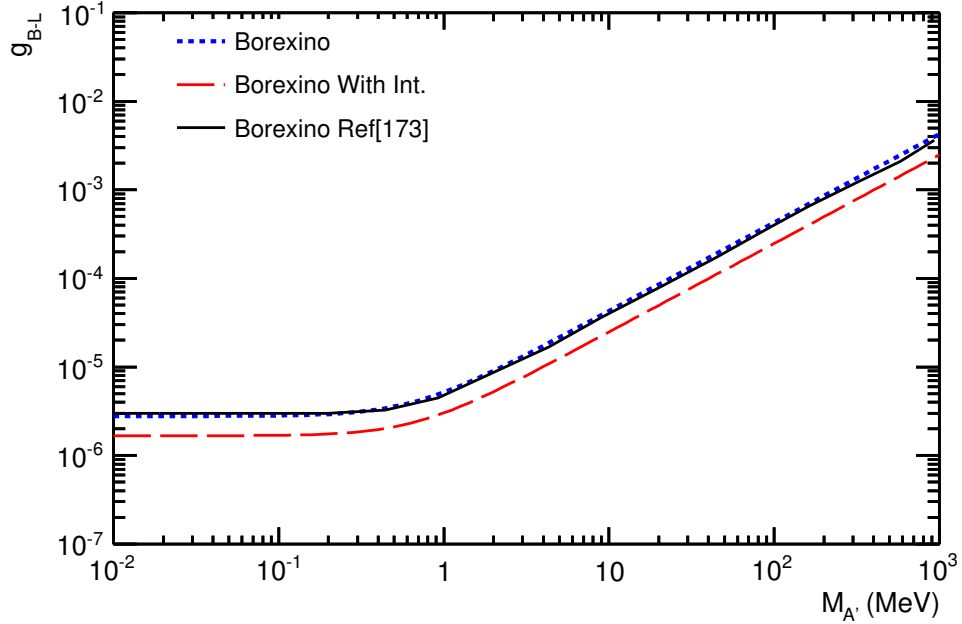


Figure 6.8: Bounds acquired from Borexino data for the DP parameters are shown in the  $m_{A'} - g_{B-L}$  plane by taking into account and neglecting the interference terms. The bounds from [173] is also shown for comparison.

Note that, even though the GEMMA and BOREXINO data were already analyzed in [173] where only pure DP interaction is considered, we reanalyzed the data by taking into account the interference effects. Our bounds from BOREXINO experiment is depicted in Figure (6.8) by showing the situation for with and without taking into

account the interference terms. Moreover, the bounds from the reference [173] are overlaid on our results for cross-check. With this plot, we conclude that the interference terms can not be neglected and bounds are affected. The role of the interference term is discussed in detail for each experiment in the following section.

### 6.5.1 Roles of Interference Terms

As we have seen from the results of BOREXINO, the interference effects have to be taken into account. Since the interference is neglected in the literature, to emphasize the role of interference on the DP terms, we decided to find the bounds on the  $g_{B-L} - m_{A'}$  plane with and without including the interference terms for each neutrino experiments that we analyzed. The bounds are shown in Figure (6.9).

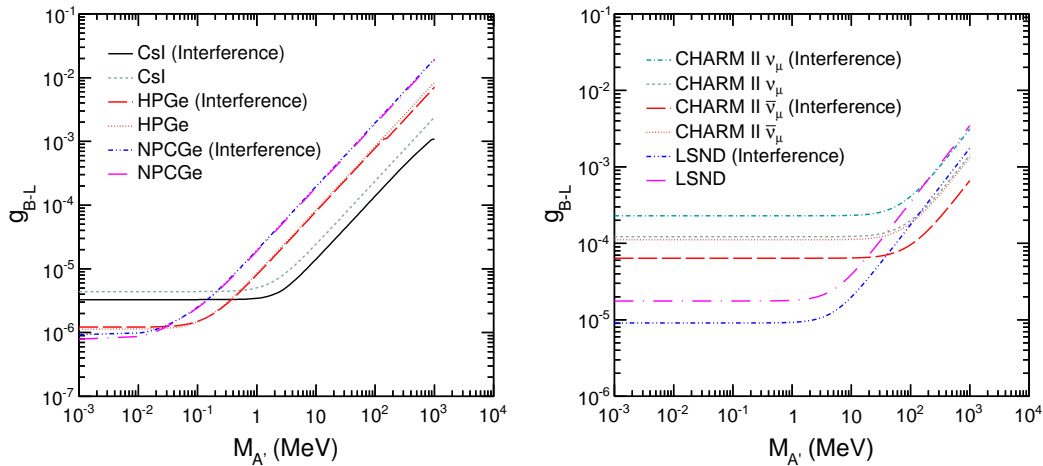


Figure 6.9: The 90% CL exclusion limits in the  $g_{B-L} - M_{A'}$  plane for various TEXONO experiments (left) and for the LSND and CHARM II experiments (right) are depicted. The results with and without the interference contributions are shown for highlighting its significance. (Figure is adapted from [170].)

We realize from Figure (6.9) that for low recoil energies the interference effects are negligible (HPGe, NPCGe) on the other hand if the recoil energies are in the range of MeV or higher then the interference effects are sizable. In fact, the reason for interference being negligible is not related with the dark photon, but related with the sensitivity of measurements. For low recoil energies, the errors are huge and there is

much room for new physics so that interference can be neglected. On the other hand, as the energy of neutrinos increase, the sensitivity of experiments enhance as well and errors become smaller and then there becomes less room for new physics. In this case, addition of the interference term is expected to alter the bounds. Thus we should not expect any difference of the bounds for the GEMMA results whether we considered interference or not. Hence we did not show that result on Figure (6.9) for clarity.

Moreover, from Figure (6.9) we also deduce that the bounds become more strict once we consider the interference effect for CsI, LSND, BOREXINO as well as CHARM II ( $\nu_\mu$ ). On the other hand the bounds are loosened for CHARM II ( $\bar{\nu}_\mu$ ). The reason is related to whether the interference term is constructive or destructive. We found out that, apart from the CHARM II ( $\bar{\nu}_\mu$ ) case, the interference is always constructive. To observe that, we can write the following limiting expressions for the interference term from Equation (6.46),

$$\begin{aligned}\frac{d\sigma_{INT}(\nu_\alpha e^-)}{dT} &\sim T(T - 2E_\nu), \\ \frac{d\sigma_{INT}(\bar{\nu}_\alpha e^-)}{dT} &\sim -T(T - 2E_\nu),\end{aligned}\tag{6.49}$$

once we take  $\sin^2\theta_W \simeq 1/4$ .

In general,  $T/2 < E_{\nu_{min}}$  and we deduce that while the interference is destructive for  $\bar{\nu}_\mu$ , it is constructive for the  $\nu_\mu$  scattering.

Having mentioned the importance of the interference terms, in Figure (6.10) we show the bounds that we obtained from all the neutrino experiments that we analyzed (with interference effects included). We found out that each neutrino experiment gives the best sensitivity for distinct part of  $m_{A'}$  regions. For instance, for  $m_{A'} \lesssim 0.1$  MeV GEMMA has better limits. On the other hand, for  $0.1 \lesssim m_{A'} \lesssim 100$  MeV, TEXONO (CsI) data leads to more stringent bounds. Moreover, CHARM II data has better limits for  $m_{A'} \gtrsim 100$  MeV among the neutrino experiments we analyzed. Note that the bounds from GEMMA collaboration is adapted from [173]. Even though the interference effects have not taken into account, we showed that the interference effect is negligible for GEMMA as well as TEXONO (HPGe and NPCGe).

One can understand the behavior of the exclusion curve clearly once we focus on the term  $(m_{A'}^2 + 2m_e T)^{-2}$  in Equation (6.39). If  $m_{A'} \ll T$  then,  $(m_{A'}^2 + 2m_e T)^{-2} \sim$

$1/T^2$  then the cross section becomes independent of  $m_{A'}$  hence, this explains the flat region in the exclusion curve (Figure (6.10)). Thus, we infer that since the current reach of the recoil energies are around keV range, the dark photon mass below keV range would not be possible to be resolved. In a similar manner, we can analyze the situation for the accelerator neutrinos. Once the incoming energy of neutrinos becomes high then even the analysis range for the recoil energy increases since the background increases (see Table 6.2). Hence, the accelerator neutrino experiments would not be as sensitive as to the dark photon mass smaller than 10 MeV.

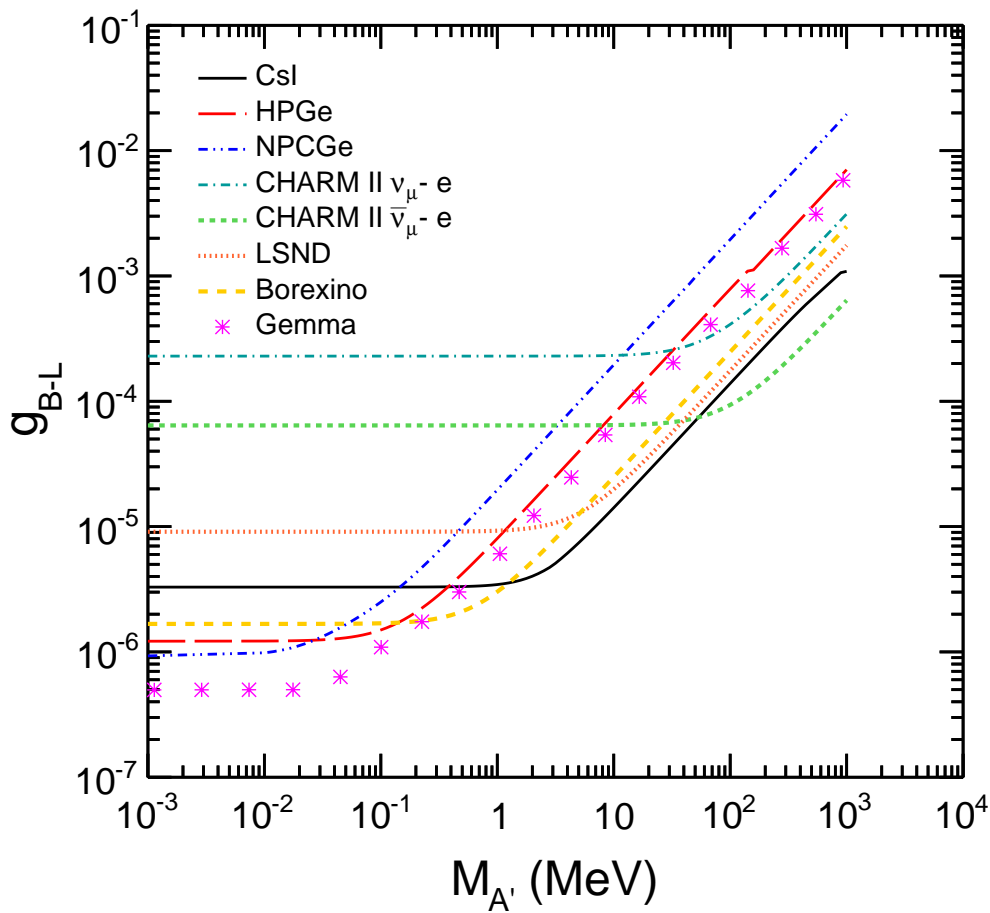


Figure 6.10: The 90% C.L. exclusion limits of the gauge coupling constant  $g_{B-L}$  of the  $U(1)_{B-L}$  group as a function of the dark photon mass  $M_{A'}$  by including the interference effects. The regions above the curves are excluded. (Figure is adapted from [170].)



## 6.5.2 Dark Photon Bounds in the Literature

Having showed the exclusion plot at 90% C.L. that we derived from the neutrino-electron scattering experiments, for completeness and also for comparing our results with the ones in the literature, we will summarize the phenomenological studies for the dark photons in the literature mostly by referring to the reviews on the dark photons published [155, 157, 174, 175].

Before we proceed further, it is important to mention that in the literature the bounds are generally given in the kinetic mixing model, hence in the  $m_{A'} - \epsilon$  plane. (Note that in the literature, instead of  $\epsilon$  and  $A'$ ,  $\xi$  and  $\gamma'$  is also used as a symbol to denote the same parameter.) However, using the relation;  $\epsilon \rightarrow \frac{B-L(f)}{Q_f} g_{B-L}$ , it is possible to convert the bounds in terms of  $g_{B-L}$ . However, note that this relation is valid unless the bounds are obtained by using the decay modes of the dark photons. To convert the parameters for decay channels of  $A'$  into fermions, one needs to have an additional factor as  $(\frac{BR(A' \xrightarrow{B-L} f\bar{f})}{BR(A' \xrightarrow{\epsilon} f\bar{f})})^{1/2}$  [170].

Since the free parameters of the model, the mass of the dark photon ( $M_{A'}$ ) and the coupling constant ( $g_{B-L}$ ) (or  $\epsilon$  in the kinetic-mixing model), can take any value, the philosophy of new physics searches relies on the motto “to reach the knowledge of what something is, one needs to identify what it is not first”. For this reason, the dark photon searches have been going on in a wide range of experiments to constrain the free parameters of the model. In general, it is possible to categorize these searches into two; for  $m_{A'} > 2m_e$  and  $m_{A'} < 2m_e$ .

Hypothesizing that the dark photon is the lightest particle of the hidden sector with  $m_{A'} > 2m_e$ , then it is natural to expect that  $A'$  decaying into the SM particles at least into the electron positron pair. Depending on the dark photon mass, the signatures can be tracked in the dimuon channel (for  $M_{A'} > 2m_\mu$ ) or into hadrons as well (for at least  $M_{A'} > 2m_\pi$ ).

One of the exciting motivation for the dark photon is that for the specific parameter region  $m_{A'} - \epsilon$ , it could be a solution to the muon magnetic moment anomaly [176]. Especially searching for that specific parameter space has a crucial role for dark photon studies (see the discussion at the end of the section for the excluded regions).

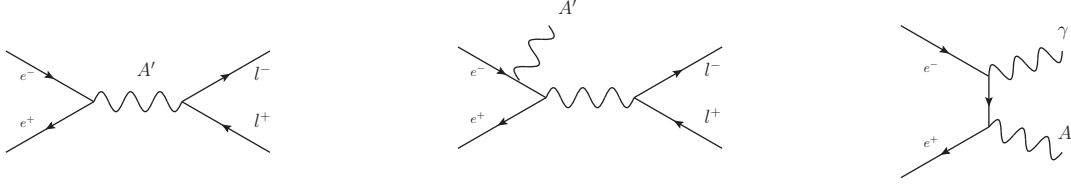


Figure 6.11: Direct dark photon production mechanism via the electron-positron annihilation channel is shown.

Before we move on to the bounds acquired from different channels, let us give brief information about the production mechanism of the dark photons.

### 6.5.3 Dark Photon Production Mechanisms

Dark photons are expected to be produced via many different channels as;

- **Annihilation Process:** In the collider experiments, dark photons are expected to be produced via the pair annihilation as shown in Figure (6.11).

The differential cross-section for the dominant channel ( $e^-e^+ \rightarrow \gamma A'$ ) is given as [155, 177];

$$\frac{d\sigma(e^+e^- \rightarrow \gamma A')}{d\cos\theta} = \frac{\alpha\epsilon^2}{2s^2(s - m_{A'}^2)} \left( \frac{s^2 + m_{A'}^4}{\sin^2\theta} - \frac{s - m_{A'}^2}{2} \right) \quad (6.50)$$

where  $\sqrt{s}$  is the center of mass energy and the mass of the electron is neglected.

- **Meson Decays:** Once kinematically allowed, the dark photon can be produced in the decay of pseudoscalar (P) or vector meson (V) decays whose relevant Feynman diagram is shown in Figure (6.12). It is possible that the dark photons are produced via  $\pi^0 \rightarrow \gamma A'$ ,  $V^\pm \rightarrow \pi^\pm A'$  and  $P^\pm \rightarrow \pi^\pm A'$ .

The branching ratio for the  $\pi^0 \rightarrow A'\gamma$  is calculated as [178];

$$Br(\pi^0 \rightarrow A'\gamma) \simeq 2\epsilon^2 \left(1 - \frac{m_{A'}^2}{m_{\pi^0}^2}\right)^3 Br(\pi^0 \rightarrow \gamma\gamma). \quad (6.51)$$

On the other hand, the branching ratio for a vector meson decaying into pseu-

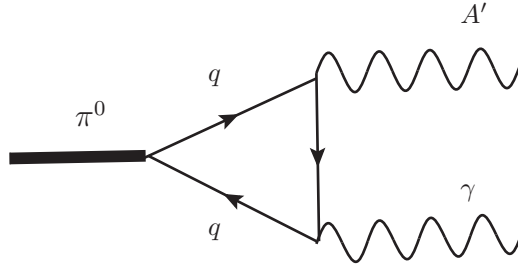


Figure 6.12: Feynman diagram of the dark photon production from  $\pi^0$  decay is shown.

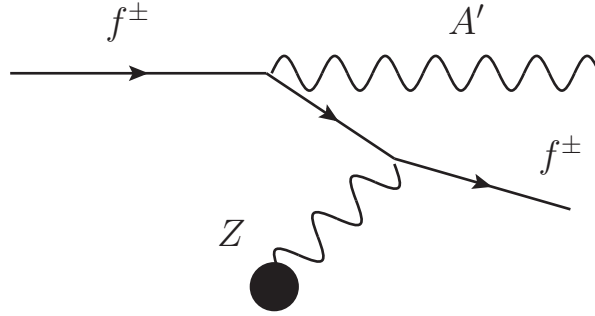


Figure 6.13: Dark photons can be produced similar to the Bremsstrahlung process called as  $A'$ -strahlung.

doctar meson and the dark photon is acquired as [178]

$$\begin{aligned}
 Br(V^\pm \rightarrow PA') &\simeq \epsilon^2 \frac{(m_V^2 - m_{A'}^2 - m_P^2)^2 \sqrt{(m_V^2 - m_{A'}^2 + m_P^2)^2 - 4m_V^2 m_P^2}}{(m_V^2 - m_{A'}^2)^3} \\
 &\times Br(V^\pm \rightarrow P\gamma),
 \end{aligned}
 \tag{6.52}$$

in which  $m_P$  and  $m_V$  are the mass of the scalar and vector mesons, respectively.

- Lepton on Target Process:** In the fixed target experiments as well as the beam dump experiments, the dark photons are also expected to be produced via mechanism called as “ $A'$ -strahlung” similar to the bremsstrahlung process. (See Figure (6.13).) Using the Weizsacker-Williams approximation, the differential cross-section for the dark photon production with energy  $E_{A'} = xE_0$  is calculated for  $m_e \ll m_{A'} \ll E_0$  and  $x\theta_{A'}^2 \ll 1$  as;

$$\frac{d\sigma}{dx d\cos\theta_{A'}} \simeq \frac{8Z^2\alpha^3\epsilon^2 E_0^2 x}{U^2} \frac{\xi}{Z^2} \quad (6.53)$$

$$\times \left[ (1-x+x^2/2) - \frac{x(1-x)m_{A'}^2 E_0^2 x \theta_{A'}^2}{U^2} \right],$$

where  $Z$  corresponds to the atomic number of the target atoms,  $E_0$  is the energy of the electron,  $\theta_{A'}$  is the angle between the dark photon and incoming electron in the lab frame and  $U$  is the virtuality of the intermediate electron in the initial-state bremsstrahlung and given as [179];

$$U(x, \theta_{A'}) = E_0^2 x \theta_{A'}^2 + m_{A'}^2 \frac{1-x}{x} + m_e^2 x.$$

$\xi$  in Equation (6.53) depends on the nuclei with the following formula;

$$\xi = \xi(E_0, m_{A'}) = \int_{t_{min}}^{t_{max}} dt \frac{t - t_{min}}{t^2} G_2(t) \quad (6.54)$$

in which  $t_{min} = (\frac{m_{A'}^2}{2E_0})^2$ ,  $t_{max} = m_{A'}^2$  and  $G_2(t)$  is a form factor [179]. This formula is used widely, however, for the  $\mathcal{O}$  (GeV) beam energies, it is shown that this approximation causes 30% overestimation of the cross-section [155, 180].

- **Proton on Target:** When the incoming beam is proton, then the dark photon production is expected to be due to proton bremsstrahlung and the dark photon production rate per proton is calculated via the Weizsacker-Williams approximation and found as [181],

$$\frac{dN}{dz} dp_{\perp}^2 = \frac{\sigma_{pA'}(s')}{\sigma_{pA'}(s)} \omega_{ba}(z, p_{\perp}^2) \quad (6.55)$$

where  $s = 2m_p E_p$ ,  $p_{\perp}$  is the transverse momentum of the  $A'$ ,  $z$  is the fraction of the momentum carried away by the dark photon in the direction of incoming proton and  $s' = 2m_p(E_p - E_{A'})$  is the reduced centre of mass energy after emission of the dark photon.  $\omega_{ba}$  is defined as,

$$\omega_{ba}(z, p_{\perp}^2) = \frac{\epsilon^2 \alpha}{2\pi H} \left[ \frac{1 + (1-z)^2}{z} - 2z(1-z) \left( \frac{2m_p^2 + m_{A'}^2}{H} - z^2 \frac{2m_p^4}{H^2} \right) \right. \\ \left. + 2z(1-z)(z + (1-z)^2) \frac{m_p^2 m_{A'}^2}{H^2} + 2z(1-z)^2 \frac{m_{A'}^4}{H^2} \right] \quad (6.56)$$

where

$$H(p_{\perp}, z) = p_{\perp}^2 + (1 - z)m_{A'}^2 + z^2m_p^2. \quad (6.57)$$

It is important to note that the above formula is derived under the assumption that the proton is a pointlike particle. Moreover it is assumed that;

$$E_p, E_{A'}, E_p - E_{A'} \gg m_p, m_{A'}, |p_{\perp}|.$$

With the mentioned mechanisms above, the dark photons are expected to be produced assuming they exist. However, to discover the dark photons via the direct detection mechanism, the dark photons decaying into the SM particles, hence, resonances should be observed. On the other hand, the dark photons can also be searched indirectly, since the observed number of events will be altered in the analyzed channel due to dark photon contribution.

The produced dark photons are expected to decay into leptons or hadrons if the mass of the dark photon is large enough. The partial decay width of the dark photons into two leptons is calculated in the kinetic mixing model as [182]

$$\Gamma_{A' \rightarrow l^+l^-} = \frac{1}{3}\alpha\epsilon^2 M_{A'} \left(1 + \frac{2m_l^2}{M_{A'}^2}\right) \sqrt{1 - \frac{4m_l^2}{M_{A'}^2}}. \quad (6.58)$$

Moreover, the partial decay width of  $A'$  into hadrons is found [182];

$$\Gamma_{A' \rightarrow hadrons} = \frac{1}{3}\epsilon^2 M_{A'} \left(1 + \frac{2m_{\mu}^2}{M_{A'}^2}\right) \sqrt{1 - \frac{4m_{\mu}^2}{M_{A'}^2}} \times \frac{\Gamma(e^+e^- \rightarrow hadrons)}{\Gamma(e^+e^- \rightarrow \mu^+\mu^-)} (E = M_{A'}). \quad (6.59)$$

Using Equations (6.58) and (6.59), the branching ratio of the dark photons into the SM particles are calculated and depicted in Figure (6.14).

Dark photon searches in the literature generally depend on the mechanisms that we mentioned above. Let us try to present the bounds acquired for the DP from various experiments. Depending on the detection techniques, experiments can be categorized as explained below.

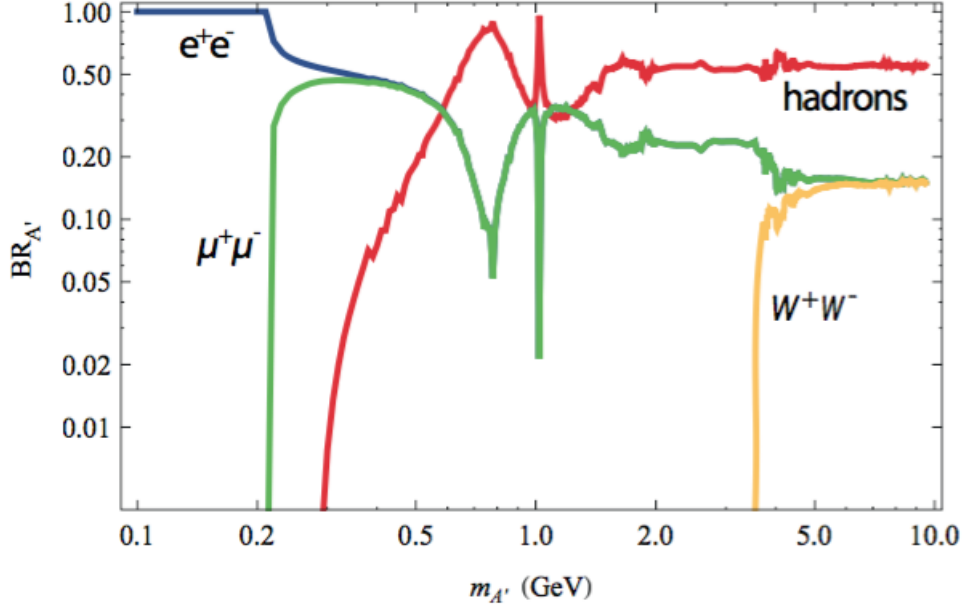


Figure 6.14: The partial width for the dark photons decaying into the SM particles in the kinetic mixing model by considering the Equations (6.58) and (6.59) are shown. (Figure is adapted from [155].)

#### 6.5.4 Beam Dump Experiments

Since the dark photons interact very weakly with the matter, to observe its effects via decaying into the SM particles, it is necessary to have high luminosity of the dark photons. Even though the dark photon production mechanism is not well known, it is expected that in the beam dump experiments, where high intensity beam of electron (proton) is impinged on a thick target, dark photons with energy  $E_{A'}$  and high intensity are produced via the  $A' - \text{strahlung}$  mechanism [155].

In the beam-dump experiments, sufficiently long shielding material is set next to the target material so that secondary produced particles will not survive through the detector, but dark photons will pass through the shielding since they feebly interact with the matter and these dark photons are expected to mix with the photon and decay into leptons which will be observed by the detector. However, note that the lifetime of the dark photon is expected to be long enough to be observed behind the shield. Hence, in this scenario, any dilepton signal over the expected background will mimic the existence of the dark photons.

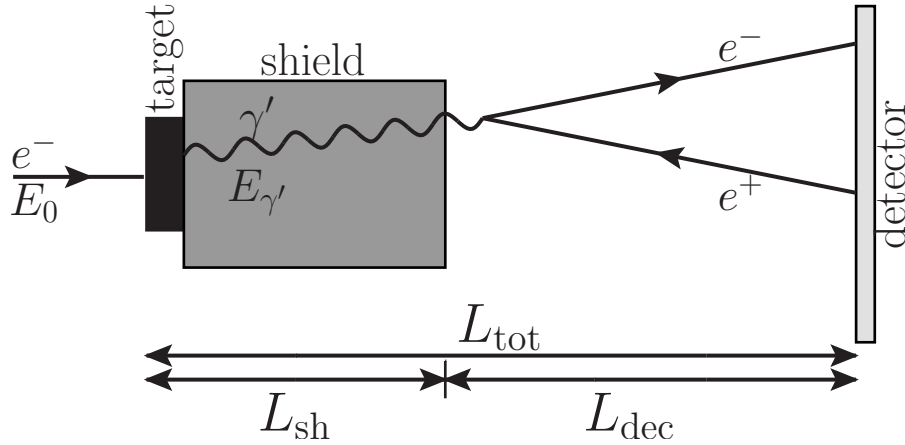


Figure 6.15: A schematic view of the electron beam-dump experiment is shown.  $L_{sh}$  and  $L_{dec}$  show the length of the shielding material and the length of the decay tube respectively. When the electron with energy  $E_0$  hits on the target, the dark photon with energy  $E_{\gamma'}$  is expected to be produced via the bremsstrahlung like process. The produced dark photons pass through the shielding without interacting and decay into the lepton pairs via mixing with the photon. (Figure is adapted from [182].)

Depending on the beam type, these experiments are classified as the electron (proton)-beam dump experiments. A schematic view of the beam-dump experiment is shown for the electron beams in Figure (6.15).

#### 6.5.4.1 Electron Beam Dump Experiments

Several experiments aimed to search for light metastable scalar or pseudo scalar particles like ALPs and Higgs like particles in the past. These experiments include the E141 [183] and E137 [184] at SLAC, the E774 [185] at Fermilab and the experiments in Orsay [186] and KEK [187]. These experiments whose characteristic parameters are summarized in Table 6.3 differ in the sense of the beam energy, the target material as well as the length of the shielding material and distance of the detector to the shielding material.

The data of these experiments are reanalyzed for the purpose of the dark photon search [182]. Depending on the experimental parameters and the production mechanism, each experiment has its own sensitivity for the different mass region of the dark photon. See Figure (6.16) for the exclusion plot. However, it is important to note that,

Table 6.3: The key parameters of the electron-beam dump experiments used to constrain the dark photon parameters is shown. For more details see [182] where the table is adapted from.

Experiment	target	$E_0$ [GeV]	$N_{el}$ electrons	Coulomb	$L_{sh}$ [m]	$L_{dec}$ [m]	$N_{obs}$	$N_{95\%up}$
E141 [183]	W	9	$2 \times 10^{15}$	0.32 mC	0.12	35	$1126^{+1312}_{-1126}$	3419
E137 [184]	Al	20	$1.87 \times 10^{20}$	30 C	179	204	0	3
E774 [185]	W	275	$5.2 \times 10^9$	0.83 nC	0.3	2	$0^{+9}_{-0}$	18
KEK [187]	W	2.5	$1.69 \times 10^{17}$	27 mC	2.4	2.2	0	3
Orsay [186]	W	1.6	$2 \times 10^{16}$	3.2 mC	1	2	0	3

since the mechanism relies on the detection of dileptons due to the dark photon mixing with photon and then decaying into leptons, it is not possible to constrain the leptophobic dark photon models with the electron-beam dump experiments. We figure out that it is possible to investigate the region for the dark photon mass upto  $\sim 100$  MeV with the electron-beam type experiments.

#### 6.5.4.2 Proton Beam Dump Experiments

As opposed to the electron beam dump experiments, there is not well-defined mechanism to describe the dark photon productions in the proton beam dump experiments. The ideas focus on the possibility of the direct production via the lepton or proton  $A'$ -strahlung mechanism or indirectly via the decay channels of the mesons as mentioned in the previous section. When protons hit on the target, mesons like  $\pi^0, \eta$  etc. with high intensity are produced. These mesons could decay into  $\gamma + A'$  with a branching ratio proportional to  $\epsilon^2$  [188].

The experimental data of CHARM [189], NOMAD [190], PS191 [191], NuCal [192] collaborations whose characteristic detector parameters are shown in Table 6.4, is



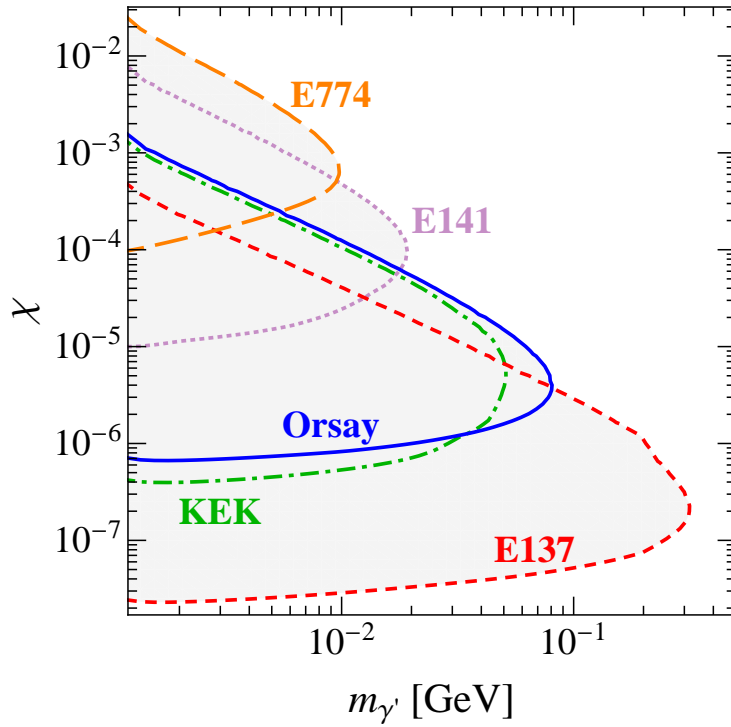


Figure 6.16: The bounds acquired from the electron beam dump experiments is shown in  $m_{\gamma'}$  ( $m_{A'}$ ) (mass of the dark photon) and  $\chi$  ( $\epsilon$ ) (kinetic mixing parameter) plane. The depicted regions are excluded. (Figure is adapted from [182]).

reanalyzed for the dark photon search [193]. The parameter region that could be surveyed via the proton-beam dump experiments is similar to the results of electron-beam dumps as shown in Figure (6.17) and constitutes a complementary result. However, while the proton beam dump experiments are sensitive to leptophobic models, leptophilic models are not suitable to search. Hence, depending on the specific models, the relevant parameter region varies.

In addition to searching the dark photons via decaying into the lepton pairs or hadrons, with the proton beam dump experiments, the invisible decay chain of  $A'$  especially if the decay products of  $A'$  is stable and re-scatter in the detector, could also be surveyed as MiniBoone collaboration proposed [194].

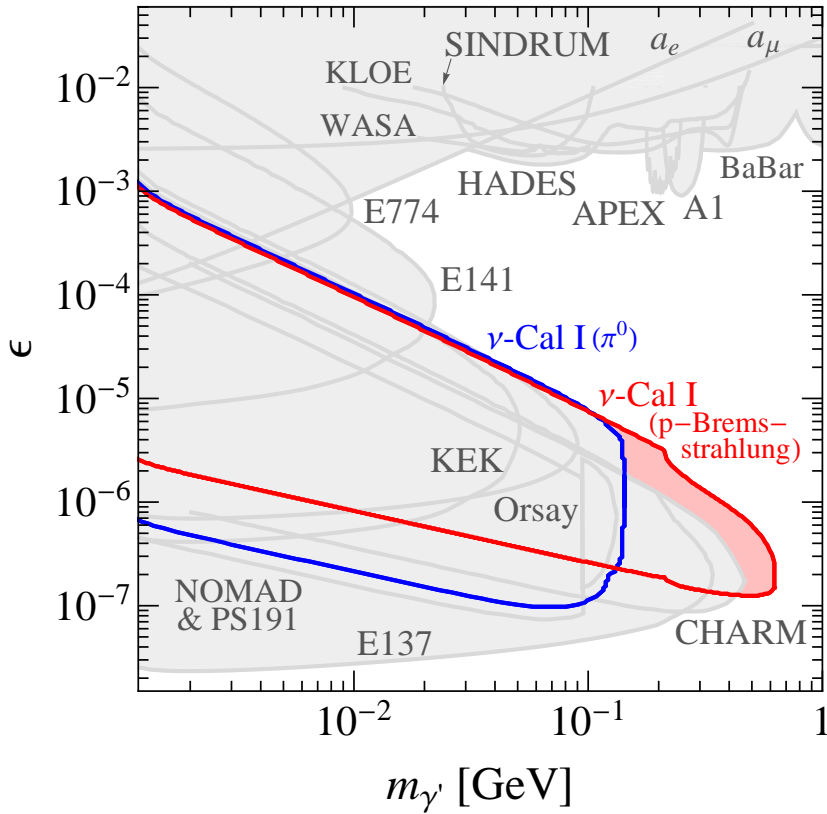


Figure 6.17: The bounds obtained from different proton beam dump experiments are shown for the kinetic-mixing model. (Figure is adapted from [181].)

### 6.5.5 Fixed Target Experiments

In the fixed target experiments, even though the production mechanism of the dark photons is similar to the electron beam dump experiments, the detection mechanism is different. There is no shielding region in this case as opposed to beam type experiments, and the expected signal is a resonance in the  $e^+ e^-$  invariant mass distribution which requires high mass resolution detectors. (See Figure (6.18) for a schematic view of the detector.) Alternative detection strategies of the dark photons are analyzed in [195].

High current electron beams are used in the fixed target experiments and the dark photons with mass  $2m_e < m_{A'} < \text{GeV}$  could be investigated. Several experiments with unique detector parameters are proposed to search the dark photon like APEX [195], HPS [196], DarkLight [197] at Jefferson Laboratory, A1 experiment [198, 199] at

Table 6.4: The relevant parameters of the most common experiments are shown. (Table is adapted from [155].)

Experiment	Target	$E_0$ (GeV)	$N_p$	$L_{sh}$ (m)	$L_{dec}$ (m)
CHARM [189]	Cu	400	$2.4 \times 10^{18}$	480	35
PS191 [191]	Be	20	$8.6 \times 10^{18}$	128	12
NOMAD [190]	Be	450	$4.1 \times 10^{19}$	835	7.5
NuCal [192]	Al	70	$1.7 \times 10^{18}$	64	23

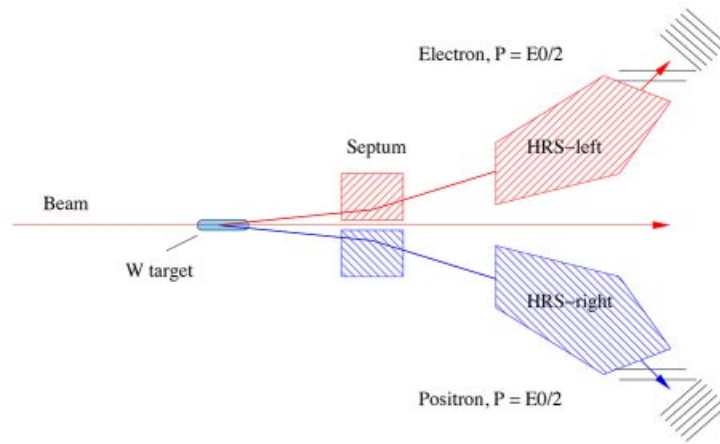


Figure 6.18: The schematic view of the APEX experiment. Electrons are impinged on a Tungsten target. Two septum magnets with opposite polarity are used to deflect the charged particles to large angles through the high resolution (HPS) spectrometers where the energy and momentum of the particles are accurately measured. Invariant mass distribution of the electron-positron pair is measured via this mechanism. (Figure is adapted from [195].)

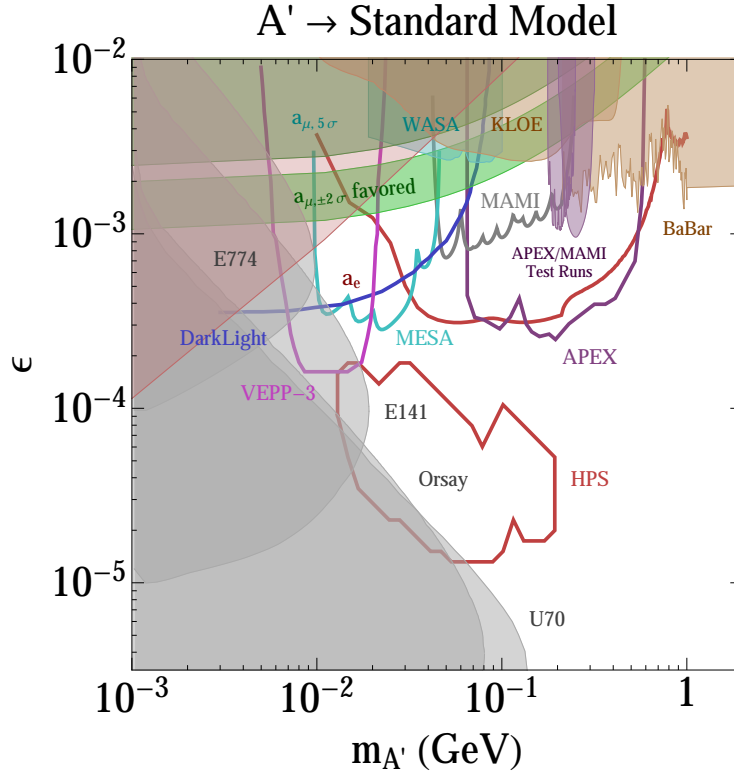


Figure 6.19: The bounds for the dark photon parameters are shown for the fixed target experiments as well as the flavor factories and colliders. (The figure is adapted from [200].)

MAMI (Mainz Microtron) each of which aims to trace the dark photon in different mass region.

The data from the fixed target experiments can constrain the kinetic mixing parameter  $\epsilon^2 > 10^{-10}$  as shown in Figure (6.19).

### 6.5.6 Flavor Factories & Colliders

Whenever a meson decays into a photon then looking for the vestige of dark photons is reasonable due to the kinetic mixing model. Hence, tracking the mesons decaying into photons is a good channel for the dark photon searches and with the advantage of vast amount of data as well as different energy ranges of flavour factories, it is possible to seek the dark photons.

Many collider experiments, focusing on different mass regions, searched the dark pho-

ton signals in different channels as we will mention briefly.

KLOE experiment is an electron-positron collider running as a  $\Phi$  factory ( $m_\phi = 1.019$  GeV) at INFN. The following decay channels are being searched;

- $\phi \rightarrow \eta A'; A' \rightarrow e^- e^+$  [201, 202] ,
- $e^+ e^- \rightarrow A' \gamma; A' \rightarrow \mu^+ \mu^-$  [203] ,
- $e^+ e^- \rightarrow A' \gamma; A' \rightarrow e^+ e^-$  [204] ,

then, the bounds on the dark photon parameters are set. See Figure (6.20).

Note that KLOE experiment is not sensitive to the mass region of around 770 MeV (mass of  $\rho$  meson) which is due to the suppression of the dark photons decaying into the dimuons since in that energy region the fraction of hadronic decay modes increases. See Figure (6.14).

Wasa at Cosy Collaboration [205] analyzed the decay of pions produced from  $pp \rightarrow pp\pi^0$  with a kinetic beam energy of 550 MeV. Note that this energy is 3 MeV below for the two pion production threshold. Searching for the decay chain of  $\pi^0$ , ( $\pi^0 \rightarrow \gamma A' \rightarrow \gamma e^+ e^-$ ) bounds from the decay channel are set for the mass range  $20 \text{ MeV} < M_{A'} < 100 \text{ MeV}$ .

HADES at GSI experiment located in Darmstadt, aimed to search the effects of the dark photon in the invariant mass distribution of the electron positron pair ( $A' \rightarrow e^- e^+$ ). 3.5 GeV proton beam impinged on the solid niobium (Nb) or a liquid hydrogen target as well as Ar + KCl reaction. Large luminosity of  $\pi^0$  and  $\eta$  mesons are acquired in these collisions and signature of the dark photon is tracked via the dielectron decay of these mesons [206, 207]. The mass region,  $m_{A'} = 0.02\text{--}0.55$  GeV is investigated.

BaBar and BELLE Experiments which are B-meson factories also looked for the dark photon signals using the advantage of their high luminosity. BaBar collaboration analyzing the reactions  $e^+ e^- \rightarrow A' \gamma; (A' \rightarrow e^+ e^-, \mu^+ \mu^-)$  investigated the mass region of the dark photon  $0.02 \text{ GeV} < m_{A'} < 10.2 \text{ GeV}$  for the dielectron channel and  $0.212 \text{ GeV} < m_{A'} < 10.2 \text{ GeV}$  for the dimuon channel [208]. The strongest limits in the mentioned mass region is acquired by BaBar Collaboration and even the large

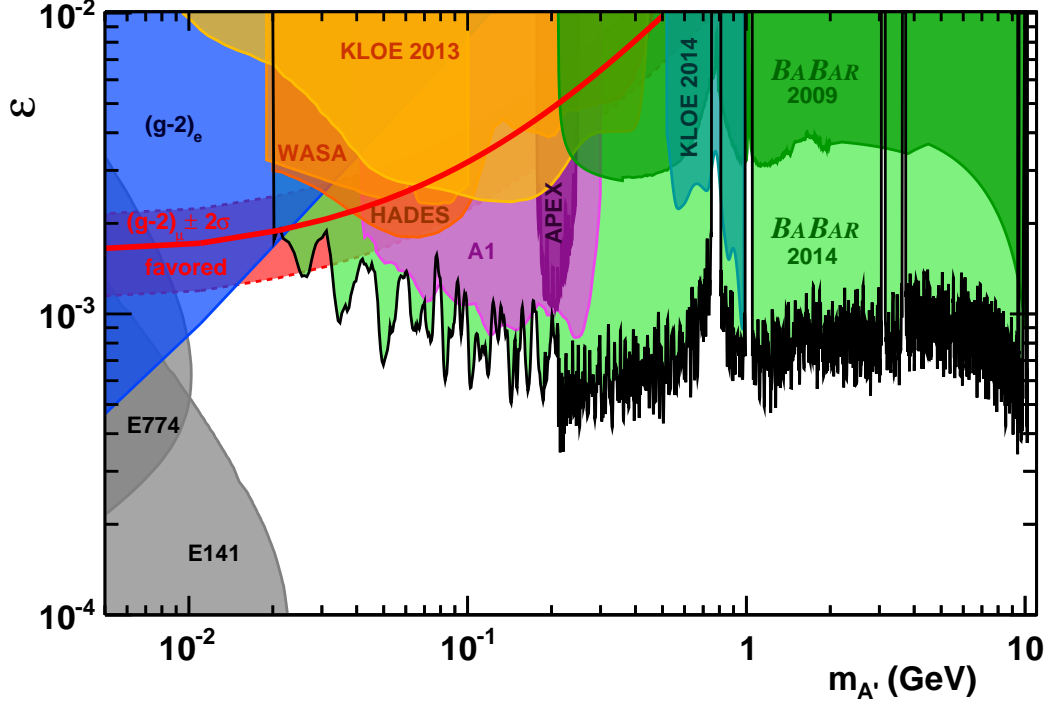


Figure 6.20: Exclusion limits obtained for the DP parameters from flavor factories are shown. (Figure is adapted from [208].)

portion of the parameter space used as an explanation for  $g_\mu - 2$  anomaly is excluded as shown in Figure (6.20).

BELLE collaboration searched the mass regions  $0.1 < m_{A'} < 3.5$  GeV for the channels  $A' \rightarrow e^+e^-, \mu^+\mu^-, \pi^+\pi^-$  and  $1.1 < m_{A'} < 3.5$  GeV for the channels  $2(e^+e^-)X, 2(\mu^+\mu^-)X$  and  $(e^+e^-)(\mu^+\mu^-)X$  where  $X$  is a dark photon candidate in which the signal is the missing energy.  $\epsilon < 8 \times 10^{-4}$  for  $m_{A'}$  is obtained from the data [209].

NA48/2 experiment at CERN which can be considered as kaon factory also searched for the dark photon signals from the decays of K mesons,  $K^\pm \rightarrow \pi^\pm\pi^0; \pi^0 \rightarrow \gamma A'; A' \rightarrow e^+e^-$ . The bounds are acquired under the assumption that the dark photon is decayed into dielectrons only [210], that is  $\text{BR}(A' \rightarrow e^+e^-) = 1$ . The bounds are shown in Figure (6.20).

Heavy ion colliders can also search the dark photon signals, since  $\pi^0, \eta$  and  $\omega$  mesons are produced with high intensity. Via the decay channels of the produced mesons, PHENIX experiment at BNL and ALICE Collaborations at CERN, also searched for

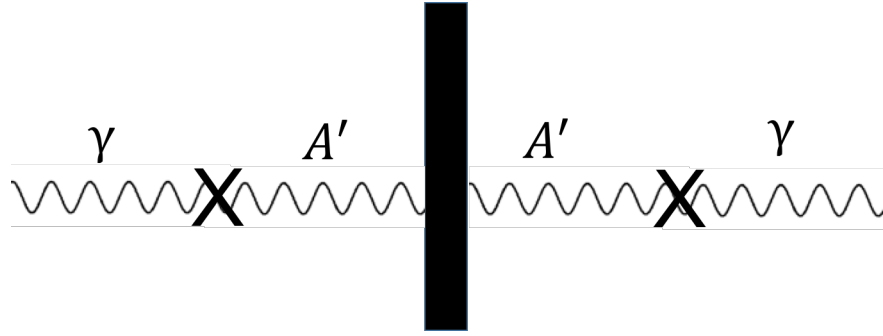


Figure 6.21: The schematic view of the detection mechanism of the dark photons via the LSW experiment is shown. If the incoming photon oscillates into the dark photon, then due to feebly interaction of dark photons they are expected to pass through the wall and oscillate back to photons which are tried to be detected.

the dark photon signal. The decay channels of  $\pi^0 \rightarrow \gamma e^+ e^-$  and  $\eta \rightarrow \gamma e^+ e^-$  are analyzed. No signal events are observed and  $\epsilon < 2 \times 10^{-6}$  is acquired for  $30 < M_{A'} < 90$  MeV by PHENIX collaboration [211].

### 6.5.7 Light Shining through Walls (LSW)

LSW experiments can delve into the parameter region of WISPs (Weakly interacting sub-eV particles) like ALPS, minicharged particles and dark photon. The schematic view for the detection is shown in Figure (6.21). The detection mechanism depends on the oscillation of the dark photon. If the incoming photon oscillates into the dark photon, then it can survive behind the wall due to very weak interaction of the dark photons. The dark photon which pass through the wall is expected to oscillate again into photon which is tried to be detected. The oscillation mechanism in this case is similar to the neutrino oscillation phenomenon. Very small mass region of the dark photon can be hunted via this method [212, 174]. The bounds acquired from the LSW experiments are depicted in Figure (6.21).

### 6.5.8 Anomalous Magnetic Moment of the Electron and Muon (g-2)

The existence of dark photon would contribute to the magnetic moment of the electron and muon at the one loop level [176]. Dark photon with the specific parameters

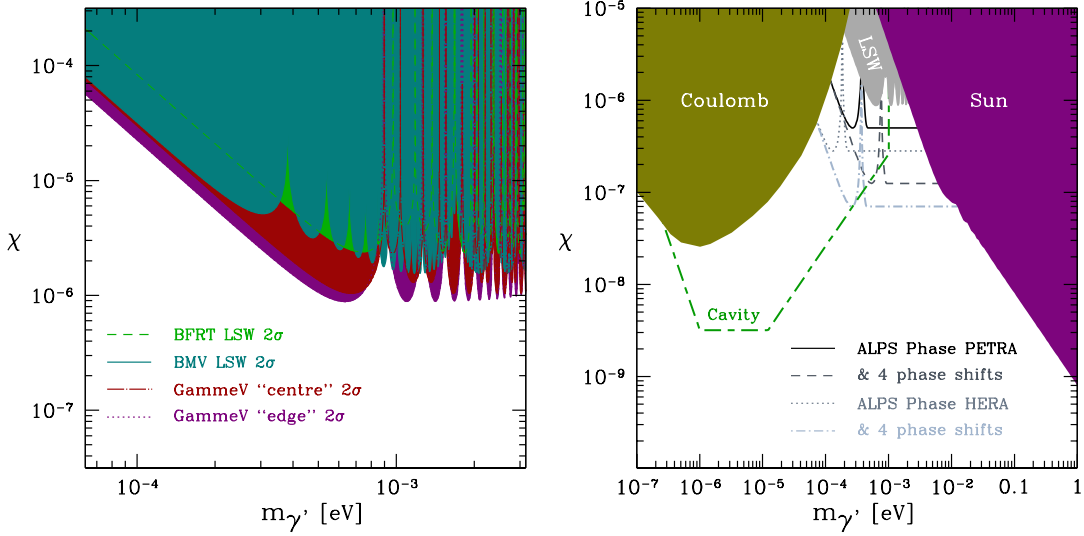


Figure 6.22: The bounds acquired from the LSW experiments are shown with a comparison from the bounds solar, cast and atomic force experiments. For more information see [212] where the figure is adapted from.

shown in Figure (6.20) could explain the  $(g - 2)_\mu$  anomaly. To test this idea, many experiments tried to search the relevant mass region as shown in Figure (6.20) and the favored region is almost all excluded. The bounds obtained from the existing measurements of magnetic moments of electron and muon are also shown in Figure (6.20).

### 6.5.9 Helioscopes

CAST (CERN Axion Solar Telescope) [228] as a helioscope could constrain the dark photon parameters by measuring the electromagnetic signals in a dark, shielded cavity. It is hypothesized that dark photons from the sun oscillate into photons after passing through the cavity and contribute to the signal measured. Strong limits can be obtained for the mass region where the dark photon flux emanating from the sun would be large [224]. However these bounds are model dependent [173].

### 6.5.10 CMB

If the dark photon mixes with the ordinary one in a frequency dependent way then the distortions in the CMB spectrum is expected [227]. Analyzing the data taken by



Table 6.5: The bounds on the gauge coupling constant of the dark photon from different sources are listed with a brief summary about the experiments as well as the relevant references.

Experiments	Comments	References
g-2	$A'$ contribution to magnetic moment of $e$ and $\mu$ .	[176, 213]
Fixed Target	$A'$ production in beam dump experiments. $A' \rightarrow e^-e^+$ in $M'_A > 2m_e$ .	[168, 179, 188, 214, 215, 216]
B-Factories	$\Upsilon \rightarrow \gamma A'$ and $A' \rightarrow \gamma l^+l^-$ . Sensitive to range $0.02 \text{ GeV} < M'_A < 10.2 \text{ GeV}$ .	[217, 218, 219, 208]
Fifth Force	Precision measurements of gravitational, Casimir and Van der Waals forces. Sensitive to $M'_A \lesssim 100 \text{ eV}$ .	[174, 220]
Atomic Physics	Corrections to Coulomb Force.	[174, 221]
Supernova	Analysis of energy loss of Supernova.	[222, 223]
Sun	Luminosity analysis in the conversion of plasmons in the sun.	[224, 225, 226]
LSW	Transition of laser $\rightarrow A' \rightarrow \gamma$ .	[174, 212]
CMB	Study of black body spectrum of Cosmic Microwave Background.	[174, 227]
CAST	Comparison of flux of dark and usual photon.	[224, 228]
Globular Clusters	Energy loss due to dark photons in Globular Clusters.	[224, 225, 226, 174]
BBN	Thermalization of Dirac neutrinos $\nu_R$ via $A'$ , contributing to the effective new neutrino species $\Delta_{N_{eff}}$	[229, 230]

COBE Satellite [231] can put constraints on the dark photon parameters as shown in Figure (6.23). However, note that as in the bounds from CAST experiment, these results are also model dependent.

Apart from the experiments mentioned above, dark photons are also searched in many channels like atomic physics, the fifth force searches and cosmology which are summarized in Table 6.5 as well as with the relevant references. Despite the fact that the bounds obtained from cosmology and the fifth force are the most stringent ones, the results are highly model dependent.

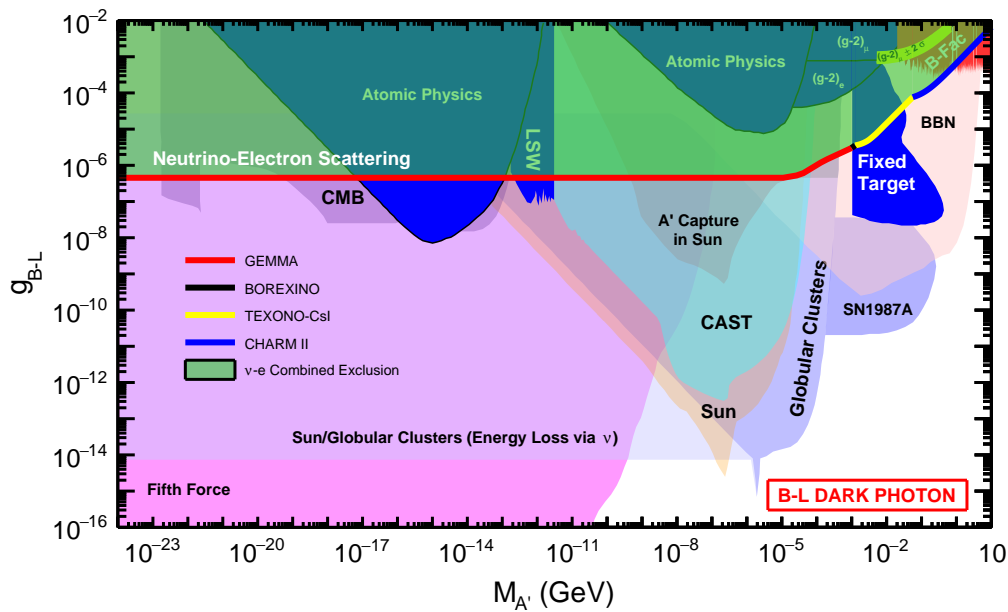


Figure 6.23: The combined limits obtained from the neutrino-electron scattering (this work) is overlaid on the bounds from different laboratory experiments as well as cosmological and astrophysical sources at 90% C.L. (Figure is adapted from [170].)

To compare the bounds that we obtained from the neutrino electron scattering experiments with the bounds in the literature we tried to overlay our results on the existing ones. Note that in the literature the bounds are generally given in terms of the kinetic mixing models. However, as we mentioned, these bounds can be converted into the  $B - L$  model. Hence, based on the bounds already mentioned in [173], we plotted our results to compare the bounds acquired from the neutrino-electron scattering experiments as shown in Figure (6.23). Note that, since each of the neutrino experiments

had their own sensitive region, we used the best bounds among them as an exclusion line.

We realize from the figure that, the bounds we acquired from the  $\nu - e^-$  scattering experiments rule out the allowed region for the dark photon which is considered as a remedy for the  $g_\mu - 2$  anomaly. Moreover, we showed that the interference effects cannot be neglected and the bounds given in the literature [173] should have been updated for at least the Borexino result. Furthermore, we figure out that for  $m_{A'} < 10$  keV the bounds on  $g_{B-L}$  is insensitive to  $m_{A'}$  for the  $\nu - e$  experiments. In addition to the  $g_{B-L}^4$  dependence of the pure DP cross-section, since it is difficult to lower the threshold of the recoil energy in the neutrino experiments, future prospects are not expected to enhance the bounds acquired especially for  $m_{A'} < 0.1$  MeV.



## CHAPTER 7

### CONCLUSIONS

Among the SM particles, neutrinos are the most mysterious ones. Even though the oscillation experiments imply that they are massive, the mass mechanism as well as mass values are not well known. Moreover, the question of whether neutrinos are Dirac or Majorana particles still keeps its secret. Despite having lots of unknowns about them, the interaction of neutrinos in the SM is well explained by the electroweak interaction where the parity is violated. Hence, searching for physics beyond the standard model in the neutrino experiments can be thought as worthwhile since the number of diagrams are very few in general with robust SM predictions. On the other hand, neutrinos interact very weakly with the matter and hence difficult to detect. In the collider experiments missing energy is the only signal for the neutrinos. Moreover, the error bars especially in the low energy neutrino experiments are very large and this makes it impossible to detect new physics signatures directly. For instance, resonances can not be observed in the  $\nu - e$  scattering experiments. Instead, indirect effects of the new physics scenarios are searched with the neutrinos. New physics effects would give additional contributions to the SM predictions, hence number of expected events will altered due to on-shell contribution of the BSM effects. The discrepancy with the observed events and the SM prediction would mimic the new physics and free parameters of the models can be constrained with the neutrino-electron scattering experiments.

In this study, we searched two beyond the standard model scenarios; Non-commutative space and the Dark photon effects from the hidden sector in the neutrino electron scattering.

The idea of non-commutative space is first used in order to get rid of the divergences encountered before the renormalization concept is set. Moreover, with the notion used in the string theory the idea became prevalent again. Similar to the commutation relation of position and momentum conjugate coordinates, the commutation relation among space-time coordinates is defined as  $[\hat{x}_\mu, \hat{x}_\nu] = i\theta_{\mu\nu} = i\frac{C_{\mu\nu}}{\Lambda_{NC}^2}$ . Where  $\Lambda_{NC}$  corresponds to the energy scale in which the coordinates become fuzzy.

Although the neutrino photon interaction is allowed in the loop corrections in the Standard Model, it is forbidden at the tree level. However, the non-commutative field theory allows neutrino photon interaction in tree level due to the new coupling of neutral particles to the  $U(1)$  gauge field. Hence, in addition to  $W$  and  $Z$  bosons, the photon exchange diagrams are also possible in the NC-space. Once we calculate the cross-section of this new diagram, we infer that the cross-section would increase either for the low recoil energy experiments or for the neutrinos with high incoming energy. Hence, bounds with better sensitivity could be set for the carefully chosen experiments. For this purpose, we decided to analyze four different data sets of experiments; TEXONO (CsI and HPGe), LSND and CHARM II depending on the recoil energy as well as the neutrino energies to constrain the  $\Lambda_{NC}$ . Among these experiments, TEXONO is a reactor neutrino experiment hence neutrinos are  $\bar{\nu}_e$ , LSND is a stopped pion experiment and the neutrinos produced from pion decays are electron type (from the muon decay) and CHARM II is an accelerator neutrinos in which the muon neutrinos are used.

We found out that the cross-section of the new photon exchange diagram is independent of the neutrino flavors and the interference between the SM diagrams is equal to zero. The limits for  $\Lambda_{NC}$  at 95% C.L. is acquired using these data sets and bounds are depicted in Table 5.1. Our results show that as the incoming neutrino energies increase then the bounds acquired become more stringent as  $\Lambda_{NC} > 3.3$  TeV from the CHARM II experiments. On the other hand, the bounds acquired from TEXONO is more stringent than LSND even though the energy of the neutrinos used in LSND is higher than TEXONO which implies that the low recoil energy experiments can also enhance the bounds. However, since lowering the analysis threshold to  $\mathcal{O}(\text{eV})$  is not practically possible in the near future, we can infer that the high energy neutrino experiments ( $\mathcal{O}(\text{GeV})$ ) would give more sensitive bounds.

The bounds on  $\Lambda_{NC}$  is also searched via many channels in the literature. We found out that, our results are complementary with the literature. Moreover, the bounds we acquired are even comparable with the ones from the collider experiments. Furthermore, our findings imply that, once the ICECUBE data, recently announced the detection of PeV neutrinos from the cosmogenic sources, is analyzed for the NC-space effects, the bounds for  $\Lambda_{NC}$  can become more stringent.

The other new physics model that we searched with the neutrino experiments is the Dark Photon. Even though the SM is very successful in explaining the most of the outcomes of the experiments conducted, there are still some phenomena that the SM becomes short to explain. For instance, dark matter can be considered as the biggest headache for the SM. Besides, excess number of events recorded by the recent Dark matter experiments still remains as a puzzle. Apart from these unexplained phenomena, there is a  $3.6\sigma$  discrepancy between the calculated and measured magnetic moment of muon. These are some of the puzzles waiting to be addressed. The existence of the Hidden sector is proposed as a solution for all these mysteries. The hidden sector may contain particles that do not interact with the SM except gravity. However if this is the case, there is no way to discover the hidden sector. On the other hand, the existence of portals may satisfy the interaction of the hidden sector with the SM sector. Dark photon which is a particle of the vector portal could be one of them. With an additional  $U(1)$  symmetry, it is possible to consider dark photons interacting with the SM particles via mixing with photon which is called as kinetic mixing model. On the other hand, one may consider the symmetry as  $U(1)_{B-L}$  for which interactions like the neutrino dark photon coupling is possible through a new gauge coupling constant,  $g_{B-L}$ . There is no theoretical restriction for the mass of dark photons, hence the mass can take any value from sub-eV to TeV. The existence of such particles could be an answer for the mentioned anomalies. For instance, for the specific parameter range of the dark photon mass, the muon magnetic moment anomaly would have been solved. To test the proposed idea, especially the pointed out region is studied heavily via many different sources in order to test the hypothesis.

Under the  $U(1)_{B-L}$  symmetry, a neutrino can couple to photons at tree level. Hence with searching for the contributions from the extra new diagram in addition to the SM predictions, constraining the dark photon parameters become possible. Once we

calculated the cross-section, we found out that interference of dark photon diagram with the SM ones can not be neglected and should be taken into consideration as opposed to the common belief in the literature. Moreover, the cross-section of the pure dark photon diagram implied that depending on the mass region of dark photon, neutrino experiments from the low energy to the high energy would give sensitive bounds in their respective parameter region. For this purpose, we preferred to analyze the neutrino electron scattering data from TEXONO (CsI, HPGE, NPCGe), LSND, CHARM II, GEMMA and BOREXINO Collaborations.

We found out that the interference effect is crucial except for experiments in which there is much room for new physics since the measurement errors are large as in the case of TEXONO (HPGE, NPCGe) and GEMMA experiment. For the other experiments we showed that the bounds are shifted around 30% percent once the interference is taken into account. Moreover, we figured out that, while the interference is destructive for the  $\bar{\nu}_\mu - e^-$  scattering, it is constructive for all the others. While the constructive interference leads to stringent bounds, they are loosened for the destructive interference. Moreover, it is important to note that, the pure DP contribution does not depend on the neutrino flavor, however the interference term would differ since the SM contributions are different.

By analyzing all the data sets, the bounds at 90% C.L are found in the  $g_{B-L} - m_{A'}$  plane. We discover that for the low  $m_{A'}$  range, the low recoil energy experiments give more stringent bounds. Moreover for the range  $m_{A'} \lesssim 10$  keV the cross-section loses its dependency on  $m_{A'}$  hence the neutrino experiments have a fixed bound as  $g_{B-L} \lesssim 10^{-6}$  in that region. As  $m_{A'}$  increases each experiment has its own sensitivity and a combined best bounds from the neutrino experiments are plotted in Figure (6.23).

In the literature, the widely studied model is the kinetic mixing one, and the bounds are generally given in the  $m_{A'} - \epsilon$  plane where  $\epsilon$  is the kinetic mixing parameter. However, these bounds can be translated into the  $m_{A'} - g_{B-L}$  plane. Having collected and converted the bounds for the  $U(1)_{B-L}$  gauge boson model, we overlaid the results that we found from the neutrino electron scattering on the literature bounds. Our results as well as the BABAR bounds exclude the possible expected parameter region where a solution to muon magnetic moment anomaly is possible. However, the future



neutrino experiments are not expected to enhance the bounds very much, due to the dependency of  $g_{B-L}^4$  in the cross-section expressions. Hence, these results also show the parameter region that can be investigated via the neutrino-electron scattering experiments. Even though the idea lost the motivation for explaining the muon magnetic moment anomaly, the existence of dark photons still contributes to the efforts for solving the puzzles in the SM and searches still go on especially for the low dark photon mass range  $10 \text{ keV} - 10 \text{ GeV}$ .



## Bibliography

- [1] A. Aguilar-Arevalo and W. Bietenholz. “NEUTRINOS: Mysterious Particles with Fascinating Features, which led to the Physics Nobel Prize 2015”.  
In: *arXiv:1601.04747 [physics.pop-ph]* (2016).  
URL: <http://arxiv.org/abs/1601.04747> (visited on 06/15/2016).
- [2] G. Gamow. *Constitution of atomic nuclei and radioactivity*. Oxford, 1931.
- [3] W. Pauli. “letter to a physicists’ gathering at Tübingen, December 4, 1930”.  
In: *Reprinted in Wolfgang Pauli, Collected Scientific Papers, ed. R. Kronig and V. Weisskopf 2* (1978), p. 1313.
- [4] O. Laporte. “Die Struktur des Eisenspektrums”. de.  
In: *Zeitschrift für Physik* 23.1 (1924), pp. 135–175.  
URL: <http://link.springer.com/article/10.1007/BF01327582>  
(visited on 06/20/2016).
- [5] A. Lesov. “The Weak Force: From Fermi to Feynman”.  
In: *arXiv:0911.0058 [physics]* (2009).  
URL: <http://arxiv.org/abs/0911.0058> (visited on 06/20/2016).
- [6] T. D. Lee and C. N. Yang.  
“Question of Parity Conservation in Weak Interactions”.  
In: *Physical Review* 104.1 (1956), pp. 254–258.  
URL: <http://link.aps.org/doi/10.1103/PhysRev.104.254> (visited on 06/20/2016).
- [7] C. S. Wu et al. “Experimental Test of Parity Conservation in Beta Decay”.  
In: *Physical Review* 105.4 (1957), pp. 1413–1415.  
URL: <http://link.aps.org/doi/10.1103/PhysRev.105.1413> (visited on 06/20/2016).
- [8] R. L. Garwin, L. M. Lederman, and M. Weinrich.  
“Observations of the failure of conservation of parity and charge conjugation

- in meson decays: the magnetic moment of the free muon”.  
In: *Physical Review* 105.4 (1957), p. 1415.
- [9] C. Sutton and F. Reines. *Spaceship Neutrino*. First Edition. Cambridge England; New York, NY, USA: Cambridge University Press, 1992.
- [10] F. Reines. “The neutrino: from poltergeist to particle”.  
In: *Reviews of Modern Physics* 68.2 (1996), pp. 317–327.  
URL: <http://link.aps.org/doi/10.1103/RevModPhys.68.317>  
(visited on 06/22/2016).
- [11] F. Reines and C. L. Cowan. “The Neutrino”.  
In: *Nature* 178.4531 (1956), pp. 446–449.  
URL: <http://www.nature.com/nature/journal/v178/n4531/abs/178446a0.html> (visited on 06/22/2016).
- [12] F. Reines and C. L. Cowan. “Detection of the Free Neutrino”.  
In: *Physical Review* 92.3 (1953), pp. 830–831.  
URL: <http://link.aps.org/doi/10.1103/PhysRev.92.830> (visited on 06/22/2016).
- [13] K. A. Olive et al. “Review of Particle Physics”. In: *Chin.Phys.* C38 (2014).
- [14] G. Danby et al. “Observation of High-Energy Neutrino Reactions and the Existence of Two Kinds of Neutrinos”.  
In: *Physical Review Letters* 9.1 (1962), pp. 36–44.  
URL: <http://link.aps.org/doi/10.1103/PhysRevLett.9.36> (visited on 06/22/2016).
- [15] C. C. F. Reines. “Reines-Cowan Experiment and Detecting the Poltergeist”.  
In: *Los Alamos Science* 25 (1997).
- [16] M. L. Perl et al.  
“Evidence for Anomalous Lepton Production in  $e^+ - e^-$  Annihilation”.  
In: *Phys. Rev. Lett.* 35 (22 1975), pp. 1489–1492.  
URL: <http://link.aps.org/doi/10.1103/PhysRevLett.35.1489>.
- [17] D. DeCamp et al. “Determination of the number of light neutrino species”.  
In: *Physics Letters B* 231.4 (1989), pp. 519–529.

URL: <http://www.sciencedirect.com/science/article/pii/S0370269389907041> (visited on 06/22/2016).

- [18] The ALEPH Collaboration and the DELPHI Collaboration and the L3 Collaboration and the OPAL Collaboration and the SLD Collaboration and the LEP Electroweak Working Group and electroweak, the SLD and groups, heavy flavour. “Precision Electroweak Measurements on the Z Resonance”. In: *Physics Reports* 427.5-6 (2006), pp. 257–454.  
URL: <http://arxiv.org/abs/hep-ex/0509008> (visited on 06/22/2016).
- [19] DONUT Collaboration. “Observation of Tau Neutrino Interactions”. In: *Physics Letters B* 504.3 (2001), pp. 218–224.  
URL: <http://arxiv.org/abs/hep-ex/0012035> (visited on 06/22/2016).
- [20] A. Franklin. *Are There Really Neutrinos?: An Evidential History*. Cambridge, Mass: Westview Press, 2000.
- [21] S. Bilenky. “Neutrino. History of a unique particle”. In: *The European Physical Journal H* 38.3 (2013), pp. 345–404.  
URL: <http://link.springer.com/10.1140/epjh/e2012-20068-9> (visited on 02/27/2016).
- [22] I. V. Anicin. “The Neutrino - Its Past, Present and Future”. In: *arXiv:physics/0503172* (2005). URL: <http://arxiv.org/abs/physics/0503172> (visited on 02/25/2016).
- [23] A. de Gouvea. “2004 TASI Lectures on Neutrino Physics”. In: *arXiv:hep-ph/0411274* (2004).  
URL: <http://arxiv.org/abs/hep-ph/0411274> (visited on 06/19/2016).
- [24] R. Mitalas and K. R. Sills. “On the photon diffusion time scale for the sun”. In: *The Astrophysical Journal* 401 (1992), p. 759.  
URL: <http://adsabs.harvard.edu/doi/10.1086/172103> (visited on 08/18/2016).
- [25] R. Davis, D. S. Harmer, and K. C. Hoffman. “Search for Neutrinos from the Sun”. In: *Physical Review Letters* 20.21 (1968), pp. 1205–1209.

URL: <http://link.aps.org/doi/10.1103/PhysRevLett.20.1205>  
(visited on 06/23/2016).

- [26] F. Suekane.  
*Neutrino Oscillations: A Practical Guide to Basics and Applications*.  
2015 edition. Tokyo ; Heidelberg: Springer, 2015.
- [27] C. Giunti and C. W. Kim.  
*Fundamentals of Neutrino Physics and Astrophysics*. First Edition.  
Oxford ; New York: Oxford University Press, 2007.
- [28] K. Zuber. *Neutrino Physics, Second Edition*.  
Boca Raton, FL: CRC Press, 2011.
- [29] C. V. Achar et al.  
“Detection of muons produced by cosmic ray neutrinos deep underground”.  
In: *Physics Letters* 18.2 (1965), pp. 196–199.  
URL: <http://www.sciencedirect.com/science/article/pii/0031916365907122> (visited on 06/23/2016).
- [30] F. Reines et al.  
“Evidence for High-Energy Cosmic-Ray Neutrino Interactions”.  
In: *Physical Review Letters* 15.9 (1965), pp. 429–433.  
URL: <http://link.aps.org/doi/10.1103/PhysRevLett.15.429>  
(visited on 06/23/2016).
- [31] T. Kajita. “Atmospheric neutrinos and discovery of neutrino oscillations”.  
In: *Proceedings of the Japan Academy. Series B, Physical and Biological Sciences* 86.4 (2010), pp. 303–321.  
URL: <http://www.ncbi.nlm.nih.gov/pmc/articles/PMC3417797/>  
(visited on 06/23/2016).
- [32] *Solar Neutrino Viewgraphs*. URL:  
<http://www.sns.ias.edu/~jnb/SNviewgraphs/snviewgraphs.html>  
(visited on 06/23/2016).
- [33] K. Hirata et al.  
“Observation of a neutrino burst from the supernova SN1987A”.  
In: *Physical Review Letters* 58.14 (1987), pp. 1490–1493.

URL: <http://link.aps.org/doi/10.1103/PhysRevLett.58.1490>  
(visited on 07/28/2016).

- [34] R. M. Bionta et al. “Observation of a Neutrino Burst in Coincidence with Supernova SN 1987a in the Large Magellanic Cloud”.  
In: *Phys.Rev.Lett.* 58 (1987), p. 1494.
- [35] E. N. Alexeyev et al. “Detection of the neutrino signal from SN 1987A in the LMC using the INR Baksan underground scintillation telescope”.  
In: *Physics Letters B* 205.2 (1988), pp. 209–214.  
URL: <http://www.sciencedirect.com/science/article/pii/0370269388916516> (visited on 08/18/2016).
- [36] T. Araki et al. “Experimental investigation of geologically produced antineutrinos with KamLAND”. In: *Nature* 436.7050 (2005), pp. 499–503.  
URL: <http://www.nature.com/nature/journal/v436/n7050/full/nature03980.html> (visited on 06/22/2016).
- [37] G. Bellini et al.  
“Measurement of geo-neutrinos from 1353 days of Borexino”.  
In: *Physics Letters B* 722.4–5 (2013), pp. 295–300.  
URL: <http://www.sciencedirect.com/science/article/pii/S0370269313003092> (visited on 06/22/2016).
- [38] V. S. Berezinsky and G. T. Zatsepin.  
“Cosmic neutrinos of superhigh energy”.  
In: *Yad.Fiz.* 11 (1970), pp. 200–205.
- [39] ARA Collaboration. “Performance of two Askaryan Radio Array stations and first results in the search for ultra-high energy neutrinos”.  
In: *arXiv:1507.08991 [astro-ph]* (2015).  
URL: <http://arxiv.org/abs/1507.08991> (visited on 06/22/2016).
- [40] S. W. Barwick et al. “Design and Performance of the ARIANNA Hexagonal Radio Array Systems”. In: *arXiv:1410.7369 [astro-ph]* (2014).  
URL: <http://arxiv.org/abs/1410.7369> (visited on 06/22/2016).
- [41] C. Spiering.  
“Towards High-Energy Neutrino Astronomy. A Historical Review”.

- In: *The European Physical Journal H* 37.3 (2012), pp. 515–565.  
URL: <http://arxiv.org/abs/1207.4952> (visited on 06/22/2016).
- [42] G. 't Hooft and M. Veltman.  
“Regularization and renormalization of gauge fields”.  
In: *Nuclear Physics B* 44.1 (1972), pp. 189–213.  
URL: <http://www.sciencedirect.com/science/article/pii/0550321372902799> (visited on 06/23/2016).
- [43] S. Weinberg. “A Model of Leptons”.  
In: *Physical Review Letters* 19.21 (1967), pp. 1264–1266.  
URL: <http://link.aps.org/doi/10.1103/PhysRevLett.19.1264>  
(visited on 06/23/2016).
- [44] S. L. Glashow. “Partial-symmetries of weak interactions”.  
In: *Nuclear Physics* 22.4 (1961), pp. 579–588.  
URL: <http://www.sciencedirect.com/science/article/pii/0029558261904692> (visited on 06/23/2016).
- [45] The ATLAS Collaboration. “Observation of a new particle in the search for the Standard Model Higgs boson with the ATLAS detector at the LHC”.  
In: *Physics Letters B* 716.1 (2012), pp. 1–29.  
URL: <http://arxiv.org/abs/1207.7214> (visited on 06/23/2016).
- [46] The CMS Collaboration. “Observation of a new boson at a mass of 125 GeV with the CMS experiment at the LHC”.  
In: *Physics Letters B* 716.1 (2012), pp. 30–61.  
URL: <http://arxiv.org/abs/1207.7235> (visited on 06/23/2016).
- [47] T. W. B. Kibble. “Symmetry Breaking in Non-Abelian Gauge Theories”.  
In: *Physical Review* 155.5 (1967), pp. 1554–1561.  
URL: <http://link.aps.org/doi/10.1103/PhysRev.155.1554> (visited on 06/23/2016).
- [48] P. W. Higgs.  
“Spontaneous Symmetry Breakdown without Massless Bosons”.  
In: *Physical Review* 145.4 (1966), pp. 1156–1163.  
URL: <http://link.aps.org/doi/10.1103/PhysRev.145.1156> (visited on 06/23/2016).



- [49] G. S. Guralnik, C. R. Hagen, and T. W. B. Kibble.  
 “Global Conservation Laws and Massless Particles”.  
 In: *Physical Review Letters* 13.20 (1964), pp. 585–587.  
 URL: <http://link.aps.org/doi/10.1103/PhysRevLett.13.585>  
 (visited on 06/23/2016).
- [50] P. W. Higgs. “Broken Symmetries and the Masses of Gauge Bosons”.  
 In: *Physical Review Letters* 13.16 (1964), pp. 508–509.  
 URL: <http://link.aps.org/doi/10.1103/PhysRevLett.13.508>  
 (visited on 06/23/2016).
- [51] P. W. Higgs. “Broken symmetries, massless particles and gauge fields”.  
 In: *Physics Letters* 12.2 (1964), pp. 132–133.  
 URL: <http://www.sciencedirect.com/science/article/pii/0031916364911369> (visited on 06/23/2016).
- [52] F. Englert and R. Brout.  
 “Broken Symmetry and the Mass of Gauge Vector Mesons”.  
 In: *Physical Review Letters* 13.9 (1964), pp. 321–323.  
 URL: <http://link.aps.org/doi/10.1103/PhysRevLett.13.321>  
 (visited on 06/23/2016).
- [53] *Science Springs*. URL: <https://sciencesprings.files.wordpress.com/2016/05/standard-model.jpg> (visited on 06/23/2016).
- [54] A. Salam. “Weak and Electromagnetic Interactions”.  
 In: *Conf.Proc.* C680519 (1968), pp. 367–377.
- [55] C. Quigg. *Gauge Theories of the Strong, Weak, and Electromagnetic Interactions: Second Edition*. English. Second edition.  
 Princeton, New Jersey: Princeton University Press, 2013.
- [56] J. D. Bjorken and S. D. Drell. *Relativistic Quantum Fields*. First Edition.  
 New York: Mcgraw-Hill College, 1965.
- [57] A. Bettini. *Introduction to Elementary Particle Physics*. English. 2 edition.  
 New York: Cambridge University Press, 2014.

- [58] D. Griffiths. *Introduction to Elementary Particles*. English. 2nd edition. Weinheim: Wiley-VCH, 2008.
- [59] P. Langacker. *The Standard Model and Beyond*. English. CRC Press, 2009.
- [60] W. Greiner and J. Reinhardt. *Quantum Electrodynamics*. English. 4th ed. 2009 edition. Berlin: Springer, 2008.
- [61] H. T. Wong and J. Li.  
“Research program of the TEXONO Collaboration: Status and highlights”.  
In: (2002), pp. 65–76.
- [62] M. Deniz et al. “Measurement of  $\bar{\nu}_e$ -Electron Scattering Cross-Section with a CsI(Tl) Scintillating Crystal Array at the Kuo-Sheng Nuclear Power Reactor”. In: *Phys.Rev. D* 81 (2010), p. 072001.
- [63] P. Vogel. “Evaluation of reactor neutrino flux: issues and uncertainties”.  
In: *arXiv:1603.08990 [hep-ph, physics:nucl-th]* (2016).  
URL: <http://arxiv.org/abs/1603.08990> (visited on 04/12/2016).
- [64] P. Huber.  
“On the determination of anti-neutrino spectra from nuclear reactors”.  
In: *Physical Review C* 84.2 (2011).  
URL: <http://arxiv.org/abs/1106.0687> (visited on 04/12/2016).
- [65] T. A. Mueller et al. “Improved predictions of reactor antineutrino spectra”.  
In: *Physical Review C* 83.5 (2011).  
URL: <http://arxiv.org/abs/1101.2663> (visited on 04/12/2016).
- [66] H. B. Li and H. T. Wong.  
“Sensitivities of low-energy reactor neutrino experiments”.  
In: *J.Phys.* G28 (2002), pp. 1453–1468.
- [67] H. T. Wong. “Prospects of scintillating crystal detector in low-energy low-background experiments”.  
In: *Astroparticle Physics* 14.2 (2000), pp. 141–152.  
URL: <http://arxiv.org/abs/hep-ex/9910002> (visited on 04/14/2016).
- [68] TEXONO Collaboration et al. “Limit on the electron neutrino magnetic moment from the Kuo-Sheng Reactor Neutrino Experiment”.  
In: *Physical Review Letters* 90.13 (2003), p. 131802.

URL: <http://link.aps.org/doi/10.1103/PhysRevLett.90.131802>  
(visited on 07/13/2016).

- [69] TEXONO Collaboration et al. “Search of neutrino magnetic moments with a high-purity germanium detector at the Kuo-Sheng nuclear power station”.  
In: *Physical Review D* 75.1 (2007), p. 012001.  
URL: <http://link.aps.org/doi/10.1103/PhysRevD.75.012001>  
(visited on 04/15/2016).
- [70] H. T. Wong. “Low energy neutrino and dark matter physics with sub-keV germanium detectors”.  
In: *International Journal of Modern Physics D* 20.08 (2011), pp. 1463–1470.  
URL: <http://www.worldscientific.com/doi/abs/10.1142/S0218271811019645>  
(visited on 04/18/2016).
- [71] J. W. Chen et al. “Constraints on millicharged neutrinos via analysis of data from atomic ionizations with germanium detectors at sub-keV sensitivities”.  
In: *Physical Review D* 90.1 (2014).  
URL: <http://arxiv.org/abs/1405.7168> (visited on 04/17/2016).
- [72] H.B. Li et al. “Differentiation of bulk and surface events in p-type point-contact germanium detectors for light WIMP searches”.  
In: *Astroparticle Physics* 56 (2014), pp. 1–8. URL: <http://www.sciencedirect.com/science/article/pii/S0927650514000176>.
- [73] J. W. Chen et al.  
“Constraining neutrino electromagnetic properties by germanium detectors”.  
In: *Phys.Rev. D* 91 (2015), p. 013005.
- [74] A. G. Beda et al. “The Results of search for the neutrino magnetic moment in GEMMA Experiment”.  
In: *Advances in High Energy Physics* 2012, 2012 (2012), e350150.  
URL: <http://www.hindawi.com/journals/ahep/2012/350150/abs/>  
(visited on 04/20/2016).
- [75] A. G. Beda et al.  
“Gemma experiment: The results of neutrino magnetic moment search”.  
In: *Physics of Particles and Nuclei Letters* 10.2 (2013), pp. 139–143. URL:

<http://link.springer.com/article/10.1134/S1547477113020027>  
(visited on 04/20/2016).

- [76] K. A. Olive et al. “Review of Particle Physics”.  
In: *Chin. Phys.* C38 (2014), p. 090001.
- [77] A. Aguilar et al. “Evidence for neutrino oscillations from the observation of electron anti-neutrinos in a muon anti-neutrino beam”.  
In: *Physical Review D* 64.11 (2001).  
URL: <http://arxiv.org/abs/hep-ex/0104049> (visited on 07/03/2016).
- [78] C. Athanassopoulos et al. “Evidence for  $\bar{\nu}_\mu \rightarrow \bar{\nu}_e$  Oscillations from the LSND Experiment at the Los Alamos Meson Physics Facility”.  
In: *Phys. Rev. Lett.* 77 (15 1996), pp. 3082–3085.  
URL: <http://link.aps.org/doi/10.1103/PhysRevLett.77.3082>.
- [79] A. Strumia.  
“Interpreting the LSND anomaly: sterile neutrinos or CPT-violation or...?”  
In: *Physics Letters B* 539.1-2 (2002), pp. 91–101.  
URL: <http://arxiv.org/abs/hep-ph/0201134> (visited on 07/03/2016).
- [80] J. M. Conrad, W. C. Louis, and M. H. Shaevitz.  
“The LSND and MiniBooNE Oscillation Searches at High  $m^2$ ”.  
In: *Annual Review of Nuclear and Particle Science* 63.1 (2013), pp. 45–67.  
URL: <http://dx.doi.org/10.1146/annurev-nucl-102711-094957>.
- [81] L. B. Auerbach et al.  
“Measurement of electron - neutrino - electron elastic scattering”.  
In: *Phys.Rev.* D63 (2001), p. 112001.
- [82] K. De Winter et al. “A detector for the study of neutrino-electron scattering”.  
In: *Nuclear Instruments and Methods in Physics Research Section A: Accelerators, Spectrometers, Detectors and Associated Equipment* 278.3 (1989), pp. 670–686. URL: <http://www.sciencedirect.com/science/article/pii/016890028991190X> (visited on 04/19/2016).
- [83] “Neutrino-electron scattering — Status of the CHARM-II experiment”.  
In: *Nuclear Physics B - Proceedings Supplements* 13 (1990), pp. 329–331.

URL: <http://www.sciencedirect.com/science/article/pii/S092056329090079A> (visited on 04/19/2016).

- [84] D. Geiregat et al. “Calibration and performance of the CHARM-II detector”.  
In: *Nuclear Instruments and Methods in Physics Research Section A: Accelerators, Spectrometers, Detectors and Associated Equipment* 325.1 (1993), pp. 92–108. URL: <http://www.sciencedirect.com/science/article/pii/S016890029391010K> (visited on 04/19/2016).
- [85] P. Vilain et al. “Precision measurement of electroweak parameters from the scattering of muon-neutrinos on electrons”.  
In: *Physics Letters B* 335.2 (1994), pp. 246–252.  
URL: <http://www.sciencedirect.com/science/article/pii/S0370269394914214> (visited on 04/19/2016).
- [86] Borexino Collaboration. “Science and Technology of BOREXINO: A Real Time Detector for Low Energy Solar Neutrinos SOLAR NEUTRINOS”.  
In: *Astroparticle Physics* 16.3 (2002), pp. 205–234.  
URL: <http://arxiv.org/abs/hep-ex/0012030> (visited on 07/04/2016).
- [87] G. Alimonti et al.  
“The Borexino detector at the Laboratori Nazionali del Gran Sasso”.  
In: *Nuclear Instruments and Methods in Physics Research Section A: Accelerators, Spectrometers, Detectors and Associated Equipment* 600.3 (2009), pp. 568–593. URL: <http://www.sciencedirect.com/science/article/pii/S016890020801601X> (visited on 04/21/2016).
- [88] Borexino Collaboration.  
“New results on solar neutrino fluxes from 192 days of Borexino data”.  
In: *Physical Review Letters* 101.9 (2008).  
URL: <http://arxiv.org/abs/0805.3843> (visited on 07/04/2016).
- [89] Borexino Collaboration.  
“Spectroscopy of geo-neutrinos from 2056 days of Borexino data”.  
In: *Physical Review D* 92.3 (2015).  
URL: <http://arxiv.org/abs/1506.04610> (visited on 07/04/2016).

- [90] Borexino Collaboration and H. O. Back.  
 “Response to a critique of the Borexino result in ”A new experimental limit for the stability of the electron” by H.V. Klapdor-Kleingrothaus, I.V. Krivosheina and I.V. Titkova”. In: *arXiv:hep-ex/0703044* (2007).  
 URL: <http://arxiv.org/abs/hep-ex/0703044> (visited on 07/04/2016).
- [91] H. O. Back et al. “New limits on nucleon decays into invisible channels with the BOREXINO counting test facility”.  
 In: *Phys.Lett.* B563 (2003), pp. 23–34.
- [92] O. Smirnov et al. “Solar neutrino with Borexino: results and perspectives”.  
 In: *Physics of Particles and Nuclei* 46.2 (2015), pp. 166–173.  
 URL: <http://arxiv.org/abs/1410.0779> (visited on 04/22/2016).
- [93] G. Bellini et al. “Precision Measurement of the  $^7\text{Be}$  Solar Neutrino Interaction Rate in Borexino”. In: *Phys. Rev. Lett.* 107 (14 2011), p. 141302.  
 URL: <http://link.aps.org/doi/10.1103/PhysRevLett.107.141302>.
- [94] B. Ydri. “Fuzzy Physics”. In: *arXiv:hep-th/0110006* (2001).  
 URL: <http://arxiv.org/abs/hep-th/0110006> (visited on 07/05/2016).
- [95] G. Birkhoff. “Von Neumann and lattice theory”. In: *Bulletin of the American Mathematical Society* 64.Number 3, Part 2 (1958), pp. 50–56.  
 URL: <http://projecteuclid.org/euclid.bams/1183522370> (visited on 07/08/2016).
- [96] S. Hossenfelder. “The Minimal Length and Large Extra Dimensions”.  
 In: *Modern Physics Letters A* 19.37 (2004), pp. 2727–2744.  
 URL: <http://arxiv.org/abs/hep-ph/0410122> (visited on 07/08/2016).
- [97] L. Randall and R. Sundrum.  
 “A Large Mass Hierarchy from a Small Extra Dimension”.  
 In: *Physical Review Letters* 83.17 (1999), pp. 3370–3373.  
 URL: <http://arxiv.org/abs/hep-ph/9905221> (visited on 07/08/2016).
- [98] R. Peierls. “Zur Theorie des Diamagnetismus von Leitungselektronen”. de.  
 In: *Zeitschrift für Physik* 80.11-12 (1933), pp. 763–791.  
 URL: <http://link.springer.com/article/10.1007/BF01342591>  
 (visited on 07/08/2016).

- [99] R. Jackiw. “Physical Instances of Noncommuting Coordinates”.  
In: *Nuclear Physics B - Proceedings Supplements* 108 (2002), pp. 30–36.  
URL: <http://arxiv.org/abs/hep-th/0110057> (visited on 07/05/2016).
- [100] P. A. Horvathy. “The non-commutative Landau problem”.  
In: *Annals of Physics* 299.1 (2002), pp. 128–140.  
URL: <http://arxiv.org/abs/hep-th/0201007> (visited on 07/05/2016).
- [101] G. Magro. “Noncommuting Coordinates in the Landau Problem”.  
In: *arXiv:quant-ph/0302001* (2003). URL:  
<http://arxiv.org/abs/quant-ph/0302001> (visited on 07/05/2016).
- [102] E. Witten. “Non-commutative geometry and string field theory”.  
In: *Nuclear Physics B* 268.2 (1986), pp. 253–294.  
URL: <http://www.sciencedirect.com/science/article/pii/0550321386901550> (visited on 07/09/2016).
- [103] W. Pauli. *Scientific Correspondence With Bohr, Einstein, Heisenberg, A.O.: 1940-1949/Wissenschaftlicher Briefwechsel Mit Bohr, Einstein, Heisenberg U.A. : 194 ... History of Mathematics and Physical Sciences*.  
Ed. by K. V. Meyenn. Berlin u.a.: Springer-Verlag, 1993.
- [104] H. S. Snyder. “Quantized Space-Time”.  
In: *Physical Review* 71.1 (1947), pp. 38–41.  
URL: <http://link.aps.org/doi/10.1103/PhysRev.71.38> (visited on 07/09/2016).
- [105] P. Aschieri. *Noncommutative spacetimes: symmetries in noncommutative geometry and field theory*. Lecture notes in physics 774.  
Berlin ; London: Springer, 2009.
- [106] N. Seiberg and E. Witten. “String Theory and Noncommutative Geometry”.  
In: *Journal of High Energy Physics* 1999.09 (1999), pp. 032–032.  
URL: <http://arxiv.org/abs/hep-th/9908142> (visited on 07/09/2016).
- [107] J. Gomis and T. Mehen.  
“Space-Time Noncommutative Field Theories And Unitarity”.  
In: *Nuclear Physics B* 591.1-2 (2000), pp. 265–276.  
URL: <http://arxiv.org/abs/hep-th/0005129> (visited on 07/09/2016).

- [108] M. Chaichian et al.  
 “Space-Time Noncommutativity, Discreteness of Time and Unitarity”.  
 In: *The European Physical Journal C* 20.4 (2001), pp. 767–772.  
 URL: <http://arxiv.org/abs/hep-th/0007156> (visited on 07/09/2016).
- [109] D. W. Chiou and O. J. Ganor.  
 “Noncommutative Dipole Field Theories And Unitarity”.  
 In: *Journal of High Energy Physics* 2004.03 (2004), pp. 050–050.  
 URL: <http://arxiv.org/abs/hep-th/0310233> (visited on 07/09/2016).
- [110] P. Schupp et al. “The photon-neutrino interaction induced by non-commutativity and astrophysical bounds”. In: *The European Physical Journal C - Particles and Fields* 36.3 (2004), pp. 405–410. URL: <http://link.springer.com/article/10.1140/epjc/s2004-01874-5> (visited on 07/12/2016).
- [111] M. M. Sheikh-Jabbari.  
 “Discrete Symmetries (C,P,T) in Noncommutative Field Theories”.  
 In: *Physical Review Letters* 84.23 (2000), pp. 5265–5268.  
 URL: <http://arxiv.org/abs/hep-th/0001167> (visited on 07/16/2016).
- [112] P. Aschieri et al. “Non-Commutative GUTs, Standard Model and C,P,T”.  
 In: *Nuclear Physics B* 651.1-2 (2003), pp. 45–70.  
 URL: <http://arxiv.org/abs/hep-th/0205214> (visited on 07/16/2016).
- [113] M. M. Etefaghi and T. Shakouri.  
 “Neutrino-electron scattering in noncommutative space”.  
 In: *Journal of High Energy Physics* 2010.11 (2010).  
 URL: <http://arxiv.org/abs/1011.5423> (visited on 07/05/2016).
- [114] P. Vilain et al. “Measurement of differential cross sections for muon-neutrino electron scattering”. In: *Physics Letters B* 302.2 (1993), pp. 351–355.  
 URL: <http://www.sciencedirect.com/science/article/pii/037026939390408A> (visited on 04/19/2016).
- [115] S. Bilmis et al. “Constraints on Non-Commutative Physics Scale with Neutrino-Electron Scattering”. In: *Physical Review D* 85.7 (2012).  
 URL: <http://arxiv.org/abs/1201.3996> (visited on 07/09/2016).



- [116] G. J. Feldman and R. D. Cousins.  
 “A Unified Approach to the Classical Statistical Analysis of Small Signals”.  
 In: *Physical Review D* 57.7 (1998), pp. 3873–3889. URL:  
<http://arxiv.org/abs/physics/9711021> (visited on 07/13/2016).
- [117] J. Kamoshita.  
 “Probing noncommutative space-time in the laboratory frame”.  
 In: *The European Physical Journal C* 52.2 (2007), pp. 451–457.  
 URL: <http://link.springer.com/article/10.1140/epjc/s10052-007-0371-y> (visited on 07/14/2016).
- [118] I. Hinchliffe, N. Kersting, and Y. L. Ma.  
 “Review of the Phenomenology of Noncommutative Geometry”. In:  
*International Journal of Modern Physics A* 19.sup02 (2004), pp. 179–204.  
 URL: <http://arxiv.org/abs/hep-ph/0205040> (visited on 07/05/2016).
- [119] G. Abbiendi et al.  
 “Test of non-commutative QED in the process  $e^+e^- \rightarrow \gamma\gamma$  at LEP”.  
 In: *Physics Letters B* 568.3-4 (2003), pp. 181–190.  
 URL: <http://www.sciencedirect.com/science/article/pii/S0370269303009523> (visited on 07/11/2016).
- [120] M. Mohammadi Najafabadi.  
 “Noncommutative standard model in the top quark sector”.  
 In: *Physical Review D* 77.11 (2008), p. 116011.  
 URL: <http://link.aps.org/doi/10.1103/PhysRevD.77.116011>  
 (visited on 07/11/2016).
- [121] IceCube Collaboration. “Constraints on ultra-high-energy cosmic ray  
 sources from a search for neutrinos above 10 PeV with IceCube”.  
 In: *arXiv:1607.05886 [astro-ph]* (2016).  
 URL: <http://arxiv.org/abs/1607.05886> (visited on 07/21/2016).
- [122] X. Calmet and M. Wohlgenannt.  
 “Effective field theories on noncommutative space-time”.  
 In: *Physical Review D* 68.2 (2003), p. 025016.  
 URL: <http://link.aps.org/doi/10.1103/PhysRevD.68.025016>  
 (visited on 07/14/2016).

- [123] X. Calmet. “What are the bounds on space-time non-commutativity?”  
In: *The European Physical Journal C - Particles and Fields* 41.2 (2005),  
pp. 269–272. URL:  
<http://link.springer.com/article/10.1140/epjc/s2005-02226-9>  
(visited on 07/14/2016).
- [124] W. Behr et al.  
“The  $Z \rightarrow \gamma\gamma; gg$  decays in the non-commutative standard model”.  
In: *The European Physical Journal C - Particles and Fields* 29.3 (2003),  
pp. 441–446.  
URL: <http://dx.doi.org/10.1140/epjc/s2003-01207-4>.
- [125] M. Burić et al. “Nonzero  $Z \rightarrow \gamma\gamma$  decays in the renormalizable gauge sector  
of the noncommutative standard model”.  
In: *Physical Review D* 75.9 (2007), p. 097701.  
URL: <http://link.aps.org/doi/10.1103/PhysRevD.75.097701>  
(visited on 07/11/2016).
- [126] A. Alboteanu, T. Ohl, and R. Rückl.  
“Probing the noncommutative standard model at hadron colliders”.  
In: *Physical Review D* 74.9 (2006), p. 096004.  
URL: <http://link.aps.org/doi/10.1103/PhysRevD.74.096004>  
(visited on 07/11/2016).
- [127] A. Alboteanu, T. Ohl, and R. Rückl.  
“The Noncommutative Standard Model at the ILC”.  
In: *arXiv:0709.2359 [hep-ph]* (2007).  
URL: <http://arxiv.org/abs/0709.2359> (visited on 07/11/2016).
- [128] J. A. Conley and J. L. Hewett.  
“Effects of the Noncommutative Standard Model on WW scattering”.  
In: *arXiv:0811.4218 [hep-ph]* (2008).  
URL: <http://arxiv.org/abs/0811.4218> (visited on 07/11/2016).
- [129] P. Mathews. “Compton scattering in noncommutative space-time at the Next  
Linear Collider”. In: *Physical Review D* 63.7 (2001), p. 075007.  
URL: <http://link.aps.org/doi/10.1103/PhysRevD.63.075007>  
(visited on 07/12/2016).

- [130] J. L. Hewett, F. J. Petriello, and T. G. Rizzo.  
“Signals for noncommutative interactions at linear colliders”.  
In: *Physical Review D* 64.7 (2001), p. 075012.  
URL: <http://link.aps.org/doi/10.1103/PhysRevD.64.075012>  
(visited on 07/12/2016).
- [131] X. G. He and X. Q. Li.  
“Probe noncommutative space–time scale using at ILC”.  
In: *Physics Letters B* 640.1–2 (2006), pp. 28–31.  
URL: <http://www.sciencedirect.com/science/article/pii/S0370269306008987> (visited on 07/12/2016).
- [132] S. Baek et al. “Signatures of noncommutative QED at photon colliders”.  
In: *Physical Review D* 64.5 (2001), p. 056001.  
URL: <http://link.aps.org/doi/10.1103/PhysRevD.64.056001>  
(visited on 07/12/2016).
- [133] T. Ohl and J. Reuter.  
“Testing the noncommutative standard model at a future photon collider”.  
In: *Physical Review D* 70.7 (2004), p. 076007.  
URL: <http://link.aps.org/doi/10.1103/PhysRevD.70.076007>  
(visited on 07/12/2016).
- [134] M. Haghight and F. Loran.  
“Three body bound state in noncommutative space”.  
In: *Physical Review D* 67.9 (2003), p. 096003.  
URL: <http://link.aps.org/doi/10.1103/PhysRevD.67.096003>  
(visited on 07/12/2016).
- [135] M. Chaichian, M. M. Sheikh-Jabbari, and A. Tureanu.  
“Hydrogen Atom Spectrum and the Lamb Shift in Noncommutative QED”.  
In: *Physical Review Letters* 86.13 (2001), pp. 2716–2719.  
URL: <http://link.aps.org/doi/10.1103/PhysRevLett.86.2716>  
(visited on 07/12/2016).
- [136] I. F. Riad and M. M. Sheikh-Jabbari.  
“Noncommutative QED and anomalous dipole moments”.  
In: *Journal of High Energy Physics* 2000.08 (2000), p. 045.

- URL: <http://stacks.iop.org/1126-6708/2000/i=08/a=045> (visited on 07/12/2016).
- [137] E. O. Iltan. “The noncommutative effects on the dipole moments of fermions in the standard model”.
- In: *Journal of High Energy Physics* 2003.05 (2003), p. 065.
- URL: <http://stacks.iop.org/1126-6708/2003/i=05/a=065> (visited on 07/12/2016).
- [138] I. Mocioiu, M. Pospelov, and R. Roiban.
- “Limits on the Non-commutativity Scale”. In: *arXiv:hep-ph/0110011* (2001).
- URL: <http://arxiv.org/abs/hep-ph/0110011> (visited on 07/12/2016).
- [139] I. Hinchliffe and N. Kersting.
- “*CP* violation from noncommutative geometry”.
- In: *Physical Review D* 64.11 (2001), p. 116007.
- URL: <http://link.aps.org/doi/10.1103/PhysRevD.64.116007> (visited on 07/12/2016).
- [140] H. Grosse and Y. Liao. “Anomalous C-violating three photon decay of the neutral pion in noncommutative quantum electrodynamics”.
- In: *Physics Letters B* 520.1–2 (2001), pp. 63–68.
- URL: <http://www.sciencedirect.com/science/article/pii/S0370269301011509> (visited on 07/12/2016).
- [141] Muon ( $g - 2$ ) Collaboration et al.
- “Precise Measurement of the Positive Muon Anomalous Magnetic Moment”.
- In: *Physical Review Letters* 86.11 (2001), pp. 2227–2231.
- URL: <http://link.aps.org/doi/10.1103/PhysRevLett.86.2227> (visited on 07/12/2016).
- [142] X. J. Wang and M. L. Yan.
- “Noncommutative QED and Muon Anomalous Magnetic Moment”.
- In: *Journal of High Energy Physics* 2002.03 (2002), p. 047.
- URL: <http://stacks.iop.org/1126-6708/2002/i=03/a=047> (visited on 07/12/2016).

- [143] N. Kersting. “ $(g-2)_\mu$  from noncommutative geometry”.  
In: *Physics Letters B* 527.1–2 (2002), pp. 115–118.  
URL: <http://www.sciencedirect.com/science/article/pii/S0370269301015180> (visited on 07/12/2016).
- [144] M. Haghghat.  
“Bounds on the parameter of noncommutativity from supernova SN1987A”.  
In: *Physical Review D* 79.2 (2009), p. 025011.  
URL: <http://link.aps.org/doi/10.1103/PhysRevD.79.025011>  
(visited on 07/12/2016).
- [145] R. Horvat and J. Trampetić. “Constraining spacetime noncommutativity with primordial nucleosynthesis”. In: *Physical Review D* 79.8 (2009), p. 087701.  
URL: <http://link.aps.org/doi/10.1103/PhysRevD.79.087701>  
(visited on 07/12/2016).
- [146] R. Horvat, D. Kekez, and J. Trampetić. “Spacetime noncommutativity and ultrahigh energy cosmic ray experiments”.  
In: *Physical Review D* 83.6 (2011), p. 065013.  
URL: <http://link.aps.org/doi/10.1103/PhysRevD.83.065013>  
(visited on 07/12/2016).
- [147] T. Ohlsson and H. Zhang.  
“Non-standard interaction effects at reactor neutrino experiments”.  
In: *Physics Letters B* 671.1 (2009), pp. 99–104.  
URL: <http://www.sciencedirect.com/science/article/pii/S0370269308014718> (visited on 07/14/2016).
- [148] R. Adhikari et al. “Non-standard interaction in neutrino oscillations and recent Daya Bay, T2K experiments”. In: *Physical Review D* 86.7 (2012).  
URL: <http://arxiv.org/abs/1201.3047> (visited on 07/14/2016).
- [149] J. Chang et al.  
“An excess of cosmic ray electrons at energies of 300–800 GeV”.  
In: *Nature* 456.7220 (2008), pp. 362–365.  
URL: <http://www.nature.com/nature/journal/v456/n7220/full/nature07477.html> (visited on 07/18/2016).

- [150] O. Adriani et al. “An anomalous positron abundance in cosmic rays with energies 1.5–100 GeV”. In: *Nature* 458.7238 (2009), pp. 607–609.  
URL: <http://www.nature.com/nature/journal/v458/n7238/full/nature07942.html> (visited on 07/18/2016).
- [151] Fermi LAT Collaboration et al. “Measurement of Separate Cosmic-Ray Electron and Positron Spectra with the Fermi Large Area Telescope”. In: *Physical Review Letters* 108.1 (2012), p. 011103.  
URL: <http://link.aps.org/doi/10.1103/PhysRevLett.108.011103> (visited on 07/18/2016).
- [152] AMS Collaboration et al. “First Result from the Alpha Magnetic Spectrometer on the International Space Station: Precision Measurement of the Positron Fraction in Primary Cosmic Rays of 0.5 – 350 GeV”. In: *Physical Review Letters* 110.14 (2013), p. 141102.  
URL: <http://link.aps.org/doi/10.1103/PhysRevLett.110.141102> (visited on 07/18/2016).
- [153] R. Bernabei et al. “First results from DAMA/LIBRA and the combined results with DAMA/NaI”. In: *The European Physical Journal C* 56.3 (2008), pp. 333–355.  
URL: <http://link.springer.com/article/10.1140/epjc/s10052-008-0662-y> (visited on 07/18/2016).
- [154] C. E. Aalseth et al. “Search for An Annual Modulation in Three Years of CoGeNT Dark Matter Detector Data”. In: *arXiv:1401.3295 [astro-ph, physics:hep-ex, physics:hep-ph]* (2014).  
URL: <http://arxiv.org/abs/1401.3295> (visited on 07/18/2016).
- [155] M. Raggi and V. Kozhuharov. “Results and perspectives in dark photon physics”. In: *Riv.Nuovo Cim.* 38 (2015), pp. 449–505. URL: <http://www.sif.it/riviste/ncr/econtents/2015/038/10/article/0>.
- [156] M. Pospelov, A. Ritz, and M. B. Voloshin. “Secluded WIMP Dark Matter”. In: *Phys. Lett. B* 662 (2008), pp. 53–61. arXiv: 0711.4866 [hep-ph].

- [157] R. Essig et al.  
 “Working Group Report: New Light Weakly Coupled Particles”.  
 In: *Proceedings, Community Summer Study 2013: Snowmass on the Mississippi (CSS2013): Minneapolis, MN, USA, July 29-August 6, 2013*.  
 2013. arXiv: 1311.0029 [hep-ph]. URL: <https://inspirehep.net/record/1263039/files/arXiv:1311.0029.pdf>.
- [158] E. Witten. “Some properties of O(32) superstrings”.  
 In: *Physics Letters B* 149.4 (1984), pp. 351–356.  
 URL: <http://www.sciencedirect.com/science/article/pii/0370269384904222> (visited on 07/19/2016).
- [159] J. P. Conlon. “The QCD Axion and Moduli Stabilisation”.  
 In: *Journal of High Energy Physics* 2006.05 (2006), pp. 078–078.  
 URL: <http://arxiv.org/abs/hep-th/0602233> (visited on 07/19/2016).
- [160] P. Svrcek and E. Witten. “Axions In String Theory”.  
 In: *Journal of High Energy Physics* 2006.06 (2006), pp. 051–051.  
 URL: <http://arxiv.org/abs/hep-th/0605206> (visited on 07/19/2016).
- [161] A. Arvanitaki et al. “String Axiverse”. In: *Physical Review D* 81.12 (2010).  
 URL: <http://arxiv.org/abs/0905.4720> (visited on 07/19/2016).
- [162] B. S. Acharya, K. Bobkov, and P. Kumar. “An M Theory Solution to the Strong CP Problem and Constraints on the Axiverse”.  
 In: *Journal of High Energy Physics* 2010.11 (2010).  
 URL: <http://arxiv.org/abs/1004.5138> (visited on 07/19/2016).
- [163] M. Cicoli, M. Goodsell, and A. Ringwald.  
 “The type IIB string axiverse and its low-energy phenomenology”.  
 In: *Journal of High Energy Physics* 2012.10 (2012).  
 URL: <http://arxiv.org/abs/1206.0819> (visited on 07/19/2016).
- [164] E. Izaguirre and I. Yavin. “A Milli-Window to Another World”.  
 In: *Physical Review D* 92.3 (2015).  
 URL: <http://arxiv.org/abs/1506.04760> (visited on 07/19/2016).
- [165] S. Alekhin et al. “A facility to Search for Hidden Particles at the CERN SPS: the SHiP physics case”.

- In: *arXiv:1504.04855 [hep-ex, physics:hep-ph]* (2015).  
 URL: <http://arxiv.org/abs/1504.04855> (visited on 07/19/2016).
- [166] S. N. Gninenko, N. V. Krasnikov, and V. A. Matveev.  
 “Muon  $g-2$  and searches for a new leptophobic sub-GeV dark boson in a missing-energy experiment at CERN”. In: *Phys.Rev. D* 91 (2015), p. 095015.
- [167] J. L. Feng et al.  
 “Evidence for a Protophobic Fifth Force from  $^8\text{Be}$  Nuclear Transitions”.  
 In: *arXiv:1604.07411 [hep-ph]* (2016).  
 URL: <http://arxiv.org/abs/1604.07411> (visited on 04/27/2016).
- [168] R. Essig et al. “Discovering new light states at neutrino experiments”.  
 In: *Physical Review D* 82.11 (2010), p. 113008.  
 URL: <http://link.aps.org/doi/10.1103/PhysRevD.82.113008>  
 (visited on 04/26/2016).
- [169] J. F. Cherry, A. Friedland, and I. M. Shoemaker.  
 “Neutrino Portal Dark Matter: From Dwarf Galaxies to IceCube”.  
 In: *arXiv:1411.1071 [astro-ph, physics:hep-ph]* (2014).  
 URL: <http://arxiv.org/abs/1411.1071> (visited on 05/10/2016).
- [170] S. Bilmiş et al.  
 “Constraints on dark photon from neutrino-electron scattering experiments”.  
 In: *Physical Review D* 92.3 (2015), p. 033009.  
 URL: <http://link.aps.org/doi/10.1103/PhysRevD.92.033009>  
 (visited on 04/21/2016).
- [171] A. Belyaev, N. D. Christensen, and A. Pukhov.  
 “CalcHEP 3.4 for collider physics within and beyond the Standard Model”.  
 In: *Computer Physics Communications* 184.7 (2013), pp. 1729–1769.  
 URL: <http://arxiv.org/abs/1207.6082> (visited on 07/21/2016).
- [172] A. G. Beda et al. “Gemma experiment: Three years of the search for the neutrino magnetic moment”.  
 In: *Physics of Particles and Nuclei Letters* 7.6 (2010), pp. 406–409. URL:  
<http://link.springer.com/article/10.1134/S1547477110060063>  
 (visited on 07/25/2016).



- [173] R. Harnik, J. Kopp, and P. A. N. Machado.  
“Exploring  $\nu$  signals in dark matter detectors”.  
In: *Journal of Cosmology and Astroparticle Physics* 2012.07 (2012), p. 026.  
URL: <http://stacks.iop.org/1475-7516/2012/i=07/a=026> (visited on 04/26/2016).
- [174] J. Jaeckel and A. Ringwald. “The Low-Energy Frontier of Particle Physics”.  
In: *Annual Review of Nuclear and Particle Science* 60.1 (2010), pp. 405–437.  
URL: <http://dx.doi.org/10.1146/annurev.nucl.012809.104433>  
(visited on 04/28/2016).
- [175] P.-F. Yin and S.-H. Zhu.  
“Light dark sector searches at low-energy high-luminosity  $e + e -$  colliders”.  
In: *Frontiers of Physics* 11.5 (2016), pp. 1–14. URL:  
<http://link.springer.com/article/10.1007/s11467-016-0541-1>  
(visited on 04/26/2016).
- [176] M. Pospelov. “Secluded U(1) below the weak scale”.  
In: *Physical Review D* 80.9 (2009), p. 095002.  
URL: <http://link.aps.org/doi/10.1103/PhysRevD.80.095002>  
(visited on 05/27/2016).
- [177] P. Fayet. “U-boson production in  $e+e-$  annihilations,  $\psi$  and Upsilon decays, and Light Dark Matter”. In: *Physical Review D* 75.11 (2007).  
URL: <http://arxiv.org/abs/hep-ph/0702176> (visited on 07/25/2016).
- [178] D. Gorbunov, A. Makarov, and I. Timiryasov. “Decaying light particles in the SHiP experiment: Signal rate estimates for hidden photons”.  
In: *Physical Review D* 91.3 (2015), p. 035027.  
URL: <http://link.aps.org/doi/10.1103/PhysRevD.91.035027>  
(visited on 05/26/2016).
- [179] J. D. Bjorken et al.  
“New fixed-target experiments to search for dark gauge forces”.  
In: *Physical Review D* 80.7 (2009), p. 075018.  
URL: <http://link.aps.org/doi/10.1103/PhysRevD.80.075018>  
(visited on 05/26/2016).

- [180] T. Beranek and M. Vanderhaeghen. “Constraints on the Dark Photon Parameter Space from Leptonic Rare Kaon Decays”.  
In: *Phys.Rev. D* 87 (2013), p. 015024.
- [181] J. Blümlein and J. Brunner. “New Exclusion Limits on Dark Gauge Forces from Proton Bremsstrahlung in Beam-Dump Data”.  
In: *Physics Letters B* 731 (2014), pp. 320–326.  
URL: <http://arxiv.org/abs/1311.3870> (visited on 05/25/2016).
- [182] S. Andreas, C. Niebuhr, and A. Ringwald.  
“New Limits on Hidden Photons from Past Electron Beam Dumps”.  
In: *Physical Review D* 86.9 (2012).  
URL: <http://arxiv.org/abs/1209.6083> (visited on 05/24/2016).
- [183] E. M. Riordan et al.  
“Search for short-lived axions in an electron-beam-dump experiment”.  
In: *Physical Review Letters* 59.7 (1987), pp. 755–758.  
URL: <http://link.aps.org/doi/10.1103/PhysRevLett.59.755>  
(visited on 07/24/2016).
- [184] J. D. Bjorken et al. “Search for neutral metastable penetrating particles produced in the SLAC beam dump”.  
In: *Physical Review D* 38.11 (1988), pp. 3375–3386.  
URL: <http://link.aps.org/doi/10.1103/PhysRevD.38.3375> (visited on 07/24/2016).
- [185] A. Bross et al.  
“Search for short-lived particles produced in an electron beam dump”.  
In: *Physical Review Letters* 67.21 (1991), pp. 2942–2945.  
URL: <http://link.aps.org/doi/10.1103/PhysRevLett.67.2942>  
(visited on 07/24/2016).
- [186] M. Davier and H. Nguyen Ngoc.  
“An unambiguous search for a light Higgs boson”.  
In: *Physics Letters B* 229.1 (1989), pp. 150–155.  
URL: <http://www.sciencedirect.com/science/article/pii/0370269389901743> (visited on 07/24/2016).

- [187] A. Konaka et al.  
 “Search for Neutral Particles in Electron-Beam-Dump Experiment”.  
 In: *Physical Review Letters* 57.6 (1986), pp. 659–662.  
 URL: <http://link.aps.org/doi/10.1103/PhysRevLett.57.659>  
 (visited on 07/24/2016).
- [188] B. Batell, M. Pospelov, and A. Ritz.  
 “Exploring portals to a hidden sector through fixed targets”.  
 In: *Physical Review D* 80.9 (2009), p. 095024.  
 URL: <http://link.aps.org/doi/10.1103/PhysRevD.80.095024>  
 (visited on 05/12/2016).
- [189] F. Bergsma et al. “Search for axion-like particle production in 400 GeV proton-copper interactions”.  
 In: *Physics Letters B* 157.5 (1985), pp. 458–462.  
 URL: <http://www.sciencedirect.com/science/article/pii/0370269385904009> (visited on 07/24/2016).
- [190] F. Vannucci and F. Vannucci.  
 “The NOMAD Experiment at CERN, The NOMAD Experiment at CERN”.  
 In: *Advances in High Energy Physics, Advances in High Energy Physics* 2014, 2014 (2014), e129694. URL:  
<http://www.hindawi.com/journals/ahep/2014/129694/abs/>, <http://www.hindawi.com/journals/ahep/2014/129694/abs/> (visited on 07/27/2016).
- [191] G. Bernardi et al. “Search for neutrino decay”.  
 In: *Physics Letters B* 166.4 (1986), pp. 479–483.  
 URL: <http://www.sciencedirect.com/science/article/pii/0370269386916023> (visited on 07/27/2016).
- [192] J. Blümlein and J. Brunner.  
 “New Exclusion Limits for Dark Gauge Forces from Beam-Dump Data”.  
 In: *Physics Letters B* 701.2 (2011), pp. 155–159.  
 URL: <http://arxiv.org/abs/1104.2747> (visited on 07/24/2016).
- [193] S. N. Gninenko. “Stringent limits on the  $\pi^0 \rightarrow \gamma X$ ,  $X \rightarrow e^+e^-$  decay from neutrino experiments and constraints on new light gauge bosons”.

- In: *Physical Review D* 85.5 (2012).  
 URL: <http://arxiv.org/abs/1112.5438> (visited on 07/24/2016).
- [194] A. A. Aguilar-Arevalo et al. “Low Mass WIMP Searches with a Neutrino Experiment: A Proposal for Further MiniBooNE Running”.  
 In: *arXiv:1211.2258 [astro-ph, physics:hep-ex, physics:hep-ph]* (2012).  
 URL: <http://arxiv.org/abs/1211.2258> (visited on 07/24/2016).
- [195] R. Essig et al. “An electron fixed target experiment to search for a new vector boson  $A'$  decaying to  $e + e^-$ ”.  
 In: *Journal of High Energy Physics* 2011.2 (2011), pp. 1–35. URL:  
[http://link.springer.com/article/10.1007/JHEP02\(2011\)009](http://link.springer.com/article/10.1007/JHEP02(2011)009)  
 (visited on 04/26/2016).
- [196] O. Moreno. “The Heavy Photon Search Experiment at Jefferson Lab”.  
 In: *arXiv:1310.2060 [hep-ex, physics:physics]* (2013).  
 URL: <http://arxiv.org/abs/1310.2060> (visited on 07/24/2016).
- [197] J. Balewski et al. “DarkLight: A Search for Dark Forces at the Jefferson Laboratory Free-Electron Laser Facility”.  
 In: *arXiv:1307.4432 [hep-ex, physics:physics]* (2013).  
 URL: <http://arxiv.org/abs/1307.4432> (visited on 07/24/2016).
- [198] A1 Collaboration et al.  
 “Search for Light Gauge Bosons of the Dark Sector at the Mainz Microtron”.  
 In: *Physical Review Letters* 106.25 (2011), p. 251802.  
 URL: <http://link.aps.org/doi/10.1103/PhysRevLett.106.251802>  
 (visited on 07/24/2016).
- [199] A1 Collaboration et al. “Search at the Mainz Microtron for Light Massive Gauge Bosons Relevant for the Muon  $g - 2$  Anomaly”.  
 In: *Physical Review Letters* 112.22 (2014), p. 221802.  
 URL: <http://link.aps.org/doi/10.1103/PhysRevLett.112.221802>  
 (visited on 07/24/2016).
- [200] R. Essig et al. “Dark Sectors and New, Light, Weakly-Coupled Particles”.  
 In: *arXiv:1311.0029 [astro-ph, physics:hep-ex, physics:hep-ph]* (2013).  
 URL: <http://arxiv.org/abs/1311.0029> (visited on 05/02/2016).

- [201] F. Archilli et al. “Search for a vector gauge boson in  $\phi$  meson decays with the KLOE detector”. In: *Physics Letters B* 706.4–5 (2012), pp. 251–255.  
URL: <http://www.sciencedirect.com/science/article/pii/S0370269311014055> (visited on 07/24/2016).
- [202] D. Babusci et al. “Limit on the production of a light vector gauge boson in  $\phi$  meson decays with the KLOE detector”.  
In: *Physics Letters B* 720.1–3 (2013), pp. 111–115.  
URL: <http://www.sciencedirect.com/science/article/pii/S037026931300124X> (visited on 07/24/2016).
- [203] D. Babusci et al. “Search for light vector boson production in interactions with the KLOE experiment”. In: *Physics Letters B* 736 (2014), pp. 459–464.  
URL: <http://www.sciencedirect.com/science/article/pii/S0370269314005723> (visited on 07/24/2016).
- [204] A. Anastasi et al. “Limit on the production of a low-mass vector boson in  $e^+e^- \rightarrow U\gamma, U \rightarrow e^+e^-$  with the KLOE experiment”.  
In: *Physics Letters B* 750 (2015), pp. 633–637.  
URL: <http://arxiv.org/abs/1509.00740> (visited on 07/24/2016).
- [205] P. Adlarson et al. “Search for a dark photon in the decay”.  
In: *Physics Letters B* 726.1–3 (2013), pp. 187–193.  
URL: <http://www.sciencedirect.com/science/article/pii/S0370269313006941> (visited on 07/24/2016).
- [206] G. Agakishiev et al. “Searching a dark photon with HADES”.  
In: *Physics Letters B* 731 (2014), pp. 265–271.  
URL: <http://www.sciencedirect.com/science/article/pii/S0370269314001336> (visited on 07/24/2016).
- [207] HADES Collaboration. “Searching a Dark Photon with HADES”.  
In: *arXiv:1311.0216 [hep-ex, physics:hep-ph]* (2013).  
URL: <http://arxiv.org/abs/1311.0216> (visited on 05/26/2016).
- [208] BaBar Collaboration.  
“Search for a Dark Photon in  $e^+e^-$  Collisions at *BaBar*”.  
In: *Physical Review Letters* 113.20 (2014), p. 201801.

- URL: <http://link.aps.org/doi/10.1103/PhysRevLett.113.201801>  
(visited on 07/24/2016).
- [209] The Belle Collaboration.  
“Search for the dark photon and the dark Higgs boson at Belle”.  
In: *Physical Review Letters* 114.21 (2015).  
URL: <http://arxiv.org/abs/1502.00084> (visited on 05/26/2016).
- [210] Evgueni Goudzovski on behalf of the NA48/2 Collaboration. “Search for the dark photon in  $\pi^0$  decays by the NA48/2 experiment at CERN”.  
In: *arXiv:1412.8053 [hep-ex]* (2014).  
URL: <http://arxiv.org/abs/1412.8053> (visited on 05/26/2016).
- [211] A. Adare et al. “Search for dark photons from neutral meson decays in  $p + p$  and  $d + Au$  collisions at  $\sqrt{s_{NN}} = 200$  GeV”.  
In: *arXiv:1409.0851 [nucl-ex]* (2014).  
URL: <http://arxiv.org/abs/1409.0851> (visited on 05/26/2016).
- [212] M. Ahlers et al. “Laser experiments explore the hidden sector”.  
In: *Physical Review D* 77.9 (2008).  
URL: <http://arxiv.org/abs/0711.4991> (visited on 07/25/2016).
- [213] Muon, Collaboration, and G. W. Bennett. “Final Report of the Muon E821 Anomalous Magnetic Moment Measurement at BNL”.  
In: *Physical Review D* 73.7 (2006).  
URL: <http://arxiv.org/abs/hep-ex/0602035> (visited on 07/25/2016).
- [214] E. Izaguirre et al.  
“Physics Motivation for a Pilot Dark Matter Search at Jefferson Laboratory”.  
In: *Physical Review D* 90.1 (2014).  
URL: <http://arxiv.org/abs/1403.6826> (visited on 07/25/2016).
- [215] S. Abrahamyan et al.  
“Search for a new gauge boson in the  $A'$  Experiment (APEX)”.  
In: *Physical Review Letters* 107.19 (2011).  
URL: <http://arxiv.org/abs/1108.2750> (visited on 07/25/2016).
- [216] M. D. Diamond and P. Schuster.  
“Searching for Light Dark Matter with the SLAC Millicharge Experiment”.

- In: *Physical Review Letters* 111.22 (2013).  
 URL: <http://arxiv.org/abs/1307.6861> (visited on 07/25/2016).
- [217] R. Essig, P. Schuster, and N. Toro. “Probing Dark Forces and Light Hidden Sectors at Low-Energy e+e- Colliders”. In: *Physical Review D* 80.1 (2009).  
 URL: <http://arxiv.org/abs/0903.3941> (visited on 07/25/2016).
- [218] C. D. Carone and H. Murayama.  
 “Possible Light U(1) Gauge Boson Coupled to Baryon Number”.  
 In: *Physical Review Letters* 74.16 (1995), pp. 3122–3125.  
 URL: <http://arxiv.org/abs/hep-ph/9411256> (visited on 07/25/2016).
- [219] M. L. Graesser, I. M. Shoemaker, and L. Vecchi. “A dark force for baryons”.  
 In: *arXiv:1107.2666 [astro-ph, physics:hep-ph, physics:hep-th]* (2011).  
 URL: <http://arxiv.org/abs/1107.2666> (visited on 07/25/2016).
- [220] E. G. Adelberger et al.  
 “Torsion balance experiments: A low-energy frontier of particle physics”.  
 In: *Progress in Particle and Nuclear Physics* 62.1 (2009), pp. 102–134.  
 URL: <http://www.sciencedirect.com/science/article/pii/S0146641008000720> (visited on 05/27/2016).
- [221] D. F. Bartlett and S. Lögl. “Limits on an Electromagnetic Fifth Force”.  
 In: *Physical Review Letters* 61.20 (1988), pp. 2285–2287.  
 URL: <http://link.aps.org/doi/10.1103/PhysRevLett.61.2285>  
 (visited on 05/27/2016).
- [222] J. B. Dent, F. Ferrer, and L. M. Krauss. “Constraints on Light Hidden Sector Gauge Bosons from Supernova Cooling”.  
 In: *arXiv:1201.2683 [astro-ph, physics:hep-ph]* (2012).  
 URL: <http://arxiv.org/abs/1201.2683> (visited on 07/25/2016).
- [223] D. Kazanas et al.  
 “Supernova Bounds on the Dark Photon Using its Electromagnetic Decay”.  
 In: *Nuclear Physics B* 890 (2015), pp. 17–29.  
 URL: <http://arxiv.org/abs/1410.0221> (visited on 07/25/2016).

- [224] J. Redondo. “Helioscope Bounds on Hidden Sector Photons”.  
In: *Journal of Cosmology and Astroparticle Physics* 2008.07 (2008), p. 008.  
URL: <http://arxiv.org/abs/0801.1527> (visited on 07/25/2016).
- [225] H. An, M. Pospelov, and J. Pradler.  
“New stellar constraints on dark photons”.  
In: *Physics Letters B* 725.4-5 (2013), pp. 190–195.  
URL: <http://arxiv.org/abs/1302.3884> (visited on 07/25/2016).
- [226] G. G. Raffelt and G. D. Starkman.  
“Stellar energy transfer by keV-mass scalars”.  
In: *Physical Review D* 40.4 (1989), pp. 942–947.  
URL: <http://link.aps.org/doi/10.1103/PhysRevD.40.942> (visited on 07/25/2016).
- [227] A. Mirizzi, J. Redondo, and G. Sigl. “Microwave Background Constraints on Mixing of Photons with Hidden Photons”. In: *Journal of Cosmology and Astroparticle Physics* 2009.03 (2009), pp. 026–026.  
URL: <http://arxiv.org/abs/0901.0014> (visited on 07/25/2016).
- [228] CAST Collaboration. “Probing eV-scale axions with CAST”. In: *Journal of Cosmology and Astroparticle Physics* 2009.02 (2009), pp. 008–008.  
URL: <http://arxiv.org/abs/0810.4482> (visited on 07/25/2016).
- [229] G. Mangano and P. D. Serpico.  
“A robust upper limit on  $N_{\text{eff}}$  from BBN, circa 2011”.  
In: *Physics Letters B* 701.3 (2011), pp. 296–299.  
URL: <http://arxiv.org/abs/1103.1261> (visited on 07/25/2016).
- [230] J. Heeck. “Unbroken B-L Symmetry”.  
In: *Physics Letters B* 739 (2014), pp. 256–262.  
URL: <http://arxiv.org/abs/1408.6845> (visited on 07/25/2016).
- [231] D. J. Fixsen et al. “The Cosmic Microwave Background Spectrum from the Full COBE/FIRAS Data Set”.  
In: *The Astrophysical Journal* 473.2 (1996), pp. 576–587. URL: <http://arxiv.org/abs/astro-ph/9605054> (visited on 07/27/2016).



## APPENDIX A

### FIERZ IDENTITIES

In general, for the calculations of physical processes, rearranging Dirac spinors become very useful which is done by the Fierz transformations. This is especially advantageous for calculation of the cross-section for the  $\nu_e - e^-$  scattering. Thus, it will be convenient to derive the Fierz identities which will be worthwhile for calculating  $\langle |\mathcal{M}|^2 \rangle_{\nu_e - e^-}$ .

The product of bispinors can be expanded as;

$$\bar{u}_\alpha u_\beta = \frac{1}{4} \sum_j (\Gamma_j)_{\beta\alpha} \bar{u} \Gamma_j u \quad (\text{A.1})$$

where  $\Gamma_i = \{\mathbb{1}, \gamma^\mu, \sigma^{\mu\nu}, i\gamma^5 \gamma^\mu, \gamma^5\}$  is the full set of Dirac matrices. Indeed, if we multiply the both sides of the Equation (A.1) with  $(\Gamma_i)_{\alpha\beta}$  and use  $Tr \Gamma_i \Gamma_j = 2g_{ij}$  we get the identity.

Assume that we need to replace the  $\bar{u}(p_4)$  with  $\bar{u}(p_3)$  in the following product of the currents:

$$I = [\bar{u}(p_4) \gamma^\mu (1 - \gamma^5) u(p_1)] [\bar{u}(p_3) \gamma_\mu (1 - \gamma^5) u(p_2)] . \quad (\text{A.2})$$

Let us define  $A^\mu = \gamma^\mu (1 - \gamma^5)$  and  $B_\mu = \gamma_\mu (1 - \gamma^5)$ , then “ $I$ ” can be written as;

$$I = [\bar{u}(p_4) A^\mu u(p_1)] [\bar{u}(p_3) B_\mu u(p_2)] . \quad (\text{A.3})$$

This expression can be written by writing the indices explicitly as

$$I = \bar{u}(p_4)_\alpha (A^\mu)_{\alpha\beta} u(p_1)_\beta \bar{u}(p_3)_\rho (B_\mu)_{\rho\sigma} u(p_2)_\sigma . \quad (\text{A.4})$$

Since we want to replace  $\bar{u}(p_4)$  and  $\bar{u}(p_3)$  let us write this in the following form

$$I = \bar{u}(p_3)_\rho u(p_1)_\beta \bar{u}(p_4)_\alpha u(p_2)_\sigma (A^\mu)_{\alpha\beta} (B_\mu)_{\rho\sigma} . \quad (\text{A.5})$$

Using the identity in Equation (A.1) we can write,

$$\begin{aligned}\bar{u}(p_3)_\rho u(p_1)_\beta &= \frac{1}{4} \sum_i (\Gamma_i)_{\beta\rho} \bar{u}(p_3) \Gamma_i u(p_1) \\ \bar{u}(p_4)_\alpha u(p_2)_\sigma &= \frac{1}{4} \sum_j (\Gamma_j)_{\sigma\alpha} \bar{u}(p_4) \Gamma_j u(p_2)\end{aligned}\tag{A.6}$$

Then, Equation (A.5) takes the following form,

$$\begin{aligned}I &= \left[ \frac{1}{4} \sum_i (\Gamma_i)_{\beta\rho} \bar{u}(p_3) \Gamma_i u(p_1) \right] \left[ \frac{1}{4} \sum_j (\Gamma_j)_{\sigma\alpha} \bar{u}(p_4) \Gamma_j u(p_2) \right] [(A^\mu)_{\alpha\beta} (B_\mu)_{\rho\sigma}] \\ &= \frac{1}{16} \sum_i \sum_j [(A^\mu)_{\alpha\beta} (\Gamma_i)_{\beta\rho} (B_\mu)_{\rho\sigma} (\Gamma_j)_{\sigma\alpha}] [\bar{u}(p_3) \Gamma_i u(p_1)] [\bar{u}(p_4) \Gamma_j u(p_2)] \\ &= \frac{1}{16} \sum_i \sum_j [(A^\mu) (\Gamma_i) (B_\mu) (\Gamma_j)]_{\alpha\alpha} [\bar{u}(p_3) \Gamma_i u(p_1)] [\bar{u}(p_4) \Gamma_j u(p_2)] \\ &= \frac{1}{16} \sum_i \sum_j Tr [A^\mu \Gamma_i B_\mu \Gamma_j] [\bar{u}(p_3) \Gamma_i u(p_1)] [\bar{u}(p_4) \Gamma_j u(p_2)].\end{aligned}\tag{A.7}$$

We need to evaluate the subsequent 16 terms in this case.

1. For  $i = 1 \rightarrow \Gamma_1 = \mathbb{1}$

(a)  $j = 1 \rightarrow \Gamma_1 = \mathbb{1}$

$$\begin{aligned}I_{11} &= Tr[\gamma^\mu(1 - \gamma^5) \mathbb{1} \gamma_\mu(1 - \gamma^5) \mathbb{1}] [\bar{u}(p_3) \mathbb{1} u(p_1)] [\bar{u}(p_4) \mathbb{1} u(p_1)] \\ I_{11} &= Tr[\gamma^\mu(1 - \gamma^5)(1 + \gamma^5) \mathbb{1} \gamma_\mu \mathbb{1}] [\bar{u}(p_3) \mathbb{1} u(p_1)] [\bar{u}(p_4) \mathbb{1} u(p_1)] \\ I_{11} &= 0,\end{aligned}\tag{A.8}$$

where we used anti-commutation relation  $\{\gamma^\mu, \gamma^5\} = 0$  in the second step and since  $(1 - \gamma^5)(1 + \gamma^5) = 0$ ,  $I_{11}$  equals to zero.

(b)  $j = 2 \rightarrow \Gamma_2 = \gamma^\mu$

$$\begin{aligned}I_{12} &= Tr[\gamma^\mu(1 - \gamma^5) \mathbb{1} \gamma_\mu(1 - \gamma^5) \gamma^\rho] [\bar{u}(p_3) \mathbb{1} u(p_1)] [\bar{u}(p_4) \gamma^\rho u(p_1)] \\ I_{12} &= Tr[\gamma^\mu(1 - \gamma^5)(1 + \gamma^5) \mathbb{1} \gamma_\mu \gamma^\rho] [\bar{u}(p_3) \mathbb{1} u(p_1)] [\bar{u}(p_4) \gamma^\rho u(p_1)] \\ I_{12} &= 0\end{aligned}\tag{A.9}$$

(c)  $j = 3 \rightarrow \Gamma_3 = \sigma^{\mu\nu}$

$$\begin{aligned}I_{13} &= Tr[\gamma^\mu(1 - \gamma^5) \mathbb{1} \gamma_\mu(1 - \gamma^5) \sigma^{\nu\rho}] [\bar{u}(p_3) \mathbb{1} u(p_1)] [\bar{u}(p_4) \sigma^{\nu\rho} u(p_1)] \\ I_{13} &= Tr[\gamma^\mu(1 - \gamma^5)(1 + \gamma^5) \mathbb{1} \gamma_\mu \sigma^{\nu\rho}] [\bar{u}(p_3) \mathbb{1} u(p_1)] [\bar{u}(p_4) \sigma^{\nu\rho} u(p_1)] \\ I_{13} &= 0\end{aligned}\tag{A.10}$$

$$(d) \quad j = 4 \rightarrow \Gamma_4 = i\gamma^5\gamma^\mu$$

$$I_{14} = Tr[\gamma^\mu(1 - \gamma^5)\mathbb{1}\gamma_\mu(1 - \gamma^5)i\gamma^5\gamma^\mu][\bar{u}(p_3)\mathbb{1}u(p_1)][\bar{u}(p_4)i\gamma^5\gamma^\mu u(p_1)]$$

$$I_{14} = Tr[\gamma^\mu(1 - \gamma^5)(1 + \gamma^5)\mathbb{1}\gamma_\mu i\gamma^5\gamma^\mu][\bar{u}(p_3)\mathbb{1}u(p_1)][\bar{u}(p_4)i\gamma^5\gamma^\mu u(p_1)]$$

$$I_{14} = 0$$

(A.11)

$$(e) \quad j = 5 \rightarrow \Gamma_5 = i\gamma^5$$

$$I_{15} = Tr[\gamma^\mu(1 - \gamma^5)\mathbb{1}\gamma_\mu(1 - \gamma^5)i\gamma^5][\bar{u}(p_3)\mathbb{1}u(p_1)][\bar{u}(p_4)i\gamma^5 u(p_1)]$$

$$I_{15} = Tr[\gamma^\mu(1 - \gamma^5)(1 + \gamma^5)\mathbb{1}\gamma_\mu i\gamma^5][\bar{u}(p_3)\mathbb{1}u(p_1)][\bar{u}(p_4)i\gamma^5 u(p_1)]$$

$$I_{15} = 0$$

(A.12)

2. For  $i = 2 \rightarrow \Gamma_2 = \gamma^\mu$ ;

$$(a) \quad j = 1 \rightarrow \Gamma_1 = \mathbb{1}$$

$$I_{21} = Tr[\gamma^\mu(1 - \gamma^5)\gamma^\nu\gamma_\mu(1 - \gamma^5)\mathbb{1}][\bar{u}(p_3)\gamma^\nu u(p_1)][\bar{u}(p_4)\mathbb{1}u(p_1)]$$

$$I_{21} = Tr[\gamma^\mu(1 - \gamma^5)(1 - \gamma^5)\gamma^\nu\gamma_\mu][\bar{u}(p_3)\gamma^\nu u(p_1)][\bar{u}(p_4)\mathbb{1}u(p_1)] \quad (A.13)$$

$$I_{21} = 2Tr[\gamma^\mu(1 - \gamma^5)\gamma^\nu\gamma_\mu][\bar{u}(p_3)\gamma^\nu u(p_1)][\bar{u}(p_4)\mathbb{1}u(p_1)]$$

$$I_{21} = 2Tr[\gamma_\mu\gamma^\mu(1 - \gamma^5)\gamma^\nu][\bar{u}(p_3)\gamma^\nu u(p_1)][\bar{u}(p_4)\mathbb{1}u(p_1)]$$

where we used the identity  $Tr(AB) = Tr(BA)$  in the last step. Moreover, since  $Tr(\gamma_\mu\gamma^\mu = 4)$ ,  $I_{21}$  can be written as;

$$I_{21} = 8Tr[(1 - \gamma^5)\gamma^\nu][\bar{u}(p_3)\gamma^\nu u(p_1)][\bar{u}(p_4)\mathbb{1}u(p_1)]$$

$$I_{21} = 8[(Tr(\gamma^\nu) - Tr(\gamma^5\gamma^\nu))][\bar{u}(p_3)\gamma^\nu u(p_1)][\bar{u}(p_4)\mathbb{1}u(p_1)] \quad (A.14)$$

$$I_{21} = 0$$

due to trace of multiplication of odd number of  $\gamma$  matrices is zero.

$$(b) \quad j = 2 \rightarrow \Gamma_2 = \gamma^\mu$$

$$I_{22} = Tr[\gamma^\mu(1 - \gamma^5)\gamma^\nu\gamma_\mu(1 - \gamma^5)\gamma^\rho][\bar{u}(p_3)\gamma^\nu u(p_1)][\bar{u}(p_4)\gamma^\rho u(p_1)]$$

$$I_{22} = Tr[\gamma^\mu(1 - \gamma^5)(1 - \gamma^5)\gamma^\nu\gamma_\mu\gamma^\rho][\bar{u}(p_3)\gamma^\nu u(p_1)][\bar{u}(p_4)\gamma^\rho u(p_1)]$$

$$I_{22} = 2Tr[\gamma^\mu(1 - \gamma^5)\gamma^\nu\gamma_\mu\gamma^\rho][\bar{u}(p_3)\gamma^\nu u(p_1)][\bar{u}(p_4)\gamma^\rho u(p_1)]$$

$$I_{22} = 2Tr[(1 + \gamma^5)\gamma^\mu\gamma^\nu\gamma_\mu\gamma^\rho][\bar{u}(p_3)\gamma^\nu u(p_1)][\bar{u}(p_4)\gamma^\rho u(p_1)]$$

(A.15)

Since  $\gamma^\mu\gamma^\nu = 2g^{\mu\nu} - \gamma^\nu\gamma^\mu$ , we can write  $I_{22}$  as;

$$\begin{aligned} I_{22} &= 2Tr[(1 + \gamma^5)(2g^{\mu\nu} - \gamma^\nu\gamma^\mu)\gamma_\mu\gamma^\rho][\bar{u}(p_3)\gamma^\nu u(p_1)][\bar{u}(p_4)\gamma^\rho u(p_1)] , \\ I_{22} &= (4g^{\mu\nu}Tr[(1 + \gamma^5)\gamma_\mu\gamma^\rho] - 2Tr[(1 + \gamma^5)\gamma^\nu\gamma^\mu\gamma_\mu\gamma^\rho]) \\ &\quad \times [\bar{u}(p_3)\gamma^\nu u(p_1)][\bar{u}(p_4)\gamma^\rho u(p_1)] . \end{aligned} \tag{A.16}$$

Using  $\gamma^\mu\gamma_\mu = 4\mathbb{1}$  Equation (A.16) takes the form,

$$\begin{aligned} I_{22} &= (4g^{\mu\nu}Tr[\gamma_\mu\gamma^\rho] + 4g^{\mu\nu}Tr[\gamma^5\gamma_\mu\gamma^\rho] - 8Tr[(1 + \gamma^5)\gamma^\nu\gamma^\rho]) \\ &\quad [\bar{u}(p_3)\gamma^\nu u(p_1)][\bar{u}(p_4)\gamma^\rho u(p_1)] , \\ I_{22} &= (4Tr[\gamma^\nu\gamma^\rho] + 4Tr[\gamma^5\gamma^\nu\gamma^\rho] - 8Tr[(1 + \gamma^5)\gamma^\nu\gamma^\rho]) \\ &\quad \times [\bar{u}(p_3)\gamma^\nu u(p_1)][\bar{u}(p_4)\gamma^\rho u(p_1)] . \end{aligned} \tag{A.17}$$

Finally, using  $Tr[\gamma^5\gamma^\mu\gamma^\nu] = 0$  and simplifying the terms, we find  $I_{22}$  as;

$$\begin{aligned} I_{22} &= (4Tr[\gamma^\nu\gamma^\rho] - 8Tr[(1 + \gamma^5)\gamma^\nu\gamma^\rho])[\bar{u}(p_3)\gamma^\nu u(p_1)][\bar{u}(p_4)\gamma^\rho u(p_1)] \\ I_{22} &= (4Tr[\gamma^\nu\gamma^\rho] - 8Tr[\gamma^\nu\gamma^\rho] - 8Tr[\gamma^5\gamma^\nu\gamma^\rho]) \\ &\quad \times [\bar{u}(p_3)\gamma^\nu u(p_1)][\bar{u}(p_4)\gamma^\rho u(p_1)] \\ I_{22} &= -4Tr[\gamma^\nu\gamma^\rho][\bar{u}(p_3)\gamma^\nu u(p_1)][\bar{u}(p_4)\gamma^\rho u(p_1)] \\ I_{22} &= -16g^{\nu\rho}[\bar{u}(p_3)\gamma^\nu u(p_1)][\bar{u}(p_4)\gamma^\rho u(p_1)] . \end{aligned} \tag{A.18}$$

(c)  $j = 3 \rightarrow \Gamma_3 = \sigma^{\mu\nu}$

$$\begin{aligned} I_{23} &= Tr[\gamma^\mu(1 - \gamma^5)\gamma^\nu\gamma_\mu(1 - \gamma^5)\sigma^{\lambda\rho}][\bar{u}(p_3)\gamma^\nu u(p_1)][\bar{u}(p_4)\sigma^{\lambda\rho} u(p_1)] \\ I_{23} &= 0 \end{aligned} \tag{A.19}$$

which is due to the fact that trace of odd number  $\gamma$  matrices is equal to zero.

(d)  $j = 4 \rightarrow \Gamma_4 = i\gamma^5\gamma^\rho$

$$\begin{aligned} I_{24} &= Tr[\gamma^\mu(1 - \gamma^5)\gamma^\nu\gamma_\mu(1 - \gamma^5)i\gamma^5\gamma^\rho][\bar{u}(p_3)\gamma^\nu u(p_1)][\bar{u}(p_4)i\gamma^5\gamma^\rho u(p_1)] , \\ I_{24} &= -Tr[\gamma^\mu(1 - \gamma^5)\gamma^\nu\gamma_\mu(1 - \gamma^5)\gamma^5\gamma^\rho][\bar{u}(p_3)\gamma^\nu u(p_1)][\bar{u}(p_4)\gamma^5\gamma^\rho u(p_1)] , \\ I_{24} &= Tr[\gamma^\mu(1 - \gamma^5)\gamma^\nu\gamma_\mu(1 - \gamma^5)\gamma^\rho][\bar{u}(p_3)\gamma^\nu u(p_1)][\bar{u}(p_4)\gamma^5\gamma^\rho u(p_1)] , \end{aligned} \tag{A.20}$$

where in the last step  $(1 - \gamma^5)\gamma^5 = -(1 - \gamma^5)$  is used. Now it is easy to see that the trace part of Equation (A.20) is same with Equation (A.15). Hence, using result of Equation (A.18) we get;

$$\begin{aligned} I_{24} &= Tr[\gamma^\mu(1 - \gamma^5)\gamma^\nu\gamma_\mu(1 - \gamma^5)\gamma^\rho][\bar{u}(p_3)\gamma^\nu u(p_1)][\bar{u}(p_4)\gamma^5\gamma^\rho u(p_1)] \\ I_{24} &= -16g^{\lambda\rho}[\bar{u}(p_3)\gamma^\nu u(p_1)][\bar{u}(p_4)\gamma^5\gamma^\rho u(p_1)]. \end{aligned} \quad (\text{A.21})$$

(e)  $j = 5 \rightarrow \Gamma_5 = i\gamma^5$

$$\begin{aligned} I_{25} &= Tr[\gamma^\mu(1 - \gamma^5)\gamma^\nu\gamma_\mu(1 - \gamma^5)i\gamma^5][\bar{u}(p_3)\gamma^\nu u(p_1)][\bar{u}(p_4)i\gamma^5 u(p_1)] \\ I_{25} &= 0. \end{aligned} \quad (\text{A.22})$$

which is again due to trace of odd number  $\gamma$  matrices being equal to zero.

3. For  $i = 3 \rightarrow \Gamma_3 = \sigma^{\mu\nu}$

(a)  $j = 1 \rightarrow \Gamma_1 = \mathbb{1}$

$$\begin{aligned} I_{31} &= Tr[\gamma^\mu(1 - \gamma^5)\sigma^{\nu\rho}\gamma_\mu(1 - \gamma^5)\mathbb{1}][\bar{u}(p_3)\sigma^{\nu\rho} u(p_1)][\bar{u}(p_4)\mathbb{1} u(p_1)] \\ I_{31} &= Tr[\gamma^\mu(1 - \gamma^5)(1 + \gamma^5)\sigma^{\nu\rho}\gamma_\mu\mathbb{1}][\bar{u}(p_3)\sigma^{\nu\rho} u(p_1)][\bar{u}(p_4)\mathbb{1} u(p_1)] \\ I_{31} &= 0 \end{aligned} \quad (\text{A.23})$$

where we have used  $(1 - \gamma^5)(1 + \gamma^5) = 0$ .

(b)  $j = 2 \rightarrow \Gamma_2 = \gamma^\mu$

$$\begin{aligned} I_{32} &= Tr[\gamma^\mu(1 - \gamma^5)\sigma^{\nu\rho}\gamma_\mu(1 - \gamma^5)\gamma^\lambda][\bar{u}(p_3)\sigma^{\nu\rho} u(p_1)][\bar{u}(p_4)\gamma^\lambda u(p_1)] \\ I_{32} &= Tr[\gamma^\mu(1 - \gamma^5)(1 + \gamma^5)\sigma^{\nu\rho}\gamma_\mu\gamma^\lambda][\bar{u}(p_3)\sigma^{\nu\rho} u(p_1)][\bar{u}(p_4)\gamma^\lambda u(p_1)] \\ I_{32} &= 0. \end{aligned} \quad (\text{A.24})$$

(c)  $j = 3 \rightarrow \Gamma_3 = \sigma^{\mu\nu}$

$$\begin{aligned} I_{33} &= Tr[\gamma^\mu(1 - \gamma^5)\sigma^{\nu\rho}\gamma_\mu(1 - \gamma^5)\sigma^{\alpha\beta}][\bar{u}(p_3)\sigma^{\nu\rho} u(p_1)][\bar{u}(p_4)\sigma^{\alpha\beta} u(p_1)] \\ I_{33} &= Tr[\gamma^\mu(1 - \gamma^5)(1 + \gamma^5)\sigma^{\nu\rho}\gamma_\mu\sigma^{\alpha\beta}][\bar{u}(p_3)\sigma^{\nu\rho} u(p_1)][\bar{u}(p_4)\sigma^{\alpha\beta} u(p_1)] \\ I_{33} &= 0. \end{aligned} \quad (\text{A.25})$$

(d)  $j = 4 \rightarrow \Gamma_4 = i\gamma^5\gamma^\mu$

$$I_{34} = Tr[\gamma^\mu(1 - \gamma^5)\sigma^{\nu\rho}\gamma_\mu(1 - \gamma^5)i\gamma^5\gamma^\lambda][\bar{u}(p_3)\sigma^{\nu\rho}u(p_1)][\bar{u}(p_4)i\gamma^5\gamma^\lambda u(p_1)]$$

$$I_{34} = Tr[\gamma^\mu(1 - \gamma^5)(1 + \gamma^5)\sigma^{\nu\rho}\gamma_\mu i\gamma^5\gamma^\lambda][\bar{u}(p_3)\sigma^{\nu\rho}u(p_1)][\bar{u}(p_4)i\gamma^5\gamma^\lambda u(p_1)]$$

$$I_{34} = 0.$$

(A.26)

(e)  $j = 5 \rightarrow \Gamma_5 = \gamma^5$

$$I_{35} = Tr[\gamma^\mu(1 - \gamma^5)\sigma^{\nu\rho}\gamma_\mu(1 - \gamma^5)\gamma^5][\bar{u}(p_3)\sigma^{\nu\rho}u(p_1)][\bar{u}(p_4)\gamma^5 u(p_1)]$$

$$I_{35} = Tr[\gamma^\mu(1 - \gamma^5)(1 + \gamma^5)\sigma^{\nu\rho}\gamma_\mu\gamma^5][\bar{u}(p_3)\sigma^{\nu\rho}u(p_1)][\bar{u}(p_4)\gamma^5 u(p_1)]$$

$$I_{35} = 0.$$

(A.27)

4. For  $i = 4 \rightarrow \Gamma_4 = i\gamma^5\gamma^\mu$

(a)  $j = 1 \rightarrow \Gamma_1 = \mathbb{1}$

$$I_{41} = Tr[\gamma^\mu(1 - \gamma^5)i\gamma^5\gamma^\nu\gamma_\mu(1 - \gamma^5)\mathbb{1}][\bar{u}(p_3)i\gamma^5\gamma^\nu u(p_1)][\bar{u}(p_4)\mathbb{1}u(p_1)]$$

$$I_{41} = -Tr[\gamma^\mu(1 - \gamma^5)\gamma^5\gamma^\nu\gamma_\mu(1 - \gamma^5)\mathbb{1}][\bar{u}(p_3)\gamma^5\gamma^\nu u(p_1)][\bar{u}(p_4)\mathbb{1}u(p_1)]$$

$$I_{41} = Tr[\gamma^\mu(1 - \gamma^5)\gamma^\nu\gamma_\mu(1 - \gamma^5)\mathbb{1}][\bar{u}(p_3)\gamma^5\gamma^\nu u(p_1)][\bar{u}(p_4)\mathbb{1}u(p_1)]$$

$$I_{41} = -Tr[\gamma^\mu(1 - \gamma^5)(1 - \gamma^5)\gamma^\nu\gamma_\mu\mathbb{1}][\bar{u}(p_3)\gamma^5\gamma^\nu u(p_1)][\bar{u}(p_4)\mathbb{1}u(p_1)]$$

$$I_{41} = -2Tr[\gamma^\mu(1 - \gamma^5)\gamma^\nu\gamma_\mu\mathbb{1}][\bar{u}(p_3)\gamma^5\gamma^\nu u(p_1)][\bar{u}(p_4)\mathbb{1}u(p_1)]$$

$$I_{41} = 0.$$

(A.28)

which is due to trace of odd number  $\gamma$  matrices being equal to zero. Moreover, in the third step notice that we used  $(1 - \gamma^5)\gamma^5 = -(1 - \gamma^5)$ .

(b)  $j = 2 \rightarrow \Gamma_2 = \gamma^\mu$

$$I_{42} = Tr[\gamma^\mu(1 - \gamma^5)i\gamma^5\gamma^\nu\gamma_\mu(1 - \gamma^5)\gamma^\rho][\bar{u}(p_3)i\gamma^5\gamma^\nu u(p_1)][\bar{u}(p_4)\gamma^\rho u(p_1)]$$

$$I_{42} = -Tr[\gamma^\mu(1 - \gamma^5)\gamma^5\gamma^\nu\gamma_\mu(1 - \gamma^5)\gamma^\rho][\bar{u}(p_3)\gamma^5\gamma^\nu u(p_1)][\bar{u}(p_4)\gamma^\rho u(p_1)]$$

$$I_{42} = Tr[\gamma^\mu(1 - \gamma^5)\gamma^\nu\gamma_\mu(1 - \gamma^5)\gamma^\rho][\bar{u}(p_3)\gamma^5\gamma^\nu u(p_1)][\bar{u}(p_4)\gamma^\rho u(p_1)].$$

(A.29)

The trace part of the above equation is same with Equation (A.15). Hence;

$$I_{42} = -16g^{\nu\rho}[\bar{u}(p_3)\gamma^5\gamma^\nu u(p_1)][\bar{u}(p_4)\gamma^\rho u(p_1)]. \quad (A.30)$$

(c)  $j = 3 \rightarrow \Gamma_3 = \sigma^{\mu\nu}$

$$\begin{aligned}
I_{43} &= Tr[\gamma^\mu(1 - \gamma^5)i\gamma^5\gamma^\nu\gamma_\mu(1 - \gamma^5)\sigma^{\lambda\rho}] \\
&\quad \times [\bar{u}(p_3)i\gamma^5\gamma^\nu u(p_1)][\bar{u}(p_4)\sigma^{\lambda\rho}u(p_1)] \\
I_{43} &= -Tr[\gamma^\mu(1 - \gamma^5)\gamma^5\gamma^\nu\gamma_\mu(1 - \gamma^5)\sigma^{\lambda\rho}] \\
&\quad \times [\bar{u}(p_3)\gamma^5\gamma^\nu u(p_1)][\bar{u}(p_4)\sigma^{\lambda\rho}u(p_1)] \\
I_{43} &= Tr[\gamma^\mu(1 - \gamma^5)\gamma^\nu\gamma_\mu(1 - \gamma^5)\sigma^{\lambda\rho}][\bar{u}(p_3)\gamma^5\gamma^\nu u(p_1)][\bar{u}(p_4)\sigma^{\lambda\rho}u(p_1)] \\
I_{43} &= -Tr[\gamma^\mu(1 - \gamma^5)(1 - \gamma^5)\gamma^\nu\gamma_\mu\sigma^{\lambda\rho}][\bar{u}(p_3)\gamma^5\gamma^\nu u(p_1)][\bar{u}(p_4)\sigma^{\lambda\rho}u(p_1)] \\
I_{43} &= -2Tr[\gamma^\mu(1 - \gamma^5)\gamma^\nu\gamma_\mu\sigma^{\lambda\rho}][\bar{u}(p_3)\gamma^5\gamma^\nu u(p_1)][\bar{u}(p_4)\sigma^{\lambda\rho}u(p_1)] \\
I_{43} &= 0 .
\end{aligned} \tag{A.31}$$

(d)  $j = 4 \rightarrow \Gamma_4 = i\gamma^5\gamma^\mu$

$$\begin{aligned}
I_{44} &= Tr[\gamma^\mu(1 - \gamma^5)i\gamma^5\gamma^\nu\gamma_\mu(1 - \gamma^5)i\gamma^5\gamma^\rho] \\
&\quad \times [\bar{u}(p_3)i\gamma^5\gamma^\nu u(p_1)][\bar{u}(p_4)i\gamma^5\gamma^\rho u(p_1)] \\
I_{44} &= Tr[\gamma^\mu(1 - \gamma^5)\gamma^5\gamma^\nu\gamma_\mu(1 - \gamma^5)\gamma^5\gamma^\rho] \\
&\quad \times [\bar{u}(p_3)\gamma^5\gamma^\nu u(p_1)][\bar{u}(p_4)\gamma^5\gamma^\rho u(p_1)] \\
I_{44} &= -Tr[\gamma^\mu(1 - \gamma^5)\gamma^\nu\gamma_\mu(1 - \gamma^5)\gamma^5\gamma^\rho] \\
&\quad \times [\bar{u}(p_3)\gamma^5\gamma^\nu u(p_1)][\bar{u}(p_4)\gamma^5\gamma^\rho u(p_1)] \\
I_{44} &= +Tr[\gamma^\mu(1 - \gamma^5)\gamma^\nu\gamma_\mu(1 - \gamma^5)\gamma^\rho][\bar{u}(p_3)\gamma^5\gamma^\nu u(p_1)][\bar{u}(p_4)\gamma^5\gamma^\rho u(p_1)] .
\end{aligned} \tag{A.32}$$

which is same with the trace part of Equation (A.15) and then we get

$$I_{44} = -16g^{\nu\rho}[\bar{u}(p_3)\gamma^5\gamma^\nu u(p_1)][\bar{u}(p_4)i\gamma^5\gamma^\rho u(p_1)] . \tag{A.33}$$

(e)  $j = 5 \rightarrow \Gamma_5 = \gamma^5$

$$\begin{aligned}
I_{45} &= Tr[\gamma^\mu(1 - \gamma^5)i\gamma^5\gamma^\nu\gamma_\mu(1 - \gamma^5)\gamma^5][\bar{u}(p_3)i\gamma^5\gamma^\nu u(p_1)][\bar{u}(p_4)\gamma^5 u(p_1)] \\
I_{45} &= -Tr[\gamma^\mu(1 - \gamma^5)\gamma^5\gamma^\nu\gamma_\mu(1 - \gamma^5)\gamma^5][\bar{u}(p_3)\gamma^5\gamma^\nu u(p_1)][\bar{u}(p_4)\gamma^5 u(p_1)] \\
I_{45} &= Tr[\gamma^\mu(1 - \gamma^5)\gamma^5\gamma^\nu\gamma_\mu(1 - \gamma^5)][\bar{u}(p_3)\gamma^5\gamma^\nu u(p_1)][\bar{u}(p_4)\gamma^5 u(p_1)] \\
I_{45} &= -Tr[\gamma^\mu(1 - \gamma^5)\gamma^\nu\gamma_\mu(1 - \gamma^5)][\bar{u}(p_3)\gamma^5\gamma^\nu u(p_1)][\bar{u}(p_4)\gamma^5 u(p_1)] \\
I_{45} &= -Tr[\gamma^\mu(1 - \gamma^5)(1 - \gamma^5)\gamma^\nu\gamma_\mu][\bar{u}(p_3)\gamma^5\gamma^\nu u(p_1)][\bar{u}(p_4)\gamma^5 u(p_1)] \\
I_{45} &= -2Tr[\gamma^\mu(1 - \gamma^5)\gamma^\nu\gamma_\mu][\bar{u}(p_3)\gamma^5\gamma^\nu u(p_1)][\bar{u}(p_4)\gamma^5 u(p_1)] \\
I_{45} &= 0 .
\end{aligned} \tag{A.34}$$

which is again due to vanishing trace of odd number  $\gamma$  matrices.

5. For  $i = 5 \rightarrow \Gamma_5 = \gamma^5$

(a)  $j = 1 \rightarrow \Gamma_1 = \mathbb{1}$

$$\begin{aligned}
I_{51} &= Tr[\gamma^\mu(1 - \gamma^5)\gamma^5\gamma_\mu(1 - \gamma^5)\mathbb{1}][\bar{u}(p_3)\gamma^5 u(p_1)][\bar{u}(p_4)\mathbb{1}u(p_1)] \\
I_{51} &= -Tr[\gamma^\mu(1 - \gamma^5)\gamma_\mu(1 - \gamma^5)\mathbb{1}][\bar{u}(p_3)\gamma^5 u(p_1)][\bar{u}(p_4)\mathbb{1}u(p_1)] \\
I_{51} &= -Tr[\gamma^\mu(1 - \gamma^5)(1 + \gamma^5)\gamma_\mu\mathbb{1}][\bar{u}(p_3)\gamma^5 u(p_1)][\bar{u}(p_4)\mathbb{1}u(p_1)] \\
I_{51} &= 0 .
\end{aligned} \tag{A.35}$$

(b)  $j = 2 \rightarrow \Gamma_2 = \gamma^\mu$

$$\begin{aligned}
I_{52} &= Tr[\gamma^\mu(1 - \gamma^5)\gamma^5\gamma_\mu(1 - \gamma^5)\gamma^\nu][\bar{u}(p_3)\gamma^5 u(p_1)][\bar{u}(p_4)\gamma^\nu u(p_1)] \\
I_{52} &= -Tr[\gamma^\mu(1 - \gamma^5)\gamma_\mu(1 - \gamma^5)\gamma^\nu][\bar{u}(p_3)\gamma^5 u(p_1)][\bar{u}(p_4)\gamma^\nu u(p_1)] \\
I_{52} &= -Tr[\gamma^\mu(1 - \gamma^5)(1 + \gamma^5)\gamma_\mu\gamma^\nu][\bar{u}(p_3)\gamma^5 u(p_1)][\bar{u}(p_4)\gamma^\nu u(p_1)] \\
I_{52} &= 0 .
\end{aligned} \tag{A.36}$$

(c)  $j = 3 \rightarrow \Gamma_3 = \sigma^{\mu\nu}$

$$\begin{aligned}
I_{53} &= Tr[\gamma^\mu(1 - \gamma^5)\gamma^5\gamma_\mu(1 - \gamma^5)\sigma^{\nu\rho}][\bar{u}(p_3)\gamma^5 u(p_1)][\bar{u}(p_4)\sigma^{\nu\rho} u(p_1)] \\
I_{53} &= -Tr[\gamma^\mu(1 - \gamma^5)\gamma_\mu(1 - \gamma^5)\sigma^{\nu\rho}][\bar{u}(p_3)\gamma^5 u(p_1)][\bar{u}(p_4)\sigma^{\nu\rho} u(p_1)] \\
I_{53} &= -Tr[\gamma^\mu(1 - \gamma^5)(1 + \gamma^5)\gamma_\mu\sigma^{\nu\rho}][\bar{u}(p_3)\gamma^5 u(p_1)][\bar{u}(p_4)\sigma^{\nu\rho} u(p_1)] \\
I_{53} &= 0 .
\end{aligned} \tag{A.37}$$



$$(d) \quad j = 4 \rightarrow \Gamma_4 = i\gamma^5\gamma^\mu$$

$$\begin{aligned} I_{54} &= Tr[\gamma^\mu(1 - \gamma^5)\gamma^5\gamma_\mu(1 - \gamma^5)i\gamma^5\gamma^\nu][\bar{u}(p_3)\gamma^5u(p_1)][\bar{u}(p_4)i\gamma^5\gamma^\nu u(p_1)] \\ I_{54} &= -Tr[\gamma^\mu(1 - \gamma^5)\gamma_\mu(1 - \gamma^5)i\gamma^5\gamma^\nu][\bar{u}(p_3)\gamma^5u(p_1)][\bar{u}(p_4)i\gamma^5\gamma^\nu u(p_1)] \\ I_{54} &= -Tr[\gamma^\mu(1 - \gamma^5)(1 + \gamma^5)\gamma_\mu i\gamma^5\gamma^\nu][\bar{u}(p_3)\gamma^5u(p_1)][\bar{u}(p_4)i\gamma^5\gamma^\nu u(p_1)] \\ I_{54} &= 0 . \end{aligned} \tag{A.38}$$

$$(e) \quad j = 5 \rightarrow \Gamma_5 = \gamma^5$$

$$\begin{aligned} I_{55} &= Tr[\gamma^\mu(1 - \gamma^5)\gamma^5\gamma_\mu(1 - \gamma^5)\gamma^5][\bar{u}(p_3)\gamma^5u(p_1)][\bar{u}(p_4)\gamma^5u(p_1)] \\ I_{55} &= -Tr[\gamma^\mu(1 - \gamma^5)\gamma_\mu(1 - \gamma^5)\gamma^5][\bar{u}(p_3)\gamma^5u(p_1)][\bar{u}(p_4)\gamma^5u(p_1)] \\ I_{55} &= -Tr[\gamma^\mu(1 - \gamma^5)(1 + \gamma^5)\gamma_\mu\gamma^5][\bar{u}(p_3)\gamma^5u(p_1)][\bar{u}(p_4)\gamma^5u(p_1)] \\ I_{55} &= 0 . \end{aligned} \tag{A.39}$$

As a result, we obtained that the only non-vanishing terms are  $I_{22}$ ,  $I_{24}$ ,  $I_{42}$  and  $I_{44}$ .

We can write Equation (A.7) as;

$$\begin{aligned} I &= \frac{1}{16}(I_{22} + I_{24} + I_{42} + I_{44}) \\ I_{ij} &= \frac{1}{16} \left( -16g^{\lambda\rho}[\bar{u}(p_3)\gamma^\nu u(p_1)][\bar{u}(p_4)\gamma^5\gamma^\rho u(p_1)] \right. \\ &\quad - 16g^{\nu\rho}[\bar{u}(p_3)\gamma^\nu u(p_1)][\bar{u}(p_4)\gamma^\rho u(p_1)] \\ &\quad - 16g^{\nu\rho}[\bar{u}(p_3)\gamma^5\gamma^\nu u(p_1)][\bar{u}(p_4)\gamma^\rho u(p_1)] \\ &\quad \left. - 16g^{\nu\rho}[\bar{u}(p_3)\gamma^5\gamma^\nu u(p_1)][\bar{u}(p_4)\gamma^5\gamma^\rho u(p_1)] \right) . \end{aligned} \tag{A.40}$$

Once we simplify Equation (A.40) we obtain

$$\begin{aligned} I &= - \left( [\bar{u}(p_3)\gamma^\nu u(p_1)][\bar{u}(p_4)\gamma^5\gamma_\nu u(p_1)] + [\bar{u}(p_3)\gamma^\nu u(p_1)][\bar{u}(p_4)\gamma_\nu u(p_1)] \right. \\ &\quad \left. + [\bar{u}(p_3)\gamma^5\gamma^\nu u(p_1)][\bar{u}(p_4)\gamma_\nu u(p_1)] + [\bar{u}(p_3)\gamma^5\gamma^\nu u(p_1)][\bar{u}(p_4)\gamma^5\gamma_\nu u(p_1)] \right) . \end{aligned} \tag{A.41}$$

When we collect the terms in the above equation we get

$$\begin{aligned}
I &= -[\bar{u}(p_3)\gamma^\nu u(p_1)]([\bar{u}(p_4)\gamma^5\gamma_\nu u(p_1)] + [\bar{u}(p_4)\gamma_\nu u(p_1)]) \\
&\quad - [\bar{u}(p_3)\gamma^5\gamma^\nu u(p_1)]([\bar{u}(p_4)\gamma_\nu u(p_1)] + [\bar{u}(p_4)\gamma^5\gamma_\nu u(p_1)]) \\
&= -[\bar{u}(p_3)\gamma^\nu u(p_1)]([\bar{u}(p_4)(1 + \gamma^5)\gamma_\nu u(p_1)]) \\
&\quad - [\bar{u}(p_3)\gamma^5\gamma^\nu u(p_1)]([\bar{u}(p_4)(1 + \gamma^5)\gamma_\nu u(p_1)]) \\
&= -[\bar{u}(p_3)(1 + \gamma^5)\gamma^\nu u(p_1)][\bar{u}(p_4)(1 + \gamma^5)\gamma_\nu u(p_1)] .
\end{aligned} \tag{A.42}$$

Moreover, if we collect ( $[\bar{u}(p_4)(1 + \gamma^5)\gamma_\nu u(p_1)]$ ) terms together in Equation (A.42) we get;

$$I = -[\bar{u}(p_3)\gamma^\mu(1 - \gamma^5)u(p_1)][\bar{u}(p_4)\gamma_\mu(1 - \gamma^5)u(p_1)] . \tag{A.43}$$

Finally, we obtained the following Fierz rearrangement formula

$$\boxed{[\bar{u}(p_4)\gamma^\mu(1 - \gamma^5)u(p_1)][\bar{u}(p_3)\gamma_\mu(1 - \gamma^5)u(p_2)] = -[\bar{u}(p_3)\gamma^\mu(1 - \gamma^5)u(p_1)] \times [\bar{u}(p_4)\gamma_\mu(1 - \gamma^5)u(p_2)] .} \tag{A.44}$$

Hence, we showed that once we replace the  $\bar{u}(p_4)$  with  $\bar{u}(p_3)$  in the amplitude of the  $\nu_\mu - e^-$  scattering, the minus sign appears, due to the anti-commuting nature of spin 1/2 particles.

## APPENDIX B

### SCALAR PRODUCTS IN THE REST FRAME OF THE ELECTRON

Since  $|\mathcal{M}|^2$  contains terms like  $p_1 \cdot p_2$ ,  $p_1 \cdot p_4$ ,  $p_1 \cdot p_3$ ,  $p_2 \cdot p_3$  and  $p_1 \cdot p_3$  let us calculate these terms in terms of the recoil energy of the electron which is the observed quantity in the low-energy neutrino experiments.

The  $\nu - e^-$  scattering before and after the interaction is shown schematically in Figure (B.1) in the rest frame of the initial electron. In the elastic scattering,  $m_1 = m_3 = m_\nu$  and  $m_2 = m_4 = m_e$ . We can find relations between these four momenta using the energy-momentum conservation,  $p_1 + p_2 = p_3 + p_4$ . Squaring this relation we have,

$$\begin{aligned}
 (p_1 + p_2)^2 &= (p_3 + p_4)^2 \\
 p_1^2 + p_2^2 + 2p_1 \cdot p_2 &= p_3^2 + p_4^2 + 2p_3 \cdot p_4 \\
 m_1^2 + m_2^2 + 2p_1 \cdot p_2 &= m_3^2 + m_4^2 + 2p_3 \cdot p_4 \\
 2p_1 \cdot p_2 &= 2p_3 \cdot p_4 \\
 \boxed{p_1 \cdot p_2 = p_3 \cdot p_4}
 \end{aligned} \tag{B.1}$$

Similarly we can relate  $p_1 \cdot p_4$  with  $p_2 \cdot p_3$  as;

$$\begin{aligned}
 (p_1 - p_4)^2 &= (p_3 - p_2)^2 \\
 p_1^2 + p_4^2 - 2p_1 \cdot p_4 &= p_3^2 + p_2^2 - 2p_3 \cdot p_2 \\
 m_1^2 + m_4^2 - 2p_1 \cdot p_4 &= m_3^2 + m_2^2 - 2p_3 \cdot p_2 \\
 -2p_1 \cdot p_4 &= -2p_3 \cdot p_2 \\
 \boxed{p_1 \cdot p_4 = p_2 \cdot p_3}
 \end{aligned} \tag{B.2}$$

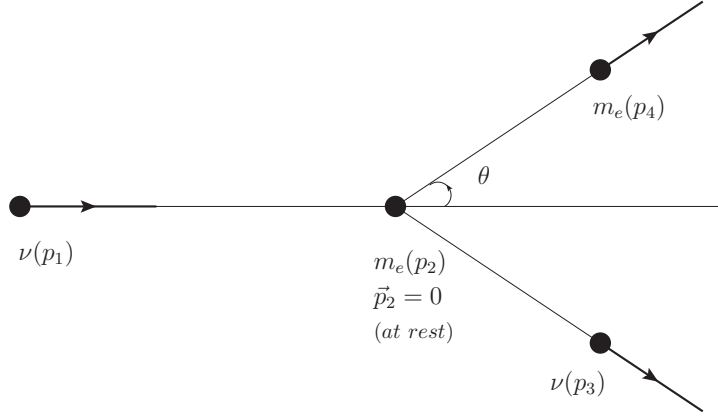


Figure B.1: The neutrino electron scattering is illustrated schematically in the rest frame of the initial electron.

For  $p_1 \cdot p_2$  we have

$$\begin{aligned} p_1 \cdot p_2 &= E_1 E_2 - \vec{p}_1 \cdot \vec{p}_2 \\ &= E_1 E_2 \end{aligned} \tag{B.3}$$

$$\boxed{p_1 \cdot p_2 = E_1 m_2}$$

For  $p_2 \cdot p_3$ :

$$\begin{aligned} p_2 \cdot p_3 &= E_2 E_3 - \vec{p}_2 \cdot \vec{p}_3 \\ &= E_2 E_3 \\ &= E_2 \overbrace{(E_1 + E_2 - E_4)}^{E_3} \\ &= m_2 (E_1 + m_2 - E_4) \end{aligned} \tag{B.4}$$

$$\boxed{p_2 \cdot p_3 = m_2 (E_1 - T)}$$

Similarly for  $p_2 \cdot p_4$  we get;

$$\begin{aligned} p_2 \cdot p_4 &= E_2 E_4 - \vec{p}_2 \cdot \vec{p}_4 \\ &= E_2 E_4 \end{aligned} \tag{B.5}$$

$$\boxed{p_2 \cdot p_4 = m_2 E_4}.$$

To find  $p_1 \cdot p_3$ , it is better to start with the relation  $(p_1 - p_3)^2 = (p_4 - p_2)^2$ . Hence,

$$\begin{aligned}
(p_1 - p_3)^2 &= (p_4 - p_2)^2 \\
p_1^2 + p_3^2 - 2p_1 \cdot p_3 &= p_4^2 + p_2^2 - 2p_4 \cdot p_2 \\
m_1^2 + m_3^2 - 2p_1 \cdot p_3 &= m_4^2 + m_2^2 - 2p_4 \cdot p_2 \\
2m_\nu^2 - 2p_1 \cdot p_3 &= 2m_2^2 - 2p_4 \cdot p_2 \\
p_1 \cdot p_3 &= m_\nu^2 - m_2^2 + \underbrace{p_2 \cdot p_4}_{m_2 E_4} \\
p_1 \cdot p_3 &= m_\nu^2 - m_2^2 + m_2 E_4 \\
p_1 \cdot p_3 &= m_\nu^2 + m_2(E_4 - m_2) \\
\boxed{p_1 \cdot p_3} &= \boxed{m_\nu^2 + m_2 T}
\end{aligned} \tag{B.6}$$

Thus, for the elastic scattering, we reach the following results for terms included in  $|\mathcal{M}|^2$ .

$$\begin{aligned}
(p_1 \cdot p_2) \cdot (p_3 \cdot p_4) &= (p_1 \cdot p_2)^2 \\
\boxed{(p_1 \cdot p_2) \cdot (p_3 \cdot p_4)} &= \boxed{E_1^2 m_2^2}
\end{aligned} \tag{B.7}$$

where we used Equation (B.1).

For the term  $(p_1 \cdot p_4) \cdot (p_2 \cdot p_3)$  using Equation (B.2) we get;

$$\begin{aligned}
(p_1 \cdot p_4) \cdot (p_2 \cdot p_3) &= (p_2 \cdot p_3)^2 \\
&= (m_2 E_1 + m_2^2 - m_2 E_4)^2 \\
\boxed{(p_1 \cdot p_4) \cdot (p_2 \cdot p_3)} &= \boxed{m_e^2 (E_1 - T)^2}
\end{aligned} \tag{B.8}$$

Collecting our findings, we get

$$\boxed{
\begin{aligned}
p_1 \cdot p_3 &= m_\nu^2 + m_e T \\
p_2 \cdot p_4 &= m_e E_4 \\
(p_1 \cdot p_4)(p_2 \cdot p_3) &= m_e^2 (E_1 - T)^2 \\
(p_1 \cdot p_2)(p_3 \cdot p_4) &= E_1^2 m_e^2
\end{aligned}
} \tag{B.9}$$



## APPENDIX C

### MAXIMUM RECOIL ENERGY OF THE ELECTRON

The recoil energy of the electron gets its maximum value when the neutrino scatters in backward direction. To find the maximum recoil energy in terms of the incoming energy of neutrinos, let us start with Equation (B.1).

$$\begin{aligned}
 p_1 \cdot p_2 &= p_3 \cdot p_4 \\
 E_1 E_2 - \vec{p}_1 \cdot \vec{p}_2 &= E_3 E_4 - \vec{p}_3 \cdot \vec{p}_4 \\
 E_1 E_2 &= E_3 E_4 - |\vec{p}_3| |\vec{p}_4| \cos(180) \\
 E_1 m_e &= E_3 E_4 + |\vec{p}_3| |\vec{p}_4|
 \end{aligned} \tag{C.1}$$

in which we used the fact that  $m_2$  is at rest, hence  $\vec{p}_2 = 0$  and  $E_2 = m_2 = m_e$ . Moreover, the angle between  $\vec{p}_3$  and  $\vec{p}_4$  is 180 degrees for the recoil energy to be maximum. (Remember  $m_1 = m_3 = m_\nu$  and  $m_2 = m_4 = m_e$ .)

We can write  $E_4$  in terms of the recoil energy of the electron as

$$E_4 = T + m_e . \tag{C.2}$$

To write  $E_3$  in terms of the recoil energy of the electron let us start with energy conservation first as;

$$\begin{aligned}
 E_3 &= E_1 + E_2 - E_4 \\
 E_3 &= E_1 + m_e - (T + m_e) \\
 E_3 &= E_1 - T
 \end{aligned} \tag{C.3}$$

Once we neglect neutrino mass then;

$$|\vec{p}_3| = E_3 = E_1 - T . \tag{C.4}$$

Using the dispersion relation we can relate  $|\vec{p}_4|$  with recoil energy  $T$  in the following way;

$$\begin{aligned}
E_4^2 - m_e^2 &= |\vec{p}_4|^2 \\
(E_4 - m_e)(E_4 + m_e) &= |\vec{p}_4|^2 \\
T(T + m_e + m_e) &= |\vec{p}_4|^2 \\
T(T + 2m_e) &= |\vec{p}_4|^2 .
\end{aligned} \tag{C.5}$$

Hence, we get;

$$|\vec{p}_4| = \sqrt{T(T + 2m_e)} . \tag{C.6}$$

Once we put Equations (C.2) to (C.4) and (C.6) into Equation (C.1) we get;

$$\begin{aligned}
E_1 m_e &= E_3 E_4 + |\vec{p}_3| |\vec{p}_4| \\
E_1 m_e &= (E_1 - T)(T + m_e) + (E_1 - T) \sqrt{T(T + 2m_e)} \\
E_1 m_e &= E_1 T + E_1 m_e - T^2 - m_e T + (E_1 - T) \sqrt{T(T + 2m_e)} \\
T^2 + m_e T - E_1 T &= (E_1 - T) \sqrt{T(T + 2m_e)} \\
\frac{T(T - E_1) + m_e T}{E_1 - T} &= \sqrt{T(T + 2m_e)} \\
-T + \frac{m_e T}{E_1 - T} &= \sqrt{T(T + 2m_e)} \\
T \left( \frac{m_e}{E_1 - T} - 1 \right) &= \sqrt{T(T + 2m_e)} .
\end{aligned} \tag{C.7}$$

Once we then square both sides of the above equation, we find;



$$\begin{aligned}
T^2\left(\frac{m_e}{E_1 - T} - 1\right)^2 &= T(T + 2m_e) \\
T\left(\frac{m_e^2}{(E_1 - T)^2} - \frac{2m_e}{E_1 - T} + 1\right) &= T + 2m_e \\
\frac{m_e^2 T}{(E_1 - T)^2} - \frac{2m_e T}{E_1 - T} + T &= T + 2m_e \\
\frac{m_e^2 T}{(E_1 - T)^2} - \frac{2m_e T}{E_1 - T} &= 2m_e \\
\frac{m_e T}{(E_1 - T)^2} - \frac{2T}{E_1 - T} &= 2 \\
\frac{m_e T}{(E_1 - T)^2} - \frac{2T(E_1 - T)}{(E_1 - T)^2} &= 2 \\
m_e T - 2T(E_1 - T) &= 2(E_1 - T)^2 \\
m_e T - 2TE_1 + 2T^2 &= 2E_1^2 + 2T^2 - 4E_1 T \\
m_e T &= 2E_1^2 - 2E_1 T \\
m_e T + 2E_1 T &= 2E_1^2 \\
T(m_e + 2E_1) &= 2E_1^2.
\end{aligned} \tag{C.8}$$

Hence we obtain the maximum recoil energy in terms of the incoming neutrino energy as;

$$\boxed{T_{\max} = \frac{2E_1^2}{m_e + 2E_1}}. \tag{C.9}$$

Once we solve this equation for  $E_1$ , we find the minimum energy of the neutrino necessary to leads to the electron having the recoil energy  $T$  as;

$$\boxed{E_{\nu_{\min}} = \frac{T + \sqrt{T^2 + 2Tm_e}}{2}} \tag{C.10}$$



## APPENDIX D

### INTERFERENCE TERM FOR $\nu_\mu - e^-$ SCATTERING IN THE NONCOMMUTATIVE SPACE

For the  $\nu_\mu - e^-$  scattering, let us calculate the interference term. The amplitude square can be written for the diagrams in Figure (D.1) as;

$$|\mathcal{M}|^2 = |\mathcal{M}_1|^2 + |\mathcal{M}_2|^2 + \mathcal{M}_1\mathcal{M}_2^* + \mathcal{M}_2\mathcal{M}_1^* \quad (\text{D.1})$$

where  $\mathcal{M}_1$  is the amplitude with  $Z$  exchange,

$$\mathcal{M}_1 = \frac{g_Z^2}{8M_Z^2} [\bar{u}(p_3)\gamma^\mu(1 - \gamma^5)u(p_1)][\bar{u}(p_4)\gamma_\mu(c_V^e - c_A^e\gamma^5)u(p_2)] \quad (\text{D.2})$$

and  $\mathcal{M}_2$  is the amplitude with photon exchange,

$$\mathcal{M}_2 = \frac{e^2}{2q^2} [\bar{u}(p_4)\gamma^\nu u(p_2)][\bar{u}(p_3)\theta_\nu^{\sigma\rho}p_{1\sigma}q_\rho(1 - \gamma^5)u(p_1)] \quad (\text{D.3})$$

where  $q = (p_1 - p_3)$  and  $\theta_\nu^{\sigma\rho} = \theta_\nu^\sigma\gamma^\rho + \theta^{\sigma\rho}\gamma_\nu + \theta_\nu^\rho\gamma^\sigma$

For the interference term let us evaluate  $|\mathcal{M}_1\mathcal{M}_2^*|$  first.

$$|\mathcal{M}_1\mathcal{M}_2^\dagger| = \frac{e^2}{2q^2} \frac{g_Z^2}{8M_Z^2} [\bar{u}(p_3)\gamma^\mu(1 - \gamma^5)u(p_1)][\bar{u}(p_4)\gamma_\mu(c_V^e - c_A^e\gamma^5)u(p_2)] \quad (\text{D.4})$$

$$[\bar{u}(p_4)\gamma^\nu u(p_2)]^* [\bar{u}(p_3)\theta_\nu^{\sigma\rho}p_{1\sigma}q_\rho(1 - \gamma^5)u(p_1)]^\dagger .$$

Once we sum over the final spin states and use the Casimir identities we get

$$\sum |\mathcal{M}_1\mathcal{M}_2^*| = \frac{e^2 g_Z^2}{16q^2 M_Z^2} Tr[\Gamma_1(p_2 + m_e)\bar{\Gamma}_2(p_4 + m_4)]Tr[\Gamma_3(p_1 + m_1)\bar{\Gamma}_4(p_3 + m_3)] \quad (\text{D.5})$$

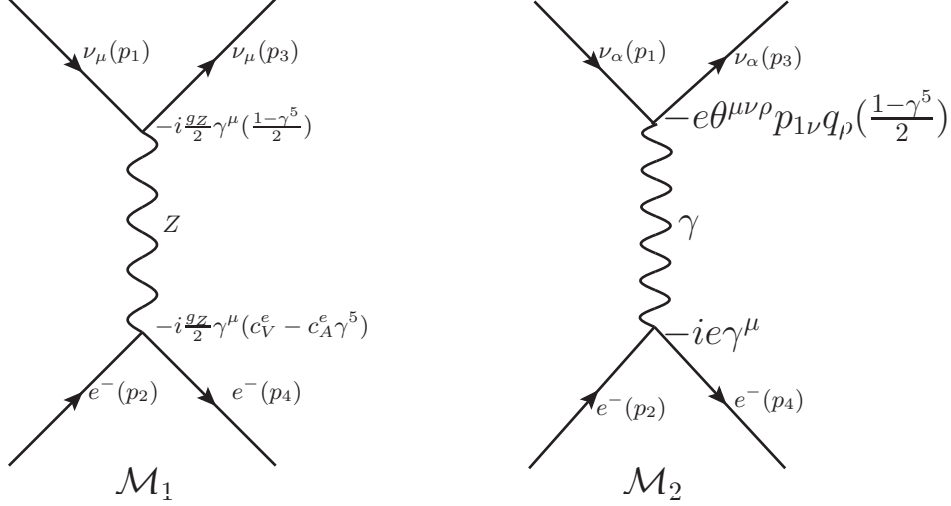


Figure D.1: Feynman Diagram of  $\nu_\mu - e^-$  scattering takes place with  $Z$  boson exchange as well as the photon exchange which takes place only in non-commutative space. Interference term between two diagrams must be calculated.

where;

$$\begin{aligned}
 \Gamma_1 &= \gamma_\mu (c_V^e - c_A^e \gamma^5), \\
 \Gamma_2 &= \gamma^\nu, \\
 \Gamma_3 &= \gamma^\mu (1 - \gamma^5), \\
 \Gamma_4 &= \theta_\nu^{\sigma\rho} p_{1\sigma} q_\rho (1 - \gamma^5).
 \end{aligned} \tag{D.6}$$

Since  $\bar{\Gamma} = \gamma^0 \Gamma^\dagger \gamma^0$ , then  $\bar{\Gamma}_2 = \Gamma_2 = \gamma^\nu$ .

Let us first evaluate  $\bar{\Gamma}_4$ .

$$\begin{aligned}
 \bar{\Gamma}_4 &= \gamma^0 \Gamma_4^\dagger \gamma^0 \\
 &= \gamma^0 (\theta_\nu^{\sigma\rho} p_{1\sigma} q_\rho (1 - \gamma^5))^\dagger \gamma^0 \\
 &= p_{1\sigma} q_\rho \gamma^0 (1 - \gamma^5)^\dagger (\theta_\nu^\sigma \gamma^\rho + \theta^{\sigma\rho} \gamma_\nu + \theta_\nu^\rho \gamma^\sigma)^\dagger \gamma^0 \\
 &= p_{1\sigma} q_\rho \gamma^0 (1 - \gamma^5) ((\gamma^\rho)^\dagger (\theta_\nu^\sigma)^\dagger + (\gamma_\nu)^\dagger (\theta^{\sigma\rho})^\dagger + (\gamma^\sigma)^\dagger (\theta_\nu^\rho)^\dagger) \gamma^0 \\
 &= p_{1\sigma} q_\rho (1 + \gamma^5) (\underbrace{(\theta_\nu^\sigma)^\dagger \gamma^0 (\gamma^\rho)^\dagger \gamma^0}_{\gamma^\rho} + \underbrace{\theta^{\sigma\rho} \gamma^0 (\gamma_\nu)^\dagger \gamma^0}_{\gamma_\nu} + \underbrace{(\theta_\nu^\rho)^\dagger \gamma^0 \gamma^\sigma \gamma^0}_{\gamma^\sigma}) \\
 &= p_{1\sigma} q_\rho ((\theta_\nu^\sigma)^\dagger \gamma^\rho + (\theta^{\sigma\rho})^\dagger \gamma^\nu + (\theta_\nu^\rho)^\dagger \gamma^\sigma) (1 - \gamma^5).
 \end{aligned} \tag{D.7}$$

Since  $\theta$  is an anti-symmetric matrix then we get;

$$\begin{aligned}(\theta_\nu^\sigma)^\dagger &= -\theta_\nu^\sigma \\(\theta^{\sigma\rho})^\dagger &= -\theta^{\sigma\rho} \\(\theta_\nu^\rho)^\dagger &= -\theta_\nu^\rho\end{aligned}\tag{D.8}$$

Hence, we can write  $\bar{\Gamma}_4$  as ;

$$\begin{aligned}\bar{\Gamma}_4 &= -p_{1\sigma}q_\rho \underbrace{(\theta_\nu^\sigma\gamma^\rho + \theta^{\sigma\rho}\gamma_\nu + \theta_\nu^\rho\gamma^\sigma)}_{\theta_\nu^{\sigma\rho}}(1 - \gamma^5) \\ &= -p_{1\sigma}q_\rho\theta_\nu^{\sigma\rho}(1 - \gamma^5) .\end{aligned}\tag{D.9}$$

With these findings, we can write Equation (D.5) as;

$$\boxed{\sum_{spin} \mathcal{M}_1\mathcal{M}_2^* = -\frac{e^2g_Z^2}{16q^2M_Z^2}Tr[\gamma_\mu(c_V^e - c_A^e\gamma^5)(\not{p}_2 + m_e)\gamma^\nu(\not{p}_4 + m_e)]Tr[\gamma^\mu(1 - \gamma^5)\not{p}_1p_{1\sigma}q_\rho\theta_\nu^{\sigma\rho}(1 - \gamma^5)\not{p}_3]}.\tag{D.10}$$

For simplicity let us denote,

$$\begin{aligned}E_\mu^\nu &= Tr[\gamma_\mu(c_V^e - c_A^e\gamma^5)(\not{p}_2 + m_e)\gamma^\nu(\not{p}_4 + m_e)] \\ F_\nu^\mu &= Tr[\gamma^\mu(1 - \gamma^5)\not{p}_1p_{1\sigma}q_\rho\theta_\nu^{\sigma\rho}(1 - \gamma^5)\not{p}_3]\end{aligned}\tag{D.11}$$

and evaluate the traces separately.

$$\begin{aligned}E_\mu^\nu &= Tr[\gamma_\mu(c_V^e - c_A^e\gamma^5)(\not{p}_2 + m_e)\gamma^\nu(\not{p}_4 + m_e)] \\ &= c_V^eTr[\gamma_\mu(\not{p}_2 + m_e)\gamma^\nu(\not{p}_4 + m_e)] - c_A^eTr[\gamma_\mu\gamma^5(\not{p}_2 + m_e)\gamma^\nu(\not{p}_4 + m_e)] \\ &= c_V^e\left(Tr[\gamma_\mu\not{p}_2\gamma^\nu\not{p}_4] + m_eTr[\gamma_\mu\not{p}_2\gamma^\nu] + m_eTr[\gamma_\mu\gamma^\nu\not{p}_4] + m_e^2Tr[\gamma_\mu\gamma^\nu]\right) \\ &\quad - c_A^e\left(Tr[\gamma_\mu\gamma^5\not{p}_2\gamma^\nu\not{p}_4] + m_eTr[\gamma_\mu\gamma^5\not{p}_2\gamma^\nu] + m_eTr[\gamma_\mu\gamma^5\gamma^\nu\not{p}_4] + m_e^2Tr[\gamma_\mu\gamma^5\gamma^\nu]\right).\end{aligned}\tag{D.12}$$

The canceled terms in the above equation are due to the trace of odd number of gamma matrices is zero. Moreover,

$$Tr[\gamma_\mu\gamma^5\gamma^\nu] = 0 .\tag{D.13}$$

Hence, we can write  $E_\mu^\nu$  as;

$$E_\mu^\nu = c_V^e \left( Tr[\gamma_\mu \not{p}_2 \gamma^\nu \not{p}_4] + m_e^2 \underbrace{Tr[\gamma_\mu \gamma^\nu]}_{4g_\mu^\nu} \right) - c_A^e \left( Tr[\gamma_\mu \gamma^5 \not{p}_2 \gamma^\nu \not{p}_4] \right). \quad (D.14)$$

Using the following identities,

$$\begin{aligned} Tr[\gamma_\mu \not{p}_2 \gamma^\nu \not{p}_4] &= 4[p_{2\mu} p_4^\nu + p_2^\nu p_{4\mu} - (p_2 \cdot p_4) g_\mu^\nu] \\ Tr[\gamma_\mu \gamma^5 \not{p}_2 \gamma^\nu \not{p}_4] &= -p_{2\alpha} p_{4\beta} Tr[\gamma^5 \gamma_\mu \gamma^\alpha \gamma^\nu \gamma^\beta] \\ &= -4i p_{2\alpha} p_{4\beta} \epsilon_\mu^{\alpha\nu\beta}. \end{aligned} \quad (D.15)$$

we get  $E_\mu^\nu$  as;

$$E_\mu^\nu = 4c_V^e \left( p_{2\mu} p_4^\nu + p_2^\nu p_{4\mu} + (m_e^2 - (p_2 \cdot p_4) g_\mu^\nu) \right) + 4i c_A^e \left( p_{2\alpha} p_{4\beta} \epsilon_\mu^{\alpha\nu\beta} \right). \quad (D.16)$$

Now let us evaluate  $F_\nu^\mu$ .

$$\begin{aligned} F_\nu^\mu &= Tr[\gamma^\mu (1 - \gamma^5) \not{p}_1 p_{1\sigma} q_\rho \theta_\nu^{\sigma\rho} (1 - \gamma^5) \not{p}_3] \\ &= p_{1\sigma} q_\rho Tr[\gamma^\mu (1 - \gamma^5) \not{p}_1 \theta_\nu^{\sigma\rho} (1 - \gamma^5) \not{p}_3] \\ &= p_{1\sigma} q_\rho Tr[\gamma^\mu (1 - \gamma^5) (1 - \gamma^5) \not{p}_1 \theta_\nu^{\sigma\rho} \not{p}_3] \\ &= 2p_{1\sigma} q_\rho Tr[\gamma^\mu (1 - \gamma^5) \not{p}_1 \theta_\nu^{\sigma\rho} \not{p}_3] \\ &= 2p_{1\sigma} q_\rho Tr[\gamma^\mu (1 - \gamma^5) \not{p}_1 (\theta_\nu^\sigma \gamma^\rho + \theta^{\sigma\rho} \gamma_\nu + \theta_\nu^\rho \gamma^\sigma) \not{p}_3] \\ &= 2p_{1\sigma} q_\rho \left( \theta_\nu^\sigma Tr[\gamma^\mu (1 - \gamma^5) \not{p}_1 \gamma^\rho \not{p}_3] + \theta^{\sigma\rho} Tr[\gamma^\mu (1 - \gamma^5) \not{p}_1 \gamma_\nu \not{p}_3] \right. \\ &\quad \left. + \theta_\nu^\rho Tr[\gamma^\mu (1 - \gamma^5) \not{p}_1 \gamma^\sigma \not{p}_3] \right). \end{aligned} \quad (D.17)$$

The form of the trace terms in the above equation is the same, thus once we evaluate one of them we can find the other results by just replacing the indices. Let us evaluate the following trace.

$$\begin{aligned} Tr[\gamma^\mu (1 - \gamma^5) \not{p}_1 \gamma^\rho \not{p}_3] &= Tr[\gamma^\mu \not{p}_1 \gamma^\rho \not{p}_3] - Tr[\gamma^\mu \gamma^5 \not{p}_1 \gamma^\rho \not{p}_3] \\ &= 4(p_1^\mu p_3^\rho + p_1^\rho p_3^\mu - (p_1 \cdot p_3) g^{\mu\rho}) + 4i p_{1\alpha} p_{3\beta} \epsilon^{\mu\alpha\rho\beta}. \end{aligned} \quad (D.18)$$

Hence  $F_\nu^\mu$  can be written as;

$$\begin{aligned}
F_\nu^\mu &= 2p_{1\sigma}q_\rho \left( 4\theta_\nu^\sigma (p_1^\mu p_3^\rho + p_1^\rho p_3^\mu - (p_1 \cdot p_3)g^{\mu\rho}) + ip_{1\alpha}p_{3\beta}\epsilon^{\mu\alpha\rho\beta} \right) \\
&\quad + 4\theta^{\sigma\rho} (p_1^\mu p_{3\nu} + p_{1\nu}p_3^\mu - (p_1 \cdot p_3)g_\nu^\mu + ip_{1\alpha}p_{3\beta}\epsilon^{\mu\alpha}{}_\nu{}^\beta) \\
&\quad + 4\theta_\nu^\rho (p_1^\mu p_3^\sigma + p_1^\sigma p_3^\mu - (p_1 \cdot p_3)g^{\mu\sigma} + ip_{1\alpha}p_{3\beta}\epsilon^{\mu\alpha\sigma\beta}) \Big). \tag{D.19}
\end{aligned}$$

Since  $q = p_1 - p_3$ , we can write the term with the first imaginary part in the above equation as;

$$\begin{aligned}
p_{1\sigma}q_\rho ip_{1\alpha}p_{3\beta}\epsilon^{\mu\alpha\rho\beta} &= ip_{1\sigma}(p_{1\rho} - p_{3\rho})p_{1\alpha}p_{3\beta}\epsilon^{\mu\alpha\rho\beta} \\
&= ip_{1\sigma} \underbrace{p_{1\rho}p_{1\alpha}}_S \underbrace{p_{3\beta}\epsilon^{\mu\alpha\rho\beta}}_{AS} - ip_{1\sigma}p_{1\alpha} \underbrace{p_{3\rho}p_{3\beta}}_S \underbrace{\epsilon^{\mu\alpha\rho\beta}}_{AS} \\
&= 0, \tag{D.20}
\end{aligned}$$

which is due to the multiplication of symmetric times anti symmetric terms.

Similarly for the last imaginary term in Equation (D.19),

$$iq_\rho \underbrace{p_{1\sigma}p_{1\alpha}}_S \underbrace{p_{3\beta}\epsilon^{\mu\alpha\sigma\beta}}_{AS} = 0. \tag{D.21}$$

Hence, we can write  $F_\nu^\mu$  as;

$$\begin{aligned}
F_\nu^\mu &= 8 \left( \theta_\nu^\sigma ((p_{1\sigma}q_\rho)(p_1^\mu p_3^\rho + p_1^\rho p_3^\mu - (p_1 \cdot p_3)g^{\mu\rho}) + \cancel{ip_{1\sigma}q_\rho p_{1\alpha}p_{3\beta}\epsilon^{\mu\alpha\rho\beta}}) \right. \\
&\quad + \theta^{\sigma\rho} ((p_{1\sigma}q_\rho)(p_1^\mu p_{3\nu} + p_{1\nu}p_3^\mu - (p_1 \cdot p_3)g_\nu^\mu) + ip_{1\sigma}q_\rho p_{1\alpha}p_{3\beta}\epsilon^{\mu\alpha}{}_\nu{}^\beta) \\
&\quad \left. + \theta_\nu^\rho ((p_{1\sigma}q_\rho)(p_1^\mu p_3^\sigma + p_1^\sigma p_3^\mu - (p_1 \cdot p_3)g^{\mu\sigma}) + \cancel{ip_{1\sigma}q_\rho p_{1\alpha}p_{3\beta}\epsilon^{\mu\alpha\sigma\beta}}) \right). \tag{D.22}
\end{aligned}$$

Once we simplify the terms we get;

$$\begin{aligned}
F_\nu^\mu &= 8 \left( \theta_\nu^\sigma ((p_{1\sigma}q_\rho)(p_1^\mu p_3^\rho + p_1^\rho p_3^\mu - (p_1 \cdot p_3)g^{\mu\rho})) \right. \\
&\quad + \theta^{\sigma\rho} ((p_{1\sigma}q_\rho)(p_1^\mu p_{3\nu} + p_{1\nu}p_3^\mu - (p_1 \cdot p_3)g_\nu^\mu) + ip_{1\sigma}q_\rho p_{1\alpha}p_{3\beta}\epsilon^{\mu\alpha}{}_\nu{}^\beta) \\
&\quad \left. + \theta_\nu^\rho ((p_{1\sigma}q_\rho)(p_1^\mu p_3^\sigma + p_1^\sigma p_3^\mu - (p_1 \cdot p_3)g^{\mu\sigma})) \right). \tag{D.23}
\end{aligned}$$

Let us contract  $E_\mu^\nu$  and  $F_\nu^\mu$ :

$$\begin{aligned}
E_\mu^\nu F_\nu^\mu &= \left( 4c_V^e (p_{2\mu} p_4^\nu + p_2^\nu p_{4\mu} + (m_e^2 - (p_2 \cdot p_4)) g_\mu^\nu) + 4ic_A^e (p_{2\alpha} p_{4\beta} \epsilon_\mu^{\alpha\nu\beta}) \right) \\
&\times 8 \left( \theta_\nu^\sigma ((p_{1\sigma} q_\rho) (p_1^\mu p_3^\rho + p_1^\rho p_3^\mu - (p_1 \cdot p_3) g^{\mu\rho})) \right. \\
&\quad + \theta^{\sigma\rho} ((p_{1\sigma} q_\rho) (p_1^\mu p_{3\nu} + p_{1\nu} p_3^\mu - (p_1 \cdot p_3) g_\nu^\mu) + ip_{1\sigma} q_\rho p_{1\alpha} p_{3\beta} \epsilon^{\mu\alpha}{}_\nu{}^\beta) \\
&\quad \left. + \theta_\nu^\rho ((p_{1\sigma} q_\rho) (p_1^\mu p_3^\sigma + p_1^\sigma p_3^\mu - (p_1 \cdot p_3) g^{\mu\sigma})) \right) \\
&= 32c_V^e \left( \theta_\nu^\sigma (p_{1\sigma} q_\rho) (p_{2\mu} p_4^\nu + p_2^\nu p_{4\mu} + (m_e^2 - (p_2 \cdot p_4)) g_\mu^\nu) \right. \\
&\quad \times (p_1^\mu p_3^\rho + p_1^\rho p_3^\mu - (p_1 \cdot p_3) g^{\mu\rho}) \\
&\quad + \theta^{\sigma\rho} (p_{1\sigma} q_\rho) (p_{2\mu} p_4^\nu + p_2^\nu p_{4\mu} + (m_e^2 - (p_2 \cdot p_4)) g_\mu^\nu) \\
&\quad \times (p_1^\mu p_{3\nu} + p_{1\nu} p_3^\mu - (p_1 \cdot p_3) g_\nu^\mu) \\
&\quad + \theta^{\sigma\rho} (p_{1\sigma} q_\rho) \underbrace{(p_{2\mu} p_4^\nu + p_2^\nu p_{4\mu} - (m_e^2 - (p_2 \cdot p_4)) g_\mu^\nu)}_{S \text{ in } \mu\nu} \underbrace{(ip_{1\alpha} p_{3\beta} \epsilon^{\mu\alpha}{}_\nu{}^\beta)}_{AS} \\
&\quad + \theta_\nu^\rho p_{1\sigma} q_\rho (p_{2\mu} p_4^\nu + p_2^\nu p_{4\mu} + (m_e^2 - (p_2 \cdot p_4)) g_\mu^\nu) \\
&\quad \left. \times (p_1^\mu p_3^\sigma + p_1^\sigma p_3^\mu - (p_1 \cdot p_3) g^{\mu\sigma}) \right) \\
&+ 32c_A^e i \left( \theta_\nu^\sigma (p_{1\sigma} q_\rho) (p_{2\alpha} p_{4\beta} \epsilon_\mu^{\alpha\nu\beta}) (p_1^\mu p_3^\rho + p_1^\rho p_3^\mu - (p_1 \cdot p_3) g^{\mu\rho}) \right. \\
&\quad + \theta^{\sigma\rho} (p_{1\sigma} q_\rho) \underbrace{(p_{2\alpha} p_{4\beta} \epsilon_\mu^{\alpha\nu\beta})}_{AS} \underbrace{(p_1^\mu p_{3\nu} + p_{1\nu} p_3^\mu - (p_1 \cdot p_3) g_\nu^\mu)}_{S \text{ in } \mu\nu} \\
&\quad + \theta^{\sigma\rho} (p_{1\sigma} q_\rho) (p_{2\alpha} p_{4\beta} \epsilon_\mu^{\alpha\nu\beta}) (ip_{1\alpha} p_{3\beta} \epsilon^{\mu\alpha}{}_\nu{}^\beta) \\
&\quad \left. + \theta_\nu^\rho p_{1\sigma} q_\rho (p_{2\alpha} p_{4\beta} \epsilon_\mu^{\alpha\nu\beta}) (p_1^\mu p_3^\sigma + p_1^\sigma p_3^\mu - (p_1 \cdot p_3) g^{\mu\sigma}) \right).
\end{aligned}
\tag{D.24}$$

Once we get rid of the terms containing symmetric times anti-symmetric terms we simplify the above equation as follows.



$$\begin{aligned}
E_{\mu}^{\nu} F_{\nu}^{\mu} &= 32c_V^e \left( \theta_{\nu}^{\sigma} (p_{1\sigma} q_{\rho}) (p_{2\mu} p_4^{\nu} + p_2^{\nu} p_{4\mu} + (m_e^2 - (p_2 \cdot p_4)) g_{\mu}^{\nu}) \right. \\
&\quad \times (p_1^{\mu} p_3^{\rho} + p_1^{\rho} p_3^{\mu} - (p_1 \cdot p_3) g^{\mu\rho}) \\
&\quad + \theta^{\sigma\rho} (p_{1\sigma} q_{\rho}) (p_{2\mu} p_4^{\nu} + p_2^{\nu} p_{4\mu} + (m_e^2 - (p_2 \cdot p_4)) g_{\mu}^{\nu}) \\
&\quad \times (p_1^{\mu} p_{3\nu} + p_{1\nu} p_3^{\mu} - (p_1 \cdot p_3) g_{\nu}^{\mu}) \\
&\quad + \theta_{\nu}^{\rho} p_{1\sigma} q_{\rho} (p_{2\mu} p_4^{\nu} + p_2^{\nu} p_{4\mu} + (m_e^2 - (p_2 \cdot p_4)) g_{\mu}^{\nu}) \\
&\quad \left. \times (p_1^{\mu} p_3^{\sigma} + p_1^{\sigma} p_3^{\mu} - (p_1 \cdot p_3) g^{\mu\sigma}) \right) \\
&\quad + 32c_A^e i \left( \theta_{\nu}^{\sigma} (p_{1\sigma} q_{\rho}) (p_{2\alpha} p_{4\beta} \epsilon_{\mu}^{\alpha\nu\beta}) (p_1^{\mu} p_3^{\rho} + p_1^{\rho} p_3^{\mu} - (p_1 \cdot p_3) g^{\mu\rho}) \right. \\
&\quad + \theta^{\sigma\rho} (p_{1\sigma} q_{\rho}) (p_{2\alpha} p_{4\beta} \epsilon_{\mu}^{\alpha\nu\beta}) (i p_{1\alpha} p_{3\beta} \epsilon^{\mu\alpha}_{\nu\beta}) \\
&\quad \left. + \theta_{\nu}^{\rho} p_{1\sigma} q_{\rho} (p_{2\alpha} p_{4\beta} \epsilon_{\mu}^{\alpha\nu\beta}) (p_1^{\mu} p_3^{\sigma} + p_1^{\sigma} p_3^{\mu} - (p_1 \cdot p_3) g^{\mu\sigma}) \right). \tag{D.25}
\end{aligned}$$

Now, let us evaluate the terms containing  $c_A^e$  first. For simplicity let us denote the terms which are factors of  $c_A^e$  in the above equation as  $E_{11}$ ,  $E_{12}$  and  $E_{13}$  as following;

$$\begin{aligned}
E_{11} &= \theta_{\nu}^{\sigma} (p_{1\sigma} q_{\rho}) (p_{2\alpha} p_{4\beta} \epsilon_{\mu}^{\alpha\nu\beta}) (p_1^{\mu} p_3^{\rho} + p_1^{\rho} p_3^{\mu} - (p_1 \cdot p_3) g^{\mu\rho}), \\
E_{12} &= \theta^{\sigma\rho} (p_{1\sigma} q_{\rho}) (p_{2\alpha} p_{4\beta} \epsilon_{\mu}^{\alpha\nu\beta}) (i p_{1\alpha} p_{3\beta} \epsilon^{\mu\alpha}_{\nu\beta}), \\
E_{13} &= \theta_{\nu}^{\rho} p_{1\sigma} q_{\rho} (p_{2\alpha} p_{4\beta} \epsilon_{\mu}^{\alpha\nu\beta}) (p_1^{\mu} p_3^{\sigma} + p_1^{\sigma} p_3^{\mu} - (p_1 \cdot p_3) g^{\mu\sigma}). \tag{D.26}
\end{aligned}$$

If we evaluate  $E_{11}$  first,

$$\begin{aligned}
E_{11} &= \theta_{\nu}^{\sigma} (p_{1\sigma} q_{\rho}) p_{2\alpha} p_{4\beta} \epsilon_{\mu}^{\alpha\nu\beta} (p_1^{\mu} p_3^{\rho} + p_1^{\rho} p_3^{\mu} - (p_1 \cdot p_3) g^{\mu\rho}) \\
&= \theta_{\nu}^{\sigma} p_{2\alpha} p_{4\beta} \epsilon_{\mu}^{\alpha\nu\beta} \left( p_{1\sigma} q_{\rho} p_1^{\mu} p_3^{\rho} + p_{1\sigma} q_{\rho} p_1^{\rho} p_3^{\mu} - p_{1\sigma} q_{\rho} (p_1 \cdot p_3) g^{\mu\rho} \right) \\
&= \theta_{\nu}^{\sigma} p_{2\alpha} p_{4\beta} \epsilon_{\mu}^{\alpha\nu\beta} \left( p_{1\sigma} (q \cdot p_3) p_1^{\mu} + p_{1\sigma} (q \cdot p_1) p_3^{\mu} - p_{1\sigma} q^{\mu} (p_1 \cdot p_3) \right) \\
&= \theta_{\nu}^{\sigma} p_{2\alpha} p_{4\beta} \epsilon_{\mu}^{\alpha\nu\beta} \left( p_{1\sigma} ((p_1 - p_3) \cdot p_3) p_1^{\mu} + p_{1\sigma} ((p_1 - p_3) \cdot p_1) p_3^{\mu} \right. \\
&\quad \left. - p_{1\sigma} (p_1^{\mu} - p_3^{\mu}) (p_1 \cdot p_3) \right) \\
&= \theta_{\nu}^{\sigma} p_{2\alpha} p_{4\beta} \epsilon_{\mu}^{\alpha\nu\beta} \left( \cancel{p_{1\sigma} p_1^{\mu} (p_1 \cdot p_3)} - p_{1\sigma} p_1^{\mu} p_3^2 + p_{1\sigma} p_3^{\mu} p_1^2 \right. \\
&\quad \left. - \cancel{p_{1\sigma} p_3^{\mu} (p_1 \cdot p_3)} - \cancel{p_{1\sigma} p_1^{\mu} (p_1 \cdot p_3)} + p_{1\sigma} p_3^{\mu} (p_1 \cdot p_3) \right) \\
&= 0. \tag{D.27}
\end{aligned}$$

we get zero once we neglect mass of neutrinos, that is  $p_1^2 = 0$  and  $p_3^2 = 0$ .

For  $E_{13}$  we get;

$$\begin{aligned}
E_{13} &= \theta_\nu^\rho p_{1\sigma} q_\rho p_{2\alpha} p_{4\beta} \epsilon_\mu^{\alpha\nu\beta} (p_1^\mu p_3^\sigma + p_1^\sigma p_3^\mu - (p_1 \cdot p_3) g^{\mu\sigma}) \\
&= \theta_\nu^\rho p_{2\alpha} p_{4\beta} \epsilon_\mu^{\alpha\nu\beta} \left( p_{1\sigma} q_\rho p_1^\mu p_3^\sigma + p_{1\sigma} q_\rho p_1^\sigma p_3^\mu - p_{1\sigma} q_\rho (p_1 \cdot p_3) g^{\mu\sigma} \right) \\
&= \theta_\nu^\rho p_{2\alpha} p_{4\beta} \epsilon_\mu^{\alpha\nu\beta} \left( \cancel{q_\rho p_1^\mu (p_1 \cdot p_3)} + p_1^2 q_\rho p_3^\mu - \cancel{p_1^\mu q_\rho (p_1 \cdot p_3)} \right) \\
&= 0.
\end{aligned} \tag{D.28}$$

Hence we can write  $E_\mu^\nu F_\nu^\mu$  as;

$$\begin{aligned}
E_\mu^\nu F_\nu^\mu &= 32c_V^e \left( \theta_\nu^\sigma (p_{1\sigma} q_\rho) (p_{2\mu} p_4^\nu + p_2^\nu p_{4\mu} + (m_e^2 - (p_2 \cdot p_4)) g_\mu^\nu) \right. \\
&\quad \times (p_1^\mu p_3^\rho + p_1^\rho p_3^\mu - (p_1 \cdot p_3) g^{\mu\rho}) \\
&\quad + \theta^{\sigma\rho} (p_{1\sigma} q_\rho) (p_{2\mu} p_4^\nu + p_2^\nu p_{4\mu} + (m_e^2 - (p_2 \cdot p_4)) g_\mu^\nu) \\
&\quad \times (p_1^\mu p_{3\nu} + p_{1\nu} p_3^\mu - (p_1 \cdot p_3) g_\nu^\mu) \\
&\quad + \theta_\nu^\rho p_{1\sigma} q_\rho (p_{2\mu} p_4^\nu + p_2^\nu p_{4\mu} + (m_e^2 - (p_2 \cdot p_4)) g_\mu^\nu) \\
&\quad \left. \times (p_1^\mu p_3^\sigma + p_1^\sigma p_3^\mu - (p_1 \cdot p_3) g^{\mu\sigma}) \right) \\
&\quad - 32c_A^e \left( \theta^{\sigma\rho} p_{1\sigma} q_\rho p_{2\alpha} p_{4\beta} \epsilon_\mu^{\alpha\nu\beta} p_{1\alpha} p_{3\beta} \epsilon^{\mu\alpha}{}_\nu{}^\beta \right).
\end{aligned} \tag{D.29}$$

Thus, we can write,

$$\sum_{spin} \mathcal{M}_1 \mathcal{M}_2^* = -\frac{e^2 g_Z^2}{16q^2 M_Z^2} E_\mu^\nu F_\nu^\mu \tag{D.30}$$

where  $E_\mu^\nu F_\nu^\mu$  is given in Equation (D.29).

Now, let us find  $|\mathcal{M}_2 \mathcal{M}_1^*|$ . Using Equation (D.2) and Equation (D.3) we obtain;

$$\begin{aligned}
|\mathcal{M}_2 \mathcal{M}_1^*| &= \frac{g_Z^2}{8M_Z^2} \frac{e^2}{2q^2} [\bar{u}(p_4) \gamma^\nu u(p_2)] [\bar{u}(p_3) \theta_\nu^{\sigma\rho} p_{1\sigma} q_\rho (1 - \gamma^5) u(p_1)] \\
&\quad [\bar{u}(p_3) \gamma^\mu (1 - \gamma^5) u(p_1)]^* [\bar{u}(p_4) \gamma_\mu (c_V^e - c_A^e \gamma^5) u(p_2)]^*.
\end{aligned} \tag{D.31}$$

Once we sum over final spin states and apply the Casimir identities as before, we get;

$$|\mathcal{M}_2 \mathcal{M}_1^*| = \frac{g_Z^2 e^2}{16q^2 M_Z^2} Tr[\Gamma_5(p_2 + m_2) \bar{\Gamma}_6(p_4 + m_4)] Tr[\Gamma_7(p_1 + m_1) \bar{\Gamma}_8(p_3 + m_3)] \tag{D.32}$$

where

$$\begin{aligned}
\Gamma_5 &= \gamma^\nu, \\
\bar{\Gamma}_6 &= \gamma^0 \Gamma_6 \gamma^0 = \gamma_\mu (c_V^e - c_A^e \gamma^5), \\
\Gamma_7 &= \theta_\nu^{\sigma\rho} p_{1\sigma} q_\rho (1 - \gamma^5), \\
\bar{\Gamma}_8 &= \gamma^\mu (1 - \gamma^5).
\end{aligned} \tag{D.33}$$

Neglecting the mass of the neutrinos we can write Equation (D.32) as;

$$\begin{aligned}
\sum_{spin} \mathcal{M}_2 \mathcal{M}_1^* &= \frac{g_Z^2 e^2}{16q^2 M_Z^2} Tr[\gamma^\nu (\not{p}_2 + m_e) \gamma_\mu (c_V^e - c_A^e \gamma^5) (\not{p}_4 + m_e)] \\
&Tr[\theta_\nu^{\sigma\rho} p_{1\sigma} q_\rho (1 - \gamma^5) \not{p}_1 \gamma^\mu (1 - \gamma^5) \not{p}_3].
\end{aligned} \tag{D.34}$$

Let us define  $K_\mu^\nu$  and  $L_\mu^\nu$  for simplicity as following;

$$\begin{aligned}
K_\mu^\nu &= Tr[\gamma^\nu (\not{p}_2 + m_e) \gamma_\mu (c_V^e - c_A^e \gamma^5) (\not{p}_4 + m_e)], \\
L_\mu^\nu &= Tr[\theta_\nu^{\sigma\rho} p_{1\sigma} q_\rho (1 - \gamma^5) \not{p}_1 \gamma^\mu (1 - \gamma^5) \not{p}_3].
\end{aligned} \tag{D.35}$$

Let us evaluate each trace one by one as before;

$$\begin{aligned}
K_\mu^\nu &= Tr[\gamma^\nu (\not{p}_2 + m_e) \gamma_\mu (c_V^e - c_A^e \gamma^5) (\not{p}_4 + m_e)] \\
&= c_V^e Tr[\gamma^\nu \not{p}_2 \gamma_\mu \not{p}_4] + c_V^e m_e \cancel{Tr[\gamma^\nu \not{p}_2 \gamma_\mu]} - c_A^e Tr[\gamma^\nu \not{p}_2 \gamma_\mu \gamma^5 \not{p}_4] - c_A^e \cancel{Tr[\gamma^\nu \not{p}_2 \gamma^5]} m_e \\
&+ m_e c_V^e \cancel{Tr[\gamma^\nu \gamma_\mu \not{p}_4]} + m_e^2 c_V^e \underbrace{Tr[\gamma^\nu \gamma_\mu]}_{4g_\mu^\nu} - m_e c_A^e \cancel{Tr[\gamma^\nu \gamma_\mu \gamma^5 \not{p}_4]} - m_e^2 c_A^e \underbrace{Tr[\gamma^\nu \gamma_\mu \gamma^5]}_0.
\end{aligned} \tag{D.36}$$

Trace of the canceled terms are zero due to odd number of gamma matrices. Using the trace identities we can easily evaluate the following traces.

$$\begin{aligned}
Tr[\gamma^\nu \not{p}_2 \gamma_\mu \not{p}_4] &= 4(p_2^\nu p_{4\mu} + p_{2\mu} p_4^\nu - (p_2 \cdot p_4) g_\mu^\nu) \\
Tr[\gamma^\nu \not{p}_2 \gamma_\mu \gamma^5 \not{p}_4] &= p_{2\alpha} p_{4\beta} Tr[\gamma^\nu \gamma^\alpha \gamma_\mu \gamma^5 \gamma^\beta] \\
&= -p_{2\alpha} p_{4\beta} Tr[\gamma^5 \gamma^\nu \gamma^\alpha \gamma_\mu \gamma^\beta] \\
&= -4i p_{2\alpha} p_{4\beta} \epsilon^{\nu\alpha\beta\mu}.
\end{aligned} \tag{D.37}$$

With these results we can simplify  $K_\mu^\nu$  as;

$$\boxed{K_\mu^\nu = 4c_V^e (p_2^\nu p_{4\mu} + p_{2\mu} p_4^\nu + (m_e^2 - (p_2 \cdot p_4)) g_\mu^\nu) + 4i c_A^e p_{2\alpha} p_{4\beta} \epsilon^{\nu\alpha\beta\mu}}. \tag{D.38}$$

Let us evaluate  $L_\mu^\nu$ .

$$\begin{aligned}
L_\nu^\mu &= \text{Tr}[\theta_\nu^{\sigma\rho} p_{1\sigma} q_\rho (1 - \gamma^5) \not{p}_1 \gamma^\mu (1 - \gamma^5) \not{p}_3] \\
&= p_{1\sigma} q_\rho \text{Tr}[\theta_\nu^{\sigma\rho} (1 - \gamma^5) (1 - \gamma^5) \not{p}_1 \gamma^\mu \not{p}_3] \\
&= 2p_{1\sigma} q_\rho \text{Tr}[\theta_\nu^{\sigma\rho} (1 - \gamma^5) \not{p}_1 \gamma^\mu \not{p}_3] \\
&= 2p_{1\sigma} q_\rho \text{Tr}[(\theta_\nu^\sigma \gamma^\rho + \theta^{\sigma\rho} \gamma_\nu + \theta_\nu^\rho \gamma^\sigma) (1 - \gamma^5) \not{p}_1 \gamma^\mu \not{p}_3] \\
&= 2p_{1\sigma} q_\rho \left( \theta_\nu^\sigma \text{Tr}[\gamma^\rho (1 - \gamma^5) \not{p}_1 \gamma^\mu \not{p}_3] + \theta^{\sigma\rho} \text{Tr}[\gamma_\nu (1 - \gamma^5) \not{p}_1 \gamma^\mu \not{p}_3] \right. \\
&\quad \left. + \theta_\nu^\rho \text{Tr}[\gamma^\sigma (1 - \gamma^5) \not{p}_1 \gamma^\mu \not{p}_3] \right). \tag{D.39}
\end{aligned}$$

Notice that all the matrices are in the same form, just the indices are different. Hence let us evaluate the first trace and deduce the others by just replacing the indices;

$$\begin{aligned}
\text{Tr}[\gamma^\rho (1 - \gamma^5) \not{p}_1 \gamma^\mu \not{p}_3] &= \text{Tr}[\gamma^\rho \not{p}_1 \gamma^\mu \not{p}_3] - \text{Tr}[\gamma^\rho \gamma^5 \not{p}_1 \gamma^\mu \not{p}_3] \\
&= 4(p_1^\rho p_3^\mu + p_1^\mu p_3^\rho - (p_1 \cdot p_3) g^{\mu\rho}) + 4i p_{1\alpha} p_{3\beta} \epsilon^{\rho\alpha\mu\beta}. \tag{D.40}
\end{aligned}$$

Hence  $L_\mu^\nu$  can be written as;

$$\begin{aligned}
L_\nu^\mu &= 8p_{1\sigma} q_\rho \theta_\nu^\sigma (p_1^\rho p_3^\mu + p_1^\mu p_3^\rho - (p_1 \cdot p_3) g^{\mu\rho}) + \cancel{8i p_{1\sigma} q_\rho \theta_\nu^\sigma p_{1\alpha} p_{3\beta} \epsilon^{\rho\alpha\mu\beta}} \\
&\quad + 8p_{1\sigma} q_\rho \theta^{\sigma\rho} (p_{1\nu} p_3^\mu + p_1^\mu p_{3\nu} - (p_1 \cdot p_3) g_\nu^\mu) + 8i p_{1\sigma} q_\rho \theta^{\sigma\rho} p_{1\alpha} p_{3\beta} \epsilon_\nu^{\alpha\mu\beta} \\
&= 8p_{1\sigma} q_\rho \theta_\nu^\rho (p_1^\sigma p_3^\mu + p_1^\mu p_3^\sigma - (p_1 \cdot p_3) g^{\mu\sigma}) + \cancel{8i p_{1\sigma} q_\rho \theta_\nu^\sigma p_{1\alpha} p_{3\beta} \epsilon^{\sigma\alpha\mu\beta}}. \tag{D.41}
\end{aligned}$$

Canceled terms are due to symmetric and anti-symmetric tensor multiplication as in Equation (D.20) and Equation (D.21). With these simplifications we get;

$$\begin{aligned}
L_\nu^\mu &= 8p_{1\sigma} q_\rho \theta_\nu^\sigma (p_1^\rho p_3^\mu + p_1^\mu p_3^\rho - (p_1 \cdot p_3) g^{\mu\rho}) \\
&\quad + 8p_{1\sigma} q_\rho \theta^{\sigma\rho} (p_{1\nu} p_3^\mu + p_1^\mu p_{3\nu} - (p_1 \cdot p_3) g_\nu^\mu) + 8i p_{1\sigma} q_\rho \theta^{\sigma\rho} p_{1\alpha} p_{3\beta} \epsilon_\nu^{\alpha\mu\beta} \\
&= 8p_{1\sigma} q_\rho \theta_\nu^\rho (p_1^\sigma p_3^\mu + p_1^\mu p_3^\sigma - (p_1 \cdot p_3) g^{\mu\sigma}). \tag{D.42}
\end{aligned}$$

Let us contract  $K_\mu^\nu L_\nu^\mu$ .

$$\begin{aligned}
K_\mu^\nu L_\nu^\mu &= \left( 4c_V^e (p_2^\nu p_{4\mu} + p_{2\mu} p_4^\nu + (m_e^2 - (p_2 \cdot p_4)) g_\mu^\nu) + 4ic_A^e p_{2\alpha} p_{4\beta} \epsilon^{\nu\alpha\ \beta}_\mu \right) \\
&\quad \times \left( 8p_{1\sigma} q_\rho \theta_\nu^\sigma (p_1^\rho p_3^\mu + p_1^\mu p_3^\rho - (p_1 \cdot p_3) g^{\mu\rho}) \right. \\
&\quad + 8p_{1\sigma} q_\rho \theta^{\sigma\rho} (p_{1\nu} p_3^\mu + p_1^\mu p_{3\nu} - (p_1 \cdot p_3) g_\nu^\mu) \\
&\quad \left. + 8ip_{1\sigma} q_\rho \theta^{\sigma\rho} p_{1\alpha} p_{3\beta} \epsilon_\nu^{\alpha\mu\beta} + 8p_{1\sigma} q_\rho \theta_\nu^\rho (p_1^\sigma p_3^\mu + p_1^\mu p_3^\sigma - (p_1 \cdot p_3) g^{\mu\sigma}) \right) \\
&= 32c_V^e \left( \theta_\nu^\sigma p_{1\sigma} q_\rho (p_2^\nu p_{4\mu} + p_{2\mu} p_4^\nu + (m_e^2 - (p_2 \cdot p_4)) g_\mu^\nu) \right. \\
&\quad \times (p_1^\rho p_3^\mu + p_1^\mu p_3^\rho - (p_1 \cdot p_3) g^{\mu\rho}) \\
&\quad + \theta^{\sigma\rho} p_{1\sigma} q_\rho (p_2^\nu p_{4\mu} + p_{2\mu} p_4^\nu + (m_e^2 - (p_2 \cdot p_4)) g_\mu^\nu) \\
&\quad \times (p_{1\nu} p_3^\mu + p_1^\mu p_{3\nu} - (p_1 \cdot p_3) g_\nu^\mu) \\
&\quad + i\theta^{\sigma\rho} p_{1\sigma} q_\rho \underbrace{(p_2^\nu p_{4\mu} + p_{2\mu} p_4^\nu + (m_e^2 - (p_2 \cdot p_4)) g_\mu^\nu)}_S p_{1\alpha} p_{3\beta} \underbrace{\epsilon_\nu^{\alpha\mu\beta}}_{AS} \\
&\quad + \theta_\nu^\rho p_{1\sigma} q_\rho (p_2^\nu p_{4\mu} + p_{2\mu} p_4^\nu + (m_e^2 - (p_2 \cdot p_4)) g_\mu^\nu) \\
&\quad \left. \times (p_1^\sigma p_3^\mu + p_1^\mu p_3^\sigma - (p_1 \cdot p_3) g^{\mu\sigma}) \right) \\
&\quad + 32ic_A^e \left( \theta_\nu^\sigma p_{1\sigma} q_\rho (p_{2\alpha} p_{4\beta} \epsilon^{\nu\alpha\ \beta}_\mu) (p_1^\rho p_3^\mu + p_1^\mu p_3^\rho - (p_1 \cdot p_3) g^{\mu\rho}) \right. \\
&\quad + \theta^{\sigma\rho} p_{1\sigma} q_\rho \underbrace{(p_{2\alpha} p_{4\beta} \epsilon^{\nu\alpha\ \beta}_\mu)}_{AS} \underbrace{(p_{1\nu} p_3^\mu + p_1^\mu p_{3\nu} - (p_1 \cdot p_3) g_\nu^\mu)}_S \\
&\quad + i\theta^{\sigma\rho} p_{1\sigma} q_\rho (p_{2\alpha} p_{4\beta} \epsilon^{\nu\alpha\ \beta}_\mu) p_{1\alpha} p_{3\beta} \epsilon_\nu^{\alpha\mu\beta} \\
&\quad \left. + \theta_\nu^\rho p_{1\sigma} q_\rho (p_{2\alpha} p_{4\beta} \epsilon^{\nu\alpha\ \beta}_\mu) (p_1^\sigma p_3^\mu + p_1^\mu p_3^\sigma - (p_1 \cdot p_3) g^{\mu\sigma}) \right).
\end{aligned}$$

(D.43)

After simplifying the above equation we get;

$$\begin{aligned}
K_\mu^\nu L_\nu^\mu &= 32c_V^e \left( \theta_\nu^\sigma p_{1\sigma} q_\rho (p_2^\nu p_{4\mu} + p_{2\mu} p_4^\nu + (m_e^2 - (p_2 \cdot p_4)) g_\mu^\nu) \right. \\
&\quad \times (p_1^\rho p_3^\mu + p_1^\mu p_3^\rho - (p_1 \cdot p_3) g^{\mu\rho}) \\
&\quad + \theta^{\sigma\rho} p_{1\sigma} q_\rho (p_2^\nu p_{4\mu} + p_{2\mu} p_4^\nu + (m_e^2 - (p_2 \cdot p_4)) g_\mu^\nu) \\
&\quad \times (p_{1\nu} p_3^\mu + p_1^\mu p_{3\nu} - (p_1 \cdot p_3) g_\nu^\mu) \\
&\quad + \theta_\nu^\rho p_{1\sigma} q_\rho (p_2^\nu p_{4\mu} + p_{2\mu} p_4^\nu + (m_e^2 - (p_2 \cdot p_4)) g_\mu^\nu) \\
&\quad \left. \times (p_1^\sigma p_3^\mu + p_1^\mu p_3^\sigma - (p_1 \cdot p_3) g^{\mu\sigma}) \right) \\
&+ 32ic_A^e \left( \theta_\nu^\sigma p_{1\sigma} q_\rho (p_{2\alpha} p_4^\beta \epsilon_{\mu\beta}^{\nu\alpha}) (p_1^\rho p_3^\mu + p_1^\mu p_3^\rho - (p_1 \cdot p_3) g^{\mu\rho}) \right. \\
&\quad + i\theta^{\sigma\rho} p_{1\sigma} q_\rho (p_{2\alpha} p_{4\beta} \epsilon_{\mu}^{\nu\alpha\beta}) p_{1\alpha} p_{3\beta} \epsilon_\nu^{\alpha\mu\beta} \\
&\quad \left. + \theta_\nu^\rho p_{1\sigma} q_\rho (p_{2\alpha} p_{4\beta} \epsilon_{\mu}^{\nu\alpha\beta}) (p_1^\sigma p_3^\mu + p_1^\mu p_3^\sigma - (p_1 \cdot p_3) g^{\mu\sigma}) \right). \tag{D.44}
\end{aligned}$$

Let us just contract the terms containing  $c_A^e$  and for simplicity let us define those terms as;

$$\begin{aligned}
K_{11} &= \theta_\nu^\sigma p_{2\alpha} p_{4\beta} \epsilon_{\mu}^{\nu\alpha\beta} (p_{1\sigma} q_\rho p_1^\rho p_3^\mu + p_{1\sigma} q_\rho p_1^\mu p_3^\rho - p_{1\sigma} q_\rho (p_1 \cdot p_3) g^{\mu\rho}), \\
K_{12} &= i\theta^{\sigma\rho} p_{1\sigma} q_\rho (p_{2\alpha} p_{4\beta} \epsilon_{\mu}^{\nu\alpha\beta}) p_{1\alpha} p_{3\beta} \epsilon_\nu^{\alpha\mu\beta}, \\
K_{13} &= \theta_\nu^\rho p_{1\sigma} q_\rho (p_{2\alpha} p_{4\beta} \epsilon_{\mu}^{\nu\alpha\beta}) (p_1^\sigma p_3^\mu + p_1^\mu p_3^\sigma - (p_1 \cdot p_3) g^{\mu\sigma}). \tag{D.45}
\end{aligned}$$

Once we replace  $q \rightarrow p_1 - p_3$  we get for  $K_{11}$ ;

$$\begin{aligned}
K_{11} &= \theta_\nu^\sigma p_{2\alpha} p_{4\beta} \epsilon_{\mu}^{\nu\alpha\beta} \left( p_{1\sigma} q_\rho p_1^\rho p_3^\mu + p_{1\sigma} q_\rho p_1^\mu p_3^\rho - p_{1\sigma} q_\rho (p_1 \cdot p_3) g^{\mu\rho} \right) \\
&= \theta_\nu^\sigma p_{2\alpha} p_{4\beta} \epsilon_{\mu}^{\nu\alpha\beta} \left( p_{1\sigma} p_{1\rho} p_1^\rho p_3^\mu - p_{1\sigma} p_{3\rho} p_1^\rho p_3^\mu + p_{1\sigma} p_{1\rho} p_1^\mu p_3^\rho \right. \\
&\quad \left. - p_{1\sigma} p_{3\rho} p_1^\mu p_3^\rho - p_{1\sigma} p_{1\rho} (p_1 \cdot p_3) g^{\mu\rho} + p_{1\sigma} p_{3\rho} (p_1 \cdot p_3) g^{\mu\rho} \right) \\
&= \theta_\nu^\sigma p_{2\alpha} p_{4\beta} \epsilon_{\mu}^{\nu\alpha\beta} \left( p_1^2 p_{1\sigma} p_{3\mu} - \cancel{p_{1\sigma} p_3^\mu (p_1 \cdot p_3)} \right) \\
&\quad + \cancel{p_{1\sigma} p_1^\mu (p_1 \cdot p_3)} - p_3^2 p_{1\sigma} p_1^\mu - \cancel{p_{1\sigma} p_1^\mu (p_1 \cdot p_3)} + \cancel{p_{1\sigma} p_3^\mu (p_1 \cdot p_3)} \\
&= \theta_\nu^\sigma p_{2\alpha} p_{4\beta} \epsilon_{\mu}^{\nu\alpha\beta} \left( p_1^2 p_{1\sigma} p_{3\mu} - p_3^2 p_{1\sigma} p_1^\mu \right) \\
&= 0. \tag{D.46}
\end{aligned}$$

This term vanishes if we neglect mass of neutrinos  $p_1^2 = 0$  and  $p_3^2 = 0$ .

Let us evaluate  $K_{13}$  in a similar way.

$$\begin{aligned}
K_{13} &= \theta_\nu^\rho p_{1\sigma} q_\rho p_{2\alpha} p_4^\beta \epsilon^{\nu\alpha}{}_{\mu\beta} (p_1^\sigma p_3^\mu + p_1^\mu p_3^\sigma - (p_1 \cdot p_3) g^{\mu\sigma}) \\
&= \theta_\nu^\rho p_{2\alpha} p_4^\beta \epsilon^{\nu\alpha}{}_{\mu\beta} \left( p_{1\sigma} q_\rho p_1^\sigma p_3^\mu + p_{1\sigma} q_\rho p_1^\mu p_3^\sigma - p_{1\sigma} q_\rho (p_1 \cdot p_3) g^{\mu\sigma} \right) \\
&= \theta_\nu^\rho p_{2\alpha} p_4^\beta \epsilon^{\nu\alpha}{}_{\mu\beta} \left( p_1^2 q_\rho p_3^\mu + \cancel{(p_1 \cdot p_3) q_\rho p_1^\mu} - \cancel{p_1^\mu q_\rho (p_1 \cdot p_3)} \right) \\
&= 0 .
\end{aligned} \tag{D.47}$$

$K_{13}$  also vanishes once we again neglect the mass of the neutrinos.

With these findings we can write  $K_\mu^\nu L_\nu^\mu$  as;

$$\begin{aligned}
K_\mu^\nu L_\nu^\mu &= 32c_V^e \left( \theta_\nu^\sigma p_{1\sigma} q_\rho (p_2^\nu p_{4\mu} + p_{2\mu} p_4^\nu + (m_e^2 - (p_2 \cdot p_4)) g_\mu^\nu) \right. \\
&\quad \times (p_1^\rho p_3^\mu + p_1^\mu p_3^\rho - (p_1 \cdot p_3) g^{\mu\rho}) \\
&\quad + \theta^{\sigma\rho} p_{1\sigma} q_\rho (p_2^\nu p_{4\mu} + p_{2\mu} p_4^\nu + (m_e^2 - (p_2 \cdot p_4)) g_\mu^\nu) \\
&\quad \times (p_{1\nu} p_3^\mu + p_1^\mu p_{3\nu} - (p_1 \cdot p_3) g_\nu^\mu) \\
&\quad + \theta_\nu^\rho p_{1\sigma} q_\rho (p_2^\nu p_{4\mu} + p_{2\mu} p_4^\nu + (m_e^2 - (p_2 \cdot p_4)) g_\mu^\nu) \\
&\quad \times (p_1^\sigma p_3^\mu + p_1^\mu p_3^\sigma - (p_1 \cdot p_3) g^{\mu\sigma}) \left. \right) \\
&\quad - 32c_A^e \left( \theta^{\sigma\rho} p_{1\sigma} q_\rho (p_{2\alpha} p_{4\beta} \epsilon^{\nu\alpha}{}_{\mu\beta}) p_{1\alpha} p_{3\beta} \epsilon_\nu{}^{\alpha\mu\beta} \right) .
\end{aligned} \tag{D.48}$$

Thus, we can write  $\mathcal{M}_2 \mathcal{M}_1^*$  as;

$$\sum_{spin} \mathcal{M}_2 \mathcal{M}_1^* = \frac{g_Z^2 e^2}{16q^2 M_Z^2} K_\nu^\mu L_\mu^\nu . \tag{D.49}$$

Finally, interference term can be written as;

$$\begin{aligned}
\mathcal{M}_1 \mathcal{M}_2^* + \mathcal{M}_2 \mathcal{M}_1^* &= \frac{g_Z^2 e^2}{16q^2 M_Z^2} K_\nu^\mu L_\mu^\nu - \frac{e^2 g_Z^2}{16q^2 M_Z^2} E_\mu^\nu F_\nu^\mu \\
&= \frac{g_Z^2 e^2}{16q^2 M_Z^2} (K_\nu^\mu L_\mu^\nu - E_\mu^\nu F_\nu^\mu) \\
&= 0 .
\end{aligned} \tag{D.50}$$

Once we compare Equation (D.47) and Equation (D.25) we easily see that interference term vanishes. Even for the  $\nu_e - e^-$  scattering, the interference term will vanish due to anti-symmetric property of  $\theta^{\mu\nu}$ .



# APPENDIX E

## COMPUTATIONAL FILES

The relevant CalcHEP and Mathematica files used to calculate interference term of dark photon diagram with the SM diagrams are depicted as snapshots of the model files. Moreover, the Mathematica file to calculate the cross-section of  $\bar{\nu}_e - e^-$  is shown for an example. The other calculations are similar.

### E.1 CalcHEP Model Files

```
SMDP(CKM=1 with hGG/AA)
Constraints
Name      <|> Expression
<|
alphaE0   | 1/137.036   % electromagnetic constant at zero energy
CW        | MW/MZ      % on-shell cos of the Weinberg angle
SW        | sqrt(1-CW^2) % sin of the Weinberg angle
GF        | EE^2/(2*SW*MW)^2/Sqrt2
LamQCD    | initQCD5(alphaSMZ,McMc,MbMb,Mtp)
Mb        | MbEff(Q)
Mt        | MtEff(Q)
Mc        | McEff(Q)
aQCD      | alphaQCD(Mh)/pi
Rqcd      | 1+149/12*aQCD+68.6482*aQCD^2-212.447*aQCD^3
Cq        | 1+11/4*aQCD
lnTop     | 2*log(Mtp/Mh)
Ctop      | 1+11/4*aQCD+ (6.1537-2.8542*lnTop)*aQCD^2+(10.999-17.93*lnTop+5.47*lnTop^2)*aQCD^3
Mcp       | McMc*(1+4/3*alphaQCD(McMc)/pi) % 1 loop formula like in Hdecay
Mbp       | MbMb*(1+4/3*alphaQCD(MbMb)/pi) % 1 loop formula like in Hdecay
LmbdGG    | -aQCD/16*sqrt(Rqcd)*EE/(2*SW*MW)*cabs(HggF((Mh/2/Mcp)^2)*Cq+HggF((Mh/2/Mbp)^2)*Cq + HggF((Mh/2/
Mtp)^2)*Ctop)
Qu        | 2/3
Qd        | -1/3
tau2c     | (Mh/2/McRun(Mh/2))^2
tau2b     | (Mh/2/MbRun(Mh/2))^2
tau2t     | (Mh/2/MtRun(Mh/2))^2
tau2l     | (Mh/2/Ml)^2
tau2W     | (Mh/2/MW)^2
LmbdAA    | -alphaE0/(8*pi)*EE/(2*MW*SW)*cabs( 3*Qu^2*(HggF(tau2c)*(1+aQCD*Hgam1F(tau2c))
+HggF(tau2t)*(1+aQCD*Hgam1F(tau2t)))+3*Qd^2*HggF(tau2b)*(1+aQCD*Hgam1F(tau2b))+HggF(tau2l)+HggV(tau2W))
=====
```

Figure E.1: Contents of the func.mdl file is presented for the DP model.

```

SMDP(CKM=1 with hGG/AA)
Particles
Full name |A |A+ | number |2*spin| mass |width |color|aux|>LaTeX(A)<|>LaTeX(A+) <|
gluon      |G |G | 21     | 2     | 0     | 0     | 8     | G   | g   | \gamma | g
photon     |A |A | 22     | 2     | 0     | 0     | 1     | G   | \gamma | \gamma
Z-boson    |Z |Z | 23     | 2     | MZ    | !wZ   | 1     | G   | Z   | Z
W-boson    |W+|W- | 24     | 2     | MW    | !wW   | 1     | G   | W^+ | W^-
Higgs      |h |h | 25     | 0     | Mh    | !wh   | 1     | |   | h   | h
electron   |e |E | 11     | 1     | Me    | 0     | 1     | |   | e   | \bar{e}
e-neutrino |ne|Ne | 12     | 1     | 0     | 0     | 1     | L   | \nu_e | \bar{\nu}_e
muon       |m |M | 13     | 1     | Mm    | 0     | 1     | |   | \mu  | \bar{\mu}
m-neutrino |nm|Nm | 14     | 1     | 0     | 0     | 1     | L   | \nu_\mu | \bar{\nu}_\mu
tau-lepton |l |L | 15     | 1     | Ml    | 0     | 1     | |   | \tau | \bar{\tau}
t-neutrino |nl|Nl | 16     | 1     | 0     | 0     | 1     | L   | \nu_\tau | \bar{\nu}_\tau
d-quark    |d |D | 1      | 1     | 0     | 0     | 3     | |   | d   | \bar{d}
u-quark    |u |U | 2      | 1     | 0     | 0     | 3     | |   | u   | \bar{u}
s-quark    |s |S | 3      | 1     | 0     | 0     | 3     | |   | s   | \bar{s}
c-quark    |c |C | 4      | 1     | Mcp   | 0     | 3     | |   | c   | \bar{c}
b-quark    |b |B | 5      | 1     | Mbp   | 0     | 3     | |   | b   | \bar{b}
t-quark    |t |T | 6      | 1     | Mtp   | wt    | 3     | |   | t   | \bar{t}
photonp    |Ap|Ap | 500022 | 2     | MAp   | wAp   | 1     | G   | \gamma^p | \gamma^p
=====

```

Figure E.2: Contents of the prtcls.mdl file is shown for the DP model.

```

SMDP(CKM=1 with hGG/AA)
Parameters
Name      <| Value      <|> Comment
<|
alphaEMZ  |0.0078180608 |MS-BAR electromagnetic alpha(MZ)
alphaSMZ  |0.1184        |Srtong alpha(MZ) for running mass calculation
EE        |0.31343       | electromagnetic constant
Me        |0.51E-3       | electron mass
|
Mm        |0.1057        | muon mass
Ml        |1.777         | tau-lepton mass
Q         |100           | QCD scale
McMc      |1.23          | Mc(Mc) MS-BAR
MbMb      |4.25          | Mb(Mb) MS-BAR
Mtp       |172.5         | t-quark pole mass
Mh        |125           | higgs mass
wt        |1.59          | t-quark width (tree level 1->2x)
MZ        |91.188        | Z-boson mass
MW        |80.385        | W-boson mass
MAp       |1E-3          | Dark Photon mass
wAp       |0             | Dark photon width
gBL       |0.0001        | Dark sector coupling
=====

```

Figure E.3: Contents of the vars.mdl file is shown for the DP model.

SMDP (CKM=1 with hGG/AA)									
Vertices									
A1	A2	A3	A4	>	Factor	< >	Lorentz part	<	
E	e	Ap			-gBL		G(m3)		
M	m	Ap			-gBL		G(m3)		
L	l	Ap			-gBL		G(m3)		
Ne	ne	Ap			-gBL		G(m3)		
Nm	nm	Ap			-gBL		G(m3)		
Nl	nl	Ap			-gBL		G(m3)		
U	u	Ap			((1/3)*gBL		G(m3)		
D	d	Ap			((1/3)*gBL		G(m3)		
S	s	Ap			((1/3)*gBL		G(m3)		
C	c	Ap			((1/3)*gBL		G(m3)		
B	b	Ap			((1/3)*gBL		G(m3)		
T	t	Ap			((1/3)*gBL		G(m3)		
G	G	G			GG		G(m3)		
G	G	G,t			GG/Sqrt2		G(m3)		
W+	W-	A			-EE		G(m3)		
W+	W-	Z			-EE/CW/SW		G(m3)		
W+	W-	Z	Z		-(EE*CW/SW)^2		G(m3)		
W+	W-	W-	W-		((EE/SW)^2		G(m3)		
W+	W-	A	Z		-EE^2		G(m3)		
W+	W-	A	A		-EE^2		G(m3)		
h	W+	W-			EE*MW/SW		G(m3)		
h	Z	Z			EE/(SW*CW^2)+MW		G(m3)		
h	h	h			(-3/2)+EE*Mh^2/(Mh*SW)		G(m3)		
h	h	h	h		(-3/4)*(EE*Mh/(Mh*SW))^2		G(m3)		
h	h	Z	Z		(1/2)*(EE/(SW*CW))^2		G(m3)		
h	h	W+	W-		(1/2)*(EE/SW)^2		G(m3)		
M	im	h			-EE*Mh/(2*Mh*SW)		G(m3)		
L	l	h			-EE*Ml/(2*Mh*SW)		G(m3)		
C	ic	h			-EE*Ml/(2*Mh*SW)		G(m3)		
B	ib	h			-EE*Mb/(2*Mh*SW)		G(m3)		
T	it	h			-EE*Mt/(2*Mh*SW)		G(m3)		
E	ie	A			-EE		G(m3)		
M	im	A			-EE		G(m3)		
L	il	A			-EE		G(m3)		
Ne	ne	W+			EE/(2*sqrt2+SW)		G(m3)		
Nm	nm	W+			EE/(2*sqrt2+SW)		G(m3)		
Nl	nl	W+			EE/(2*sqrt2+SW)		G(m3)		
E	ne	W-			EE/(2*sqrt2+SW)		G(m3)		
M	nm	W-			EE/(2*sqrt2+SW)		G(m3)		
L	nl	W-			EE/(2*sqrt2+SW)		G(m3)		
E	e	Z			-EE/(4+SW*CW)		G(m3)		
M	im	Z			-EE/(4+SW*CW)		G(m3)		
L	il	Z			-EE/(4+SW*CW)		G(m3)		
Ne	ne	Z			EE/(4+SW*CW)		G(m3)		
Nm	nm	Z			EE/(4+SW*CW)		G(m3)		
Nl	nl	Z			EE/(4+SW*CW)		G(m3)		
U	u	A			(2/3)*EE		G(m3)		
D	d	A			(-1/3)*EE		G(m3)		
C	c	A			(2/3)*EE		G(m3)		
S	s	A			(-1/3)*EE		G(m3)		
B	b	A			(-1/3)*EE		G(m3)		
T	t	A			(2/3)*EE		G(m3)		
U	u	Z			-EE/(12+SW*CW)		G(m3)		
D	d	Z			-EE/(12+SW*CW)		G(m3)		
C	c	Z			-EE/(12+SW*CW)		G(m3)		
S	s	Z			-EE/(12+SW*CW)		G(m3)		
B	b	Z			-EE/(12+SW*CW)		G(m3)		
T	t	Z			-EE/(12+SW*CW)		G(m3)		
U	u	W+			EE/(2*sqrt2+SW)		G(m3)		
C	s	W+			EE/(2*sqrt2+SW)		G(m3)		
T	ib	W+			EE/(2*sqrt2+SW)		G(m3)		
D	lu	W-			EE/(2*sqrt2+SW)		G(m3)		
S	lc	W-			EE/(2*sqrt2+SW)		G(m3)		
B	lt	W-			EE/(2*sqrt2+SW)		G(m3)		
U	u	G			GG		G(m3)		
D	u	G			GG		G(m3)		
E	c	G			GG		G(m3)		
S	is	G			GG		G(m3)		
T	it	G			GG		G(m3)		
B	ib	G			GG		G(m3)		
C	is	W+,f			-1*EE/(2*sqrt2+MW+SW)		G(m3)		
T	ib	W+,f			-1*EE/(2*sqrt2+MW+SW)		G(m3)		
S	lc	W-,f			-1*EE/(2*sqrt2+MW+SW)		G(m3)		
B	lt	W-,f			-1*EE/(2*sqrt2+MW+SW)		G(m3)		
C	ic	Z,f			-1*EE*Ml/(2*Mh*SW)		G5		
B	ib	Z,f			-1*EE*Mb/(2*Mh*SW)		G5		
M	nm	W-,f			-1*EE*Mm/(2*sqrt2+MW+SW)		G5		
L	nl	W-,f			-1*EE*Ml/(2*sqrt2+MW+SW)		G5		
Nm	im	W+,f			-1*EE*Mm/(2*sqrt2+MW+SW)		G5		
Nl	il	W+,f			-1*EE*Ml/(2*sqrt2+MW+SW)		G5		
M	im	Z,f			1*EE*Mm/(2*Mh*SW)		G5		
L	il	Z,f			1*EE*Ml/(2*Mh*SW)		G5		
h	Z,f	Z			1*EE/(2*CW*SW)		G5		
h	W+,f	W+			1*EE/(2*SW)		G5		
h	W+,f	W-			1*EE/(2*SW)		G5		
Z,f	W+,f	W-			EE/(2*SW)		G5		
Z,f	W-,f	W+			EE/(2*SW)		G5		
W-,f	W+,f	Z			EE/(2*CW*SW)		G5		
W-,f	W+,f	A			EE		G5		
W-,f	W+	A			-1*EE*MW		G5		
W-,f	W-	A			-1*EE*MW		G5		
W-,f	W+	Z			-1*EE*MW+SW/CW		G5		
W-,f	W-	Z			-1*EE*MW+SW/CW		G5		
W-,f	W+,f	h			-EE*Mh^2/(2*Mh*SW)		G5		
Z,f	Z,f	h			-EE*Mh^2/(2*Mh*SW)		G5		
W-,f	W+,f	A	A		2*EE^2		G5		
W-,f	W+,f	Z	Z		((EE/(CW+SW))^2/2)		G5		
W-,f	W+,f	W-	W+		EE^2/(2*SW+SW)		G5		
W-,f	W+,f	Z	A		EE^2/(2*SW+SW)		G5		
Z,f	Z,f	Z	Z		((EE/(SW+CW))^2/2)		G5		
Z,f	Z,f	W-	W+		EE^2/(2*SW+SW)		G5		
W-,f	Z,f	W+	A		-EE^2/(2*SW)		G5		
W-,f	Z,f	W-	A		-EE^2/(2*SW)		G5		
W-,f	Z,f	W+	Z		EE^2/(2*CW)		G5		
W-,f	h	W+,f	A		-1*EE^2/(2*SW)		G5		
W-,f	h	W-	A		1*EE^2/(2*SW)		G5		
W-,f	h	W+	Z		1*EE^2/(2*CW)		G5		
W-,f	h	W-	Z		-1*EE^2/(2*CW)		G5		
Z,f	Z,f	Z,f	Z,f		-3*(EE*Mh/(2*Mh*SW))^2		G5		
Z,f	Z,f	W-,f	W+,f		-(EE*Mh/(2*Mh*SW))^2		G5		
W-,f	W-,f	W+,f	W+,f		-(EE*Mh/(2*Mh*SW))^2/2		G5		
Z,f	Z,f	h	h		-(EE*Mh/(2*Mh*SW))^2		G5		
W+,f	W-,f	h	h		-(EE*Mh/(2*Mh*SW))^2		G5		
G,c	G,c	G			-GG		G5		
W-,c	Z,c	W+			EE*CW/SW		G5		
W-,c	Z,c	W-			-EE*CW/SW		G5		
Z,c	W-,c	W+			-EE*CW/SW		G5		
Z,c	W-,c	W-			EE*CW/SW		G5		
W-,c	W+,c	Z			-EE*CW/SW		G5		
W-,c	W+,c	Z			EE*CW/SW		G5		
W-,c	W+,c	A			-EE		G5		
W-,c	W+,c	A			EE		G5		
Z,c	Z,c	h			-EE*MW/(2*SW+CW+SW)		G5		
W-,c	W+,c	h			-EE*MW/(2*SW)		G5		
W-,c	W+,c	h			EE*MW/(2*SW)		G5		
W-,c	W+,c	Z,f			1*EE*MW/(2*SW)		G5		
W-,c	W+,c	Z,f			-1*EE*MW/(2*SW)		G5		
W-,c	Z,c	W+,f			-1*EE*MW/(2*CW+SW)		G5		
W-,c	Z,c	W-,f			1*EE*MW/(2*CW+SW)		G5		
Z,c	W-,c	W+,f			1*EE*MW/(2*CW+SW)		G5		
Z,c	W-,c	W-,f			-1*EE*MW/(2*CW+SW)		G5		
W-,c	A,c	W+			EE		G5		
W-,c	A,c	W-			-EE		G5		
A,c	W+,c	W+			EE		G5		
A,c	W+,c	W-			EE		G5		
W-,c	A,c	W+,f			-1*EE*MW		G5		
W-,c	A,c	W-,f			1*EE*MW		G5		
G	G	h			-4*LmbdGG		G5		
A	A	h			-4*LmbdAA		G5		

Figure E.4: Contents of the lgrng.mdl file is shown for the DP model.

## E.2 Contents of the “sum\_22\_low\_weak.m”

```
initSum:=(
  If[Length[inParticles] !=2 || Length[outParticles] !=2,
    Print["Current summation is for 2->2 processes only"];
    Quit ];

  MM$1=SC[p1,p1] /. substitutions;
  MM$2=SC[p2,p2] /. substitutions;
  MM$3=SC[p3,p3] /. substitutions;
  MM$4=SC[p4,p4] /. substitutions;

  massSum=Simplify[MM$1+MM$2+MM$3+MM$4];
  sum=0;
);

addToSum:=Module[
  {sqm},
  sqm=totFactor*numerator/denominator /. {propDen[p_, MW, w_] -> MW^2, propDen[p_, MZ, w_] -> MZ^2} /.
  propDen[p_,m_,w_]->(m^2-SC[p,p]);

  sqm=sqm /. substitutions;

  sqm=sqm /. {SC[p1,p2]->( s - MM$1 -MM$2)/2 ,
    SC[p1,p3]->(-t + MM$1 +MM$3)/2};
  sum=sum+sqm;
];

finishSum:=Module[
  {sumU,u},
  If[Part[outParticles,1]==Part[outParticles,2],
    sumU=sum /. t-> u;
    sum=(sum+ (sumU /. u-> (massSum -s-t)))/2;
  ];
  sum=Apart[sum];
];
```

Figure E.5: Contents of the “sum\_22\_low\_weak.m” file is shown.

### E.3 Mathematica Notebook File to Calculate the Cross-section for $\bar{\nu}_e - e^-$ Scattering

```
<< "sum_22_low_weak.m";

(*
sum_22.m:
It combines the expressions from the squared diagrams
and presents it as a sum of pole terms
*)

(*-----
OUR NOTE:
Difference between sum_22_low_weak.m versus sum_22.m:
For W and Z propagators i*g_mu_nu/M^2 is used.
We added the following substitution in sum_22.m;
propDen[p_, MW, w_] -> MW^2, propDen[p_, MZ, w_] -> MZ^2
-----*)

(*
=====
* CalcHEP 3.4.7 *
=====
process ne(p1)+e(p2)->e(p3)+ne(p4)
*)

(*parameters={
EE -> 0.00000000000*10^(0)
,Me -> 0.00000000000*10^(0)
,MZ -> 0.00000000000*10^(0)
,MW -> 0.00000000000*10^(0)
,MAp -> 0.00000000000*10^(0)
,gBL -> 0.00000000000*10^(0)
};
*)

(*-----
OUR NOTE:
For the "substitutions" rule, we postpone making the necessary
changes all the way to the end as below.
But we have to keep it here as a trivial operation (MZ->MZ)
since it is needed by sum_22.m
-----*)

substitutions = {
(*SW->Sqrt[1-CW^2]
,CW->MW/MZ*)(*
MZ^2->MW^2/(1-SW^2),
EE->Sqrt[8GF*MW^2*SW^2/Sqrt[2]],
CW->Sqrt[1-SW^2]*)
MZ -> MZ
};

inParticles = {"Ne", "e"};
outParticles = {"e", "Ne"};

SetAttributes[ SC, Orderless ];

SC[ a_ , b_ + c_ ] := SC[a, b] + SC[a, c];

SC[ x_?NumberQ * a_ , b_ ] := x * SC[ a, b ]

p4 = +p1 + p2 - p3;
p1 /: SC[p1, p1] = 0^2;
p2 /: SC[p2, p2] = Me^2;
p3 /: SC[p3, p3] = Me^2;
p2 /: SC[p2,p3] = -1*(0^2 - 0^2 - Me^2 - Me^2 - 2*SC[p1, p2] + 2*SC[p1, p3])/2;
```

```

initSum;

(*)
Diagram 1 in subprocess 1
      Ne      e      e      Ne
==<==\      /==>== ==>==\      /==<==
P1 |      | P3      P3 |      | P1
  |      |      |      |      |
  e | W+ | Ne      Ne | W+ | e
==>==@--<--@==<== ==<==@--<--@==>==
      P2      P4      P4      P2

*)
totFactor = ((2*EE^4)/(SW^4));
numerator = (SC[p1,p3]^2);
denominator = (propDen[-p1-p2,MW,wW]^2);

addToSum;

(*)
Diagram 2 in subprocess 1
      Ne      e      Ne      Ne
==<==\      /==>== ==<==@==<==
P1 |      | P3      P4 | P1
  |      |      |      |
  e | W+ | Ne      e | e
==>==@--<--@==<== ==>==@==>==
      P2      P4      P3      P2

*)
totFactor = ((2*EE^4)/(SW^4*CW^2));
numerator = (2*SC[p1,p3]^2*SW^2-SC[p1,p3]^2+SC[p1,p3]*SW^2*Me^2-SC[p1,p2]*SW^2*Me^2);
denominator = (propDen[-p1-p2,MW,wW]*propDen[-p1+p4,MZ,0]);

addToSum;

(*)
Diagram 3 in subprocess 1
      Ne      e      Ne      Ne
==<==\      /==>== ==<==@==<==
P1 |      | P3      P4 | P1
  |      |      |      |
  e | W+ | Ne      e | e
==>==@--<--@==<== ==>==@==>==
      P2      P4      P3      P2

*)
totFactor = ((4*gBL^2*EE^2)/(SW^2));
numerator = (2*SC[p1,p3]^2+SC[p1,p3]*Me^2-SC[p1,p2]*Me^2);
denominator = (propDen[-p1-p2,MW,wW]*propDen[-p1+p4,MAp,0]);

addToSum;

(*)
Diagram 4 in subprocess 1
      Ne      Ne      Ne      Ne
==<==@==<== ==<==@==<==
P1 | P4      P4 | P1
  |      |      |      |
  Z | e      e | e
==>==@==>== ==>==@==>==
      P2      P3      P3      P2

*)
totFactor = ((EE^4)/(2*SW^4*CW^4));

```

```

numerator = (4*SC[p1,p3]^2*SW^4-4*SC[p1,p3]^2*SW^2+SC[p1,p3]^2+4*SC[p1,p3]*
  SW^4*Me^2-2*SC[p1,p3]*SW^2*Me^2+4*SC[p1,p2]^2*SW^4-4*SC[p1,p2]*SW^4*Me^2+2*
  SC[p1,p2]*SW^2*Me^2);
denominator = (propDen[-p1+p4,MZ,0]^2);

addToSum;

(*
  Diagram 5 in subprocess 1
      Ne   Ne       Ne   Ne
      ==<==@==<==   ==<==@==<==
      P1 | P4       P4 | P1
      z |           Ap|
      e | e         e | e
      ==>==@==>==   ==>==@==>==
      P2   P3       P3   P2
*)
totFactor = ((2*gBL^2*EE^2)/(SW^2*CW^2));
numerator = (4*SC[p1,p3]^2*SW^2-2*SC[p1,p3]^2+4*SC[p1,p3]*SW^2*Me^2-
  SC[p1,p3]*Me^2+4*SC[p1,p2]^2*SW^2-4*SC[p1,p2]*SW^2*Me^2+SC[p1,p2]*Me^2);
denominator = (propDen[-p1+p4,MZ,0]*propDen[-p1+p4,MAp,0]);

addToSum;

(*
  Diagram 6 in subprocess 1
      Ne   Ne       Ne   Ne
      ==<==@==<==   ==<==@==<==
      P1 | P4       P4 | P1
      Ap|           Ap|
      e | e         e | e
      ==>==@==>==   ==>==@==>==
      P2   P3       P3   P2
*)
totFactor = ((8*gBL^4)/(1));
numerator = (SC[p1,p3]^2+SC[p1,p3]*Me^2+SC[p1,p2]^2-SC[p1,p2]*Me^2);
denominator = (propDen[-p1+p4,MAp,0]^2);

addToSum;

finishSum;
sumstu = sum;
sumstu = sumstu;
(*sumstu>>enen_smdp _stu.txt*)

```

```

(*-----
                                OUR NOTE:

Standard Model Check:
Differential cross section dsigma/dT in the
lab frame from the literature (XXXX.XXXX(hep-ph),Eqn.XX):

ruleantiab=
{a→-SW^2,b→-1/2-SW^2} (*for electron anti-neutrino-electron scattering*)

sigmadTSMLit =2*GF^2*Me/(Pi*e1^2)*(a^2*e1^2+b^2*(e1-T)^2-a*b*Me*T)

where
e1:incident neutrino total energy
T:The recoil energy of the electron

Notation:
ne(p1)+e(p2)→e(p3)+ne(p4)
s=(p1+p2)^2=Me^2+2 e1*Me
t=(p1-p3)^2=(p4-p2)^2=Me^2-2*Me*(e1-T)
PhaseSpaceFact=1/(32*Pi*Me*e1^2)
-----

mysubs = {MZ → MW/Sqrt[1 - SW^2], EE^4 → (8 GF * MW^2 * SW^2 / Sqrt[2])^2,
          EE^2 → (8 GF * MW^2 * SW^2 / Sqrt[2]), CW → Sqrt[1 - SW^2]};
rulekin = {s → Me^2 + 2 e1 * Me, t → Me^2 - 2 * Me * (e1 - T)};
ruleantiab = {a → -SW^2, b → -1 / 2 - SW^2};
PhaseSpaceFact = 1 / (32 * Pi * Me * e1^2);

dsigmatdTSMLit = 2 * GF^2 * Me / (Pi * e1^2) *
(a^2 * e1^2 + b^2 * (e1 - T)^2 - a * b * Me * T) / . ruleantiab;
ampsquareSM = Expand[sumstu /. gBL → 0] /. mysubs /. rulekin // Expand // Simplify;
dsigmatdTSMOur = PhaseSpaceFact * ampsquareSM
dsigmatdTSMOur - dsigmatdTSMLit // ExpandAll

GF^2 Me (e1^2 (1 + 4 SW^2 + 8 SW^4) - 2 e1 (1 + 2 SW^2)^2 T + (1 + 2 SW^2) T (-2 Me SW^2 + T + 2 SW^2 T))
-----
2 e1^2 π
0

(*-----
                                OUR NOTE:

Pure Dark Photon (DP) Check:(1202.6073(hep-ph),Eqn .11)
dsigmatdTDPLit=
gBL^4*Me/(4*Pi*e1^2)/(MAp^2+2*T*Me)^2*(2*e1^2+T^2-2*T*e1-T*Me)
-----

dsigmatdTDPLit = gBL^4 *
Me / (4 * Pi * e1^2) / (MAp^2 + 2 * T * Me)^2 * (2 * e1^2 + T^2 - 2 * T * e1 - T * Me);

ampsquareDP =
gBL^4 Collect[Coefficient[Expand[sumstu] /. {gBL^4 → gBL4, gBL^2 → gBL2},
gBL4], gBL4] /. rulekin // FullSimplify;
dsigmatdTDPOur = PhaseSpaceFact * ampsquareDP
dsigmatdTDPOur - dsigmatdTDPLit // ExpandAll

```



$$\frac{gBL^4 Me (2 e1^2 - (2 e1 + Me) T + T^2)}{4 e1^2 \pi (MAp^2 + 2 Me T)^2}$$

0

(\*-----)

OUR NOTE:

Interference term:

-----\*)

```

ampsquareINT = gBL^2 Collect [
  Coefficient[Expand[sumstu] /. {gBL^4 -> gBL4, gBL^2 -> gBL2}, gBL2];
dsigmatTINT = PhaseSpaceFact * ampsquareINT /. mysubs /. rulekin // Expand //
Simplify
zerotest = (PhaseSpaceFact * sumstu - dsigmatTSMOur - dsigmatTDPOur - dsigmatTINT) /.
mysubs /. rulekin // Expand // Simplify

```

$$\frac{(gBL^2 GF Me (e1^2 (2 + 8 SW^2) - 4 e1 (T + 2 SW^2 T) + T (-Me - 4 Me SW^2 + 2 T + 4 SW^2 T)))}{(2 \sqrt{2} e1^2 \pi (MAp^2 + 2 Me T))}$$

0



# CURRICULUM VITAE

## PERSONAL INFORMATION

**Surname, Name:** Bilmiş, Selçuk

**Date and Place of Birth:** 1984, Rize

**Languages:** English (Advanced), German (Beginner), Japanese (Beginner),  
Turkish (Native)

**e-mail:** sbilmis@metu.edu.tr, selcukbilmis@gmail.com

**Phone:** +905369706048

## EDUCATION

<b>Degree</b>	<b>Institution</b>	<b>Year of Graduation</b>
PhD.	Middle East Technical University	2016
M.S.	Middle East Technical University	2010
B.S.	Middle East Technical University	2007

## PROFESSIONAL EXPERIENCE

Year	Place	Enrollment
December 2008 - Present	Middle East Technical University	Research Assistant
September-November 2013	BELLE (Japan)	Student
April-October 2009	TEXONO (Taiwan)	Student
July-September 2008	CERN (Switzerland)	Student

## PUBLICATIONS

- “Constraints on Dark Photon from Neutrino-Electron Scattering Experiments”, *Phys. Rev. D* **92** (2015) 033009
- “Constraints on Non-Commutative Physics Scale with Neutrino-Electron Scattering”, *Phys. Rev. D* **85** (2012) 073011
- “Constraints on Non-Standard Neutrino Interactions and Unparticle Physics with Neutrino-Electron Scattering at the Kuo-Sheng Nuclear Power Reactor”, *Phys. Rev. D* **82** (2010) 033004
- “Measurement of Neutrino-Electron Scattering Cross-Section with a CsI(Tl) Scintillating Crystal Array at the Kuo-Sheng Nuclear Power Reactor”, *Phys. Rev. D* **81** (2010) 072001

## International Conference Publications

- “Final Results of  $\bar{\nu}_e$ - $e^-$  Electron Scattering Cross-Section Measurements and Constraints on New Physics”, *arXiv:1201.4675v1 [hep-ex]*
- “Measurement of  $\bar{\nu}_e$ - $e^-$  Scattering Cross-Section and Constraints on New Physics with a CsI(Tl) Crystal Array at the Kuo-Sheng Reactor Laboratory”, *EPS-HEP* (2011)

## PROJECTS

- TÜBİTAK 108T502, “Study on neutrino physics and dark matter with dedicated detector and DAQ (Data Acquisition) systems at low energy and low background experiments” (2008-2011)
- METU-BAP-08-11-2013-028 “Beyond the physics model search at LHC (Standard model ötesi fiziğin büyük hadron çarpıştırıcısında araştırılması)” (2013-2015)

## ATTENDED CONFERENCES & SUMMER SCHOOLS

- Ankara YEF Gunleri (12-14 February 2015)
- International Neutrino Summer School, **Virginia Tech** - Blacksburg, Virginia, US (10-21 July 2012)
- Ankara YEF Gunleri (27-30 December 2011)
- International Europhysics Conference on High Energy Physics (**EPS-2011**), Grenoble, France (21-27 July 2011) (Contributed talk **on behalf of TEXONO Collaboration**)
- Practical Statistics Lecture Series, Feza Gursey Institute, Istanbul, TURKEY (30 April - 3 May 2010 )
- International Summer School and Conference on High Energy Physics: Standard Model and Beyond, Mugla, Turkey (27 August - 4 September 2010)
- The Eighth Particle Physics Phenomenology Workshop (PPP 8) in **Tainan, Taiwan** (20-23 May 2009)
- TR-Grid School, Ankara, Turkey (30 April-2 May 2008)
- **Cern Summer School 2008** Lectures (10 July- 15 Augustus 2008)
- International Summer School and Conference on High Energy Physics: Standard Model and Beyond, Mugla, Turkey (10-18 September 2008)

## **SCHOLARSHIP & AWARDS**

- Scholarship of TUBITAK-2228 (The Scientific and Technological Research Council of Turkey) for graduate students (2007 - 2009)
- Scholarship of TUBITAK-2211 (The Scientific and Technological Research Council of Turkey) for doctorate students (2010 - 2015)

## **FIELDS OF INTERESTS**

- High Energy Physics
- Neutrino Physics
- Beyond the Standard Model Physics

## **TECHNICAL SKILLS**

**Languages:** C++, Shell scripting (Bash), Mathematica

**Applications:** FeynCalc, MadGraph, CalcHEP, ROOT, PAW, gnuplot, Emacs, L<sup>A</sup>T<sub>E</sub>X, MS Office

**Operating Systems:** Linux (Ubuntu), Mac OS and Windows